Climate Change and Global Crop Yield: Impacts, Uncertainties and Adaptation

Delphine Deryng

A thesis submitted to
the School of Environmental Sciences of the University of East Anglia
in partial fulfilment of the requirements for the degree of Doctor of Philosophy

September 2014

UEA
University of East Anglia

Abstract

Climate change and global crop yield:
Impacts, uncertainties and adaptation

by Delphine Deryng

As global mean temperature continues to rise steadily, agricultural systems are projected to face unprecedented challenges to cope with climate change. However, understanding of climate change impacts on global crop yield, and of farmers' adaptive capacity, remains incomplete as previous global assessments: (1) inadequately evaluated the role of extreme weather events; (2) focused on a small subset of the full range of climate change predictions; (3) overlooked uncertainties related to the choice of crop modelling approach and; (4) simplified the representation of farming adaptation strategies. This research aimed to assess climate change impacts on global crop yield that accounts for the knowledge gaps listed above, based on the further development and application of the global crop model PEGASUS. Four main research topics are presented. First, I investigated the roles of extreme heat stress at anthesis on crop yield and uncertainties related to the use of seventy-two climate change scenarios. I showed large disparities in impacts across regions as extreme temperatures adversely affects major areas of crop production and lower income countries, the latter appear likely to face larger reduction in crop yields. Second, I coordinated the first global gridded crop model intercomparison study, comparing simulations of crop yield and water use under climate change. I found modelled global average crop water productivity increases by up to $17\pm20.3\%$ when including carbon fertilisation effects, but decreases to $-28\pm13.9\%$ when excluding them; and identified fundamental uncertainties and gaps in our understanding of crop response to elevated carbon dioxide. Third, to link climate impacts with adaptation, I introduced the recently developed concept of representative agricultural pathways and examined their potential use in models to explore farming adaptation options within biophysical and socio-economic constraints. Finally, I explored tradeoffs between increasing nitrogen fertiliser use to close the global maize yield gap and the resulting nitrous oxide emissions. I found global maize production increases by 62% based on current harvested area using intensive rates of nitrogen fertiliser. This raises the share of nitrous oxide emissions associated with maize production from 20 to 32% of global cereal related emissions. Finally, these results demonstrated that in some regions increasing nitrogen fertiliser application, without addressing other limiting factors such as soil nutrient imbalance and water scarcity, could raise nitrous oxide emissions without enhancing crop yield.

Acknowledgements

I am deeply thankful to several amazing people who helped me in countless ways throughout this doctoral research and compile this thesis.

First of all, I would like to express my immense gratitude to Declan Conway for his valuable advice, encouragement, support and patience all through this research and writing up process.

I owe my deepest appreciation to Navin Ramankutty, for offering a constant source of intellectual inspiration and sound advice.

I am also greatly in debt to Cynthia Rosenzweig for sharing her tremendous energy and enthusiasm with me, as well as for giving me the responsibility to coordinate the first gridded crop modelling intercomparison.

My next words of acknowledgements go to Joshua Elliott for being the funniest and brightest colleague, and an incredible person to work with. I am also especially thankful to Alex Ruane for encouraging me to join the AgMIP initiative in the first place.

Then I would like to thank the fast-track GGCMI people: Christoph Müller, Stefan Olin, Thomas Pugh, Christian Folberth, Erwin Schmid, and Hong Yang; Katja Fieler and Franziska Piontek from ISI-MIP; and Hermann Lotze-Campen, Jerry Nelson and John Antle from the AgMIP economic team. Special thanks as well to Dieter Gerten and Sibyll Schaphoff for welcoming me at PIK and providing stimulating research collaboration.

I am in debt to the Tyndall Centre and the University of East Anglia for financing my research. I am extremely grateful to Corinne Le Quéré, for her support and for providing exceptional inspiration.

I am thankful to Parvhada Suntharalingam for a support throughout my doctorate and commenting on the final version of my thesis.

As well, I would like to express my gratitude to Sudipta Goswami and Chris Collins, from the high performance computing service, for their precious technical supports when dealing with zillion bits of data.

I would like to thank Andy Challinor and Andrew Lovett for examining my thesis and for providing extremely useful comments that helped improve the presentation of my research and think more critically about the outcome of my work.

I also would like to thank my office mates, Tara, Jenny, Amy, James and Miranda, for sharing bites of life at UEA and numerous cups of tea. A special thanks to my

Contents

List of Figures

List of Tables

xiv

Chapter 1

Introduction

1.1 Background and motivation

Global food production needs to increase to feed a growing population that is mostly expanding in cities of the developing world and additionally contributing to rising per-capita food demand (Beddington et al., 2012). However, increasing global food production throughout the 21$^{\text{st}}$ century is a major challenge for our civilisation at the edge of a global environmental collapse (Beddington, 2009; Ehrlich and Ehrlich, 2013). To feed seven billion people living today[1], agricultural activities appropriate ~34% of terrestrial land (Ramankutty et al., 2008), 70% of global freshwater withdrawal (Gleick et al., 2009; Postel et al., 1996), and contribute to 15-25% of global greenhouse gas (GHG) emissions consisting of carbon dioxide (CO_2), methane (CH_4) and nitrous oxide (N_2O) (Eggleston et al., 2006; Vermeulen et al., 2012b). Agricultural impacts on ecosystems and natural resources are unprecedented and there is no extra land suitable to expand cropland areas, unless we further exploit tropical forests, which would create a substantial loss for the planet's biodiversity and enhance climate change by altering surface albedo and releasing a considerable amount of carbon dioxide (CO_2) into the atmosphere through subsequent deforestation (Foley et al., 2011; Lambin and Geist, 2006).

In fact, global cropland areas have remained fairly steady over the last fifty years (Ramankutty et al., 2008) and most of the increase in crop production occurred due

---

[1]among those seven billion, 850 million people suffer from hunger and two billion people suffer from undernutrition (Wheeler and von Braun, 2013)

to large scale development of intensive agriculture between the late sixties and nineties, relying heavily on mineral fertiliser and pesticide application, irrigation, advanced crop breeding technology and eventually genetically modified crops (Godfray and Garnett, 2014). This so called "green revolution" marked a great success for food supply and contributed to reduce the percentage of hungry people from 23% to 15% of the world's population (The Millennium Development Goals Report, 2013; Wheeler and von Braun, 2013), but it occurred with huge environmental costs (Godfray and Garnett, 2014; Tilman et al., 2011). For instance, despite its beneficial effect on crop carbon intake and thus crop yield, inadequate timing and overuse of nitrogen fertiliser application leads to N_2O emissions into the atmosphere (Levis, 2010) and pollutes groundwater, nearby lakes and rivers (Galloway et al., 2008; Schlesinger, 2008). Furthermore, irrigation expansion not only threatens river flows and groundwater reserves (Haddeland et al., 2006; Siebert et al., 2010), but also involves complex feedbacks with the climate system, e.g. by accelerating the water cycle, with more evapotranspiration (ET) from irrigated crops to the atmosphere, and increasing cloud cover, so that a smaller fraction of incoming solar radiation reaches the land surface (Boucher et al., 2004; Sacks et al., 2008).

Today, the planet's natural capital – land, water, soil minerals, biodiversity – are seriously jeopardised across the world resulting from large scale unsustainable agricultural intensification and land cover change (Foley et al., 2011; Lambin and Meyfroidt, 2011; Rockström et al., 2009). The large contribution of agriculture to global GHG emissions is particularly important as crops, in return, depend largely on climatic conditions. Climate change, especially the increasing risk of extreme weather events and indirect impacts on freshwater resources, threatens agricultural systems and food security (Field et al., 2012; Hertel et al., 2010; Porter et al., 2014; Wheeler and von Braun, 2013). In 2009, Beddington rightly described these complex global interactions as a "perfect storm", and called for a "new green revolution" to achieve sufficient food supply to feed the world's population in the future while reducing agricultural energy and water uses, and GHG emissions (Beddington, 2009; Beddington et al., 2012). Agricultural development must follow a radically different way of conceiving food production in the 21st century; in which increasing crop yield must be addressed together with the environmental conservation agenda (Foley et al., 2011; Garnett et al., 2013; Phalan et al., 2014; Poppy et al., 2014), which is contextualised to local social, political and cultural factors (Ejeta, 2010; Godfray and Garnett, 2014; Horlings and Marsden, 2011;
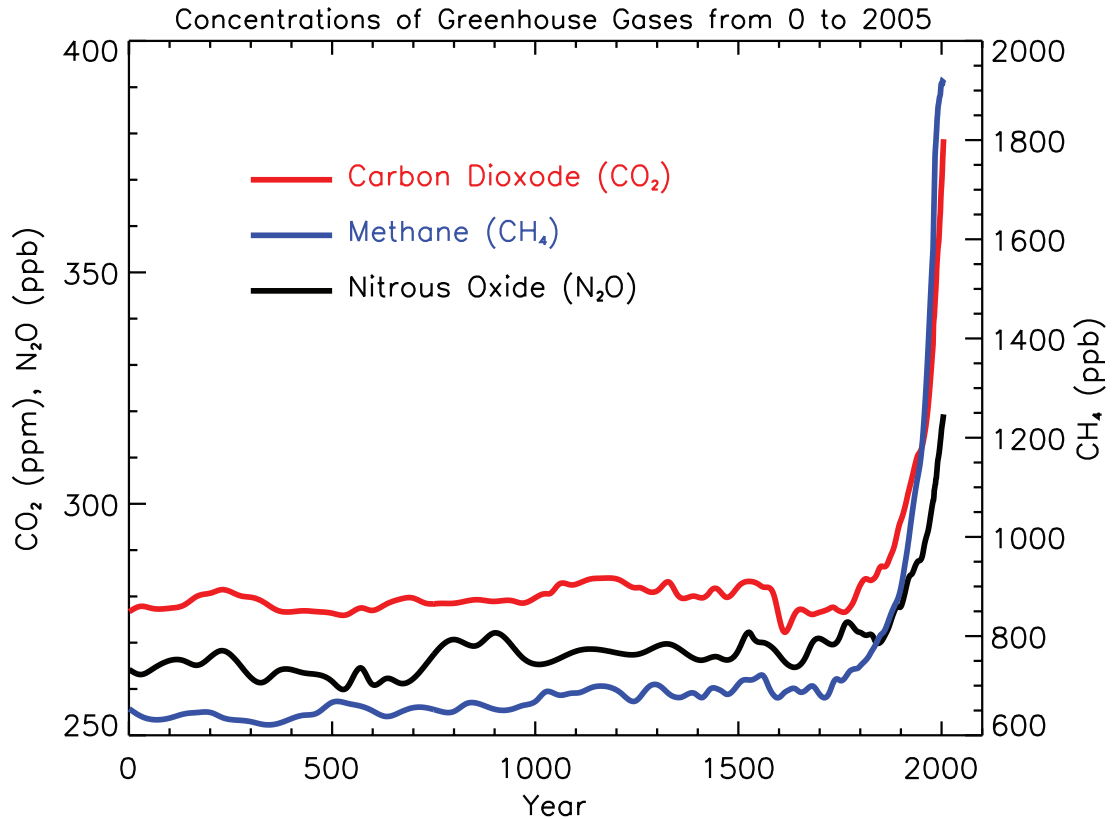
FIGURE 1.1: Atmospheric concentrations of important long-lived greenhouse gases over the last 2,000 years. Increases since about 1750 are attributed to human activities in the industrial era. Concentration units are parts per million (ppm) or parts per billion (ppb), indicating the number of molecules of the GHG per million or billion air molecules, respectively, in an atmospheric sample (Solomon et al., 2007, FAQ 2.1, Figure 1).

Sayer and Cassman, 2013).

1.1.1 Climate change impacts on agriculture

The research presented in this thesis deals with one important aspect of global environmental change and its impacts on crop yields, namely climate change, a phenomenon that is strongly debated in the political arena (Berkhout, 2010; Giddens, 2009) but widely accepted in the scientific community (Solomon et al., 2007; Stocker et al., 2013; Weart, 2010). Figure 1.1 clearly illustrates the surge in GHG concentrations manifested since the start of the industrial revolution (circa 1750), which has and will continue to alter the Earth's energy balance and hence change climate (Joos and Spahni, 2008).

Climate plays a central role in crop growth, such that climate change threatens global agricultural production and food security (Hertel et al., 2010; Wheeler and von Braun, 2013). An extensive review of the drivers of climate change impacts on crop yields is provided by Gornall et al. (2010) and Rosenzweig and Neofotis (2013) and summarised in Table 1.1. Direct drivers of climate impacts on crop yields include long-term change in average temperature and precipitation conditions, and the increasing occurrence of extreme weather events such as extreme temperatures, droughts, floods and tropical storms. In addition, crop yields are sensitive to indirect effects of climate change on freshwater resources, pests and diseases, and sea level rise. Finally, changes in atmospheric composition resulting from GHG emissions, chiefly carbon dioxide (CO_2) and ozone (O_3) concentrations, also play a crucial role in photosynthesis and crop yield.

TABLE 1.1: Direct and indirect drivers of climate change impacts on crop yields.

Drivers	Impacts
Mean climate change	Shift in crop growing season (Burke et al., 2009; Kucharik, 2008)
Extreme temperatures	Heat stress; reduce crop fertility (Ferris et al., 1998a; Semenov and Shewry, 2011)
Droughts	Water stress; crop development alteration (Li et al., 2009; Savage, 2013)
Floods	Fungal disease; crop failure (Rosenzweig et al., 2002; Schiermeier, 2011)
Tropical storms	Loss of cropland area; crop failure (Schiermeier, 2011)
Freshwater resources	Shortage of water for irrigation (Kundzewicz et al., 2008; Vörösmarty et al., 2010)
Pests and diseases	Crop failure; reduce quality (Rosenzweig et al., 2001)
Sea level rise	Inundation of coastal cropland (Dasgupta et al., 2011; Wassmann et al., 2004)
CO_2 increase	Enhance photosynthesis rate; reduce stomata transpiration; reduce protein content (Kimball, 2011; Myers et al., 2014)
O_3 increase	Reduce photosynthesis rate; accelerate leaf senescence (Van Dingenen et al., 2009)

The chapter on food of the latest assessment report of Working Group II of the Intergovernmental Panel on Climate Change (IPCC WGII AR5, Porter et al., 2014) states the high probability of negative impacts resulting from global warming, with substantial negative impacts already observed in Australia, sub-Saharan Africa and South America (Field et al., 2014, figure TS.2.A). The IPCC WGII AR5 (Porter et al., 2014) also confirms previous findings of large regional disparity in future impacts, with vulnerable countries in the tropics and sub-tropics predicted to face larger negative impacts (Müller et al., 2010, 2011; Rosenzweig and Parry, 1994); and countries in high latitudes to benefit from a moderate increase in mean temperatures, especially if farmers

take full advantage of longer growing seasons to grow adequate cultivars (Challinor et al.,
2014b; Deryng et al., 2011). A more detailed review of global analyses of climate change
impacts on crop yields is presented in Chapter 3.

1.1.2 Crop modelling and uncertainties

The IPCC findings are supported by a comprehensive review of climate impacts studies
on crops published before September 2013 (Porter et al., 2014) based on observations of
recent climate change impacts and field experiments (Rosenzweig and Neofotis, 2013),
and simulations (Carter, 2010). Modelling techniques include empirical models based on
crop yield-climate statistics (Lobell and Gourdji, 2012), or agroecological zone (AEZ)
indicators derived from climate and soil information combined with simple soil water
budget estimates (Fischer et al., 2005, 2002), process-based crop models representing
detailed biophysical processes and requiring a substantial amounts of agronomic data
(Jones et al., 2003; Parry et al., 2004) and large-scale ecosystem models designed to
simulate the terrestrial carbon cycle with some representation of managed land requiring
a minimal amount of input data (Deryng et al., 2011; Kucharik, 2003; Müller et al., 2010;
Osborne et al., 2007).

Process-based crop models include the highest level of detail in simulating biophysical
crop responses to multiple drivers of climate change and diverse farming management
practices; however these models need to be calibrated to a specific location and their
aggregation for global scale climate impacts assessments, as done by Parry et al. (2004)
and Nelson et al. (2009), can be problematic (Challinor et al., 2009). Statistical models
on the other hand are very useful to assess global scale trends in crop yield–climate
relationships (Lobell and Burke, 2010; Lobell and Gourdji, 2012; Lobell et al., 2011b).
Yet, statistical models fail to capture adequately non-linearity in crop–climate responses
(Challinor et al., 2009). Furthermore, statistical models are limited to reproducing
historical behaviour of cropping systems, hence presenting important limitations when
dealing with large uncertainties in our understanding of biophysical processes and
unknown future climate change (Vermeulen et al., 2012b). Alternatively, the AEZ
approach presents a useful method for exploring climate change impacts on global
cropland suitability and productivity (Fischer et al., 2005, 2002) but similar to statistical
models, this method overlooks the role of agricultural management practices and farming

adaptation responses. Another statistical modelling approach that indirectly includes farming adaptation is called the "Ricardian approach", which instead of considering crop yield–climate relationships, focuses on land values–climate relationships, i.e. climate impacts on farmers' allocations of activities across time and across landscapes (Cline, 2007; Mendelsohn et al., 1994). However, as for statistical models based on crop yield–climate relationships, Ricardian models build on historical trends and do not capture non-linearity of climate impacts. In contrast, global ecosystem models, or global gridded crop models (GGCMs), enable a more robust evaluation of the role of management practices in response to climate change (Deryng et al., 2011), and offer great capability to deal with the global nature of climate change and the complexity of crop-climate interactions (Challinor et al., 2009; Gerten et al., 2011). These tools are also well suited for combining biophysical impacts on crops with monetary dimensions of crop production when coupled with global economic models to explore global climate change implication on food security (Schmitz et al., 2012). Two generations of GGCMs can be distinguished. A first generation includes global ecosystem models initially developed to simulate natural vegetation dynamics and net primary productions (Sitch et al., 2003) and eventually extended to simulate cropland systems (Bondeau et al., 2007; Deryng et al., 2011; Stehfest et al., 2007). A second generation of GGCMs has recently emerged, thanks to major progress in parallel computing technologies and geographic information systems that now enable point-specific process-based crop models to be run on a grid simultaneously (Elliott et al., 2013; Liu et al., 2007).

Yet, each of these modelling techniques presents important uncertainties that need to be clearly identified and quantified as much as possible for robust impact assessments and sound decision making. First of all, some uncertainties in crop modelling results arise from uncertainties in the input data. Projections of future climate change vary widely among global climate models (GCMs), reflecting poorly understood processes related to complex land-atmosphere-ocean interactions and the random nature of climate variability. Furthermore, unknown future socio-economic development and radiative concentration pathways (RCPs) necessitate comparison of different assumptions and scenarios of future GHG emissions, that directly infer with the climate system. These climate uncertainties are transferred to the impact simulations so that crop models are typically run using multiple climate change scenarios that span a wide range of possible climate change futures. Recent improvements in computational capacity and

techniques such as model emulations have enabled such comparative methods (see Chapter 3). For example, Osborne et al. (2013) identified large disagreement in the relative magnitude of impacts resulting from the use of 14 different GCMs to drive one single crop model. As well, the use of differing downscaling and bias-correction methods to generate suitable climate data from raw GCM outputs can lead to large differences in crop yield simulations and thus increase the range of uncertainty (Falloon et al., 2014). In addition, uncertainties within soil and farming management data (e.g. crop calendar dataset, irrigated cropping areas, and fertiliser application) required to drive crop models, and also within crop yield data used for model calibration and/or validation, propagate to the crop simulations (Falloon et al., 2014; Lobell, 2013).

Secondly, some uncertainties in crop modelling results emerge from different representation of crop processes and parameterisation assumptions, which can lead to significant differences in simulated impacts (White et al., 2011). For instance, different crop models use different levels of complexity to represent CO_2 fertilisation effects, either based on leaf-level biogeochemistry or semi-empirical representations, which leads to contrasting results in simulations (Müller et al., 2010). In fact, the actual role of CO_2 on crops remains highly uncertain, especially in sub-tropical and tropical cropping systems, as large scale experiments have all been located in temperate regions and have focused on a limited number of crops (Leakey et al., 2012; Long et al., 2006; Rosenthal et al., 2012). However, crop models tend to focus on impacts on yield and do not address CO_2 effects on crop quality, which is nonetheless crucial for examining climate change implications for food security (Myers et al., 2014). A detailed review of the CO_2 fertilisation effects on crops is presented in Chapter 5. Moreover, while the role of change in mean temperatures and precipitation patterns has been widely simulated, there has been less focus on the role of extremes on crops (Carter, 2010; Porter et al., 2014). In addition, complex interactions between multiple biophysical drivers of crop yields, such as the relative role of CO_2 interaction with O_3, water and temperature stresses are poorly represented in crop models (Kimball, 2011). Finally, there is no global scale quantitative assessment of the role of pests, diseases, and extreme events such as tropical storms and floods on crop yields as those factors are extremely difficult to represent in crop models (Carter, 2010).

To deal with these model-based uncertainties, modelling assessment studies can follow a probabilistic approach that uses results from multi-model ensembles to determine

the range and likelihood of possible impacts (Falloon et al., 2014). These multi-model ensembles may consist of a combination of multiple climate models and emission scenarios driving a single crop model as done in Osborne et al. (2013) and also in Chapter 3 of this thesis; or in a combination of multiple climate models and emissions scenarios driving multiple crop models as done in Asseng et al. (2013); Bassu et al. (2014) and further explored in Chapters 4 and 5 of this thesis. For instance, Asseng et al. (2013) led a crop model intercomparison analysis of 27 crop models that focused on site-level wheat simulations and concluded that differences in crop models' structure and parameterisation resulted in a greater range of impacts than differences in climate change scenarios. In particular, crop model differences were greater in respect to variations in temperature and atmospheric CO_2 concentration. Bassu et al. (2014) came to the same conclusion in respect to simulated maize yield by an ensemble of 23 crop models. In addition, Bassu et al. (2014) found that model responses to temperature and CO_2 were independent of whether models were run under low or high levels of calibration information. Standardised crop modelling intercomparisons such as these two present unique opportunities to identify modelling strengths and weaknesses, establish causes of uncertainties in models and prioritise future research directions for model improvement and greater accuracy and precision (Challinor et al., 2014a; Rosenzweig et al., 2013; Rötter et al., 2011).

Another statistical method to address model-based uncertainty consists in evaluating the role of model parameter specification. Techniques such as Monte-Carlo simulation and Bayesian-based statistics can be used to explore the entire parameter space and assess crop model sensitivity to the choice of parameter values (Chen and Cournède, 2014; Falloon et al., 2014). It is also possible to emulate the behaviour of complex models to study their sensitivity to the variation of multiple parameters (Lee et al., 2011).

1.1.3 The role of adaptation

Adding to the list of biophysical uncertainties, large gaps exist in our understanding of future socio-economic development and farmers' adaptive capacity and vulnerability. In response to climate change impacts, farmers can apply various adaptation strategies. Direct adaptation options at the farm scale include switching to crop cultivars better suited for longer growing seasons in high latitudes or even switching to different crop

types; planting earlier in the growing season as mean temperatures increase in temperate regions and irrigating in response to water stress (Challinor et al., 2014b). Increasing nitrogen fertiliser application is to some extent another important adaptation measure as crops could potentially respond more positively to carbon fertilisation effects when they are not nutrient limited (Kimball, 2011). Chapters 6 and 7 review in more depth the current state of knowledge on the role of adaptation in future crop production. Additional agricultural adaptation options often rely on investments and medium and long-term planning such as crop breeding to develop drought and/or heat tolerant cultivars and expansion of irrigation infrastructure (Vermeulen et al., 2012a). Successful adaptation measures also need to consider local factors (Vincent, 2007). For instance, Sanchez (2010) argued that the use of high yielding cultivars on African cropland was not as successful as in the case of Asia due to poor soil nutrients, which remain a key limiting factor of crop growth in much of the continent. In addition, cropping systems in sub-Saharan Africa rely mostly on rainfed water and are thus highly vulnerable to variations in precipitation patterns (Challinor et al., 2007b; Knox et al., 2012); these patterns are extremely uncertain according to insufficient climate model projections (Conway et al., 2009).

All these factors must be characterised and evaluated to comprehensively assess possible options for adaptation. Ziervogel and Ericksen (2010) also point out the need for evaluating vulnerability and adaptive capacity in respect to other dimensions of food security, chiefly food access and utilisation, which have been understudied in comparison to the dimensions of food supply. More generally, trans-disciplinary research efforts to fully analyse biophysical and socio-economic dimensions of climate impacts, adaptation and vulnerability are emerging, but major challenges must be addressed to connect research knowledge to concrete action and decision-making at different scales (Adger et al., 2005; Barnett, 2010).

Given the high level of uncertainties in climate and crop simulations, the impact research community has given particular attention to improving the predictive skills of models. But as the representation of climate impacts on agriculture becomes more detailed and elaborate, the range of uncertainty increases (Rötter, 2014). Giving priority to better predictions is increasingly questioned by decision-makers and the adaptation research community, who argue that robust adaptation planning can be developed despite unknown future climate change and its impacts, by focusing on potential vulnerabilities

of diverse adaptation strategies (Dessai and Hulme, 2004; Dessai et al., 2011, 2005). Indeed, successful adaptation policy should not be impeded by existing uncertainties; on the contrary, adaptation measures must be designed to be robust to "deep uncertainties" (Haasnoot et al., 2013; Hallegatte et al., 2011).

Crop modelling predictions are inevitably uncertain given all the factors mentioned in section 1.1.2, but their use in exploratory instead of predictive analyses of the range of climate impacts and sectorial vulnerability can be extremely valuable for adapting to climate change (Challinor et al., 2013; Vermeulen et al., 2013). In the water sector, robust adaptation planning is often designed by inviting experts to assess local risks and vulnerability and explore options via a range of possible impacts (Dessai and Hulme, 2007; Krueger et al., 2012). Nonetheless, a bottom-up approach for decision-making brings additional uncertainties sometimes referred as "conflict-based" – as opposed to "model-based" – uncertainties that are generated by conflicting opinions from multiple experts (Patt, 2007; Wilby and Dessai, 2010). Patt (2007) suggests greater emphasis on the distinction between model-based and conflict-based uncertainties can help evaluate the likelihood of an event and better use of impact assessments for adaptation planning.

1.2   Objectives and research questions

In the previous section, I reviewed in essence the current state of knowledge and methods commonly employed to assess global agricultural impacts of climate change, uncertainties and adaptation, and identified several shortcomings, setting the agenda for new research development and improvements to impact assessment. This doctoral research aims to fill some of these key knowledge gaps by:

- examining the roles of extreme heat stress and carbon fertilisation effects on global crop yield and crop water productivity (CWP);

- producing more robust estimates of the full range of uncertainties related to climate change scenarios and impact simulation throughout the 21$^{\text{st}}$ century;

- building on an innovative agricultural scenario framework to evaluate socio-economic and environmental tradeoffs linked to farming adaptation response to climate change at the global scale.

This research uses primarily quantitative analyses based on spatially gridded numerical crop models run at the global scale, which are fully described in two methodology chapters: namely, Chapter 2, which presents the global crop model PEGASUS; and Chapter 4, which describes the global gridded crop model intercomparison (GGCMI) initiative.

The research is organised around the following research questions:

1. To what extent are global crop yields vulnerable to extreme heat stress?

2. How much is known about carbon fertilisation effects on global crop yield and CWP and what are the key sources of uncertainty?

3. How can biophysical elements of cropping systems be effectively integrated with socio-economic dimensions of global environmental change to explore the role of agricultural development and farming adaptive capacity?

4. What are the climate mitigation tradeoffs associated with global cropland intensification?

To answer these questions, I investigate in Chapter 3 the role of extreme temperature stress at anthesis on crop yield and uncertainties related to the use of 72 climate change scenarios. In Chapter 5, I compare six GGCM simulations of crop yield and water use under climate change and identify fundamental uncertainties and gaps in our understanding of crop response to elevated CO_2. Evaluation of uncertainties in both Chapters 3 and 5 focuses on model-based uncertainties using a probabilistic approach. In Chapter 3, I estimate median change in crop yield and corresponding median absolute deviation from the median (MAD) resulting from the use of alternative climate informations produced by 18 different GCMs. I also evaluate PEGASUS' response to two processes: chiefly, CO_2 fertilisaiton effects and extreme temperature stress at anthesis. Similarly, in Chapter 5, I estimate median change in crop yield, ET and CWP, and corresponding MAD, resulting from the use of six different GGCMs driven by alternative climate information produced by five different GCMs. I also evaluate GGCMs' sensitivity to CO_2 fertilisation effects and water stress.

In Chapter 6, I expand recent work on representative agricultural pathways (RAPs) to integrate future land productivity scenarios with economic impact assessments of climate

change in agriculture. Uncertainties in Chapter 6 are treated using an exploratory approach focusing on the development of scenarios to evaluate adaptive capacity and vulnerability.

Finally, in Chapter 7, I estimate potential maize production on current harvested area resulting from optimum nitrogen fertiliser use and associated N_2O emissions from soils, to identify tradeoffs between climate mitigation policy and global food security. Here, uncertainties are only broadly reviewed as this chapter is simply intended to illustrate concepts developed in Chapter 6. I focus on the predictive skills of the method by taking into account a range and median value of emission factors, and comparing model results to another modelling approach.

1.3   Thesis outline

This thesis comprises eight chapters, including the introduction and conclusion chapters (1 and 8 respectively). Apart from Chapters 2 and 4, which focus on the methodological background of this research, each chapter addresses at least one of the research questions presented in section 1.2.

In Chapter 3, I use the global crop yield model PEGASUS, driven by a vast ensemble of climate change scenarios, to quantify the range of impacts of extreme heat stress on global crop yield and the uncertainties related to a large range of climate change futures. Chapter 3 is preceded by a methodology chapter (2) that describes in detail PEGASUS and the modelling protocol used in Chapter 3.

In Chapter 4, I review the GGCMI fast-track process. I describe my contribution to its coordination and the production of the global modelling ensemble that supports the analysis presented in Chapter 5, looking at the role of elevated atmospheric CO_2 concentration levels on crop yield and water use, and uncertainties in current crop modelling methods.

Chapter 6 addresses the role of adaptation in climate change impact assessments and builds on new storylines and scenarios development for use with GGCMs to simulate future trends in global land productivity in response to agricultural management practices consistent with alternative socio-economic pathways. Finally, to explore

some of the RAP socio-economic and environmental challenges presented in Chapter 6, Chapter 7 analyses tradeoffs associated with closing the global crop yield gap by adding optimum levels of nitrogen fertiliser to maize production systems and resulting N_2O emissions from cultivated soils.

Each chapter is preceded by a preface, which links chapters together and details my contribution along with that of my co-authors. All figures and tables included in this thesis are original and were produced by myself unless explicitly specified.

Chapter 2

Global crop yield modelling

Preface

The research presented in this thesis relies for the most part on the use of global gridded crop models (GGCMs) typically developed to assess crop response to climate change impacts at the global scale. All results chapters of this thesis make use of the global crop yield model PEGASUS (Predicting Ecosystem Goods and Services Using Simulation), a state-of-the-art GGCM primarily developed and used by myself since 2007 (Deryng, 2009; Deryng et al., 2011). Chapter 3 employs PEGASUS to look at the effects of extreme heat stress on crop yields. Chapter 5 is based on the first GGCM intercomparison analysis consisting of six GGCMs including PEGASUS. The framework of the intercomparison project and methodology behind the other GGCMs are presented in Chapter 4. Chapter 7 uses PEGASUS to explore tradeoffs associated with increasing nitrogen fertiliser use and resulting nitrous oxide (N_2O) emissions from soils.

2.1 Introduction

PEGASUS is a global crop model designed to simulate effects of climate change and the role of agricultural management practices on global crop yield (Deryng et al., 2011). PEGASUS originates from a global ecosystem model and is thus capable of simulating carbon dynamics in cropland and natural vegetation. For my doctoral thesis, I have developed a new version of PEGASUS (version 1.1, Deryng et al., 2014) that includes

several improvements since version 1.0. These include the ability to simulate the effects of heat-stress at anthesis (HSA) on crop fertility, and elevated atmospheric carbon dioxide concentration ($[CO_2]$) on photosynthesis rate and transpiration demand. In addition, PEGASUS 1.1 can generate stochastic weather data at a daily time-step from monthly climate inputs allowing for a more accurate representation of climate variability when daily climate data are not available. This chapter presents a detailed description of PEGASUS: the modelling approach (section 2.2), input data (section 2.3) and model calibration and validation (section 2.4). An overview of the ISI-MIP/AgMIP framework and participating GGCMs is presented in Chapter 4.

2.2 The PEGASUS model

2.2.1 Carbon dynamics

PEGASUS combines a radiation use efficiency (RUE) model with a surface energy and soil water balance model to estimate daily photosynthesis and annual net primary production (NPP) for natural vegetation and crops comprising maize, soybean and spring wheat. The diagram in Figure 2.1 illustrates interactions between the different modules within PEGASUS.

A dynamic allocation algorithm, specific to each crop type, partitions daily biomass production into the different organs of the crop, i.e. leaves, stem, roots, and storage organs, and crop yield is eventually derived from the amount of carbon contained in the storage organs at harvest date (Deryng et al., 2011; Penning de Vries et al., 1989). Carbon allocation fractions vary with crop development so that all biomass produced after crop anthesis is allocated to the storage organs. In addition PEGASUS accounts for leaves and roots turnover as the crop reaches its maturity state (Deryng et al., 2011; Penning de Vries et al., 1989).

The RUE model assumes photosynthesis in unstressed conditions is proportional to incoming solar radiation, but temperature, soil moisture availability, and nutrient availability can limit daily net biomass production ($\mathcal{P}$). $\mathcal{P}$ is expressed in mol C m^{-2} s^{-1} as:

$$\mathcal{P} = \beta APAR f_T f_W f_N \qquad (2.1)$$
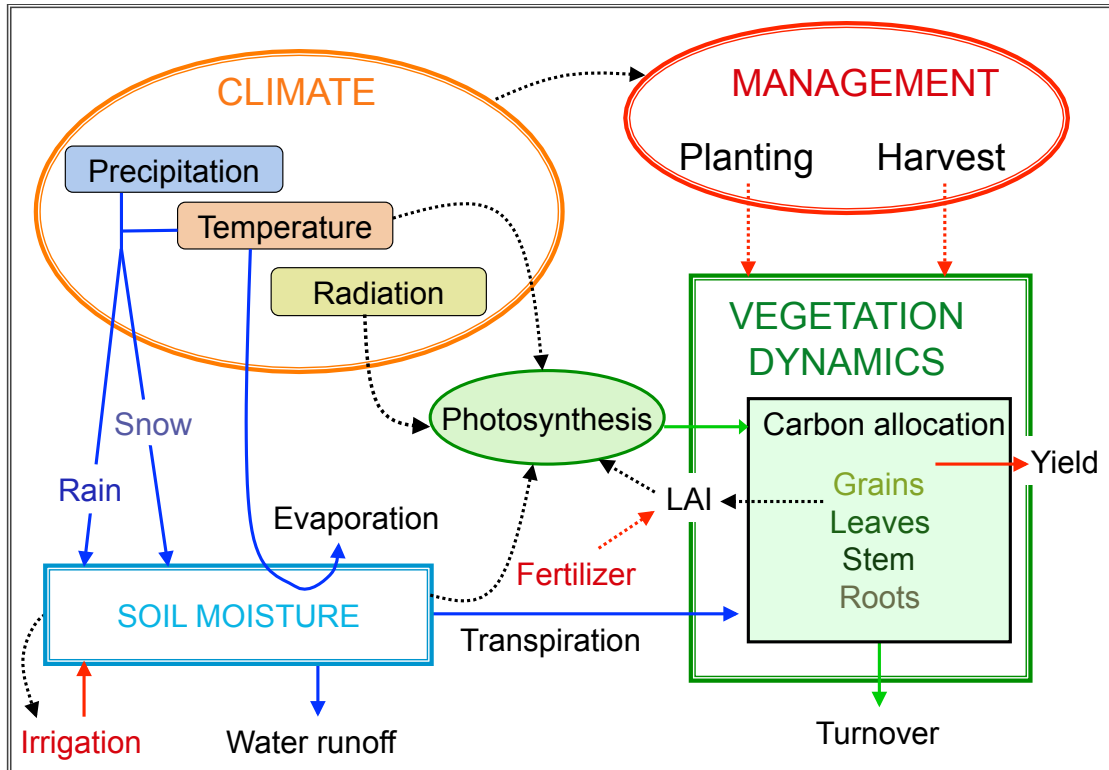
FIGURE 2.1: Flowcharts of the global crop model PEGASUS (Deryng, 2009). Rectangles represent the stock of water in soil and carbon in vegetation. Blue arrows stand for water fluxes. Green arrows stand for carbon fluxes. Dashed arrows represent the relationship between variables. The management components are shown in red.

where β (mol C mol quanta^{-1}) is the RUE coefficient, which is a crop specific global parameter that increases with atmospheric [CO_2] (see section 2.2.6). $APAR$ (mol quanta m^{-2} s^{-1}) represents the daily average Absorbed Photosynthetically Active Radiation and is expressed using Beer-Lambert's law for light interception on a surface, which depends on leaf surface area and its carbon content (Deryng et al., 2011; Foley, 1994). f_T, f_W, and f_N are three limiting factors varying between 0 (high stress) and 1 (no stress) of daily mean air surface temperature, daily soil moisture, and soil nutrient status, respectively. Other limiting factors such as pests and diseases, air pollution, soil erosion, level of mechanisation and farmer-style of management are not taken into consideration, assuming soil nutrient content has a predominant effect on crop yield relative to these other limiting factors (Deryng et al., 2011). In fact, PEGASUS is based on the assumption that the rate of fertiliser application is positively correlated with other limiting factors, i.e. places with high rates of chemical fertiliser application should have higher levels of mechanisation and higher use of chemical pesticides (see section 2.2.4).

2.2.2 Temperature stress

The temperature stress factor (f_T) is defined according to a global temperature envelope specific for each crop type (Figure 2.2(a)) to represent the range of optimum temperature allowing daily biomass production (Deryng et al., 2011); an additional heat-stress factor is defined to simulate the impact of extreme heat stress on crop fertility (see section 2.2.5).

2.2.3 Water stress and irrigation

The water stress factor (f_W) is a function of the potential plant water uptake rate (Campbell and Norman, 2000), which is a non-linear function of the ratio of the daily soil moisture to the soil available water capacity (AWC) (Deryng et al., 2011). Potential plant water uptake is high as long as soil water exceeds half of the soil AWC, but it decreases rapidly below this threshold (Figure 2.2(b)). Soil AWC is prescribed from the ISRIC-WISE soil dataset (Batjes, 2005).The calculation of daily soil moisture follows a simple two-layer bucket approach (Deryng et al., 2011) where soil water inflow results from rainfall and snow melt, and soil water outflow accounts for soil evapotranspiration, soil percolation, canopy interception loss and transpiration (Gerten et al., 2004). The calculation of crop transpiration is based on the Priestley-Taylor equation to estimate potential evapotranspiration (PET) (Deryng et al., 2011; Gerten et al., 2004; Ramankutty et al., 2002) and varies with [CO_2] to account for CO_2 effect on crop water use efficiency (see section 2.2.6).

When irrigation water is supplied, the potential water uptake rate is kept above 0.9 to ensure soil water remains at minimum at half of its AWC. Various approaches can be used to simulate rainfed and irrigated yields. In Deryng et al. (2011), actual yield was directly estimated using a f_W that combined plant water uptake rates in irrigated and rainfed crop areas using global maps of fraction of crop-specific irrigated areas. In all simulations presented in this thesis however, both fully irrigated and rainfed systems were simulated separately over potential climatic-suitable cropland areas. Irrigated and rainfed yields were then combined together to form actual yield using a combination of the Earthstat dataset (Monfreda et al., 2008) for present-day harvested areas and the MIRCA2000 dataset (Portmann et al., 2009) for present-day irrigated and rainfed areas.
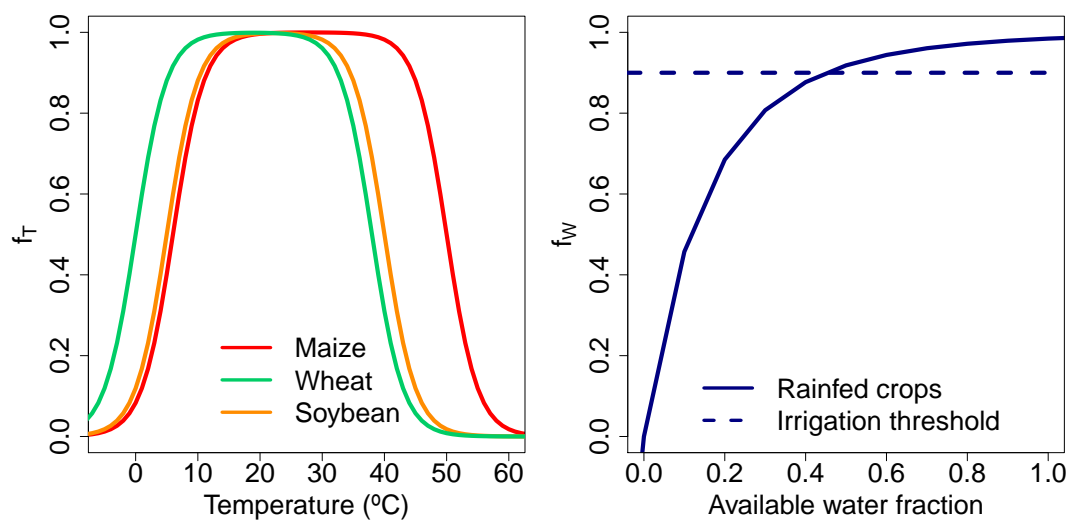
(a) Temperature stress factor (f_T)

(b) Water stress factor (f_W)
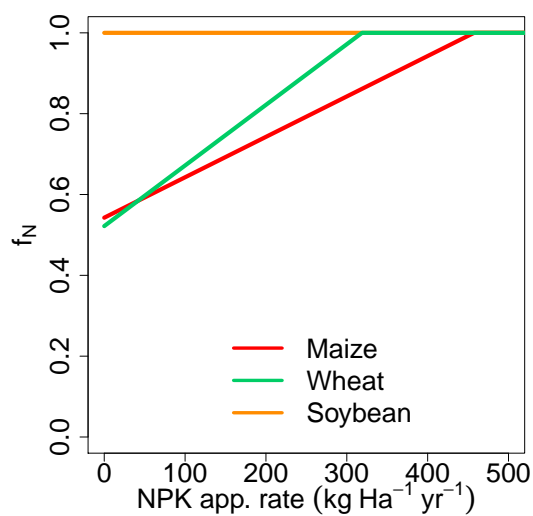
(c) Nutrient stress factor (f_N)

FIGURE 2.2: Temperature (a), water (b), and nutrient (c) stress factors for each crop. The water stress factor is identical for each crop. In irrigated cropland, f_W is kept above 0.9.

2.2.4 Nutrient stress and fertiliser application

Unlike the temperature and water stress factors that vary daily with daily average temperature, soil moisture and crop water demand, the nutrient stress factor (f_N) is estimated from annual rates of fertiliser application and remain constant throughout the growing season. f_N in PEGASUS is estimated after a linear regression between yield gap data – derived from actual and potential yields achievable according to specific soil moisture and temperature conditions (Deryng et al., 2011) – and annual rates of nitrogen–phosphorus–potassium (NPK) fertiliser application from the International Fertiliser Industry Association (IFA) (Deryng et al., 2011; IFA, 2002). The yield gap can be attributed to water and nutrient deficits and we assumed that in irrigated cropland, yield gap is uniquely a result of nutrient limitation. The regression was therefore performed using data points with more than 20% of the cropland area under irrigation to establish a direct yield–fertiliser relationship (Deryng et al., 2011).

Figure 2.2(c) illustrates f_N response to national annual rates of NPK fertiliser application. Note among the three crops simulated in PEGASUS, the regression analysis produced significant results for maize and wheat only so that in the case of soybean, f_N remains equal to 1 (i.e. no stress). The limitations of this approach are discussed in (Deryng et al., 2011).

Chapter 7 explores scenarios for closing the global yield gap by increasing rates of fertiliser application using subnational fertiliser data comprising both organic and inorganic fertilisers (Mueller et al., 2012) instead of the national IFA dataset, and by applying a non-linear algorithm to account for yield plateau at high fertiliser application.

2.2.5 Heat stress at anthesis

Crops are sensitive to extreme temperatures, particularly around the reproductive stage, called anthesis, which last about a few weeks depending on crop types and varieties (Ferris et al., 1998a; Wheeler et al., 2000). Following the methodology developed by Challinor et al. (2005) and used in several other studies (Moriondo et al., 2011; Teixeira et al., 2011), PEGASUS' account of extreme temperature stress on crop yield follows three steps:

1. estimation of the crop thermal sensitivity period (TSP);

2. identification of an extreme temperature event according to crop specific temperature tolerance threshold;

3. application of a heat stress factor f$_{\text{HSA}}$ on storage organ production, which depends on duration and intensity of the high temperature event.

Crop TSP includes a couple of days before and after anthesis and is estimated as a function of crop growing period length (GPL), which depends on growing degree days (GDD) accumulation (Deryng et al., 2011) and varies with crop cultivars. Anthesis is scheduled when the number of days since emergence reaches half of crop GPL (calculated between emergence and maturity), i.e. $0.5\ GPL$; TSP starts a few days before anthesis at $0.45\ GPL$ and ends after anthesis at $0.7\ GPL$. A high temperature event occurs when daily effective temperature (T$_{\text{eff}}$) exceeds a critical temperature (T$_{\text{cr}}$) threshold. Above this threshold, the daily heat stress factor f$_{\text{HSAd}}$ during the TSP is calculated according to:

$$f_{HSAd} = \begin{cases} 1 & \text{if } T_{eff} < T_{cr} \\ 1 - \dfrac{T_{eff} - T_{cr}}{T_{lim} - T_{cr}} & \text{if } T_{cr} \leq T_{eff} < T_{lim} \\ 0 & \text{if } T_{eff} \geq Tlim \end{cases} \tag{2.2}$$

T_{eff} is defined as $(T_{mean} + T_{max})/2$, where T_{mean} is the daily mean temperature and T$_{\text{max}}$ is the daily maximum temperature (Penning de Vries et al., 1989), T$_{\text{lim}}$ is the limit temperature above which f$_{\text{HSAd}}$ is maximal. Crop specific T$_{\text{cr}}$ and T$_{\text{lim}}$ come from a synthesis of values found in the literature (Ferris et al., 1998a; Lobell et al., 2011a; Modhej et al., 2008; Moriondo et al., 2011; Porter and Gawith, 1999; Semenov and Shewry, 2011; Spiertz et al., 2006; Teixeira et al., 2011; Thuzar et al., 2010) (Table 2.1). Temperature tolerance differs for each crop. Here, critical temperature thresholds for HSA are 25℃ for spring wheat, 32℃ for maize and 35℃ for soybean. Hence, as temperatures increases, spring wheat yield is impacted first, followed by maize and finally soybean. However, HSA impact functions differ among crop type as temperature thresholds at zero pod-set are 35℃ for spring wheat, 45℃ for maize and 40℃ for soybean.

The daily heat stress factor is accumulated and averaged over the TSP so that f$_{\text{HSA}}$ is expressed as:

$$f_{HSA} = \frac{1}{TSP} \sum_{1}^{TSP} f_{HSAd} \tag{2.3}$$

Finally, crop yield (Y in t Ha^{-1}) affected by HSA is expressed as:

$$Y = \frac{EF}{0.45\ DF} C_{so} \times f_{HSA} \tag{2.4}$$

where C_{so} represents the amount of dry carbon accumulated in the storage organs at harvesting date, EF is the economic fraction of the storage organs, DF is the dry fraction of the economic yield to convert weight of dry matter to weight of fresh matter, and 0.45 is the mass of carbon contained in one unit of dry matter (Deryng et al., 2011).

TABLE 2.1: Temperature critic (T_{cr}) and limit (T_{lim}) (in ℃) for maize, wheat and soybean used in this study (PEGASUS 1.1) and corresponding values found in the literature.

Reference	Maize		Wheat		Soybean	
	T_{cr}(℃)	T_{lim}(℃)	T_{cr}(℃)	T_{lim}(℃)	T_{cr}(℃)	T_{lim}(℃)
PEGASUS 1.1	32	45	25	35	35	40
Moriondo et al. (2011)	31	40				
Teixeira et al. (2011)	35	45	27	40	35	40
Lobell et al. (2011a)	30					
Semenov and Shewry (2011)			27			
Thuzar et al. (2010)					34	
Modhej et al. (2008)			22			
Spiertz et al. (2006)			25			
Porter and Gawith (1999)			24	31		
Ferris et al. (1998a)			25	35		

2.2.6 Carbon dioxide effects

PEGASUS takes into account photosynthesis enhancement from elevated [CO_2] and reduction in transpiration demand. While the CO_2 effect on RUE coefficient is crop specific, CO_2 influence on PET is identical for all crops.

In equation 2.1, β increases with [CO_2] so that:

$$\beta = \frac{100 \cdot CO_2}{CO_2 + e^{r1 - r2\ \cdot\ CO_2}} \tag{2.5}$$

where CO_2 is the concentration of carbon dioxide in the atmosphere (ppm), and r1 and r2 are shape coefficients. The shape coefficients are calculated by solving equation 2.5 using two known points (β_{amb}, $CO_{2_{amb}}$) and (β_{hi}, $CO_{2_{hi}}$). β_{amb} is tuned to simulate present-day global crop yield data (from the Earthstat dataset Monfreda et al., 2008) at $CO_{2_{amb}} = 380$ ppm as in Deryng et al. (2011). During the calibration procedure,

PEGASUS is run for a wide range of β_{amb} values to identify an optimum value for each crop according to the Willmott index of agreement (Deryng et al., 2011; Willmott et al., 1985).

At $CO_{2_{hi}} = 550$ ppm, parameters are $\beta_{hi} = 1.06 \times \beta_{amb}$ for maize, $\beta_{hi} = 1.13 \times \beta_{amb}$ for wheat, and $\beta_{hi} = 1.19 \times \beta_{amb}$ for soybean according to Free-Air CO_2 Enrichment (FACE) results (Long et al., 2006):

$$r1 = ln\left[\frac{CO_{2_{amb}}}{0.01 \cdot \beta_{amb}} - CO_{2_{amb}}\right] + r2 \cdot CO_{2_{amb}} \tag{2.6}$$

$$r2 = \frac{ln\left[\frac{CO_{2_{amb}}}{0.01 \cdot \beta_{amb}} - CO_{2_{amb}}\right] - ln\left[\frac{CO_{2_{hi}}}{0.01 \cdot \beta_{hi}} - CO_{2_{hi}}\right]}{CO_{2_{hi}} - CO_{2_{amb}}} \tag{2.7}$$

In PEGASUS 1.1, elevated [CO_2] reduces daily PET demand following a similar and simplified approach to Easterling et al. (1992), also used in later versions of EPIC (Williams, 1995) and SWAT (Neitsch et al., 2005) models , so that:

$$PET = PET_{amb} \times \left(1.5 - 0.5 \frac{CO_2}{CO_{2_{amb}}}\right) \tag{2.8}$$

where PET_{amb} corresponds to PET estimated under $CO_{2_{amb}}$. The water stress factor f_W is indirectly affected by elevated [CO_2] due to its dependency on potential plant water uptake rate, which in turn depends on daily PET demand.

2.2.7 Planting and harvesting decisions

In PEGASUS, planting date decision is made according to a simple algorithm based on temperature and precipitation conditions and crop PET (Deryng et al., 2011). The main rationale behind planting date decision is farmers tend to plant when temperatures become mild enough to allow the crop to grow in temperature-limited regions and when the ratio of precipitation to PET reaches a threshold signalling the start of the rainy season in moisture-limited regions. PEGASUS takes also into account the influence of winter snow, which can delay planting since farmers have to wait until the soil is dry enough to drive tractors in the fields (Deryng et al., 2011; Sacks et al., 2010). However, PEGASUS does not account for multiple cropping systems, which are common farming

system in tropical agriculture (Waha et al., 2013). In region where double cropping is possible (i.e. the same crop is grown twice successively in the same field in the same year), PEGASUS only simulates the primary crop but not the secondary one, so the field is left bare after harvest of the primary crop until the following year.

Harvesting date decision is triggered by the crop reaching maturity, which is estimated from GDD accumulation. PEGASUS simulates choice of crop cultivars, defined by their GGD requirement, according to annual GDD so that cultivars grown in colder climates have smaller GDD requirements than those grown in warmer climates:

$$GDD_{T_b} = \sum_{i=1}^{N} max(0, \min(T_i, T_{max}) - T_b) \tag{2.9}$$

where T_i is the daily mean temperature at day i, T_b is the base temperature, T_{max} is the maximum temperature threshold, and N is the total number of days, e.g. 365 for annual GDD calculation. Different crops have different minimum and maximum temperature thresholds for thermal accumulation (Deryng et al., 2011).

When adaptation to climate change by changing crop planting date and cultivar is enabled in PEGASUS, timing of critical crop development stages such as crop anthesis and grain filling period vary accordingly, which can influence the duration and timing of crop TSP (section 2.2.5) and thus the intensity of heat stress at anthesis. Figure 2.3 illustrates the effect of adapting planting dates and crop cultivars to simulated climate change on crop flowering dates as simulated by PEGASUS driven by daily climate input from HadGEM2-ES under RCP 8.5 (see Chapter 4).

2.3   PEGASUS input data

PEGASUS is driven by daily climate data of average, minimum and maximum temperatures, precipitation and fraction of sunshine hours. Fraction of cloud cover can be used instead of sunshine hours. In that case, PEGASUS converts fraction of cloud cover to sunshine hours following Doorenbos and Pruitt (1984). PEGASUS also requires information on soil AWC, and annual rates of crop specific chemical fertiliser application. The use of crop-specific irrigated areas is optional and is used here in a post-processing step. PEGASUS can be run at various spatial resolutions but the simulations presented
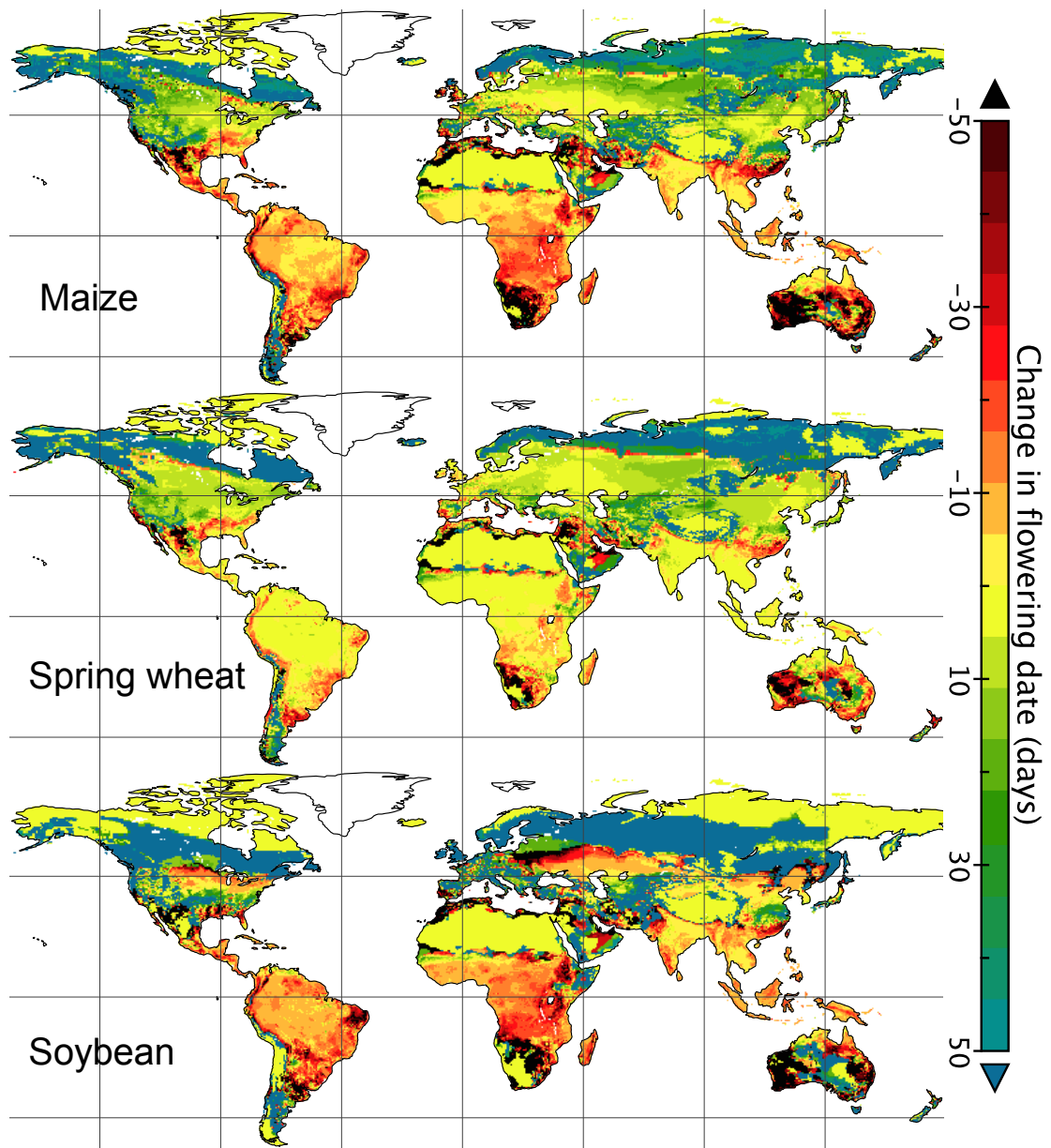
FIGURE 2.3: Simulated change in flowering dates for maize, spring wheat and soybean for PEGASUS driven by HadGEM2-ES under RCP 8.5 (using 10–year average for 2081–2090 relative to 1991–2000 generated with the ISI-MIP fast-track data archive, see www.isi-mip.org). Temperature-limited regions show unchanged or slightly later flowering dates resulting mainly from longer growing period due to higher temperatures, which is more influential than the effect of earlier planting; on the opposite, moisture-limited regions tend to show earlier flowering dates resulting from faster crop development due to higher temperatures, thus leading to overall shorter crop duration. Unchanged flowering dates (yellow areas) in the Sahel and in high latitudes represent areas where the crop is not planted (so flowering dates remain equal to 0). In addition, regions where flowering dates occur more than 50 days later than present (dark green areas) are regions where climate conditions in the 2080s become suitable for growing crops (corresponding flowering dates are equal to 0 at present-day).

in this thesis were run on a $0.5° \times 0.5°$ grid. Similarly to Müller and Lucht (2007), $0.5°$ appears to be optimum for robustness and accuracy of results when dealing with coarse climate data, as well as finer resolution of agricultural data. Table 2.2 summarises the input dataset, excluding the climate data, used to drive PEGASUS in Chapters 3 and 5.

Daily mean temperature and fraction of sunshine hours (or cloud cover) are used to estimate the land-surface energy balance, and thus, incoming photosynthetically active radiation as described in Foley (1994); Gerten et al. (2004); Ramankutty et al. (2002). In addition, the soil water balance module uses daily precipitation and temperature data to estimate daily inflow of water in the soil layers as well as daily outflow via soil evaporation and leaf evapotranspiration similar to Gerten et al. (2004). Daily mean and maximum temperatures also directly affect the rate of biomass production in equation 2.1. In addition, daily maximum and mean temperatures are used in the heat-stress functions (see equation 2.2 in section 2.2.5). Finally, phenology in PEGASUS makes use of GDD accumulation, and hence uses temperature data to estimate duration and timing of development stage of crop growth. Last, information on precipitation and temperature conditions are also used in the automatic planting date decision algorithm.

TABLE 2.2: Minimum soil and management data requirements to run PEGASUS and crop yield and harvested areas used for calibration (see section 2.4)

Dataset	Variable name	Spatial Reference	Temporal Reference	Source
Soil information	Available water capacity (top 50cm, top 20cm, 50-150cm soil columns)	$0.5°$ lon $\times 0.5°$ lat	-	ISRIC-WISE (Batjes, 2005)
Irrigation	Annual irrigated harvested area	$0.5°$ lon $\times 0.5°$ lat (original is 5' lon $\times$ 5' lat)	2000	MIRCA2000 (Portmann et al., 2009)
Fertiliser application	Total NPK application rates	National average	Mid-1990s	(IFA, 2002)
Present-day yield & harvested areas	Yield, harvested areas	$0.5°$ lon $\times 0.5°$ lat (original is 5' lon $\times$ 5' lat)	2000	Earthstat (Monfreda et al., 2008)

Ideally, daily climate data are required to run PEGASUS. However, as daily data are not always available, PEGASUS 1.1 can also be run using monthly climate data that feed in an internal weather generator producing daily inputs (see section 2.3.3). The next subsection describes the approach taken in Chapter 3 that combines monthly climate data generated by the Community Integrated Assessment System (CIAS) and PEGASUS' weather generator. Note at the time of the study performed in Chapter

3, GCMs had yet to be run for the representative concentration pathways (RCPs) and downscaled globally so that CIAS provided the largest ensemble of GCMs inputs available with the RCPs. The approach taken in Chapter 5 in which daily climate data are used is described in Chapter 4.

2.3.1 Monthly climate data

Monthly climate data used in Chapter 3 comprise historical climate data from the CRU TS 2.10 (Mitchell and Jones, 2005) dataset and 72 global climate change patterns derived from eighteen global climate models (GCMs) combined with four RCPs generated using CIAS (Warren et al., 2008): a modular integrated assessment model (IAM) linking an emission scenarios module (ESM), a simple global climate module (SCM), MAGICC 6 (Meinshausen et al., 2011), and a climate scenario downscaling module (DSM), ClimGEN (Osborn, 2009). Designed for modelling climate change policy and effectiveness, CIAS is a unique multi-institutional modular and flexible integrated assessment system offering a single framework to create multiple IAMs by interchanging the coupling of the different modules (Warren et al., 2008). CIAS is supported by a software framework called SoftIAM, which allows various combinations of modules to be connected together into alternative IAMs and provides a graphical interface to let users interact with the system, as well as configure and perform various kinds of simulations to answer different scientific and policy questions. In Chapter 3, CIAS modules are configured to emulate the behaviour of eighteen GCMs used in the Fourth Assessment Report of the IPCC (IPCC AR4) (Solomon et al., 2007) coupled to four RCPs used in the Fifth Assessment Report of the IPCC (IPCC AR5) (Stocker et al., 2013; van Vuuren et al., 2011) (the eighteen GCMs are listed in Table 2.3).

The ESM provides atmospheric concentration data of greenhouse gas (GHG) emissions for various scenarios database such as the IPCC SRES (Nakicenovic et al., 2000) and RCPs, the latter being used in Chapter 3. Alternatively, GHG concentrations can be estimated from emission scenarios generated from an economic module linked to an emission converter as presented in (Warren et al., 2008). GHG concentration data are then input to MAGICC 6.

The MAGICC model (Wigley, 2001) has been developed and updated over two decades and widely used in integrated modelling studies (Rotmans et al., 1994; van Vuuren

TABLE 2.3: Model identification and originating group from the CMIP3 archive.

IPCC ID	Centre and location
CGCM3.1(T47)	Canadian Centre for Climate Modelling and Analysis (Canada)
CSIRO-Mk3.0	CSIRO Atmospheric Research (Australia)
CNRM-CM3	Météo-France, Centre National de Recherches Météorologiques (France)
GFDL-CM2.0	US Dept. of Commerce, NOAA
GFDL-CM2.1	Geophysical Fluid Dynamics Laboratory (United States)
GISS-EH GISS-ER	NASA/Goddard Institute for Space Studies (United States)
FGOALS-g1.0	LASG/Institute of Atmospheric Physics (China)
INM-CM3.0	Institute for Numerical Mathematics (Russia)
IPSL-CM4	Institut Pierre Simon Laplace (France)
MIROC3.2(medres) MIROC3.2(hires)	Center for Climate System Research (The University of Tokyo), National Institute for Environmental Studies, and Frontier Research Center for Global Change (JAMSTEC) (Japan)
MRI-CGCM2.3.2a	Meteorological Research Institute (Japan)
ECHAM5/MPI-OM	Max Planck Institute for Meteorology (Germany)
NCAR-CCSM3.0 NCAR-PCM1	National Center for Atmospheric Research (United States)
UKMO-HadCM3 UKMO-HadGEM1	Hadley Centre for Climate Prediction and Research, Met Office (UK)

et al., 2008). MAGICC is a single piece of software comprising a set of linked internal components to simulate GHGs cycles, radiative forcing, and ice melt. Radiative forcing drives an upwelling diffusion energy balance model to estimate future climate changes. MAGICC 6 (Meinshausen et al., 2011) is an updated version of the original MAGICC, with an improved representation of the carbon cycle. Climate feedback on the carbon cycle is included; the resulting [CO_2] depends on the forcing, the climate sensitivity and the ocean heat uptake efficiency. Sulphate aerosol forcing is scaled directly with the emissions because of the short residence time in the atmosphere. Thus the model allows the user to emulate GCM output, specifically changes in [CO_2], global-mean surface air temperature and sea level between the years 2000 and 2100 resulting from anthropogenic emissions of CO_2, methane, N_2O, chlorofluorocarbons, hydrofluorocarbons, perfluorocarbons, as well as sulfur dioxide. In Chapter 3, MAGICC 6 is tuned to emulate eighteen state-of-the-art GCMs listed in Table 2.3 to create global temperature projections for the four RCPs (van Vuuren et al., 2011).

The DSM generates spatially explicit climate data at various temporal scales from the single global-mean surface air temperature calculated by the SCM. The current DSM is CLIMGEN, which produces monthly, seasonal and annual mean climate data at a spatial resolution of $0.5° \times 0.5°$ grid-cell covering both the terrestrial land surface excluding

Antarctica (Mitchell and Jones, 2005). CLIMGEN follows a pattern-scaling methodology currently based on GCM patterns from the third Coupled Model Intercomparison Project (CMIP3) archive (Meehl et al., 2007): any given change in annual mean temperature as simulated by MAGICC 6 can be linearly rescaled to represent spatial and temporal patterns of change in each climate variable. ClimGEN combines these patterns of change with the observed climatology, currently provided by the CRU TS 2.10 dataset, to produce patterns of mean absolute climate, and then combines them with observed time series of deviations from climatology to produce realisations of climate change over 2001 to 2100 with realistic yearly variability superimposed. CLIMGEN can generate monthly climate data for eight variables including mean, maximum and minimum temperatures, precipitation, vapour pressure, cloud cover and wet-day frequency. In the case of precipitation, change in GCM precipitation patterns is expressed as fractional change from present-day precipitation that is applied to the observed climatology by multiplication. To simulate a future change in both precipitation variability and mean precipitation, ClimGEN includes a gamma shape method where a gamma shape parameter represents the temporal distribution of precipitation (Aksoy, 2000). Change in the gamma shape parameter output by the GCMs is scaled by the required global-mean temperature change (Osborn, 2009). Future changes in the frequency of temperature extremes are not, however, as yet incorporated (Osborn, 2009; Warren et al., 2012).

Figure 2.4 presents the spread among the 72 climate change scenarios used in Chapter 3 in terms of global average temperature increase and total annual precipitation change for medium (2050s) (Figure 2.4(a)) and long (2080s) (Figure 2.4(b)) time horizons relative to the 1910s. Note the CRU TS 2.1 dataset begins in 1901 so that comparison to pre-industrial climate conditions, as typically done by the IPCC, was not possible here. Nonetheless, comparison to the 1910s time horizon gives a valuable indiction of the spread in the climate change scenarios ensemble. We calculated 30-year climatologies for each time-period. Most GCMs agree in a general increase in annual total precipitation globally except GFDL-CM21 that predicts a small decrease. Relative change in global average temperature varies widely among GCMs and RCPs. GCM differences are exacerbated by high temperatures (2.4(b) for the 2080s).
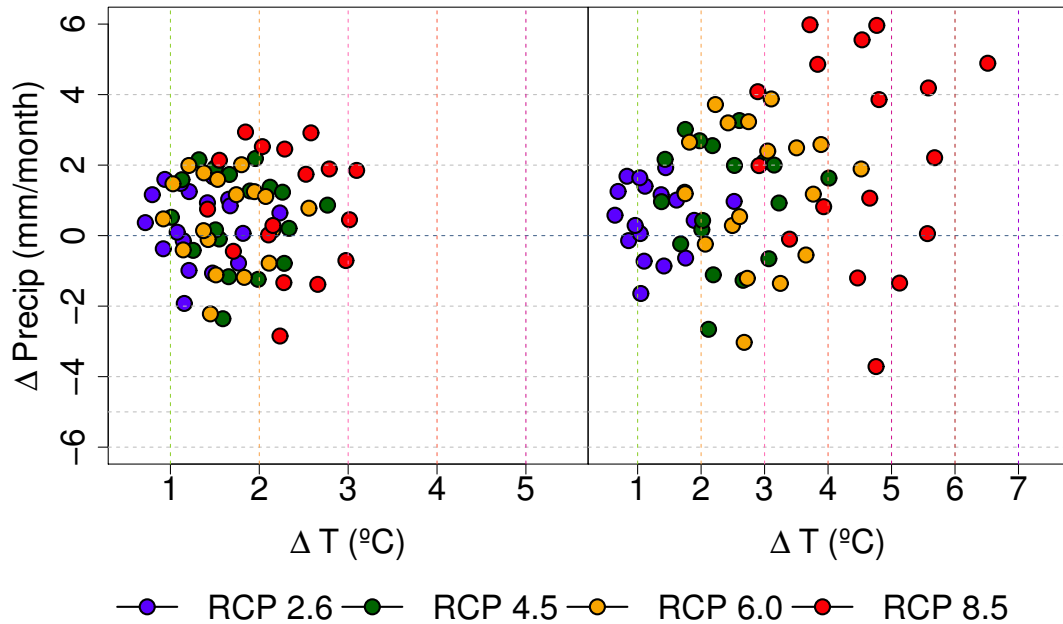
FIGURE 2.4: Scatter-plots showing distribution of relative change between the 2050s and the 1910s (left) and between the 2080s and the 1910s (right) in global mean temperature and precipitation among the 4 RCPs × 18 GCMs. Each circle represents a combination of one RCP–GCM. Data for each RCP are presented in a different colour.

2.3.2 The representative concentration pathways

RCPs were especially designed for the IPCC AR5 by identifying a level of radiative forcing in the year 2100 and a specific emission scenario including GHG emissions from land use and land cover change. Four distinct RCPs were finally selected corresponding to a radiative forcing of 2.6, 4.5, 6.0 and 8.5 W/m^2 respectively. Each of these RCPs follows an independent socio-economic and emission trajectory modelled by independent IAMs:

- The RCP 2.6 was developed by the IMAGE modelling team and is representative for scenarios in the literature leading to very low GHG concentration level. In this scenario, the global radiative forcing level reaches a peak value of 3.1 W/m^2 in the mid-century, before it eventually returns to 2.6 W/m^2 by 2100 thanks to substantial reduction in GHG emissions (van Vuuren et al., 2007).

- The RCP 4.5 was developed by the GCAM modelling team and characterises a scenario for which the global radiative forcing is stabilised before 2100 owing to a range of technologies and strategies for reducing GHG emissions (Wise et al., 2009).

- The RCPs 6.0 was developed by the AIM modelling team and describes a scenario for which the global radiative forcing is stabilised after 2100 (Fujino et al., 2006)

- The RCP 8.5 was developed by the MESSAGE modelling team and represents a scenario of increasing GHG emissions, in which the global radiative forcing rises and does not stabilised by 2100 (Riahi et al., 2007).

As a result, these well-spaced concentration pathways produce discernible and independent climate change consequences and offer the opportunity to explore alternative stabilisation levels and uncertainties in biophysical processes.

2.3.3 PEGASUS' weather generator

Monthly climate data generated within CIAS are interpolated to a daily time-step using PEGASUS' internal weather generator. First, PEGASUS derives fraction of sunshine hours from CIAS cloud cover data following Doorenbos and Pruitt (1984). Then, PEGASUS uses monthly mean climate input of total precipitation, wet day frequency, fraction of sunshine hours and minimum, maximum and mean temperatures to feed into an extended version of the Richardson weather generator (Parlange and Katz, 2000; Richardson and Wright, 1984). Daily precipitation follows a two-states first order Markov chain according to the number of wet days per month and a gamma shape distribution of precipitation centred on monthly average precipitation per wet day (Parlange and Katz, 2000; Richardson, 1981). The method for wet and dry day transition probabilities is described in Geng (1986). Daily temperature and fraction of sunshine hours follow a multivariate model for which mean and standard-deviation of each variable are tied to the wet or dry status of the day (Richardson, 1981). Furthermore, daily mean temperature estimates are tied to daily minimum and maximum temperature estimates (Parlange and Katz, 2000), so that changes in daily mean temperatures reflect changes in minimum and maximum temperature extrema.

2.4 Model calibration and validation

Identical versions of PEGASUS 1.1 described in this chapter are used throughout the research presented in this thesis. PEGASUS was calibrated against the Earthstat crop yield data for the year 2000 (Monfreda et al., 2008). The calibration procedure follows a similar approach used by Deryng et al. (2011) but uses climate data spanning six years, circa 2000 (1996-2002) instead of the 30-year climatology. As in Deryng et al. (2011), only the RUE coefficient under ambient [CO_2] (β_{amb}) is tuned to calibrate, at the grid-cell level, simulated yield to observed yield as stated in section 2.2.6 (Deryng et al., 2011; Willmott et al., 1985).

Although an identical version of PEGASUS is used in Chapters 3 and 5, two distinct climate datasets are used for the six-year calibration period. In Chapter 3, PEGASUS is calibrated using a six-year subset from the CRU-TS 2.10 monthly climate time-series linked to PEGASUS' weather generator. In Chapter 5, PEGASUS is calibrated using a six-year subset from the WATCH daily climate time-series (Weedon et al., 2011), to ensure consistency with the ISI-MIP climate data (see Chapter 4 for more details). The use of different climate inputs, however, led to identical β_{amb} values between the two studies for maize and soybean (0.035 and 0.011 mol C m^{-2}s^{-1}APAR, respectively) and slightly different values in the case of spring wheat (0.029 and 0.027 mol C m^{-2}s^{-1}APAR, when using CRU TS 2.10 versus WATCH climate inputs respectively). β_{amb} values remain close to those of Deryng et al. (2011).

PEGASUS' performance in simulating present-day crop yields is assessed by comparing simulated yields to the same Earthstat crop yield data but aggregated to national levels as in (Deryng et al., 2011). Although identical yield data is used for both calibration and validation purposes (as in Deryng et al., 2011), the calibration modified only the global average β_{amb} values, whereas the validation focused on model's ability to match the spatial variability of observed yields. PEGASUS' performance is systematically better when driven by the WATCH daily climate data (higher r^2 and smaller RMSE) than driven the CRU monthly climate data disaggregated with the weather generator (2.5 a-c-e).

A detailed comparison of simulated crop yields between PEGASUS and other GGCMs is described in Deryng et al. (2011), where I demonstrated equivalent aptitude in simulating
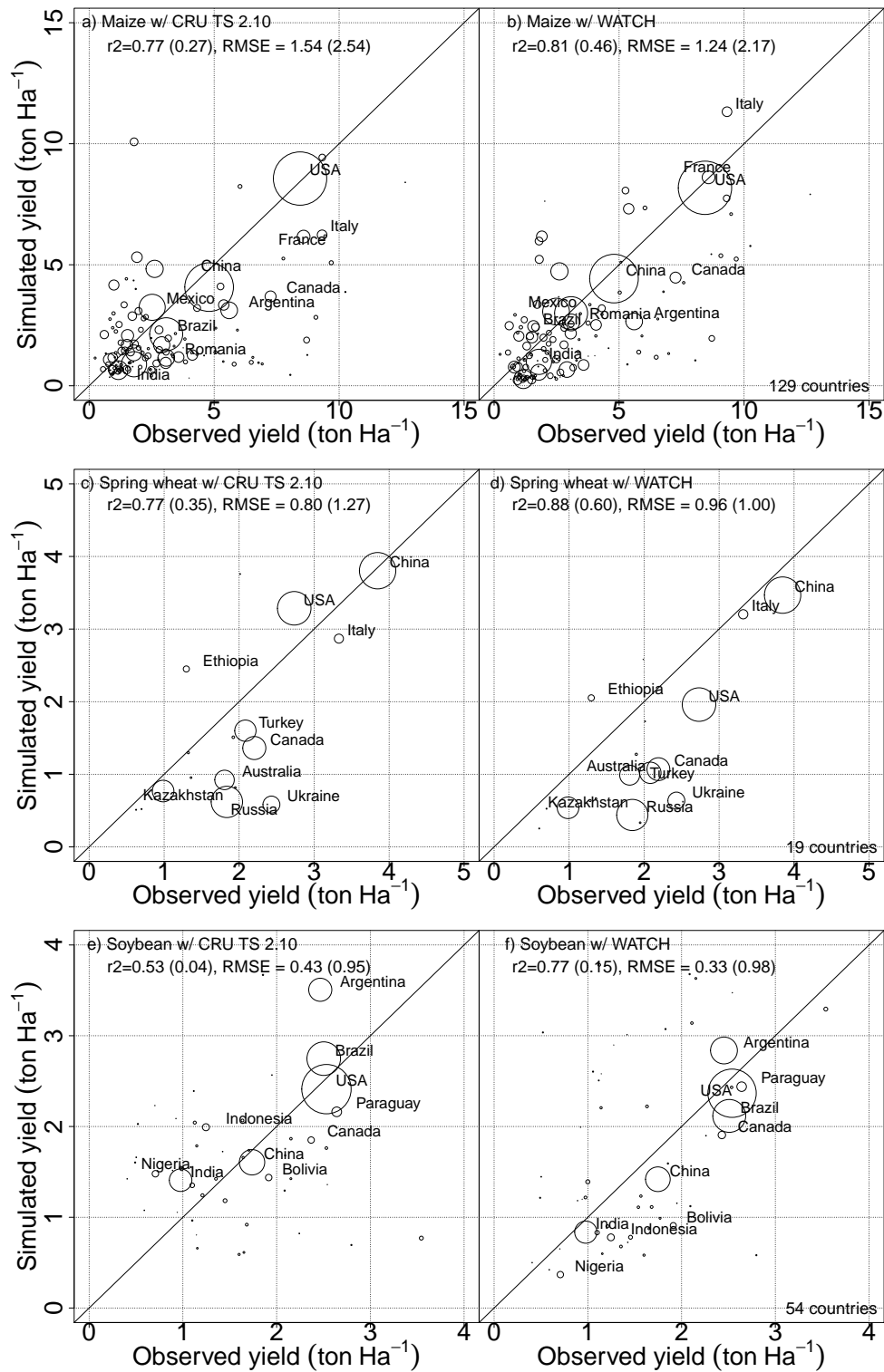
FIGURE 2.5: Comparison of simulated crop yields and corresponding observations (Monfreda et al., 2008) for maize (a-b), spring wheat (c-d) and soybean (e-f) aggregated by country using CRU TS 2.10 (a-c-e) & WATCH (b-d-f) climate data. Areas of circles represent crop harvested area. Weighted r^2 and RMSE are based on crop harvested area for each country. Numbers in bracket correspond to unweighted r^2 and RMSE.

present-day crop yields between PEGASUS, LPJmL and DayCent global crop models. In fact, PEGASUS' strengths in comparison to these other models consist in a more extensive representation of farming management practices and the inclusion of the effects of extreme heat stress at anthesis, particularly relevant for climate change impacts and adaptation analyses. Note that a rigorous GGCM intercomparison effort to evaluate ability of models to simulate historical yields is currently ongoing and is described in Chapter 4 of this thesis.

2.5 Concluding remarks

This chapter presented a detailed description of the global crop model PEGASUS along with modelling methodology behind the analysis presented in the next chapter (3) focusing on the effect of extreme temperature stress at anthesis. The version of PEGASUS as described here is also used in subsequent chapters of this thesis, chiefly Chapter 5, presenting results from the first GGCM intercomparison study, and Chapter 7, presenting PEGASUS estimates of potential yield resulting from no nutrient stress.

Chapter 3

Global crop yield response to extreme heat stress under multiple climate change futures

Preface

This chapter consists of a paper published in *Environmental Research Letters*, in March 2014, with the same title: Deryng et al. (2014). The manuscript is largely unchanged from the published paper apart from minor superficial changes to the figures and minor changes to the text as well as inclusion of figures from the paper's supplemental information. The text in the appendix of the paper has also been moved to Chapter 2. I designed and performed research, analysed data and wrote the paper. Conway, Ramankutty and Warren provided scientific input; Price and Warren assisted with the provision of revised climate data from Community Integrated Assessment System and all co-authors helped revise the text for publication. The comments of two anonymous reviewers also helped to improve the manuscript.

Abstract

Extreme heat stress during the crop reproductive period can be critical for crop productivity. Projected changes in the frequency and severity of extreme climatic events

are expected to negatively impact crop yields and global food production. This study applies the global crop model PEGASUS to quantify, for the first time at the global scale, impacts of extreme heat stress on maize, spring wheat and soybean yields resulting from 72 climate change scenarios for the 21st century. Our results project maize to face progressively worse impacts under a range of representative concentration pathways (RCPs) but spring wheat and soybean to improve globally through to the 2080s due to carbon dioxide (CO_2) fertilisation effects, even though parts of the tropic and sub-tropic regions could face substantial yield declines. We find extreme heat stress at anthesis (HSA) by the 2080s (relative to the 1980s) under RCP 8.5, taking into account CO_2 fertilisation effects, could double global losses of maize yield ($\Delta Y = -12.8 \pm 6.7\%$ versus $-7.0 \pm 5.3\%$ without HSA), reduce projected gains in spring wheat yield by half ($\Delta Y = 34.3 \pm 13.5\%$ versus $72.0 \pm 10.9\%$ without HSA) and in soybean yield by a quarter ($\Delta Y = 15.3 \pm 26.5\%$ versus $20.4 \pm 22.1\%$ without HSA). The range reflects uncertainty due to differences between climate model scenarios; soybean exhibits both positive and negative impacts, maize is generally negative and spring wheat generally positive. Furthermore, when assuming CO_2 fertilisation effects to be negligible, we observe drastic climate mitigation policy as in RCP 2.6 could avoid more than 80% of the global average yield losses otherwise expected by the 2080s under RCP 8.5. We show large disparities in climate impacts across regions and find extreme heat stress adversely affects major producing regions and lower income countries.

3.1   Introduction

Anthropogenic climate change challenges current and future global food production due to the direct effects of changes in mean climatic conditions, increasing risks from extreme weather events, increased atmospheric carbon dioxide (CO_2) concentration and increasing pest damage (Gornall et al., 2010; Hillel and Rosenzweig, 2011). The IPCC AR4 reports moderate increase in global crop yield for global mean temperature increase up to 3℃ – mostly due to beneficial CO_2 fertilisation effects on photosynthesis rate and transpiration demand – but general decrease above this threshold (Easterling et al., 2007). The report further concludes projected changes in the frequency and severity of extreme climatic events will have more serious consequences for food production and food insecurity, than changes in mean climate alone (Easterling et al., 2007).

Yet global climate impact assessments to date fail to address adequately effects of changes in climate extremes on crops (Deryng et al., 2011; Gornall et al., 2010; Hillel and Rosenzweig, 2011; Müller et al., 2010; Nelson et al., 2010; Parry et al., 2004), especially the negative impact of heat waves during the reproductive stage, identified as a major threat to yield in many parts of the world. Previous analyses modelling the effect of extreme heat stress on crops have been limited to single regions (Hawkins et al., 2013; Lobell et al., 2013; Moriondo et al., 2010; Semenov and Shewry, 2011; Wahid et al., 2007) or do not quantify impacts on yield (Gourdji et al., 2013; Teixeira et al., 2011). Moreover, most previous studies present only a partial estimate of uncertainty related to the range of climate change projections by considering at most four GCMs using the older SRES emissions scenarios (Easterling et al., 2007; Müller et al., 2010; Nelson et al., 2010; Parry et al., 2004). Finally, anticipated benefits from CO_2 fertilisation effects remain a large source of uncertainty (Kirkham, 2012).

This chapter addresses a major gap in crop simulations by studying the effect of HSA on crop yield globally. Effects of HSA are expected to impact crop yields negatively and occur unevenly across regions. It is not clear however, whether negative effects of HSA could outweigh potential gains in yields of C_3 crops due to CO_2 fertilisation. Furthermore, previous impact assessments found yield of C_4 crops to be more negatively impacted than C_3 crops. Since different crops have different heat tolerance thresholds, yields of C_3 crops typically grown in colder climate, such as spring wheat, could be more negatively impacted in future than yields of C_4 crops, even with carbon enhancement, because of their lower tolerance threshold to extreme temperatures. Another interesting hypothesis explored in this chapter is whether regional divides in climate change impacts between high and low latitudes are preserved when including HSA effects. Finally, this chapter aim at validating findings that the range of impacts due to climate model differences, and thus uncertainty, increases with radiative forcing.

Here we use a new version of the global crop yield model PEGASUS (Deryng et al., 2011) that takes into consideration crop sensitivity to HSA (Challinor et al., 2005; Moriondo et al., 2010) and CO_2 fertilisation effects for maize, spring wheat and soybean. We use an ensemble of 72 climate change projections spanning the 21st century together with the CRU TS 2.10 observed climate dataset (Mitchell and Jones, 2005) for the years 1971–2000 to drive PEGASUS and produce a robust estimate of uncertainties related to future climate change. Our approach takes into account impacts of change in mean

climate conditions, extreme temperatures and elevated atmospheric CO_2 concentration. We explore PEGASUS' sensitivity to HSA and CO_2 fertilisation effects and show impacts on global crop yield and production on present-day harvested areas. We present results from different RCPs (van Vuuren et al., 2011) to evaluate potential benefits of mitigation policy. Although we make use of one single global gridded crop model and do not evaluate across-model uncertainty, PEGASUS enables a first assessment of the effect of HSA on global crop productivity, currently missing in other comparable state-of-the-art global gridded crop models (Rosenzweig et al., 2013). Key sources of uncertainty resulting from the use of a single crop model (i.e. consisting primarily of uncertainty in the magnitude of CO_2 fertilisation effects, temperature thresholds for HSA, and model representation of water, temperature and nitrogen stresses), the use of static harvested areas, and assumptions about farmers' adaptation responses (i.e. decision of planting dates and choice of crop cultivars) are addressed in the discussion section.

3.2 Methods

3.2.1 Crop modelling

PEGASUS 1.1 is an improved version of the global crop yield model PEGASUS (Deryng et al., 2011) that simulates crop response to elevated CO_2 and better represents effects of climate variability and extremes. A specific heat stress factor is calculated as a function of intensity and duration of extreme temperature events during crop anthesis according to crop specific temperature thresholds (Challinor et al., 2005; Moriondo et al., 2010; Teixeira et al., 2011) (see Chapter 2, section 2.2.5). A literature review indicates spring wheat starts to face HSA at a lower critical temperature (T_{cr}) threshold than for the other crops and maize can tolerate a higher limit temperature (T_{lim}) (Table 3.1). Soybean experiences a shorter range of elevated temperatures and a steeper decline in yield between the critical threshold and limit temperatures (Table 3.1).

Farm management practices represented in PEGASUS include irrigation and fertiliser application, decision of planting dates and choice of crop cultivars. Our simulations allow for adaptation in decision of planting dates and choice of crop cultivars, according to temperature and precipitation conditions as in Deryng et al. (2011). In temperature-limited regions, PEGASUS typically allows for earlier sowing dates and

longer growing season varieties due to warming temperatures. In moisture-limited regions, PEGASUS tends to coincide sowing dates with the start of the rainy season (the crop calendar methodology is described in detail in (Deryng et al., 2011)). As a result of adaptation of planting dates and cultivars, timing of crop anthesis can vary with climate change and thus influences net HSA effects on crops: temperature-limited regions show unchanged or slightly later flowering dates resulting mainly from longer growing periods, which is more influential than the effect of earlier planting; moisture-limited regions tend to show earlier flowering dates resulting from earlier planting-dates (Figure 2.3 in Chapter 2).

Total harvested area, along with fraction of total irrigated and rainfed areas, are kept constant to present-day (circa the year 2000) and irrigation water is applied to prevent irrigated crops from experiencing water stress, assuming unlimited availability of irrigation water as in Deryng et al. (2011). We use the Earthstat dataset (www.earthstat.org) for global crop harvested area (Monfreda et al., 2008) in combination with the MIRCA2000 dataset (Portmann et al., 2009) for crop specific irrigated areas to define present-day harvested areas and fraction of irrigated and rainfed areas. Similarly, we use national annual rates of nitrogen–phosphorus–potassium (NPK) fertiliser application from the International Fertiliser Industry Association (IFA) (IFA, 2002) corresponding to the mid–1990s and maintain application rates constant throughout the simulations.

PEGASUS is calibrated and validated for the year 2000 using the CRU TS 2.10 climate data (Mitchell and Jones, 2005) for the period 1997–2002 and the Earthstat dataset for global crop yield and harvested area (Monfreda et al., 2008). Average simulated crop yield for the period 1997–2002 is used to approximate yield for the year 2000.

3.2.2   Climate modelling

PEGASUS is driven by climate data from the CRU TS 2.10 dataset for the period 1971–2000 and from the CIAS (Warren et al., 2008) for the period 2001–2100 (see Chapter 2, section 2.3.1). CIAS uses GHG emissions time-series corresponding to the four RCPs emission scenarios (van Vuuren et al., 2011) to drive a global climate change model MAGICC 6 (Meinshausen et al., 2011) capable of reproducing global mean warming from complex GCMs. The resultant projections of global temperature change

drive a pattern-scaling module ClimGen (Osborn, 2009) capable of reproducing climate change patterns diagnosed from eighteen alternative GCM simulations combined with a baseline observed climate using the CRU TS 2.10 dataset. We produce 72 spatially explicit time-series projections of monthly mean, minimum and maximum temperatures, total monthly precipitation, wet day frequency and percentage of cloud cover downscaled to $0.5° \times 0.5°$ resolution (~ 50 km^2 at the Equator) and consistent with the RCPs (Meehl et al., 2007). Monthly mean climate data are interpolated to daily using a stochastic weather generator within PEGASUS (see Chapter 2, section 2.3.3).

Changes in temporal distribution of precipitation are scaled according to changes in global mean temperature using a gamma shape parameter such that ClimGen outputs of total monthly precipitation and wet day frequency account for changes in present and future precipitation variability (Osborn, 2009). Changes in monthly mean, minimum and maximum temperatures are estimated according to changes in global mean temperature so that the weather generator within PEGASUS generates warmer temperature extrema as global mean temperature increases. However, potential changes in the frequency of extreme temperature events are not yet simulated within ClimGen (see Chapter 2). As those might also change in future (Stocker et al., 2013), results presented here might be more conservative than with fully realised changes in temperature variability (see section 3.8 for further discussion).

3.2.3 Global average yield and production estimates

Global average actual yield is calculated by combining yields simulated from full irrigation and no irrigation runs weighted by irrigated and rainfed areas. We consider three time periods averaged over 30 years: baseline corresponding to the 1980s (1971–2000), medium time horizon corresponding to the 2050s (2036–2065) and long time horizon corresponding to the 2080s (2071–2100). Total production is estimated by multiplying actual yield by corresponding harvested area assuming harvested area remains constant as present-day using the Earthstat dataset (Monfreda et al., 2008).

We use the World Bank definition to classify countries by income level: Economies are divided according to 2012 gross national income per capita, calculated using the World Bank Atlas method (World Bank, 2013 and see Appendix D). The groups are: low income, \$1,035 or less; lower middle income, \$1,036 - \$4,085; upper middle income, \$4,086

- \$12,615; and high income,\$12,616 or more. We calculated country level production for the year 2000 (average over the six-year period: 1997–2002) using the CRU TS 2.10 climate dataset and selected the top-five producing countries according to PEGASUS yield estimates multiplied by crop harvested area. The top-five countries for maize and soybean production agree with the FAO rankings (FAOSTAT, 2013) for the year 2000. In the case of spring wheat, we use spring wheat harvested area generated by combining wheat harvested area (Monfreda et al., 2008) and global spring wheat planting and harvesting calendar (Sacks et al., 2010), assuming that farmers do not grow both winter and spring varieties in the same location.

3.2.4 Representative concentration pathways and climate change futures

The four RCPs encompass a mitigation pathway in which radiative forcing is reduced to 2.6 W m^{-2} (RCP 2.6) by 2100, a *business as usual* pathway in which radiative forcing increases to 8.5 W m^{-2} (RCP 8.5) by 2100, and two stabilisation pathways in which forcing levels out at 4.5 W m^{-2} (RCP 4.5) and 6.0 W/m^{-2} (RCP 6.0) by 2100 respectively. The IPCC AR5 reports RCP 2.6 engenders a world with global mean surface temperature stabilised at 1℃ by the 2050s with respect to 1986–2005 (Stocker et al., 2013) resulting in moderate heat stress and low CO_2 fertilisation effects. Similarly, RCP 8.5 leads to a global mean warming exceeding 1.4℃ and up to 4.8℃ by the 2080s (Stocker et al., 2013), along with unprecedented extreme heat stress and high potential CO_2 fertilisation effects.

Here we evaluate and explore uncertainties in crop sensitivity to direct physiological effects of increased CO_2 and HSA for the two most contrasting RCPs (i.e. RCP 2.6 and 8.5). Consequently, results presented consist of 72 simulations to account for combined impacts of mean climate change, HSA, and direct CO_2 fertilisation effects (CO_2) denoted as CC, 36 simulations to account for impacts of mean climate change and direct CO_2 fertilisation only ($CC_{\text{w/o HSA}}$), and 36 simulations to account for impacts of mean climate change and extreme temperatures only ($CC_{\text{w/o CO}_2}$), for each of the three crops.

3.3 Global average trends

We find global average yield decreases for all maize simulations (ΔY ranges from $-2.9 \pm 2.6\%$ under RCP 2.6 to $-12.8 \pm 6.7\%$ under RCP 8.5 by the 2080s for CC) whereas corresponding yields of spring wheat and soybean, when CO_2 fertilisation effects are included, increase throughout the 21st century owing to large positive responses in C_3 crops (ΔY ranges from $9.9 \pm 3.6\%$ under RCP 2.6 to $34.3 \pm 13.5\%$ under RCP 8.5 for spring wheat and from $7.1 \pm 7.0\%$ under RCP 2.6 to $15.3 \pm 26.5\%$ under RCP 8.5 for soybean by the 2080s for CC) (Figure 3.1 and Table 3.1). HSA strongly influences maize and spring wheat yields, contributing to nearly half of expected losses for maize by the 2080s under RCP 8.5 (ΔY $= -12.8 \pm 6.7\%$ for CC compared to ΔY $= -7.0 \pm 5.3\%$ for $CC_{\text{w/o HSA}}$) and substantial reductions in expected yield gains for spring wheat (ΔY $= 34.3 \pm 13.5\%$ for CC compared to ΔY $= 72.0 \pm 10.9\%$ for $CC_{\text{w/o HSA}}$). In contrast, HSA moderately affects soybean global yield trajectories due to its higher critical temperature threshold to HSA (see section 3.2 and see Chapter 2, section 2.2.5) (ΔY $= 15.3 \pm 26.5\%$ for CC compared to ΔY $= 20.4 \pm 22.1\%$ for $CC_{\text{w/o HSA}}$). Soybean exhibits a larger range of results spanning both positive and negative outcomes globally whereas maize results are mostly negative and wheat results mostly positive with CO_2 fertilisation effects. Differences between crop responses and the larger range of results for soybean reflect differences in specific temperature tolerance to HSA (e.g. soybean has higher critical temperature tolerance but lower limit temperature tolerance in comparison to maize – see Chapter 2, section 2.2.5) as well as differences in GCM precipitation and temperature patterns and in spatial patterns of production specific to each crop. Figure 3.3 illustrates level of agreement in GCM simulations for each crop. In the case of soybean, there are as many areas showing a net decrease in yield as there are showing a net increase. However, in some important soybean production areas such as the United States and Brazil, there is no agreement on whether the sign of the projected yield changes is positive or negative (see also section 3.4).

When CO_2 fertilisation effects are excluded from simulations (dashed lines in Figure 3.1), spring wheat and soybean yields follow maize's negative trend, soybean being the most affected crop: ΔY $= -26 \pm 17.3\%$ for soybean, ΔY $= -22.0 \pm 5.7\%$ for maize, and ΔY $= -24.1 \pm 7.1\%$ for spring wheat respectively for RCP 8.5 by the 2080s (see table
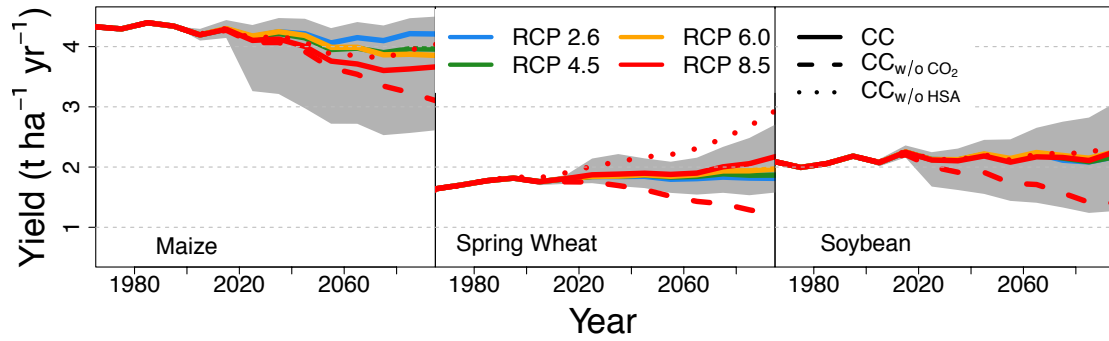
FIGURE 3.1: Global average yield trends simulated by PEGASUS under all 4 RCPs × 18 GCMs ensemble for maize, spring wheat and soybean. Thick lines represent median value across each set of simulations. Full lines are for simulations including both CO_2 fertilisation effect and HSA (CC). Dotted lines are for simulations not taking into account HSA ($CC_{\text{w/o HSA}}$) and dashed lines are for simulations with no CO_2 fertilisation effects ($CC_{\text{w/o CO}_2}$). Grey areas represent the range of global average yield estimates in the case of CC simulations.

TABLE 3.1: Median of relative change in global crop yield ΔY (%) by the 2050s and the 2080s relative to the 1980s for maize, spring wheat, and soybean derived from 30–year average yield calculated for each period. The range represents the median absolute deviation (MAD) from median.

Crop sensitivity	RCP	Maize 2050	Maize 2080	Spring wheat 2050	Spring wheat 2080	Soybean 2050	Soybean 2080
CC	RCP 2.6	-3.1 ± 2.4	-2.9 ± 2.6	9.8 ± 3.0	9.9 ± 3.6	9.5 ± 7.3	7.1 ± 7.0
	RCP 4.5	-4.9 ± 3.3	-6.8 ± 4.2	13.0 ± 4.0	16.7 ± 5.3	10.8 ± 8.9	9.4 ± 12.6
	RCP6.0	-4.2 ± 3.1	-8.3 ± 5.2	13.3 ± 3.7	23.0 ± 6.8	11.4 ± 8.4	13.0 ± 16.1
	RCP8.5	-7.4 ± 3.2	-12.8 ± 6.7	16.9 ± 6.3	34.3 ± 13.5	11.1 ± 12.5	15.3 ± 26.5
$CC_{\text{w/o HSA}}$	RCP 2.6	-2.2 ± 2.1	-2.2 ± 2.1	16.6 ± 3.1	15.9 ± 3.4	10.2 ± 7.1	7.7 ± 6.8
	RCP 8.5	-4.7 ± 3.3	-7.0 ± 5.3	31.9 ± 4.9	72.0 ± 10.9	12.4 ± 11.6	20.4 ± 22.1
$CC_{\text{w/o CO}_2}$	RCP 2.6	-4.7 ± 2.4	-4.4 ± 2.5	-4.5 ± 3.3	-2.9 ± 3.5	1.9 ± 6.8	0.9 ± 6.6
	RCP 8.5	-10.5 ± 3.2	-22.0 ± 5.7	-10.1 ± 5.0	-24.1 ± 7.1	-6.9 ± 9.6	-26.0 ± 17.3

3.1). Soybean also shows the widest range of simulated yields when including HSA with and without CO_2 effects.

Maize is by far the most negatively affected crop and our results suggest a climate change future following RCP 2.6 could avoid fairly significant losses otherwise expected with higher RCPs, due to their larger heat and water stress conditions – since CO_2 fertilisation effects are minimal for maize, a C_4 crop. On the contrary, spring wheat and soybean, both C_3 crops, could benefit greatly from higher CO_2 concentration in the atmosphere arising from RCP 8.5 or RCP 6.0 as, in these cases, beneficial CO_2 fertilisation effects outweigh negative effects of mean climate change and extremes. However, crop response to elevated CO_2 remains the largest source of uncertainty as little is known about their actual response in the field throughout the world, especially under tropical climatic conditions and varied soil nutrient availability (all experiments

to date have been conducted either in chambers or in fields located in the United States and in Europe, i.e. under temperate climatic conditions – see section 3.7).

Finally, maize, spring wheat and soybean have different tolerance thresholds to extreme temperatures (see Chapter 2, section 2.2.5), leading to substantial differences in yield response. Spring wheat is the most affected by extreme temperatures and soybean is the least affected. By the 2080s for RCP 8.5, HSA accounts for 45% of total negative impacts on maize, offsets 25% of positive impacts on soybean and 52% of positive impacts on spring wheat when averaged at the global scale (Table 3.1).

3.4 Spatial patterns

We confirm previous findings of regional disparities in crop yield impacts, with yield increases in high latitudes and large yield reductions in mid and low latitudes (Figure 3.2). Maize, with the largest cultivated area, shows a uniform decrease in yield over mid and low latitudes by the 2080s (Figure 3.2(a)). In contrast, spring wheat and soybean present disparate results owing to contradictory effects resulting from beneficial CO_2 fertilisation and detrimental extreme heat stress, the latter playing a critical role in some regions (Figure 3.2(d-g) respectively). The number of simulations agreeing in the sign of change in yield is also higher for maize than for the other crops (see Figure 3.3, which presents corresponding maps of ensemble simulations and their agreement).

Comparison between maps from top (CC) and middle ($CC_{\text{w/o HSA}}$) rows in Figure 3.2, indicates crop harvested areas at risk of HSA. In the case of maize (Figure 3.2(a-b)), greater HSA sensitivity occurs in the American corn-belt, the Middle East, western and southern Asia, and north-east China. Within the top-five producing countries (Figure 3.4(b)), Brazil, Mexico and Argentina experience large decreases in national production, exacerbated by HSA (blue and yellow bars). The United States also faces a notable decrease in all simulations. China's small gain owing to CO_2 fertilisation effects is cancelled out by HSA. These losses among the top-five producing countries (i.e. accounting for 80% of global maize production) could play a major role in future world supply of maize, with consequences for stability of international crop markets and higher risks of future food insecurity as already experienced during the 2008 global food crisis (Abbott et al., 2008; Piesse and Thirtle, 2009).
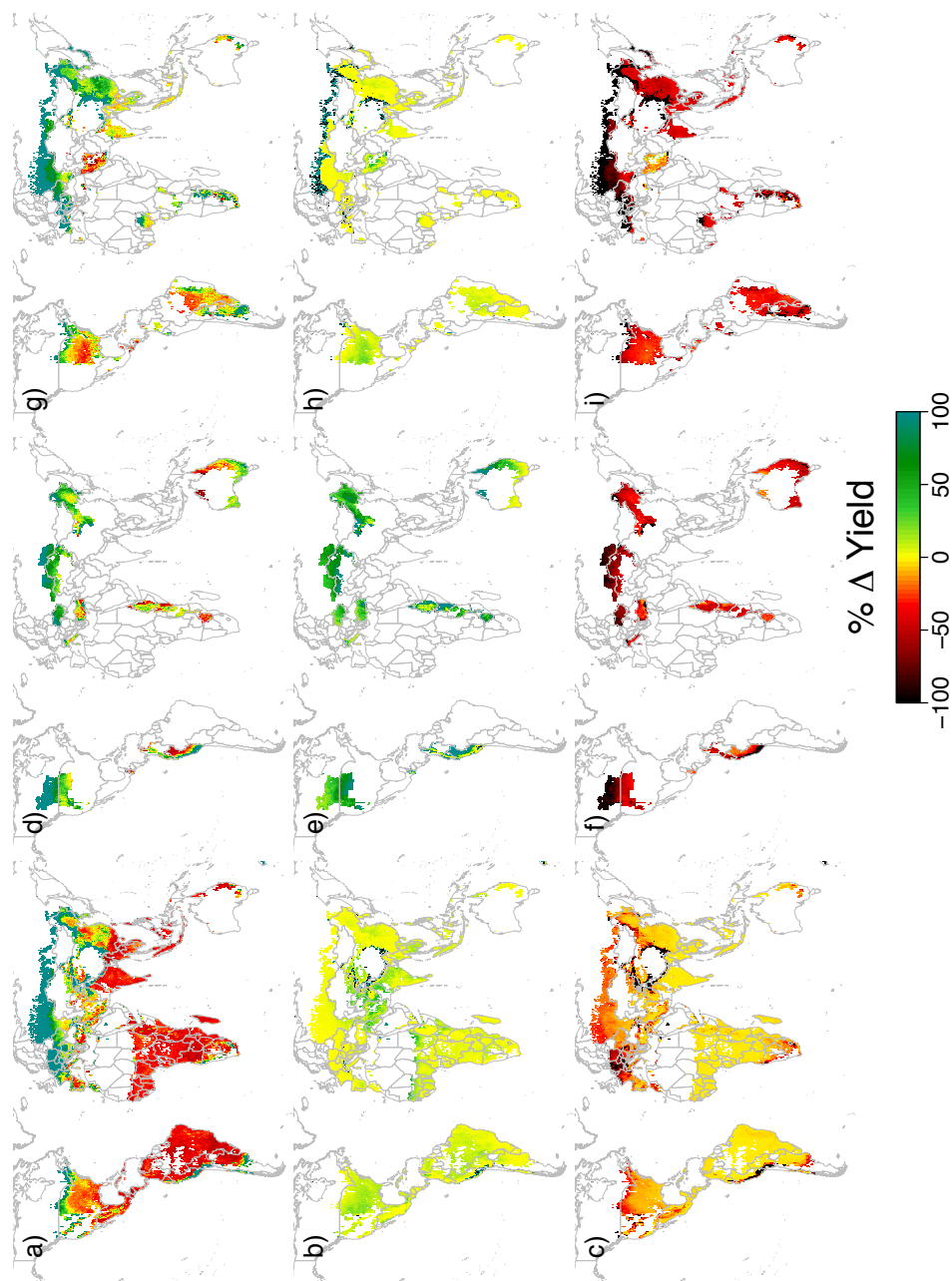
FIGURE 3.2: Maps of median ΔY (%) across the 18 GCMs ensemble for RCP 8.5 in the 2080s relative to the 1980s for maize (a), spring wheat (d) and soybean (g). Maps (b-e-h) show corresponding ΔY differences (%) between $CC_{\text{w/o HSA}}$ and CC simulations (green areas show important yield gains without HSA). Similarly, maps (c-f-i) show corresponding ΔY differences between $CC_{\text{w/o CO}_2}$ and CC simulations (red to black areas show important yield losses without CO_2 fertilisation).
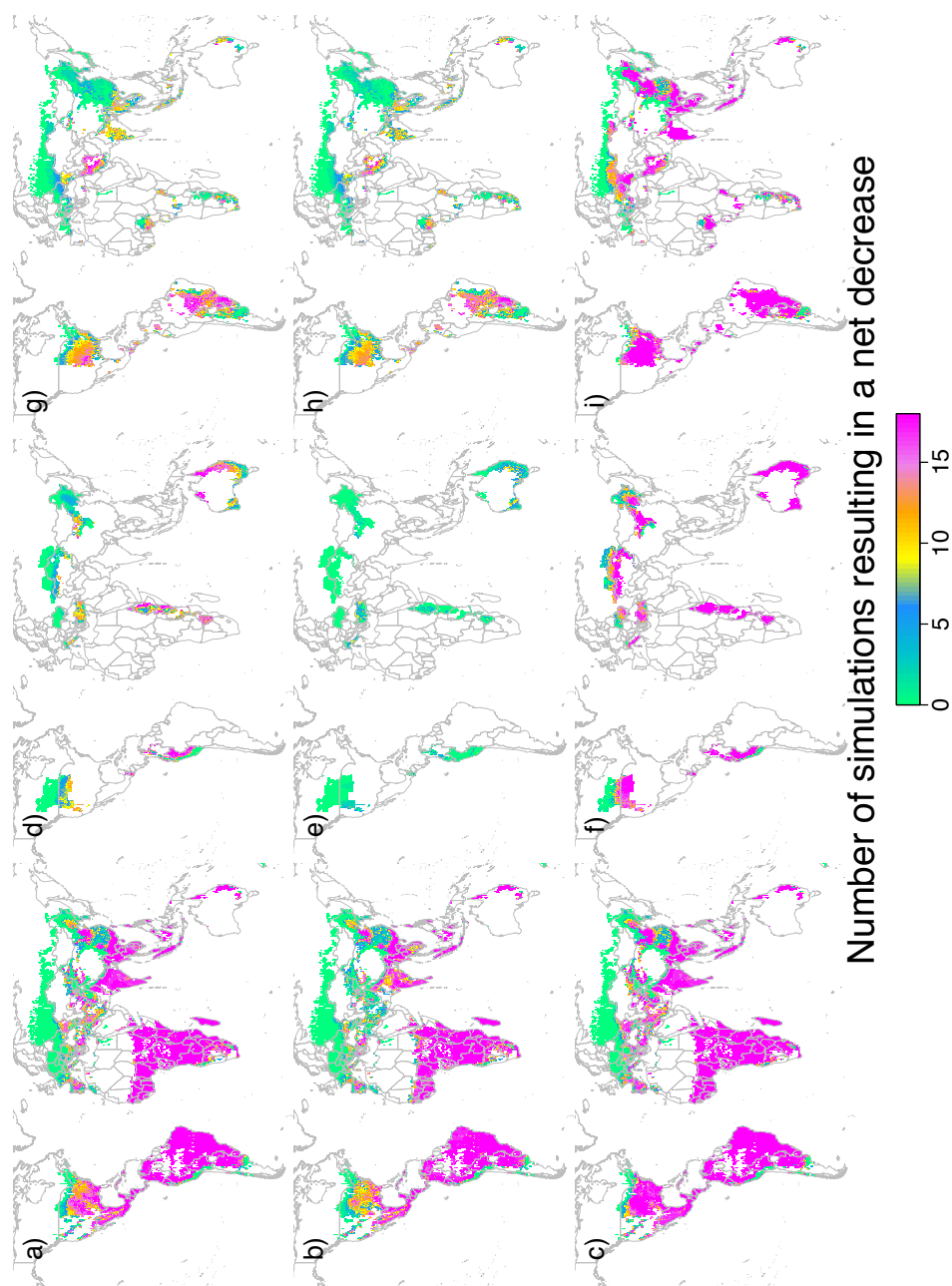
FIGURE 3.3: Maps of agreement among the 18 GCMs driven simulations in the sign of change in yield according to Figure 3.2. When the value is 0 (green), all the simulations agree that yield change is positive. Other colours indicate number of simulation that agree with a net decrease in yield by 2080s. Strongest agreement corresponds to either a value of 0, i.e. a net increase in yield, or a value of 18, i.e. a net decrease in yield by the 2080s relative to the 1980s. Top row is for CC, middle row is for $CC_{\text{w/o HSA}}$ and bottom row is for $CC_{\text{w/o CO}_2}$

In the case of spring wheat (Figure 3.2(d-e)), all current cultivated areas experience heat stress damage: the most severely impacted regions are again the mid and low latitudes, including the northern part of the United States, Near East and eastern part of Australia. In fact, all top-five producing countries exhibit drastic reductions in anticipated production increases due to HSA (Figure 3.4(b)). Note country ranking is estimated according to PEGASUS spring wheat harvested area (Sacks et al., 2010), which does not include winter wheat and hence differs from country rankings that include both winter and spring wheat (see section 3.2).

Finally, in the case of soybean (Figure 3.2(g-h)), the United States, Brazil and India (accounting for more than 60% of global soybean production) are the most affected among the top-five producing countries (Figure 3.4(b)). In contrast, Argentina, the third largest soybean producing country, shows a large increase in its production, which could increase its ranking to second in terms of world production, before Brazil. China also displays large gains in production but only when CO_2 fertilisation effects are included and little change under $CC_{\text{w/o } CO_2}$. Finally, the main region of production, the central part of the United States, faces the most critical HSA effects.

When CO_2 fertilisation effects are not taken into account (Figure 3.2(c-f-i)), yields of all three crops decrease uniformly in mid and low latitudes whereas changes in yields in high latitudes remain positive. In addition, we find a net decrease in yields for the top-five producing countries of each crop, including even Canada, a high latitude country, in the case of spring wheat (red bars in Figure 3.4(b)).

3.5   Country income levels

Impacts by the 2080s follow a regular gradient among income levels of nations (as defined by the World Bank (2013) – see section 3.2) for maize and partly for spring wheat, whereas impacts are mixed in the case of soybean (Figure 3.5(b)). For maize, we find high income (HI) economies face the least damage while low income (LI) ones suffer the most. As seen in the global average trends (Figure 3.1), maize yields decrease under nearly all simulations.

For spring wheat, yields increase from HI to medium low income (MLI) countries when CO_2 fertilisation effects are included. LI countries are less positively affected. Under
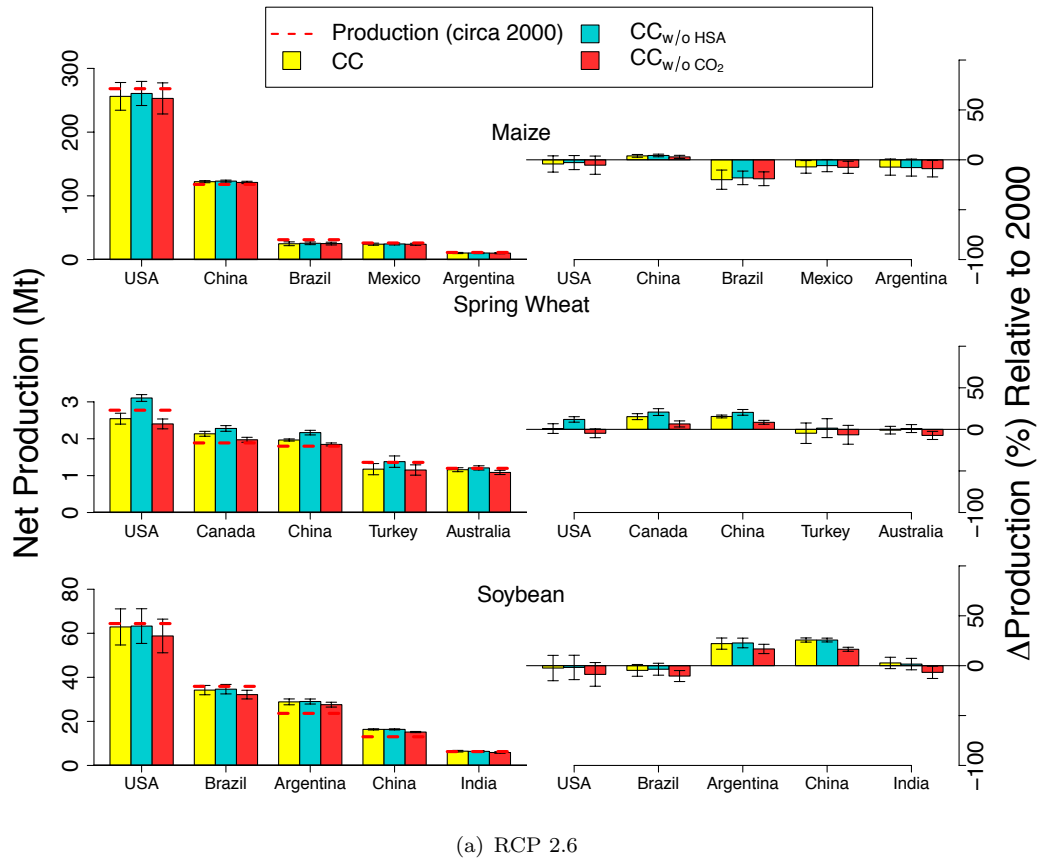
(a) RCP 2.6
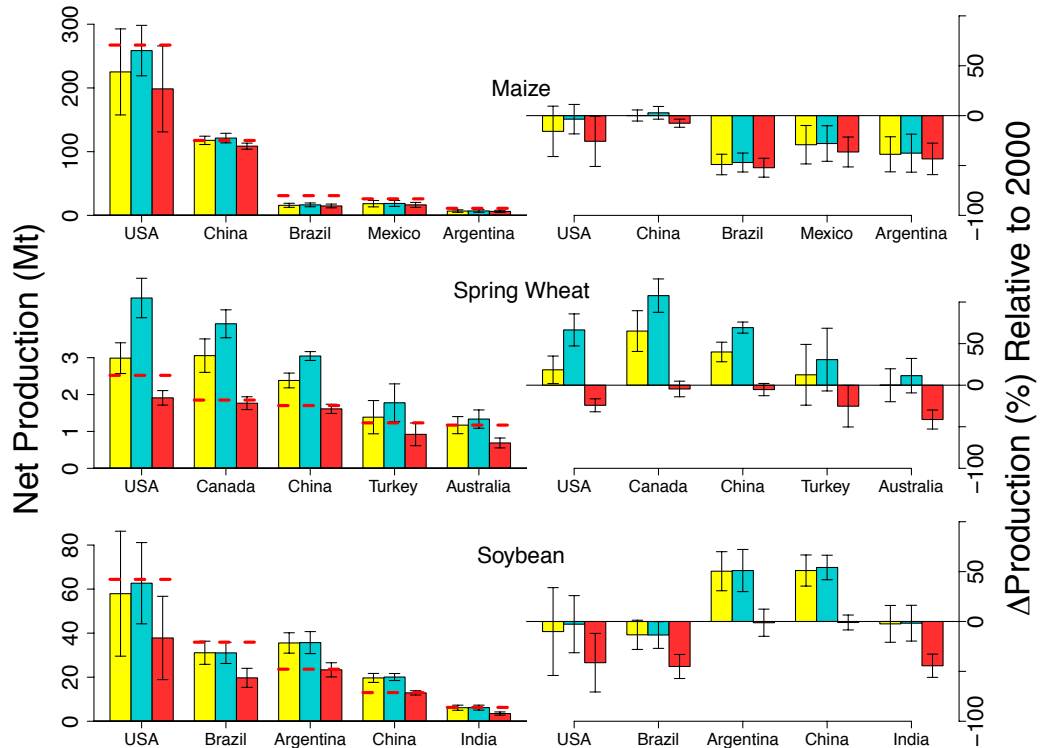
(b) RCP 8.5

FIGURE 3.4: Bar-plots showing net production (left side) and relative change in production (right side) for RCP 2.6 (a) and RCP 8.5 (b) by the 2080s among top-5 producing countries for maize, spring wheat and soybean. The top of the bar stands for median value and whiskers show range for each data. Dashed red lines on the left plots show current level of production, circa the year 2000. Production is estimated using present-day harvested area.

$CC_{\text{w/o CO}_2}$, yields decrease the most for LI and HI groups. Spring wheat displays the strongest response to CO_2 fertilisation effects and greater HSA compared to the other crops (Figure 3.5(b)).

In the case of soybean, medium high income (MHI) countries experience large increases in yield when including CO_2 effects and small decreases under $CC_{\text{w/o CO}_2}$. LI economies also experience a small increase in yield when including CO_2 effects and a decrease without it. HI and MLI economies are the most impacted regions experiencing a large decrease in yield under $CC_{\text{w/o CO}_2}$, which is cancelled out with positive CO_2 fertilisation effects. Spread in the results is similar within all groups, whereas HI economies exhibit larger uncertainties in impacts, which is also the case for maize.

Apart from maize, which shows greater impacts with decreasing income level, we find relative differences in results due to HSA or CO_2 fertilisation effects do not show systematic patterns by income levels and repeat global trends illustrated in Figures 3.1 & 3.5(a).

3.6 Representative concentration pathways trajectories

PEGASUS is more responsive to CO_2 effects and HSA than different pathways of radiative forcing. Yet CO_2 effects on C_3 and C_4 crops vary greatly, resulting in quite different outcomes depending on crop–RCP combination. When all factors are taken into account, global average maize yield by the 2080s displays much greater reduction under RCP 8.5 ($\Delta Y = -12.8 \pm 6.7\%$) than under RCP 2.6 ($\Delta Y = -2.9 \pm 2.6\%$), and moderate losses under RCP 4.5 ($\Delta Y = -6.8 \pm 4.2\%$) and 6.0 ($\Delta Y = -8.3 \pm 5.2\%$) (Figure 3.1). In contrast, yields of spring wheat and soybean increase the most under RCP 8.5 (up to $34.3 \pm 13.5\%$), followed by RCP 6.0 (up to $23.0 \pm 6.8\%$), RCP 4.5 (up to $16.7 \pm 5.3\%$) and RCP 2.6 (up to $9.9 \pm 3.6\%$). By the 2050s, maize yield may be a little higher under RPC 4.5 than under RCP 6.0. Similarly, soybean yield could be slightly higher under RCP 6.0 than RCP 8.5. These differences highlight the complexity of crop–climate–CO_2 interactions.

Relative changes in production (Figure 3.4(a) for top-five countries) and yield (Figure 3.5(a) for income level groups) under RCP 2.6 are much smaller than under RCP 8.5 (Figures 3.4(b) & 3.5(b) respectively). However, the range of uncertainties is greatly
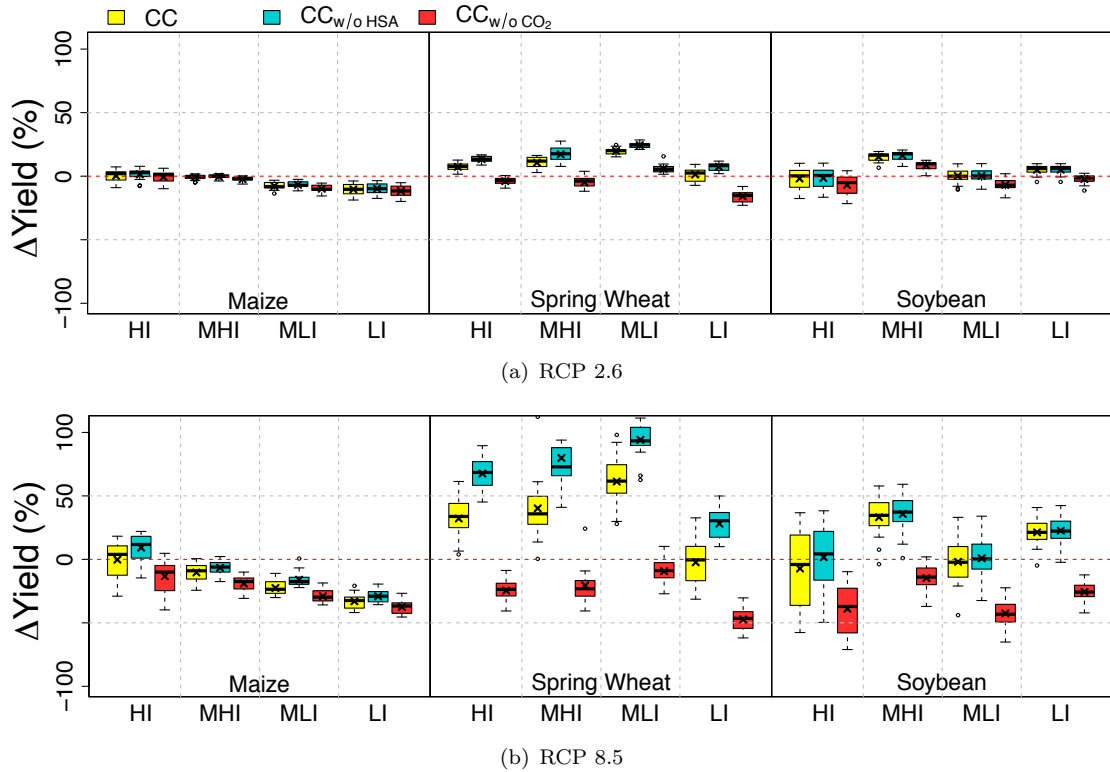
FIGURE 3.5: Box-plots of ΔY (%) simulated for RCP 2.6 (a) and RCP 8.5 (b) $\times$ 18 GCMs for the 2080s relative to the 1980s among different income-level countries as defined by the World Bank: high income (HI), medium high income (MHI), medium low income (MLI) and low income (ML) levels for maize, spring wheat and soybean. The bottom and top of the box are lower and upper quartiles, respectively, the band near the middle of the box is the median value across each set of simulations, and the cross is the mean value.

reduced. A strong mitigation scenario resulting in a low stabilised radiative forcing (i.e. RCP 2.6) could therefore contribute to reduced uncertainties in projections of overall impacts and thus facilitate adaptation planning. In contrast, a *business as usual* future such as RCP 8.5 is associated with large uncertainties in projected impacts, and designing adaptation strategies for such an uncertain future is much more challenging.

Finally, when assuming CO_2 fertilisation to be negligible (i.e. $CC_{\text{w/o } CO_2}$), we find dramatic yield losses for all three crops by the 2080s under RCP 8.5; whereas corresponding yield losses are reduced by more than 80% under RCP 2.6 (see two last rows in Table 3.1). In this case, our findings present major differences between RCP trajectories and further emphasise the importance of better quantifying the role of elevated atmospheric CO_2 on crops (see discussion, section 3.7).

3.7 Discussion

Our paper fills an important gap in previous assessments of climate change impact on global crop yield by simulating, for the first time at the global scale, effects of extreme heat stress during the crop reproduction phase and an extensive range of future climate scenarios (72) encompassing differences in GHG emissions and GCMs. Table 3.2 compares key results presented here against other global scale impact assessments. We identified studies using different crop simulation approaches, including the LPJmL model (Müller et al., 2010), the DSSAT suite of crop models (Nelson et al., 2010; Parry et al., 2004) and version 1.0 of PEGASUS (Deryng et al., 2011) under climate change only (referred to in the table as $CC_{\text{w/o HSA,CO}_2}$) and $CC_{\text{w/o HSA}}$ scenarios. Table 3.2 also includes results from a statistical model using historical observed data (Lobell et al., 2011b). PEGASUS 1.1 differs from 1.0 by including an improved interpolation algorithm of monthly climate data to daily values using a weather generator and being sensitive to specific extreme heat stress (see section 3.2 and Chapter 2). Some studies reported results for each individual crop and some reported multi-crop averages. Effects of HSA in PEGASUS 1.1 lead to more pessimistic outcomes. Importantly, PEGASUS 1.1 produces a wider range of estimated ΔY than any previous study. For instance, impacts on soybean yields may be largely positive or negative even when CO_2 fertilisation effects are taken into account. Previous studies listed in Table 3.2 considered only two to four GCMs to drive their crop models, whereas our study, using PEGASUS 1.1, takes into account an ensemble of eighteen GCMs, which increases the range of uncertainties, due to climate model scenarios.

TABLE 3.2: Comparison of changes in global crop yield relative to present-day $\Delta Y(\%)$ with previous assessments from peer reviewed literature. Wheat results for PEGASUS include only spring variety whereas the other studies include both winter and spring varieties. The range represents extrema of global average yield change reported in previous studies and estimated by PEGASUS 1.1. Median change in crop yield due to changes in temperature (T), precipitation (P) and CO_2 is reported for the statistical model.

Crop sensitivity	Model & reference	Number of scenarios	Time horizon	Maize	Wheat	Soybean	Multi crops
T, P, CO$_2$	Statistical model(Lobell et al., 2011b)	Historical	1980–2008	− 4	− 3	1	
$CC_{\text{w/o HSA,CO}_2}$	LPJmL(Müller et al., 2010)	3 SRES × 4 GCMs					[− 8 ; − 4]
	DSSAT (rainfed only)(Nelson et al., 2010)	1 SRES × 2 GCMs	2050	[− 12 ; − 2]	[− 10 ; − 4]		
	PEGASUS 1.0(Deryng et al., 2011)	2 SRES × 2 GCMs		[− 12 ; − 6]	[− 10 ; − 4]	[− 26 ; − 12]	
$CC_{\text{w/o CO}_2}$	PEGASUS 1.1	2 RCPs × 18 GCMs		[− 16 ; − 1]	[− 20 ; − 14]	[− 33 ; 8]	[− 11 ; 0]
$CC_{\text{w/o HSA}}$	LPJmL(Müller et al., 2010)	3 SRES × 4 GCMs					[12 ; 13]
	PEGASUS 1.1	2 RCPs × 18 GCMs	2050	[− 11 ; 2]	[10 ; 86]	[− 19 ; 25]	[− 5 ; 26]
CC	PEGASUS 1.1	4 RCPs × 18 GCMs		[− 13 ; 1]	[3 ; 52]	[− 21 ; 24]	[− 5 ; 18]
$CC_{\text{w/o CO}_2}$	PEGASUS 1.1	2 RCPs × 18 GCMs	2080	[− 32 ; 0]	[− 39 ; 3]	[− 55 ; 7]	[− 21 ; 3]
$CC_{\text{w/o HSA}}$	DSSAT(Parry et al., 2004)	7 SRES × 2 GCMs					[− 5 ; 1]
$CC_{\text{w/o HSA}}$	PEGASUS 1.1	2 RCPs × 18 GCMs	2080	[− 15 ; 2]	[10 ; 121]	[− 25 ; 46]	[− 7 ; 26]
CC	PEGASUS 1.1	4 RCPs × 18 GCMs		[− 25 ; 1]	[4 ; 60]	[− 32 ; 44]	[− 9 ; 22]

Our results include some important scientific uncertainties and assumptions. First, we use global values of temperature thresholds for HSA for each crop whereas in reality temperature thresholds vary not only among crop types but also among crop cultivars. Second, this analysis omits winter wheat and therefore gives only a partial assessment on total global wheat yield (spring wheat as simulated in PEGASUS accounts for 35% of total wheat harvested area). Third, PEGASUS does not include negative impacts related to crop pest and disease factors, which have yet to be explicitly examined in crop models (Gornall et al., 2010), or crop interactions with pollutants such as ozone, and nutrient–CO_2 interactions. Fourth, our study assumes no adaptation in fertiliser application rates, which does not represent realistic scenarios of future fertiliser application rates. In fact, we constrain our analysis to focus on biophysical aspects of climate impacts without speculating on future developments in the world economy and trade and gain in yield due to improvements in agro-technologies. Adaptation scenarios taking into account future fertiliser application rates would require additional information on economy and trade, which is beyond the scope of this study. Similarly, irrigation scenarios here do not rely on actual water resources available, assuming water is available in irrigated cropland. A more realistic assessment would require linkage to a global water model, which could lead to reductions in irrigated crop yield due to water scarcity. Fifth, CO_2 fertilisation effects on crops, which are included here, remain controversial (Ainsworth and Rogers, 2007; Long et al., 2006; Tubiello et al., 2007). Atmospheric CO_2 concentrations continue to rise rapidly, having recently surpassed 400 parts per million. The potential for CO_2 fertilisation effects to alleviate the largely negative impacts of climate change on crops, and ultimately food security, is unclear. Little is known about actual crop response to elevated CO_2 effects in many parts of the world. Current FACE experiments (Kimball, 2011) have been conducted in temperate climates, principally in the United States and a few in Europe. CO_2 effects in tropical climates could be very different and possibly more sensitive to soil nutrient availability. Differences in the impacts found here with and without CO_2 fertilisation highlight the urgency for further study of CO_2 effects on crops across agroecosystems (Leakey et al., 2012). In addition, elevated CO_2 could affect temperature tolerance threshold to heat stress (Wang et al., 2008), and is expected to reduce C–N ratios in crops, hence reducing the quality of grains by reducing the overall protein content (Taub et al., 2008). Although this last point is paramount for global food security, CO_2 effects on grain protein content are omitted from current global crop models. Sixth, monthly

temperature series generated within CIAS do not take into account changes in the frequency of extreme temperatures, which would increase risk of HSA. As a result, our simulation results are probably conservative and may underestimate the yield impact of extreme temperatures. Finally, our study uses only one crop model and therefore omits a key source of uncertainty in crop response to changing climate inputs. The need for research into uncertainties associated with different impact models is increasingly recognised (Bassu et al., 2014; Rosenzweig et al., 2013).

3.8   Conclusion

To conclude, our results quantify the importance of extreme weather events on crop yield and confirm regional disparities in climate change impacts, with greater negative impacts in the tropics and sub-tropics than in temperate regions for maize and spring wheat in particular. Our results confirm previous findings that low latitudes are generally more negatively impacted than higher latitudes as a results of climate change. By the 2080s under RCP 8.5, we find strong HSA effects for maize (responsible for up to 45% of global average yield losses under RCP 8.5 by the 2080s relative to the 1980s) and spring wheat (responsible for up to 52% reduction of global average yield gains) and smaller consequences for soybean (responsible for up to 25% reduction of global average yield gains). Yet, we found large HSA impacts on soybean yields of major producing countries, including Brazil and the United Sates. In addition, future GHG emission pathways are shown here to play an important role in determining future crop production. Another important finding is that even though results show important negative effects of HSA on crop yield, positive effects of elevated $[CO_2]$ on crop yields appear more important on average for all crops, and as early as the 2050s in the business as usual scenario. However, regional impacts of extreme heat stress appear to be more important than CO_2 in some places, highlighting the importance of climate mitigation. Strong radiative forcing, leading to a large increase in global mean temperature and hence higher extreme temperatures, will impact crops negatively in some of the regions contributing most to global production and across different income countries. The potential effects on global food prices and crop yield reduction in currently food insecure areas represent significant consequences for global food security. The wide range of

impacts across regions underscores the need for carefully targeted adaptation responses including breeding and technology programs for greater crop heat tolerance.

Chapter 4

The global gridded crop modelling intercomparison and improvement initiative

Preface

In Chapter 3, I presented a climate impact study using PEGASUS driven by a large ensemble of climate change scenarios. This approach, although achieving an important advancement by using one of the largest ensemble of climate change scenarios, is nonetheless constrained by the use of one single global crop model. Indeed, PEGASUS is a model based on several assumptions about crop-climate interactions and covering only *some* – yet *key* – aspects of climate change impacts on crops. Thus, results presented in Chapter 3 do not fully capture uncertainties related to the use of a single crop modelling approach. In the subsequent chapters of this thesis (Chapters 5 & 6), I explore in more depth the range of uncertainties related to different approaches for modelling complex biophysical processes (Chapter 5) and farming adaptation responses (Chapter 6). Research presented in these chapters was completed during my active participation in the Agricultural Model Intercomparison and Improvement Project (AgMIP) during April 2012–January 2013. Along with Dr. Cynthia Rosenzweig and Dr. Joshua Elliott, based at the NASA Goddard Institute for Space Studies at Columbia University, I designed and coordinated the first global gridded crop modelling intercomparison

(GGCMI) exercise, which was made possible thanks to the collaboration between AgMIP, the Inter-Sectoral Impact Model Intercomparison Project (ISI-MIP) and the participation of seven modelling groups. My contribution to the project included: coordination of six modelling groups along with my participation running PEGASUS; organisation of biweekly conference calls; collection of model metadata; and production of the summary tables and the model genealogy diagram that are presented further in this chapter (see Tables 4.1 to 4.5 and Figure 4.2, which can also be found in the supplementary information of Rosenzweig et al., 2014). This model intercomparison study resulted in the production of more than 2240 simulations spanning 130 years of climate data using seven distinct GGCMs driven by five different GCMs coupled to four RCPs. The inclusion of the multiple GGCMs extended the range of uncertainties in impact simulation by a factor of three and proved to be a major advancement for identifying strengths and weaknesses of the different GGCMs (see Chapter 5). This chapter presents background and motivation behind AgMIP and ISI-MIP, along with a detailed description of the GGCM ensemble and the simulation protocol of the joint AgMIP/ISI-MIP fast-track.

4.1 Introduction

For more than a decade, climate scientists have largely recognised the inadequacy of using one single global climate model (GCM) to represent the full range of uncertainties in climate projections (Meehl et al., 1997). The same philosophy has recently emerged across disciplines of climate impact research; where the use of one single impact model in the fields of agronomy, hydrology, ecology, global health and economy is recognised to be insufficient for assessing the full range of impacts and uncertainties. With the increasing variety of crop productivity models developed and used at both regional and the global scales, modelling intercomparison programs (MIPs) such as the Agricultural Model Intercomparison and Improvement Project (AgMIP) since 2010 (www.agmip.org, Rosenzweig et al., 2013) and the Inter-Sectoral Impact Model Intercomparison Project (ISI-MIP) since 2012 (www.isi-mip.org, Warszawski et al., 2014) have become key in coordinating international modelling efforts across research groups to better assess the extent of current knowledge and related uncertainties of climate change impacts on agriculture and other sectors, and design a strategic plan of action to advance climate

impact simulations (Challinor et al., 2014a). This chapter begins with a presentation of the AgMIP (section 4.2) and ISI-MIP (section 4.3) initiatives. Section 4.4 provides a detailed description of the seven GGCMs involved in the ISI-MIP fast-track and the simulation protocol, which is central to methodology of Chapter 5. The chapter concludes with a summary of ongoing activities and next steps for global gridded crop model intercomparison (GGCMI) (section 4.5).

4.2 The agricultural model intercomparison and improvement project

AgMIP is an international collaborative initiative committed to coordinating crop and agricultural economic model intercomparison exercises to improve the characterisation of world food security in response to climate change and address global adaptive capacity within a trans-disciplinary framework (Rosenzweig et al., 2013). AgMIP facilitates collaborative research across a vast array of modelling and food security experts, regrouped into four research teams focusing on climate data, crop and agricultural economic modelling and information technology to perform systematic and robust model comparison and improvement, climate impact assessment, and facilitate data access and knowledge transfer for decision making (Figure 4.1). In addition, AgMIP provides a framework for addressing issues of scale, multidimensionality and uncertainty across disciplines (Rosenzweig et al., 2013).

In particular, the climate team aims to develop and improve standardisation of climate scenarios for historical validation, sensitivity and future impact analyses. The crop modelling team performs crop modelling simulations at global, regional and field-scales to analyse key crop–climate interactions, the role of carbon dioxide (CO_2) fertilisation, pests, diseases and farming management practices. The economic team integrates crop productivity outputs from crop models into economic models to explore economic impacts and adaptation options across a range of representative agricultural pathways (RAPs) at regional and the global scales (Rosenzweig et al., 2013; see also Chapter 6 for more details on the RAPs).

Some of the crop modelling intercomparison activities have to date included multi-site – crop-specific analyses (e.g. Bassu et al., 2014 for maize; Asseng et al., 2013 for
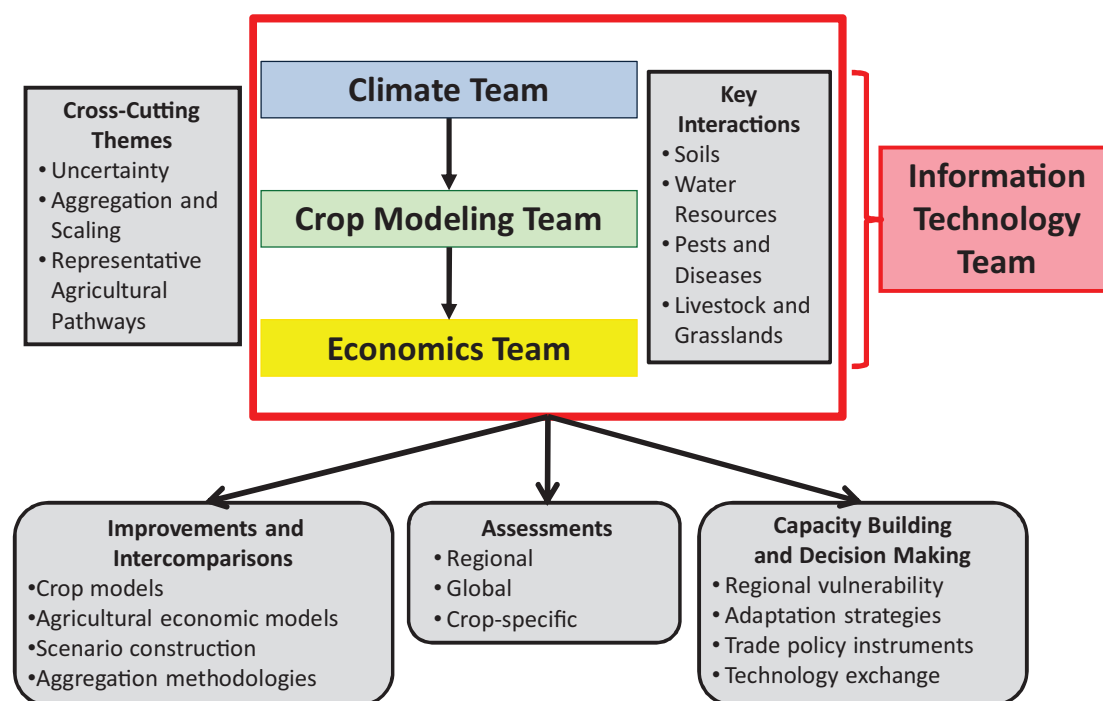
FIGURE 4.1: AgMIP Teams, Cross-Cutting Themes, key interactions and expected outcomes (Rosenzweig et al., 2013, Figure 1).

wheat; Singels et al., 2013 for sugarcane), regional studies (e.g. Ruane et al., 2013b in Bangladesh; Ruane et al., 2013a in Panama) and the first GGCMI exercise in collaboration with ISI-MIP (see following sections 4.3 & 4.4).

4.3 The inter-sectoral impact model intercomparison project

ISI-MIP was launched to integrate climate impact assessment across multiple sectors, thus complementing MIPs designed to look at specific sectors (such as AgMIP: www.agmip.org; Rosenzweig et al., 2013 & WaterMIP: www.eu-watch.org; Haddeland et al., 2011). The ISI-MIP fast-track exercise, which took place between January 2012 and January 2013, consisted in the integration of societal and environmental impact models representing one to several sectors among water, agriculture, ecosystem, health, infrastructure and the economy at the global scale (most participating impact models represented a single sector with the exception of three models capable of simulating two/three sectors) (Warszawski et al., 2014).

For the fast-track, ISI-MIP provided harmonised GHG emission scenarios and bias-corrected climate forcings issued from the CMIP5 archive (Hempel et al., 2013) along with a centralised data storage and transfer system to facilitate data access and sharing across participating modelling groups (www.isi-mip.org). The ISI-MIP fast-track effort culminated in the production of twelve articles published in the special feature "Global climate impacts: a cross-sector, multi-model assessment" of the *Proceedings of the National Academy of Sciences*, volume 111 issue 9 (see Schellnhuber et al., 2014 for the editorial introduction), among which four articles were directly based on the GGCM simulation results: Elliott et al. (2014a); Nelson et al. (2014); Piontek et al. (2014); Rosenzweig et al. (2014). Rosenzweig et al. (2014) provided a general overview of the GGCMI results, focusing on simulated yield, confirming regional disparities in impacts, with developing countries showing particularly strong negative impacts. In addition, the paper highlighted sources of uncertainties related to the representation of CO_2, nitrogen and high temperature effects. Nelson et al. (2014) summarised the economic impacts of climate change effects on crops as simulated by nine global economic models driven by seven harmonised crop yield shocks from climate change. In particular, their results showed that assumptions about ease of land use conversion, intensification, and trade are responsible for important differences in economic impacts. Elliott et al. (2014a) presented a cross-sectoral analysis looking at climate impacts on irrigation water use by comparing results from ten global hydrological models (GHMs) and six GGCMs, demonstrating the importance of CO_2 fertilisation effects on water use, which are yet to be adequately simulated in GHMs. As well, the paper identified freshwater limitation in some important irrigated regions, including western United States, China, and western, southern and central Asia. Piontek et al. (2014) presented a multi-sectoral analysis combining impact simulations on water, agriculture, ecosystems and malaria, identifying regions at risk of high impact exposure of multiple sectors under future climate change. In addition, I led an in-depth analysis looking at uncertainties resulting from modelled carbon fertilisation effects on crop yield and water use, which is presented in Chapter 5.

4.4 The agricultural sector of the inter-sectoral impact model intercomparison project fast-track

4.4.1 Presentation of the seven participating global gridded crop models

The seven GGCMs that participated in the ISI-MIP fast-track are listed in Table 4.1 and consist of:

1. the Environmental Policy Integrated Climate (EPIC) model (Gassman et al., 2004; Izaurralde et al., 2006; Williams, 1990, 1995 – originally the Erosion Productivity Impact Calculator; Williams, 1990);

2. the Geographic Information System-based Environmental Policy Integrated Climate (GEPIC) model (Liu et al., 2007; Williams, 1990, 1995);

3. the Global AgroEcological Zone model in the Integrated Model to Assess the Global Environment (GAEZ-IMAGE; Bouwman et al., 2006; Leemans and Solomon, 1993);

4. the Lund-Potsdam-Jena managed Land (LPJmL) dynamic global vegetation and water balance model (Bondeau et al., 2007; Fader et al., 2010; Waha et al., 2011);

5. the Lund-Potsdam-Jena General Ecosystem Simulator (LPJ-GUESS) with managed land (Bondeau et al., 2007; Lindeskog et al., 2013; Smith et al., 2001);

6. the parallel Decision Support System for Agro-technology Transfer [pDSSAT; Elliott et al., 2013; Jones et al., 2003; using the Crop Environment Resource Synthesis (CERES) models for maize, wheat, and rice and the Crop Template approach (CROPGRO) for soybean];

7. the Predicting Ecosystem Goods And Services Using Scenarios (PEGASUS) model (Deryng et al., 2014, 2011 and Chapter 2 & 3).

These GGCMs can be grouped into three families spanning more than three decades of model development (Figure 4.2):

TABLE 4.1: Model name and contact details

Model	Version	References for model description and applications	Institution	Contact person / Web address
EPIC	0810	Izaurralde et al. (2006) Williams (1990, 1995)	BOKU; University of Natural Resources and Life Sciences, Vienna	Erwin Schmid erwin.schmid@boku.ac.at
GEPIC	EAWAG	Liu et al. (2007) Williams (1990)	EAWAG Swiss Federal Institute of Aquatic Science and Technology	Christian Folberth/Hong Yang christian.folberth@eawag.ch hong.yang@eawag.ch
IMAGE	2.4	Bouwman et al. (2006) Leemans and Solomon (1993)	Netherland Environmental Assessment Agency (PBL)	Elke Stehfest/Kathleen Neumannl elke.stehfest@pbl.nl kathleen.neumann@pbl.n
LPJmL	-	Bondeau et al. (2007) Fader et al. (2010) Waha et al. (2011)	Potsdam Institute for Climate Impact Research	Christoph Müller christoph.mueller@pik-potsdam.de www.pik-potsdam.de/lpj
LPJ-GUESS	2.1	Bondeau et al. (2007) Lindeskog et al. (2013) Smith et al. (2001)	Lund University, department for Physical Geography and Ecosystem Science, IMK-IFU, Karlsruhe Institute of Technology, Garmisch-Partenkirchen, Germany	Stefan Olin/Thomas Pugh stefan.olin@nateko.lu.se thomas.pugh@imk.fzk.de
pDSSAT	pDSSAT 1.0 (DSSAT 4.0)	Elliott et al. (2013) Jones et al. (2003)	University of Chicago Computation Institute	Joshua Elliott jelliott@ci.uchicago.edu
PEGASUS	1.1	Deryng et al. (2014, 2011)	Tyndall Centre for Climate Change Research, University of East Anglia, UK McGill University, Canada	Delphine Deryng d.deryng@uea.ac.uk

- site-based crop models – extended for global analyses using geographical information system (EPIC and GEPIC) and advanced parallel simulation system (pDSSAT);

- ecosystem models – initially developed to simulate terrestrial carbon cycle for natural vegetation using downscaled global climate data and then extended to represent managed land (LPJmL, LPJ-GUESS and PEGASUS);

- agro-ecological zone (AEZ) models – designed to represent cropland suitability and crop growing period according to elevation, soil and climate characteristics (IMAGE).

The site-based crop models tend to include a more detailed representation of cropping systems but necessitate substantial computing resources, whereas the ecosystem and AEZ models typically include less detail on crop management but present the advantage of being run globally in a short fraction of time. In addition, since the ecosystem models simulate global carbon and water cycles, they are useful tools for assessing crop production in the context of global environmental change.

Biophysical processes represented in GGCMs include CO_2 effects, environmental stresses, soil nutrient cycling and soil water dynamic, which are based on different approaches. Firstly, photosynthesis is described with either a simple radiation use efficiency (RUE) (e.g. PEGASUS, described in Chapter 2) or a detailed leaf-level photosynthesis respiration (referred further as *Farqhuar*, Farquhar et al.,
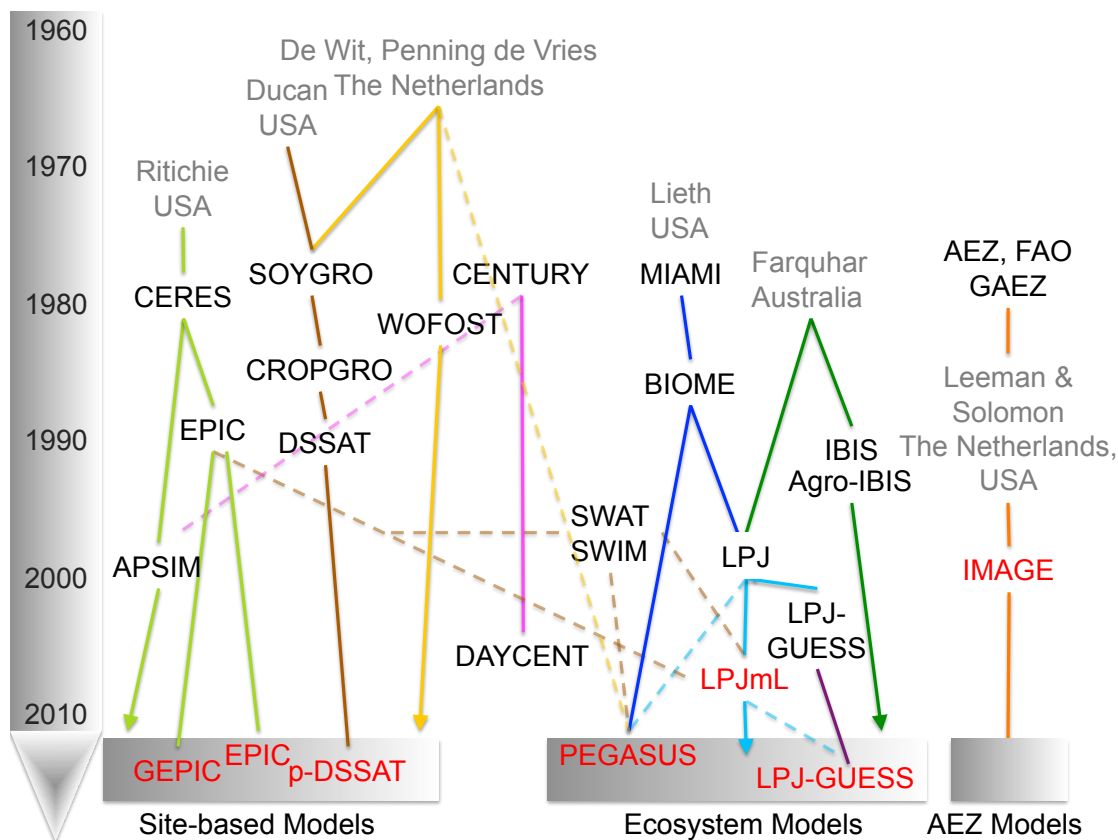
FIGURE 4.2: Crop model genealogy for site-based, ecosystem, and AEZ models. The GGCMs that participated in the ISI-MIP fast-track are highlighted in red (Rosenzweig et al., 2014, Figure S1).

1980) approach. Representation of CO_2 fertilisation effects on photosynthesis and transpiration rates thus follow either a descriptive (RUE-type models) or explanatory approach (Farqhuar-type models) (see Chapter 5 section 5.4.2). Secondly, all GGCMs take into account temperature and water stress. Most models include nitrogen stress as well (except the LPJ-type models and IMAGE). Both EPIC-type models also represent aluminium and oxygen stresses. PEGASUS represents heat stress effect at anthesis (see Chapter 2 & Deryng et al., 2014). Thirdly, GGCMs differ in respect to crop water demand and estimated evapotranspiration (ET): the EPIC-type models use the Penman-Monteith approach (Monteith, 1965; Penman, 1948), whereas the other GGCMs use Priestley-Taylor (Priestley and Taylor, 1972). In addition, the number of soil layers varies among GGCMs and roots are either linearly or exponentially distributed throughout the soil depth. Finally, crop phenology in GGCMs depends on temperature, which is common to all models, using growing degree day (GDD) accumulation, which varies with models' definition of base and maximum temperature thresholds (see section 2.2.7 in Chapter 2) that are also crop specific (Table 4.2).

Model	Leaf area development[1]	Light interception[2]	Light utilization[3]	Yield formation[4]	Stresses[5]	Type of heat stress[6]	Crop phenology[7]	Type of water stress[8]	Evapo-transpiration[9]	Soil water dynamics[10]	Root distribution over depth[11]	Soil processes[12]	CO_2 effects[13]
EPIC	D	S	RUE	HI_{ws} Prt B	W, T, H, A, N, P, BD, Al	V	T(HU), V, O	E	PM	10	Lin, W	C, N, B(1), P(6)	RUE, TE
GEPIC	D	S	RUE	HI_{ws} Prt B	W, T, H, A, N, P, BD, Al	V	T(HU), V, O	E	PM	5	Lin, W	C, N, B(1), P(6)	RUE, TE
IMAGE	D	S	RUE	HI	W, T, BD	na	T	E	PT	1	W	na	RUE
LPJmL	PS	S	P-R	HI_{ws}	W, T	na	T, V	S	PT	5	Exp	na	LF, SC
LPJ-GUESS	D	S	P-R	HI_{ws}	W, T	na	T, V	S	PT	2	Lin	na	LF, SC
pDSSAT	D	S; Soy: D	RUE; Soy: P-R	Gn	W, T, H, A, N	V, R, F	T, V, DL, O	E	PT	4	Exp	C, N, P(3)	RUE, TE, Soy: LF, TE
PEGASUS	D	S	RUE	Prt	W, T, H, N, P, K	V, F	T(HU)	E	PT	3	Non	na	RUE, TE

Table 4.2: Biophysical processes (Rosenzweig et al., 2014, Table S3).

Notes (na = Not applicable): (1) D: Dynamic simulation based on development and growth processes; PS: Prescribed shape of LAI curve as function of phenology, modified by water stress & low productivity (2) S: Simple approach; D: Detailed approach (3) RUE: Simple (descriptive) radiation use efficiency approach; P-R: Detailed (explanatory) gross photosynthesis-respiration (for more details, see Adam et al., 2011) (4) Yield formation depending on: HI: Fixed harvest-index; HI_{ws}: HI modified by water stress; Prt: Partitioning during reproductive stages; B: Total (above-ground) biomass; Gn: Number of grains and grain growth rate (5) W: Water stress; T: Temperature stress; H: Specific heat stress; A: Oxygen stress; N: Nitrogen stress; P: Phosphorus stress; K: Potassium stress; BD: Bulk density; Al: Aluminium stress (based on pH and base saturation) (6) V: Vegetative (source); R: Reproductive organ (sink); F: Number of grain (pod) set during the flowering period (7) Crop phenology function of: T: Temperature; HU: Heat unit index; V: Vernalisation; O: Other water/nutrient stress effects considered; DL: photoperiod (day length) (8) E: Ratio of supply to demand of water; S: Soil available water in root zone (9) PM: Penman-Monteith; PT: Priestley-Taylor (10) Number of soil layers (11) Lin: Linear; W: Actual water depends on water availability in each soil layer; Exp: Exponential; Non: No roots-just soil depth zone (12) Carbon model; Nitrogen model; B(x): x number of microbial biomass pools; P(x): x number of organic matter pools (13) Elevated CO_2 effects: RUE: Radiation use efficiency; TE: Transpiration efficiency; LF: Leaf-level photosynthesis (via rubisco or quantum-efficiency and leaf-photosynthesis saturation; SC: Stomatal conductance.

Representation of farm management practices is also a source of difference in GGCMs results: whether and how fertiliser application, irrigation, crop residue management, crop cultivar selection and planting date decision are simulated strongly influence yield and other outputs. The site-specific models (i.e. EPIC, GEPIC & pDSSAT) apply fertiliser dynamically through the crop growing season: application occurs at specific stages of the crop development to take into account the role of both application quantity and timing. PEGASUS, the only ecosystem model, applies fertiliser as a daily stress function and thus does not simulate effect of fertiliser application timing (see Chapter 2 section 2.2.4 and Deryng et al., 2014, 2011). As well, although ISI-MIP provided

Model	Spatial scale	Temporal scale[1]	Climate input variables[2]	Soil input data[3]	Spin Up[4]	Planting date[5]	Crop cultivars[6]	Irrigation[7,8]	Fertilizer application[9]	Crop residue[10]	CO_2 level[11]
EPIC	0.5° lon x 0.5° lat	D, H,	Tmn, Tmx, P, Rad, RH, WS	ISRIC-WISE ROSETTA AWC (van Genuchten) Albedo (Dobos) HYD (USDA)	Soil OM, C, NH_3, NO_3, H_2O, P(1)	S (fraction of PHU) - fixed planting window	GDD - fixed	90/100/500/50/20[8] maximum applied irrigation: 500 mm yr^{-1}	High N input (max 200 kg ha^{-1} yr^{-1}) PK (national stat. IFA) dynamic application	No, can be simulated	380 ppm (2005)
GEPIC	0.5° lon x 0.5° lat	D	Tmn, Tmx, P, Rad, RH, WS	ISRIC-WISE	Soil OM, C, NH_3, NO_3, H_2O, P, CR (20)	S (fraction of PHU) - clim. adapt	GDD, 2 cultivars for mai - fixed	90/100/2000/1000/0.01[8]	NP (national stat. FertiSTAT), dynamic application	Yes, Crop-specific	364 ppm (2000)
IMAGE	0.5° lon x 0.5° lat	M, WG	Ta,P	Soil reduction factor (Wood & Dent) on FAO soil map	CR(210)	clim. adapt (implicit planting date)	GDD + clim. adapt	NA	na	Yes, does not affect yield	370 ppm (2000)
LPJmL	0.5° lon x 0.5° lat	D	Ta, P, cld (or Rad)	HWSD STC HYD (Cosby) THM (Lawrence & Slater)	H_2O (200)	S - fixed planting window	GDD+V (whe, sunfl, rapes); BT (mai); static (others) - fixed	300/90/100/varies[7]	na	Yes, does not affect yield	370 ppm (2000)
LPJ-GUESS	0.5° lon x 0.5° lat	D	Ta, P, cld (or Rad)	HWSD STC HYD (Cosby) THM (Lawrence & Slater)	H_2O (30)	S - fixed planting window	GDD+V (whe, sunfl, rapes); BT (mai); static (others) + clim. adap	200/90/100/100[7]	na	Yes, does not affect yield	379 ppm (2005)
pDSSAT	0.5° lon x 0.5° lat	D	Tmn, Tmx, P, Rad	HWSD	Soil OM, C, NH_3, NO_3, H_2O (1)	S - fixed planting window	GDD and/or latitude, 2-3 for each cell - fixed	40/80/100/75[7] ric: 30/50/100/100[7]	SPAM, dynamic application	Crop-specific, does not affect yield	330 ppm (1975)
PEGASUS	0.5° lon x 0.5° lat	D	Ta, Tmn, Tmx, P, cld (or sun)	AWC (ISRIC-WISE)	H_2O (4)	S - clim. adapt	GDD + clim. adapt	40/90/100/100[7]	NPK (national stat. IFA), annual application	na	369 ppm (2000)

Table 4.3: GGCM inputs and agricultural management practices. (Rosenzweig et al., 2014, Table S4).

Notes (na = Not applicable): (1) D: Daily time-step; H: Hourly time-step; M: Monthly time-step; WG: Monthly climate data interpolated to daily using a weather-generator (2) Tmn: Minimum temperature, Tmx: Maximum temperature, P: Precipitation, Rad: Percentage of radiation, RH: Relative humidity, WS: Wind speed, Ta: Average temperature, Cld: Percentage of cloud cover, Sun: Fraction of sunshine hours (3) Source of soil property inputs (i.e. source of basic soil properties), plus method for deriving parameters required by models); AWC: Available water capacity; HYD: Hydraulic soil parameters; THM: Thermal parameters; STC: Soil texture classification based on USDA soil texture classification (http://edis.ifas.ufl.edu/ss169); Reference: HWSD: Harmonised world soil database (FAO/IIASA, 2012); ISRIC-WISE (Batjes, 2005); ROSETTA (Schaap and Bouten, 1996); FAO soil map (FAO, 1991); Cosby et al. (1984); Dobos (2006); Lawrence and Slater (2008); USDA/NRCS (2012); van Genuchten et al. (1988); Wood and Dent (1983) (4) Number years for spin up (x); OM: Organic matter, C: Carbon; NH_3: Ammonia; NO_3: Nitrate; H_2O: Soil water; P: Phosphorus; CR: Crop residue (5) S: Simulation of planting dates according to climatic conditions; F: Fixed planting dates; source of planting date data if applicable; PHU: Potential heat unit; Fixed planting window: Does not allow for adaptation to climate change; clim. adapt: Dynamic planting window: adapts to climate change (6) GDD: Simulates crop Growing Degree Days (GDDs) requirement according to estimated annual GDDs from daily temperature; Number of cultivars; GDD+V GDD requirements and vernalisation requirements computed based on past climate experience; BT: Base Temperature computed based on past climate; fixed: Static GDD requirement (no adaptation); clim. adapt: Dynamic GDD requirement (adaptation to climate change) (7) Irrigation rules: IMDEP(cm): Depth of soil moisture measured; ITHRL(%): Critical lower soil moisture threshold to trigger irrigation event; ITHRU(%): Upper soil moisture threshold to stop irrigation; IREFF(%): Irrigation application efficiency (8) Irrigation rules: EPIC and GEPIC models: BIR(%): Water stress in crop to trigger automatic irrigation; EFI(%): Irrigation efficiency - runoff from irrigation water; VIMX(mm): Maximum of annual irrigation volume; ARMX(mm): Maximum of single irrigation volume allowed; ARMN(mm): Minimum of single irrigation volume allowed (9) Fertiliser application, timing of application; NPK annual application of total NPK (nutrient-stress factor); Source of fertiliser application data; Timing: Annual or dynamic (10) Remove residue or not (Yes/No) (11) CO_2 concentration baseline for "no CO_2" simulations (corresponding year).

Model	Model origin[1]	Calibration method	Parameters for calibration[2]	Output variable and dataset for calibration[3]	Spatial scale of calibration	Temporal scale of calibration	Method for model evaluation[4]
EPIC	Site-based	Site-specific (EPIC 0810)	na	Yield (FE & FAO)	Field-scale & National	Various	na
GEPIC	Site-based	Site-specific (EPIC 0810) & Global*	F, HI_{pot} (maize, rice)	Yield (FE & FAO)	National	Average for 1997-2003	R^2
IMAGE	GAEZ	NA	na	Potential Yield	National	Average for 1970-2005	na
LPJmL	Ecosystem	Global	LAI_{max}, HI, α_a	Yield (FAO)	National	Average for 1998-2003	Wilmott
LPJ-GUESS	Ecosystem	Uncalibrated	na	NA	na	na	na
pDSSAT	Site-based	Site-specific (DSSAT)	na	Yield (FE)	Field-scale	Various	na
PEGASUS	Ecosystem	Global	β	Yield (M3)	Gridcell level (0.5°lon x0.5°lat resolution)	Average for 1997-2004	Wilmott

Table 4.4: Model calibration and validation (Rosenzweig et al., 2014, Table S5). Notes (na = Not applicable): (1) Site-based crop model; GAEZ: Global agro-ecological zones; Ecosystem: Global ecosystem model (2) F: Fertiliser application rate; HI_{pot}: Potential harvest index; LAI_{max}: Maximum LAI under unstressed conditions; HI: Harvest index; α_a: Factor for scaling leaf-level photosynthesis to stand level; β: Radiation use efficiency factor (3) FE: Field experiments; FAO: FAOSTAT national yield statistics; Earthstat: Gridded dataset of crop-specific yields and harvested areas for the year 2000 (29) (4) Wilmott: Maximise Wilmott index of agreement (d) and RMSEu>RMSEs (RMSE: Root-mean-square error; RMSEu: Unsystematic RMSE; RMSEs: Systematic RMSE) (30) * GEPIC: Default parameters from field scale model EPIC0810 are mostly used. Potential HI has been adjusted for maize cultivars and rice based on literature (i.e. field trials). Fertiliser application rates have been modified for a few countries that report very high yields and low fertiliser use, whereas most of these countries are known for their intensive use of manure.

harmonised climate data, models did not necessarily use the same climate variables as input or other input data, such as soil characteristics and national fertiliser application rates, which were not harmonised in time for the fast-track process (Table 4.3).

Finally, GGCMs calibration methods also differ significantly between site-specific and ecosystem models. Ecosystem models are calibrated to global crop yield data (PEGASUS, see Chapter 2 section 2.4) and FAO national statistics (LPJmL, Bondeau et al., 2007) by tuning a limited number of parameters, whereas the site-specific models use a large set of parameters previously calibrated at various study sites (Table 4.4). Given all these differences, models from similar origins, such as EPIC/GEPIC and LPJmL/LPJ-GUESS, differ enough to be considered each as an independent GGCM within the ensemble.

4.4.2 Fast-track simulation protocol

All GGCMs were run at 0.5°lat × 0.5°lon spatial resolution using the twenty ISI-MIP bias-corrected climate scenarios resulting from five GCMs and four RCPs for the period:

1971–2099 (Hempel et al., 2013). The five GCMs were (see also Table 2.3 in Chapter 2 and Stocker et al., 2013):

1. HadGEM2-ES (developed at the Hadley Centre for Climate Prediction and Research in the UK);

2. IPSL-CM5A-LR (developed at the Institut Pierre Simon Laplace in France);

3. MIROC-ESM-CHEM (cooperatively developed at the Center for the University of Tokyo, the National Institute for Environmental Studies, and the Frontier Research Center for Global Change in Japan);

4. GFDL-ESM2M (developed at the Geophysical Fluid Dynamics Laboratory in the United States);

5. NorESM1-M (developed at the Norwegian Climate Centre in Norway).

All GGCMs simulated maize, wheat, rice and soybean except PEGASUS, which does not simulate rice. The default simulations included carbon fertilisation so that all GGCMs simulated effects of CO_2 for the five GCMs. All models simulated the HadGEM2-ES climate model without CO_2 effects, but only LPJmL, pDSSAT, PEGASUS, and EPIC simulated the other four GCMs. All models provided yield and seasonal ET outputs except IMAGE so that the analysis presented in Chapter 5 includes only six GGCMs: EPIC, GEPIC, LPJmL, LPJ-GUESS, pDSSAT and PEGASUS. Table 4.5 summarises the ensemble of simulation experiments and the complete list of simulated crops and submitted output variables.

4.5 Moving forwards

Following the success of the fast-track but also the identification of challenges and limitations in the partially harmonised results ensemble, new activities have taken place involving additional modelling groups. The first phase of GGCMI is ongoing and focuses on historical simulation and GGCM evaluation using harmonised inputs (see Chapter 6 section 6.4; Appendix B; and Elliott et al., 2014b) and nine different reanalysis-based weather datasets spanning 1948-present and harmonised by the climate team of AgMIP (www.agmip.org/ag-grid/ggcmi). A second phase of GGCMI is planned to analyse

G G C Ms	GCMs-RCPs-CO$_2$	C R O P	OUTPUT[1]
EPIC	HADGEM2-ES + 4RCPs-CO$_2$ + 4RCPs-noCO$_2$ IPSL-CM5A-LR + 4RCPs-CO$_2$ + RCP8.5-noCO$_2$ MIROC-ESM-CHEM + 4RCPs-CO$_2$ + RCP8.5-noCO$_2$ GFDL-ESM2M + 4RCPs-CO$_2$ + RCP8.5-noCO$_2$ NorESM1-M + 4RCPs-CO$_2$ + RCP8.5-noCO$_2$	Maize, wheat, soybean, rice, barley, managed grass, millet, rapeseed, sorghum, sugarcane, drybean, cassava, cotton, sunflower, groundnut	YIELD, PIRRWW, AET
GEPIC[2]	HADGEM2-ES + 4RCPs-CO$_2$ + 4RCPs-noCO$_2$ IPSL-CM5A-LR + 4RCPs-CO$_2$ MIROC-ESM-CHEM + 4RCPs-CO$_2$ GFDL-ESM2M + 4RCPs-CO$_2$ NorESM1-M + 4RCPs-CO$_2$	Maize, wheat, soybean, rice	YIELD, PIRRWW, AET
IMAGE	HADGEM2-ES + 4RCPs-CO$_2$ + 4RCPs-noCO$_2$ IPSL-CM5A-LR + 4RCPs-CO$_2$ MIROC-ESM-CHEM + 4RCPs-CO$_2$ GFDL-ESM2M + 4RCPs-CO$_2$ NorESM1-M + 4RCPs-CO$_2$	Maize, wheat, soybean, rice	YIELD
LPJmL	HADGEM2-ES + 4RCPs-CO$_2$ + 4RCPs-noCO$_2$ IPSL-CM5A-LR + 4RCPs-CO$_2$ + 4RCPs-noCO$_2$ MIROC-ESM-CHEM + 4RCPs-CO$_2$ + 4RCPs-noCO$_2$ GFDL-ESM2M + 4RCPs-CO$_2$ + 4RCPs-noCO$_2$ NorESM1-M + 4RCPs-CO$_2$ + 4RCPs-noCO$_2$	Maize, wheat, soybean, rice, millet, cassava, sugar beet, field pea, rapeseed, sunflower, groundnut, sugarcane	YIELD, PIRRWW, AET, PLANT-DAY, MATY-DAY, BIOM, GSPRCP, GSRSDS, SUMT
LPJ-GUESS	HADGEM2-ES + 4RCPs-CO$_2$ + 4RCPs-noCO$_2$ IPSL-CM5A-LR + 4RCPs-CO$_2$ MIROC-ESM-CHEM + 4RCPs-CO$_2$ GFDL-ESM2M + 4RCPs-CO$_2$ NorESM1-M + 4RCPs-CO$_2$	Maize, wheat, soybean, rice	YIELD, PIRRWW, AET
pDSSAT	HADGEM2-ES + 4RCPs-CO$_2$ + 4RCPs-noCO$_2$ IPSL-CM5A-LR + 4RCPs-CO$_2$ + 4RCPs-noCO$_2$ MIROC-ESM-CHEM + 4RCPs-CO$_2$ + 4RCPs-noCO$_2$ GFDL-ESM2M + 4RCPs-CO$_2$ + 4RCPs-noCO$_2$ NorESM1-M + 4RCPs-CO$_2$ + 4RCPs-noCO$_2$	Maize, wheat, soybean, rice	YIELD, PIRRWW, AET, GSPRCP
PEGASUS[3]	HADGEM2-ES + 4RCPs-CO$_2$ + 4RCPs-noCO$_2$ IPSL-CM5A-LR + 4RCPs-CO$_2$ + RCP8.5-noCO$_2$ MIROC-ESM-CHEM + 4RCPs-CO$_2$ + RCP8.5-noCO$_2$ GFDL-ESM2M + 4RCPs-CO$_2$ + RCP8.5-noCO$_2$ NorESM1-M + 4RCPs-CO$_2$ + RCP8.5-noCO$_2$	Maize, wheat, soybean	YIELD, PIRRWW, AET, PLANT-DAY, ANTH-DAY, MATY-DAY, INITR, ONITR, BIOM, LEACH, GSPRCP, GSRSDS, SUMT

Table 4.5: List of simulation experiments and GGCMs outputs (Rosenzweig et al., 2014, Table S6).

Outputs description: (1) YIELD (t ha^{-1} yr^{-1}): dry matter; PIRRWW (mm yr^{-1}): potential irrigation water withdrawal; AET (mm yr^{-1}): actual growing season evapotranspiration; PLANT-DAY (julian day): planting date; ANTH-DAY (day from planting): date of anthesis; MATY-DAY (day from planting): maturity date; INITR (t ha^{-1} yr^{-1}): inorganic nitrogen application rate; ONITR (t ha^{-1} yr^{-1}): organic nitrogen application rate; BIOM (t ha^{-1} yr^{-1}): total above ground biomass yield; LEACH (t ha^{-1} yr^{-1}): nitrogen leached; GSPRCP (mm yr^{-1}): growing season precipitation; GSRSDS (W m^{-2} yr^{-1}): growing season incoming solar radiation; SUMT (Co-day yr^{-1}): sum of daily mean temperature over growing season

models' sensitivity to carbon-temperature-water-nitrogen (CTWN) organised around a set of simulations driven by the harmonised data products prepared in Phase 1 and using perturbation signals. Finally, a third phase of GGCMI will focus on climate vulnerability, impacts and adaptation, using climate change projections from CMIP5 and a detailed set of adaptation scenarios developed as part of the RAP framework (see Chapter 6).

4.6 Concluding remarks

This chapter has provided a general overview of AgMIP and the recent and ongoing GGCMI activities. In addition, this chapter presented a detailed description of the ISI-MIP fast-track modelling protocol and a comprehensive review of the seven participating GGCMs, central to results presented in the next chapter (5). Chapter 5 focuses in particular on evaluating GGCM differences in simulating carbon fertilisation effects on crop yield and water use. Materials presented in this chapter are also essential to Chapter 6, which presents a perspective analysis to address agricultural adaptation capacity within the AgMIP trans-disciplinary framework.

Chapter 5

Disentangling uncertainties in future crop water productivity under climate change

Preface

This chapter describes research conducted for the ISI-MIP fast-track exercise in 2012 looking at global crop model responses to increasing atmospheric CO_2 concentrations ([CO_2]). This intercomparison analysis considers six global gridded crop models (GGCMs) from various modelling backgrounds as described in Chapter 4 and provides a unique assessment of modelling techniques with respect to CO_2 fertilisation effects and evaluation against available observed data. The text is a revised version of that initially submitted for publication in the *Proceedings of the National Academy of Sciences* as part of the ISI-MIP special features: Deryng et al.. My role here has been substantial as I designed the research, coordinated the modelling intercomparison effort, ran PEGASUS' simulations, developed analytic tools, analysed data and wrote the paper. Rosenzweig, Elliott, Ruane, Boote, Jones, Gerten and Schaphoff co-designed the research; Elliott, Folberth, Müller, Pugh, Schmid, Khabarov, Olin, and Yang also performed research; Elliott and Ruane contributed scientific inputs to analyse data; and all co-authors helped revise the text. This new version of the manuscript includes a number of substantial improvements suggested by two anonymous reviewers, including:

1. A better description of the methodology developed to handle differences in GGCM outputs due to the use of different $[CO_2]$ baselines in climate change only simulations;

2. A comprehensive review of existing FACE measurements for maize, wheat, rice and soybean on CO_2 fertilisation effects on both yield and actual evapotranspiration and comparison with simulated effects from the GGCM ensemble.

Abstract

Projected future population growth and dietary shifts will require a substantial increase in global food production, which will be constrained by freshwater availability, climate change impacts, and a variety of socioeconomic factors. The direct influence of increasing atmospheric CO_2 concentration ($[CO_2]$) on crops is possibly the only effect that could act to reduce pressure on water resources and increase attainable yields and thus increase crop water productivity (CWP). This study compares for the first time CWP for maize, wheat, rice, and soybean, as computed by six global gridded crop models (GGCMs) under projections from five General Circulation Models (GCMs) following the RPC 8.5 emission trajectory, focusing on potential beneficial effects of elevated $[CO_2]$. Global average CWP increases by 5.6 ± 26.6 (in the case of rice) to $17.3 \pm 20.3\%$ (in the case of wheat) by the 2080s when both climate change and CO_2 effects are considered, but decreases by -14 ± 16.5 (in the case of maize) to $-28.4 \pm 13.9\%$ (in the case of soybean) in the absence of CO_2 fertilisation effects. Disparities among GGCMs simulations by the 2080s double when including CO_2 effects. Moreover, substantially larger uncertainties result from the use of multiple GGCMs than from the use of multiple GCMs, reflecting fundamental uncertainties and gaps in our understanding of crop response to elevated CO_2. These results show that rising atmospheric $[CO_2]$ may have beneficial effects on crop water use, and crop yields, but also emphasise an urgent need for better understanding and modelling of crop response to elevated CO_2 and climate change, to support more robust assessments of future food production.

5.1   Introduction

5.1.1   The effects of carbon dioxide on crops

Increasing greenhouse gas (GHG) emissions into the atmosphere, including CO_2 emissions from various activities (transportation, energy, industry, agriculture, and land use change), are transforming the Earth's land surface energy balance and its global biogeochemistry (Stocker et al., 2013). CO_2 contributes to the greenhouse effect by directly affecting the Earth's climate and plays a crucial role in vegetation growth by stimulating photosynthesis and reducing stomatal conductance (Kimball, 2011; Vanuytrecht et al., 2012). Through this mechanism, elevated atmospheric CO_2 concentrations ($[CO_2]$) can improve overall crop water productivity (CWP), i.e. the ratio of crop yield to seasonal evapotranspiration (ET) (Burkart et al., 2011; Kimball, 2011).

The general effects of CO_2 on crops are well established but quantified estimates of actual fertilisation effects on crops based on observations continue to be controversial due to their dependence on experimental methodology: to date, it is not clear whether results from enclosure and Free-Air-Carbon-Enrichment (FACE) experiments agree or not and further comparison analyses need to be conducted (Ainsworth et al., 2008; Kimball, 2011; Long et al., 2006; Tubiello et al., 2007). Quantification is extremely challenging as understanding of complex field-scale crop-CO_2 interactions with temperature, soil water and nutrients content and surface ozone (O_3) concentration is patchy across biomes (Leakey et al., 2012; Rosenthal et al., 2012). Atmospheric $[CO_2]$ recently reached 400 parts per million (ppm)[1], a 43% increase from pre-industrial concentration levels (280 ppm), and it continues to rise rapidly. Therefore a thorough understanding of CO_2 effects on crops and interactions with environmental factors is urgently needed to anticipate climate change impacts on future global crop productivity and design valuable climate mitigation and adaptation strategies in the agriculture sector.

Results from FACE experiments show crops grown under elevated $[CO_2]$ display higher rates of photosynthesis (up to 45%), increases in crop yield (up to 50%) and lower crop ET (down by 20%) (Kimball, 2011). These ranges of effects are large and reflect differences in CO_2 fertilisation effects among crop types (C_3 versus C_4 crops, cereals

---

[1]on 10 May 2013

versus legumes and tubers) (Kimball, 2011) and among crop growing conditions (Leakey et al., 2009). CO_2 fertilisation effects are higher for C_3 crops, with legumes – such as soybean – and tubers – such as cassava and potato – being the most responsive crop species (Rosenthal et al., 2012). On the other hand, C_4 crops – such as maize and sorghum – are less responsive to direct CO_2 enhancement of photosynthesis. However, yield of C_4 crops do increase under elevated $[CO_2]$ when soil water availability is limited, because elevated $[CO_2]$ decreases stomatal conductance and therefore contributes to a more efficient use of water (Ainsworth and Rogers, 2007). In fact, soil water and nutrients, chiefly nitrogen (N), play a crucial role in CO_2 fertilisation effects. Crops grown under N limited conditions exhibit smaller positive effects on photosynthesis and yield under elevated $[CO_2]$ than when soil N content is abundant (Brooks et al., 2000; Farage et al., 2013; Kim et al., 2003; Romanova et al., 2002; Vilhena-Cardoso and Barnes, 2001; Weerakoon et al., 2000). On the contrary, crops grown in dry conditions show larger increases in relative crop yield and overall CWP (Baker et al., 1997; Bernacchi et al., 2006; Chun et al., 2011; Conley et al., 2001; Ferris et al., 1998b; Manderscheid and Weigel, 2007; Markelz et al., 2011; Widodo et al., 2003). Experimental results show temperature optima for some processes are shifted under elevated CO_2 (Berry and Bjorkman, 1980; Fleisher et al., 2011; Long, 1991; McMurtrie et al., 1992; McMurtrie and Wang, 1993; Stuhlfauth and Fock, 1990). Dieleman et al. (2012) show both elevated $[CO_2]$ and warming exert fundamentally different effects on photosynthesis and soil C and N cycling, which interact with crop development in a non-additive manner. Crops exposed to high O_3 concentrations exhibit lower photosynthesis and yield as O_3 damages photosynthetic pigments and proteins, but elevated $[CO_2]$ alleviates and sometimes completely cancels out the negative effects of O_3, owing to the reduction in stomatal conductance, which reduces O_3 uptake (Ainsworth, 2008; Booker, 2000; Booker et al., 2005; Clausen et al., 2011; Feng and Kobayashi, 2009; Heagle et al., 2000; Pleijel and Uddling, 2011; Reid and Fiscus, 1998; Vilhena-Cardoso and Barnes, 2001).

Enclosure experiments, especially designed for characterising crop responses to CO_2 and temperature and other abiotic factors, do not reflect realistic growing conditions in the field (Fleisher et al., 2011). Whilst current FACE experiments are overwhelmingly located in temperate regions (e.g. in Illinois for soybean, Arizona for maize, Germany for wheat, and China and Japan for rice), experimental data are scarce in high latitudes, as well as in the tropics and subtropics where food security is most threatened (Leakey

et al., 2012; Rosenthal et al., 2012).

5.1.2 Process-based crop models

Modelling techniques, including statistical and process-based dynamic models, offer valuable tools to examine the full range of climate change impacts on agriculture, however CO_2 effects remain the main source of uncertainty so that crop modelling studies either purposefully omit them or present results both with and without them to provide a range of uncertainty (Nelson et al., 2009; Parry et al., 2004). In order to improve modelling of CO_2 effects, crop models needs to be thoroughly evaluated against observations and against each other. A joint effort between the model intercomparison projects AgMIP and ISI-MIP (Chapter 4 & Rosenzweig et al., 2014) enables, for the first time, a comparative assessment of six global gridded crop models (GGCMs) introduced in Chapter 4, with simulations using climate input data from five global climate models (GCMs) and four Representative Concentration Pathways (RCPs) (Hempel et al., 2013; Moss et al., 2010).

This chapter focuses on GGCM structural differences in simulating the CO_2 effects on photosynthesis and crop water use for four of the world's major crops (maize, wheat, rice and soybean), and how this affects future projections of crop yields. We consider two sets of simulations including or excluding CO_2 effects on crops. To synthesise both yield and water use variables given the effects of CO_2 on photosynthesis and transpiration, we compare GGCM simulations using CWP, defined by the United Nations Food and Agriculture Organisation (FAO) as the ratio of crop yield to total water use throughout the crop development period, i.e. actual evapotranspiration (AET) during the growing period (Kassam and Smith, 2001). CWP changes are complex due to the interactions between crop biomass production and water use. Yield increases due to the direct fertilisation effect on photosynthesis, and indirectly through a possible reduction in water stress caused by the decrease in stomatal conductance (Leakey et al., 2009; Wullschleger et al., 2002). However, AET increases or decreases depending on which effect is predominant: the effect of decreasing stomatal conductance or the effect of increasing leaf area driven by increasing biomass productivity (Long et al., 2006; Tubiello et al., 2007). In addition, the radiative effects of $[CO_2]$ mediated through climate change affect both yield and AET directly. Among the GGCMs considered here, only GEPIC (Liu

et al., 2007) and LPJmL (Fader et al., 2010; Gerten et al., 2011), were used previously to estimate CWP. GEPIC analysis focused on present-day estimates of CWP and its spatial variability, LPJmL analyses showed a global increase in CWP when considering both climate change and CO_2 effects, even though many regions potentially face decreases in CWP and responses differ among crop types.

This chapter addresses one of the most controversial effects of climate change on crop growth: the role of carbon fertilisation. Indeed, we expect this process to contribute to a greater extent to divergence in simulated yields than direct effects of changes in temperature and precipitation patterns. As reviewed at the beginning of this section, knowledge on actual effects of CO_2 fertilisation in the field across the world is limited. Although level of agreement among GGCMs in the sign of change in simulated crop yields, AET and CWP should be fairly good, we expect level of agreement in the intensity of the effect to vary extensively due to GGCM structural, parametric and calibration differences that influence greatly their response to elevated [CO_2]. Yet, it is not clear which of these factors would be the most influential in driving model differences. We aim to assess whether GGCMs reproduce well findings from FACE experiments. For instance, CO_2 fertilisation effects should be stronger under water-stress conditions because elevated [CO_2] improves crop water use efficiency and under high rates of fertiliser application. Finally, due to spatial differences in agroclimatic conditions, CO_2 fertilisation effects should vary in intensity across regions and we aim to identify hot-spots of impacts and agreements.

This analysis first presents global average results of future relative change in CWP up to 2099 compared to a present-day (30-years average 1980-2010) baseline with and without inclusion of CO_2 effects on crops. We evaluate the uncertainties arising from multiple GGCMs (EPIC (Izaurralde et al., 2006; Williams, 1990, 1995), GEPIC (Folberth et al., 2012), LPJmL (Bondeau et al., 2007; Waha et al., 2011), LPJ-GUESS (Lindeskog et al., 2013), pDSSAT(Jones et al., 2003) and PEGASUS (Deryng et al., 2011); see section 3.2) and GCMs in the ensemble under RCP 8.5. As well, we report spatial differences between CWP calculated by each GGCM with, and without, CO_2 effects. Finally, we identify and attribute the main drivers of differences among GGCMs response to CO_2 fertilisation effects before discussing the findings and concluding on further GGCM development and improvement needs.

5.2 Methods

5.2.1 Simulations protocol

We compare crop yield and corresponding AET for two sets of experiments: CC (taking into account both climate change and CO_2 effects) and $CC_{\text{w/o } CO_2}$ (taking into account the climate signal with constant $[CO_2]$) as simulated by six GGCMs using daily climate input from 1971 to 2099 provided by the ISI-MIP fast-track (Hempel et al., 2013). This study considers three C_3 crops (wheat, rice, soybean) and one C_4 crop (maize). We calculate CWP (in kg m^{-3} yr^{-1}) for a specific year following the equation: $CWP = 100Y/AET$ where Y is the crop yield in ton ha^{-1} yr^{-1} and AET is the total actual evapotranspiration in mm over the growing season of that specific year. Note we use annual AET for EPIC and pDSSAT as these model did not compute AET over the growing season but since this study focuses on normalised percent change, the results are still comparable.

The GGCMs used different $[CO_2]$ baselines when performing their $CC_{\text{w/o } CO_2}$ simulations. Therefore, relative changes in yield, AET and CWP between CC and $CC_{\text{w/o } CO_2}$ simulations are calculated here, rescaled to a common baseline, to take into account the differences and ensure consistency among results. PEGASUS simulated spring wheat everywhere for the wheat simulations and does not simulate rice (Chapter 2).

Each year of crop yield data is averaged over a 30-year or a 10-year period according to the ISI-MIP protocol. GGCMs performed simulations over the entire land surface according to climate suitability to grow crops (Chapter 4 section 4.4.1). Four different sets of runs were performed: no irrigation (i.e. rainfed) and fully irrigated with and without CO_2. We then mask out results to current cropland harvest area using the Earthstat dataset (Monfreda et al., 2008) and calculate global average CWP from actual yield combining both fully irrigated and rainfed yields according to the MIRCA data for irrigated cropland areas (Portmann et al., 2009).

Climate inputs are taken from five downscaled GCMs under four RCPs (Hempel et al., 2013). All GGCMs computed yield and AET with and without CO_2 effects using climate input from HadGEM2-ES under four RCPs (2.6, 4.5, 6.0, and 8.5). Only EPIC, LPJmL, pDSSAT and PEGASUS computed yield and AET with and without CO_2 effects for the

other GCMs but solely under RCP 8.5 (Chapter 4 section 4.4.2. For some part of this analysis, we use the full set of results (i.e. HadGEM2-ES×4RCPs and 4GCMs×RCP8.5) but for some other parts, we only use results under RCP 8.5 as this study focuses mostly on assessing the effect of elevated atmospheric $[CO_2]$.

A comprehensive description of the GGCM modelling approaches and settings for this intercomparison exercise is described in Chapter 4 section 4.4.

5.2.2 Application of a scaling factor ϵ_0 to account for different carbon dioxide baselines

We apply a scaling factor to estimate relative change in yield, AET and CWP to account for the different $[CO_2]$ baselines in models.

Relative change in yield between future (t_1) and present-day (e.g. $t_0 = 2000$ and $[CO_2]_{t_0=2000} = 368$ ppm) simulated under CC is expressed as:

$$\Delta Y_{1_{CC}} = \frac{Y_{1_{CC}}}{Y_{0_{CC}}} - 1 \tag{5.1}$$

where $Y_{1_{CC}}$ is the absolute yield at time t_1 under CC and $Y_{0_{CC}}$ is the absolute yield at time t_0 under CC.

Relative change in yield simulated under $CC_{w/o\ CO_2}$ is expressed as:

$$\Delta Y_{1_{CCw/o\ CO_2}} = \frac{Y_{1_{CCw/o\ CO_2}}}{Y_{0_{CCw/o\ CO_2}}} - 1 - \epsilon_0 \tag{5.2}$$

where $Y_{1_{CCw/o\ CO_2}}$ is the absolute yield at time t_1 under CC and $Y_{0_{CCw/o\ CO_2}}$ is the absolute yield at time t_0 under CC and ϵ_0 is the scaling factor for the CO_2 effect and expressed as:

$$\epsilon_0 = \frac{Y_{0_{CC}}}{Y_{0_{CCw/o\ CO_2}}} - 1 \tag{5.3}$$

Finally, the relative difference in yield with (CC) and without the CO_2 ($CC_{w/o\ CO_2}$) effect at time t_1 (e.g. the 2050s or 2080s) is expressed as:

$$\Delta Y_{1_{\Delta CO_2}} = \frac{Y_{1_{CC}}}{Y_{1_{CCw/o\ CO_2}}} - 1 - \epsilon_0 \tag{5.4}$$

Similar equations are used for AET and for CWP.

5.2.3   Comparison of model and site–specific FACE experiments

We identified four FACE study sites reporting CO_2 effects on CWP:

- Braunschweig, Germany (52°29'N, 10°45'E) for maize;

- Maricopa, Arizona, United States (33°06'N,112°05'W) for wheat;

- Iwate, Japan (39°38'N, 140°57'E) for rice;

- Illinois, United States (40°03'N, 88°12'W) for soybean;

and selected corresponding yield and AET values from the GGCM simulations at grid-cells matching their coordinates to calculate $\Delta CWP_{\Delta CO_2}$ (for which a scaling factor was applied as described above). Ambient atmospheric $[CO_2]$ in the FACE experiments varied between 360 and 380 ppm and elevated CO_2 corresponds to 550 ppm. We used 10-year average around the year corresponding to the same CO_2 level (e.g. year circa 2005 for CO_2 = 380 ppm and the 2050s for 550 ppm) to compare relative change in CWP for the same increment of CO_2 rise (Table 5.1). Table 5.2 summarises N fertiliser application rates for each GGCMs at each FACE location.

5.3   Results

5.3.1   Climate signal

Global average temperature by the 2080s relative to the 2000s increases between 3.1℃ (GFDL-ESM2M on current harvested areas for maize and soybean) and 6℃ (MIROC-ESM-CHEM on current wheat harvested area), given the RCP 8.5 scenario in which $[CO_2]$ increases from 338 parts per million (ppm) in 1980 to 927 ppm in 2099. Median increases in global average temperature are 3.2℃, 4.3℃, 5.3℃, and 5.7℃ on current harvested areas for maize, rice, soybean and wheat respectively. Corresponding changes in annual precipitation range between a decrease of 47 mm yr^{-1} (GFDL-ESM2M on current harvested areas for maize and soybean) and an increase of 240 mm yr^{-1}

TABLE 5.1: Summary table of relative change in CWP at ambient and elevated CO_2 for FACE observations and GGCM simulations.

Crop	Reference	Ambient CO_2 (ppm)	Elevated CO_2 (ppm)	N fertiliser	H_2O	ΔCWP (%) median[range]
Maize	Manderscheid et al., 2012	378	550	High + bare soil	wet	[-3;8]
					dry	[1;39]
				High + mulch soil	wet	10
					dry	44
	This study	380	550	High (N app. varies with GGCM)	irrigated	13.1[8.6;17.9]
					rainfed	14.3[6.6;25.9]
Wheat	Hunsaker et al., 1996	370	550	High	wet	18
					dry	24
	Hunsaker et al., 2000	370	550	High	wet	[19;23]
				Low		[7;12]
	Kimball et al., 1999	360	550	High	wet	29
	This study	370	550	High (N app. varies with GGCM)	irrigated	15.4[9.6;52.7]
					rainfed	21.4[-4.2;84.9]
Rice	Shimono et al., 2013	365	548	High	paddy	20
	This study	365	550	High (N app. varies with GGCM)	irrigated	16.4[6.2;27.2]
					rainfed	16.4[6.2;30.8]
Soybean	Bernacchi et al., 2006	380	550	High	wet	29.4
	This study	380	550	High (N app. varies with GGCM)	irrigated	26.1[-19.0;35.4]
					rainfed	31.3[-15.0;47.1]

TABLE 5.2: Table summary of N fertiliser application rates (kg-N ha^{-1} yr^{-1}) for each GGCM at each FACE location.

Crop	EPIC	GEPIC	LPJmL	LPJ-GUESS	pDSSAT	PEGASUS
Maize	high	150	na	na	150	150
Wheat	high	63	na	na	70	63
Rice	high	110	na	na	80	na
Soybean	high	21	na	na	0	58.8

(MIROC-ESM-CHEM on current wheat harvested area). The median changes are -22, +25, +60 and +170 mm yr^{-1} on current harvested areas for maize, rice, soybean and wheat, respectively. Changes in annual mean temperature and precipitation are, however, not necessarily representative for changes in climate conditions during the cropping season. Depending on region, crop and GCM, changes within the cropping season can be either stronger or weaker than the annual mean.

5.3.2 Crop response to climate change only

We estimate relative change in global crop yield (ΔY), actual evapotranspiration (ΔAET) and crop water productivity (ΔCWP) for each of the four crops for near, medium and long time horizons (30-year averages around the 2020s, 2050s and 2080s, respectively) (see section 5.2). The GGCM-GCM ensemble simulates a strong decrease in yield ($-27.8 \pm 9.5\%$) and CWP ($-20.4 \pm 12.9\%$) and a moderate decrease in AET ($-6.3 \pm 8.9\%$) by the 2080s (Table 5.3).

TABLE 5.3: Relative change in global average yield, AET and CWP (%): Median values and corresponding median absolute deviation (MAD) defined as the median of the absolute deviations from the data's median across all GCMs–GGCMs combinations for CC simulations and CC$_{w/o\ CO_2}$ simulations as shown in Figures 5.1(a) & 5.1(b) for the long time horizon, i.e. the 2080s, under RCP 8.5.

	Yield		AET		CWP	
	CC	CC$_{w/o\ CO_2}$	CC	CC$_{w/o\ CO_2}$	CC	CC$_{w/o\ CO_2}$
Maize	-10.6±10.8	-24.2±10.8	-18.5±11.1	-10.5±10.9	12.4±22.5	-14.0±16.5
Rice	0.4±23.4	-26.5±8.7	-3.4±5.5	-2.0±6.1	5.6±26.6	-19.5±6.7
Soybean	-2.0±20.0	-37.2±10.6	-10.1±19.1	-7.1±15.3	7.1±29.8	-28.4±13.9
Wheat	3.9±8.9	-23.3±7.9	-10.5±8.5	-5.0±3.2	17.3±20.3	-19.5±14.5
All Crops	-2.1±15.8	-27.8±9.5	-10.6±11.1	-6.3±8.9	10.6±24.8	-20.4±12.9

While most GGCMs simulate decreasing CWP, which is largely independent of the climate scenarios (red boxes Figure 5.1(a)), there is considerable spread across GGCM

and crop, constituting the largest part of overall uncertainty in CWP response to $CC_{w/o\ CO_2}$ (grey boxes in Figure 5.1(a)). The main reason for GGCM uncertainty is differences in climate change effects on AET. While the six GGCMs tend to agree on a general decline in global yield over time when CO_2 effects are not included (Figure 5.2(a) and Rosenzweig et al., 2014), they tend to disagree in the sign and magnitude of change in simulated global average AET (Figure 5.3(a)), especially for maize and soybean, which is reflected in corresponding estimates of ΔCWP (Figure 5.1(a)). The GGCMs in this study use different methods to simulate crop water use and soil water dynamics (see section 5.2 and Chapter 4 section 4.4.1 and Rosenzweig et al., 2014), which drives notable differences in simulated AET and CWP responses to $CC_{w/o\ CO_2}$.

5.3.3 Crop responses to climate change and elevated carbon dioxide

When both climate change and CO_2 fertilisation effects are included (CC), median global impacts on CWP are positive ($10.6 \pm 24.8\%$ by the 2080s when $[CO_2]$ reaches 800 ppm). Compared to the $CC_{w/o\ CO_2}$ simulations, negative impacts on yield lessen ($-2.1 \pm 15.8\%$) and AET is more strongly reduced ($-10.6 \pm 11.1\%$) (Table 5.3). Impacts vary among crop types and GGCMs, reflecting differences in crop photosynthetic pathways and the way GGCMs handle those processes. Wheat, the only crop for which all GGCMs agree in a net positive change in ΔCWP, shows the highest gains in yield ($3.9 \pm 8.9\%$) and CWP ($17.3 \pm 20.3\%$) resulting from rising $[CO_2]$. As a C_4 crop, maize benefits the least from increases in $[CO_2]$ in respect to yield ($-10.6 \pm 10.8\%$), yet benefits the most in respect to CWP ($12.4 \pm 22.5\%$). Finally, rice and soybean show smaller gains in CWP ($5.6 \pm 26.6\%$ and $7.1 \pm 29.8\%$, respectively). Yield and CWP of rice and soybean exhibit larger disparities among GGCMs, with a clearer distinction between LPJmL and LPJ-GUESS and the other four GGCMs (Figures 5.1(b) & 5.2(b)). These differences are driven by model differences in simulating CO_2 effects, with strong CO_2 effects on stomatal conductance in the case of the LPJ models, contrasting with the radiation use efficiency (RUE) approach used in the other GGCMs (Chapter 4 section 4.4 & Rosenzweig et al., 2014).

In the case of rice and soybean in particular, LPJ-GUESS simulates an overall increase in AET, triggered by important CO_2 enhancement of photosynthesis leading to an expansion of the leaf area available for transpiration (Figures 5.2(b) & 5.3(b)). pDSSAT

(a) $CC_{w/o\ CO_2}$

(b) CC
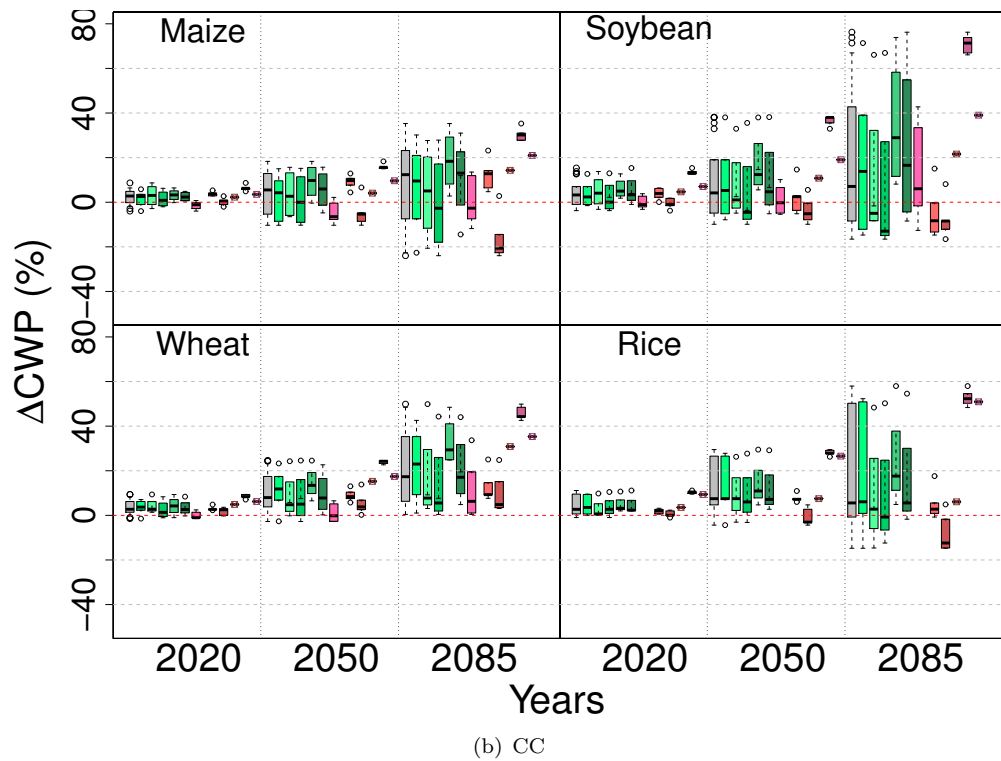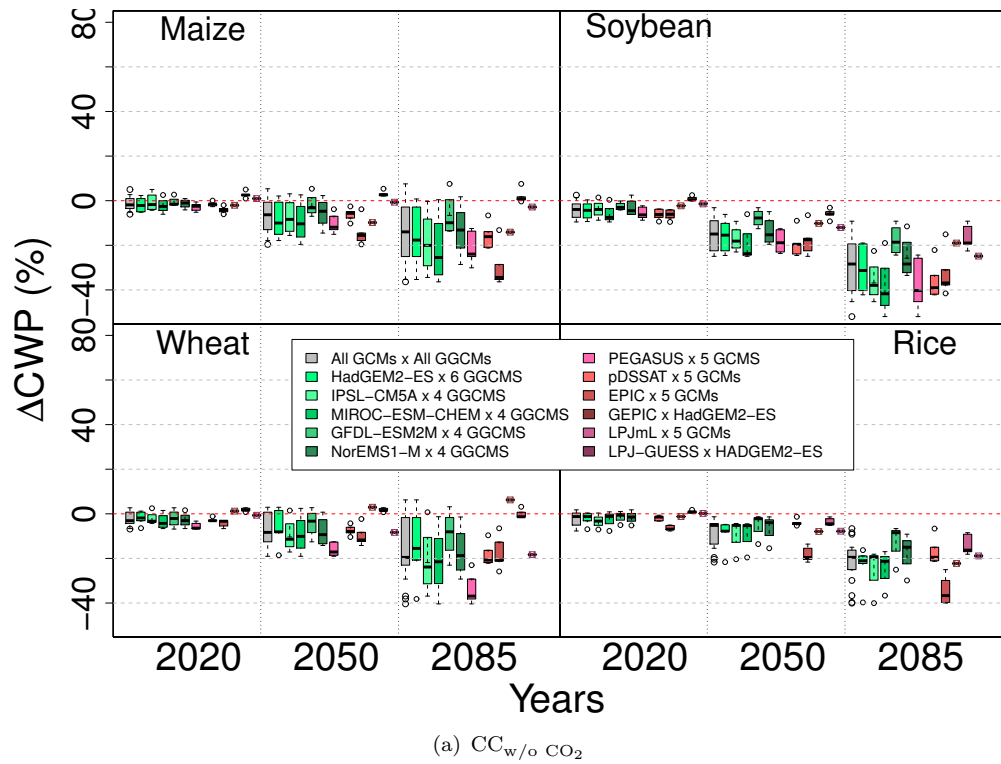
FIGURE 5.1: Global average ΔCWP (%) simulated under RCP 8.5 for all GGCMs–GCMs combinations for maize, wheat, soybean and rice for $CC_{w/o\ CO_2}$ simulations without CO_2 (a) and for CC (b). The bottom and top of the box are lower and upper quartiles,respectively, and the band near the middle of the box is the median value across each set of simulations. Grey boxplot represent the set of all GGCMs and GCMs combination. Green boxplots represent the set of multiple GGCMs combined to one GCM. Red boxplots represent the set of one GGCM combined to multiple GCMs. GEPIC and LPJ-GUESS show one unique data point as they were only run with HadGEM2-ES for this experiment.
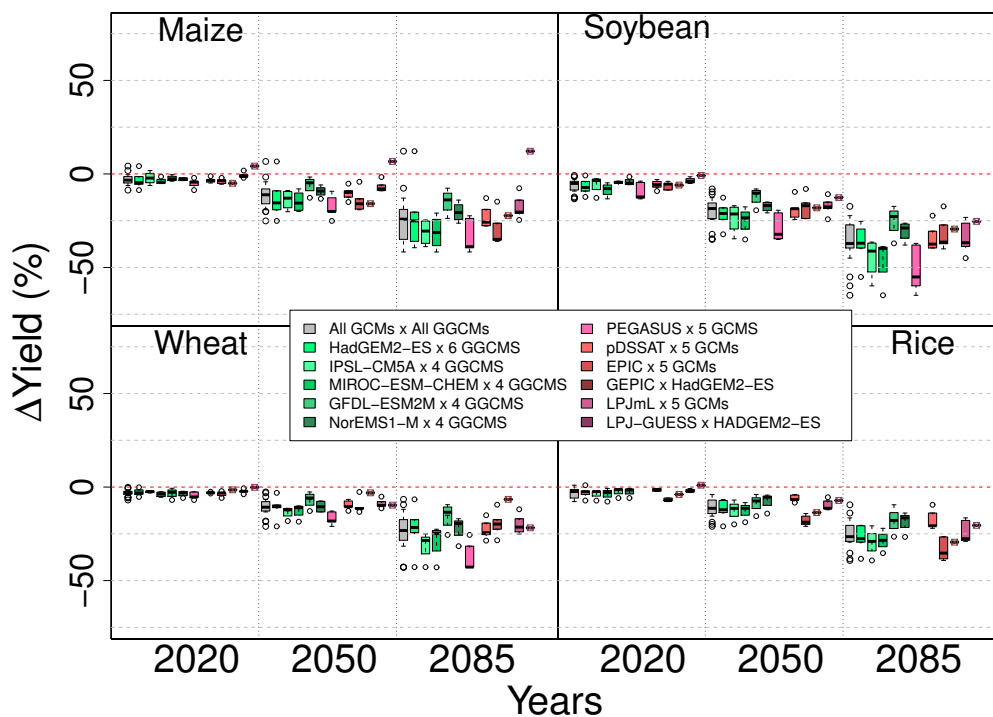
(a) $CC_{w/o\ CO_2}$
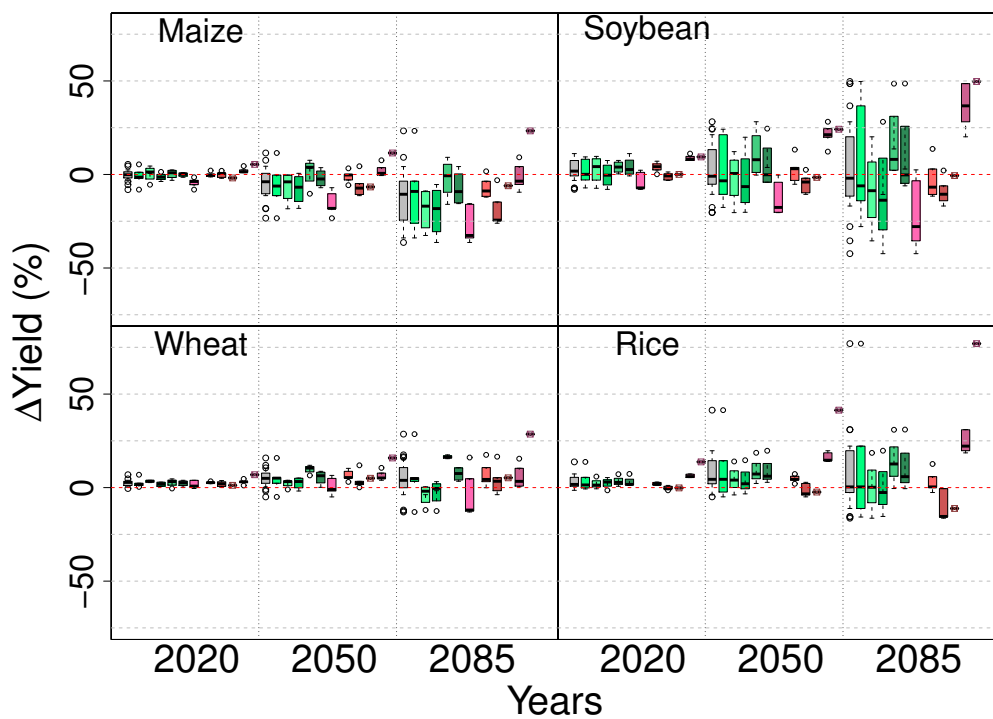
(b) CC

FIGURE 5.2: Same as Figure 5.1 for global average ΔYield (%)
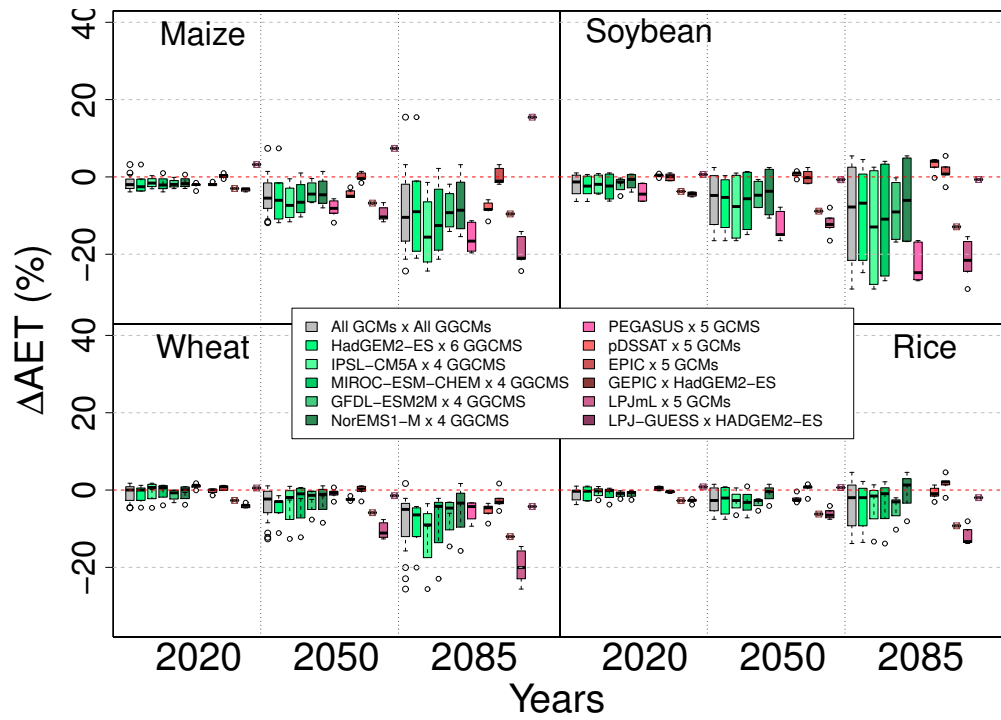
(a) $CC_{w/o\ CO_2}$
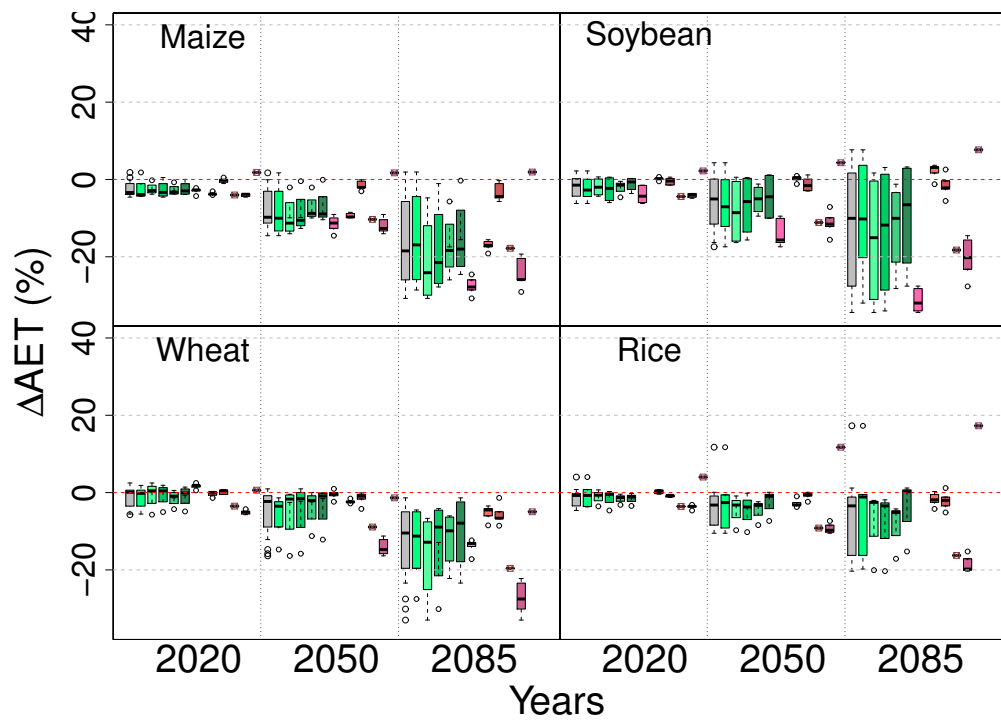
(b) CC

FIGURE 5.3: Same as Figure 5.1 for global average ΔAET (%)

also simulates an increase in ΔAET for soybean (Figure 5.3(b)) but because of greater water stress, manifested by a corresponding reduction in soybean yield, ΔCWP decreases (Figures 5.1(b) & 5.2(b)). PEGASUS shows the highest sensitivity to CC due to its stronger response to extreme temperature variability; with ΔCWP increasing or decreasing depending on the GCM used to drive the model.

Even when considering the CO_2 fertilisation effects, EPIC consistently simulates a decrease in ΔCWP for maize, rice and soybean, whereas GEPIC, which is based on the same crop model version but uses a different parameterisation and different management practices assumptions (Chapter 4 section 4.4.1), simulates large increases in CWP. In general, CO_2 effects in rainfed conditions tend to be stronger for maize in particular but the spread in the ensemble is similar in rainfed and fully irrigated conditions (Figure 5.4).
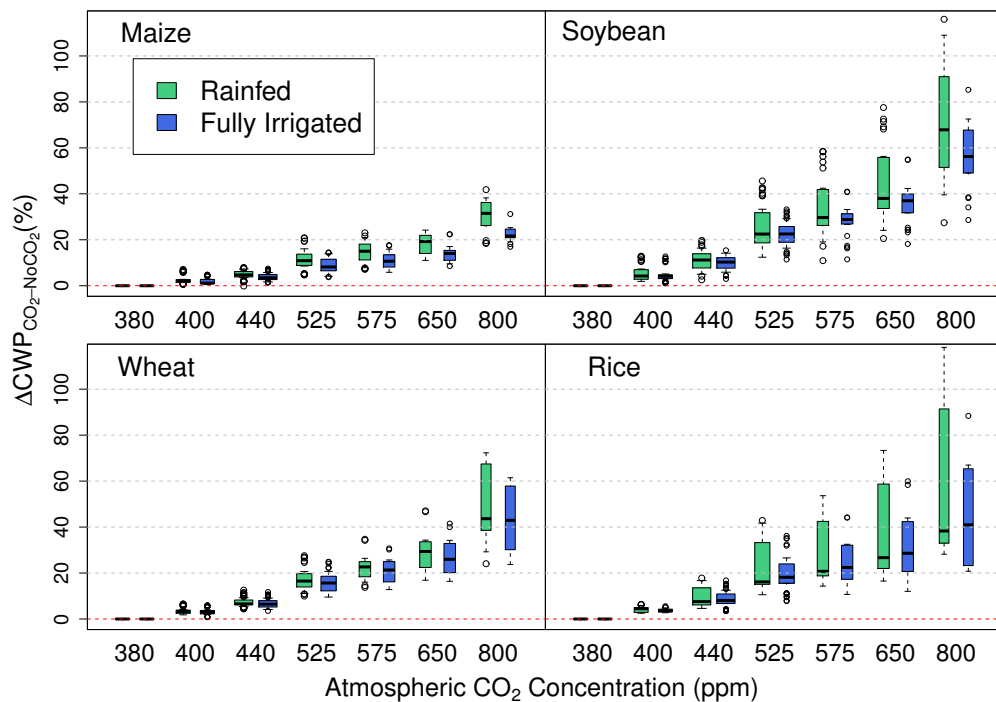
FIGURE 5.4: Relative difference between CWP under CC effects and CWP under $CC_{w/o\ CO_2}$ only ($\Delta CWP_{\Delta CO_2}$) for 40 RCP–GCMs–GGCMs combinations (including RCP 8.5 for all GCMs and also RCP 2.6, 4.5 and 6.0 for HadGEM2-ES) for rainfed (green boxes) and fully irrigated (blue boxes) scenarios. The bottom and top of the box are lower and upper quartiles,respectively, and the band near the middle of the box is the median value in the ensemble.

Among GGCMs run with multiple GCM input data, PEGASUS and LPJmL show higher AET sensitivity to the climate signal than pDSSAT and EPIC, especially for maize and soybean as they simulate the largest decreases in ΔAET (Figure 5.5(b)).
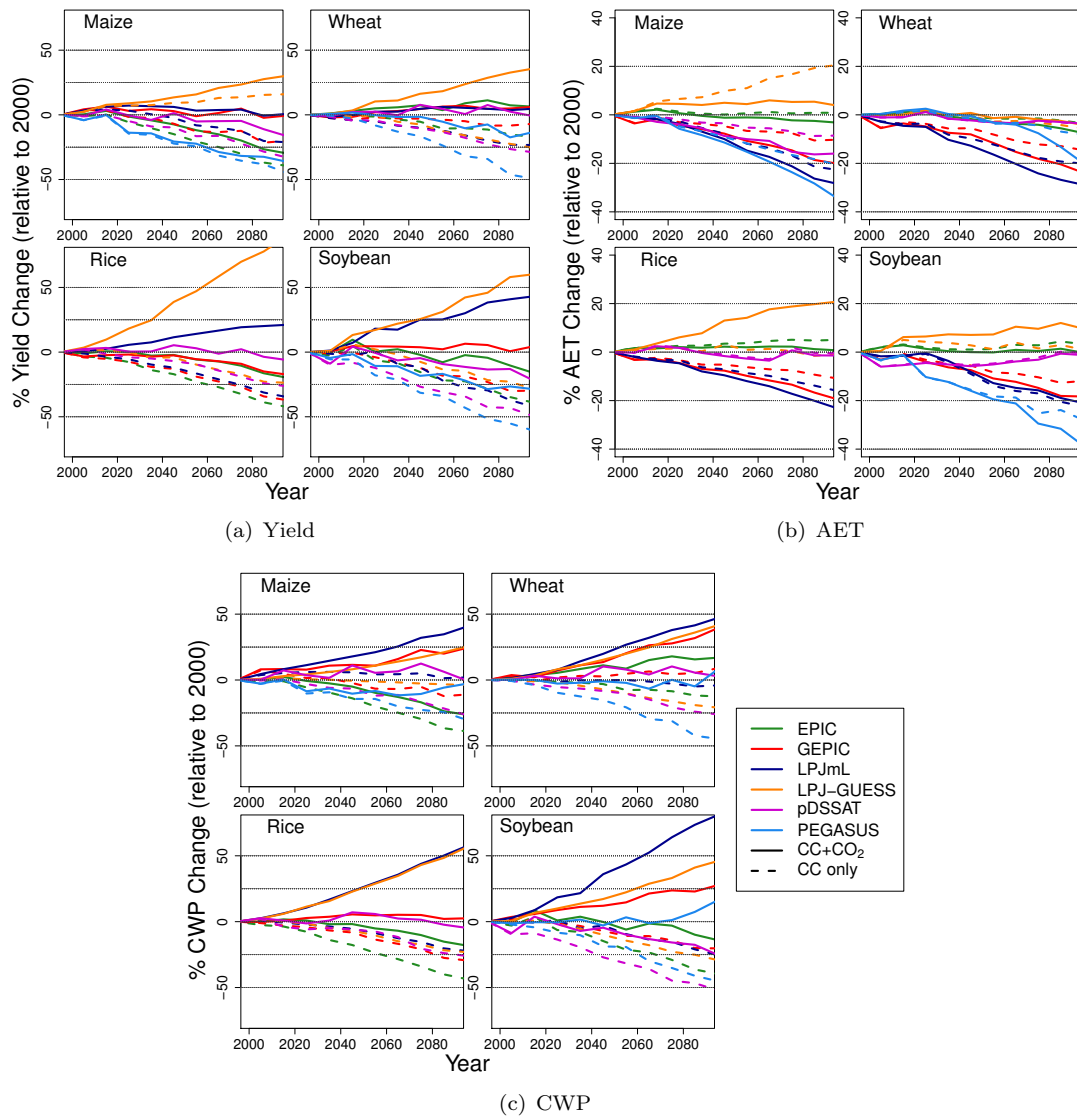
FIGURE 5.5: Global average ΔYield (a), ΔAET (b) and ΔCWP (c) (%) relative to 2010 simulated under RCP 8.5 for HadGEM2-ES. Solid lines show simulation under both climate change and CO_2 effects whereas dashed-lines show simulation under climate change effects only, i.e. with constant atmospheric $[CO_2]$.

However, LPJmL simulates the least impact on ΔCWP in comparison to the other GGCMs displaying a similar level of yield sensitivity but a lower AET sensitivity. Since PEGASUS is the only model simulating detrimental effect of extreme heat stress at anthesis (Chapter 3 & Deryng et al., 2014), it is the most sensitive and pessimistic with respect to global average yield (Rosenzweig et al., 2014 & Figure 5.5(a)), which results in a larger reduction in ΔCWP. In the case of wheat, GEPIC actually simulates a 6% increase in ΔCWP due to a small decrease in global average yield along with a large reduction in global average AET by the 2080s.

5.3.4 Comparison of model and site–specific FACE experiments

ΔCWP of the GGCMs is generally in the range of the observed ΔCWP values in FACE under comparable CO_2 enrichment (Figure 5.6 and Table 5.1). GGCMs capture differences between wet and dry conditions, with higher increases in CWP under water stress, as shown in the case of wheat and soybean but also the wider range of results (Figure 5.6). However, fully irrigated and rainfed simulations of ΔCWP for maize and rice are very similar because the corresponding locations (in Germany for maize and in Japan for rice) experience little water stress. Model simulations and observations indicate soybean is the most responsive to CO_2 under wet conditions, whereas maize is the most responsive under dry conditions according to FACE measurements (GGCMs results for maize correspond to minor water stress and cannot be compared to dry condition experiments which artificially minimised rainfall). Finally, Maize ΔCWP differs little from C_3 crops indicating water conservation is more important for C_4 crops since yield is less responsive to CO_2.
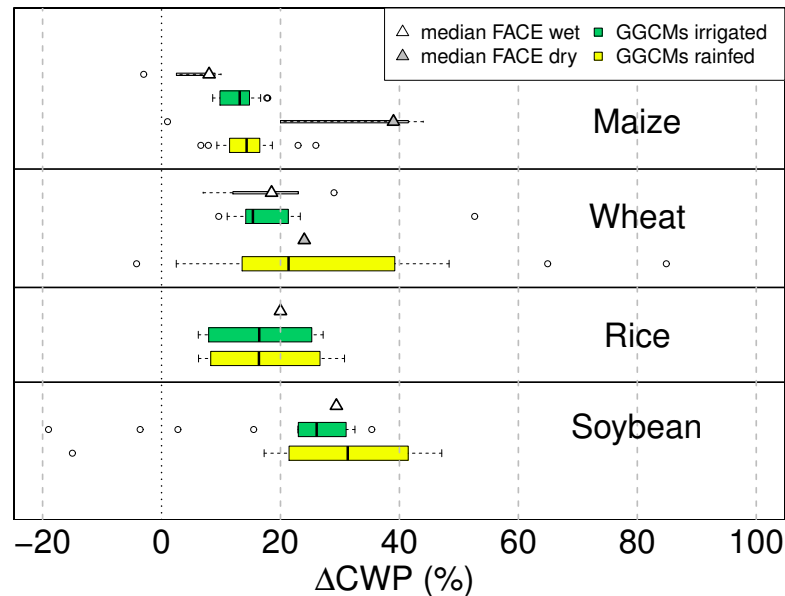
FIGURE 5.6: Crop water productivity responses (median $\pm$ standard error) to elevated CO_2 (550 ppm from FACE and corresponding grid-cell values extracted from GGCM simulations in this study) for maize, wheat, rice and soybean at ample and limited soil water. FACE data were collected from references summarised in Table 5.1. The left and right sides of the box are lower and upper quartiles, respectively, and the band near the middle of the box is the median value across each set of simulations. Open circles are outliers.

5.3.5   Carbon dioxide effects in rainfed versus irrigated cropland

Figure 5.4 shows calculated differences in CWP with and without CO_2 effects ($\Delta CWP_{\Delta CO_2}$), plotted as a function of $[CO_2]$, for the 40 RCP/GCM/GGCM combinations (results include RCP 8.5 for all GCMs and also RCP 2.6, 4.5 and 6.0 for HadGEM2-ES) and for rainfed and fully irrigated scenarios (where irrigation requirements are satisfied accross all cropland regardless of freshwater supply). Median values of $\Delta CWP_{\Delta CO_2}$ are found to be higher for rainfed maize, which is a C_4 crop and mostly responds to elevated $[CO_2]$ via increased water use efficiency in arid conditions. The magnitudes of differences between $\Delta CWP_{\Delta CO_2}$ in rainfed and fully irrigated conditions are equivalent for soybean and wheat, except at extremely high $[CO_2]$ (> 800ppm), when CO_2 effects overshoot in LPJmL and LPJ-GUESS models. Rice, which is mostly grown in flooded environments, shows a large spread in the RCP/GCM/GGCM ensemble but does not show large differences in $\Delta CWP_{\Delta CO_2}$ between irrigated and rainfed conditions. In fact, $\Delta Y_{\Delta CO_2}$ is almost identical under rainfed or irrigated conditions.

5.3.6   Spatial patterns of carbon dioxide effects

Global gridded crop models from similar families, i.e. EPIC and GEPIC, LPJmL and LPJ-GUESS, tend to agree on the spatial variation of the CO_2 response (Figure 5.7). Yet EPIC simulates lower CO_2 effects in low N input regions. In fact, PEGASUS, with similar $\Delta CWP_{\Delta CO_2}$ to the magnitude of the EPIC models, tends to follow LPJ spatial variations; all three GGCMs use the same modified Priestley-Taylor approach (Gerten et al., 2004) to simulate ET. On the other hand, the EPIC GGCMs both use the Penman-Monteith method (Monteith, 1965; Penman, 1948) (and Chapter 4 section 4.4.1). pDSSAT uses the Priestley-Taylor method (Priestley and Taylor, 1972). The use of different ET equations influences GGCMs response especially in arid regions, confirming recent studies that compare both methods (Sumner and Jacobs, 2005; Utset et al., 2004; Vinukollu et al., 2011).

Note that we intentionally show spatial patterns for the case of soybean, which is a N-fixing crop, to minimise uncertainties from differences among various modelling approaches regarding N limitations (Chapter 4 section 4.4.1). Indeed, some GGCMs

from this comparison study reported optimum yields with no nutrient limitation (LPJmL, LPJ-GUESS), while some reported nutrient limited yields using static – not accounting for the role of timing of application – N fertilisation from observation (PEGASUS) or dynamic N fertilisation from observation (pDSSAT & GEPIC), or dynamic N fertilisation using a high input thresholds (EPIC) (Chapter 4 section 4.4.1). N-limited crops are likely to have reduced sensitivity to $[CO_2]$ changes. PEGASUS and LPJmL show lower $\Delta CWP_{\Delta CO_2}$ in the United States than in Brazil unlike EPIC, GEPIC, and pDSSAT. LPJ-GUESS shows a similar range of $\Delta CWP_{\Delta CO_2}$ in the United States and in northern Brazil, where results are higher than in southern Brazil. Higher $\Delta CWP_{\Delta CO_2}$ is found in southern Asia than in northern Asia for LPJmL, LPJ-GUESS and PEGASUS, with the reverse true in pDSSAT and no clear difference in the EPIC models. Overall, PEGASUS shows higher $\Delta CWP_{\Delta CO_2}$ in low yielding areas while the EPIC models show the opposite pattern. For PEGASUS these spatial patterns are induced by a stronger relative CO_2 photosynthesis enhancement in low yielding areas than in already optimum yielding areas, such as in the United States, which is driven by a positive feedback due to leaf-area-index reaching a specific threshold value at which biomass production kicks-off.

5.4 Global gridded crop model uncertainties and differences

5.4.1 Spread in the ensemble

This study reveals large uncertainties in the responses of GGCMs to elevated $[CO_2]$, with variability in GGCM responses increasing with $[CO_2]$. For each time horizon, results display larger uncertainties resulting from multiple GGCM responses than from GCM differences, especially when CO_2 effects are included. In general, ΔCWP tends to increase when CO_2 effects are included but uncertainties among GGCMs increase, especially for maize, soybean, and rice. Uncertainties in simulated ΔAET appear to be large both with and without simulation of CO_2 effects and are substantially larger than uncertainty in the climate signal. For maize, AET tends to decrease greatly as atmospheric $[CO_2]$ rises due to a much smaller CO_2 fertilisation effect for C_4 crops allowing the stomatal response to dominate. However, AET reduction for C_3 crops is
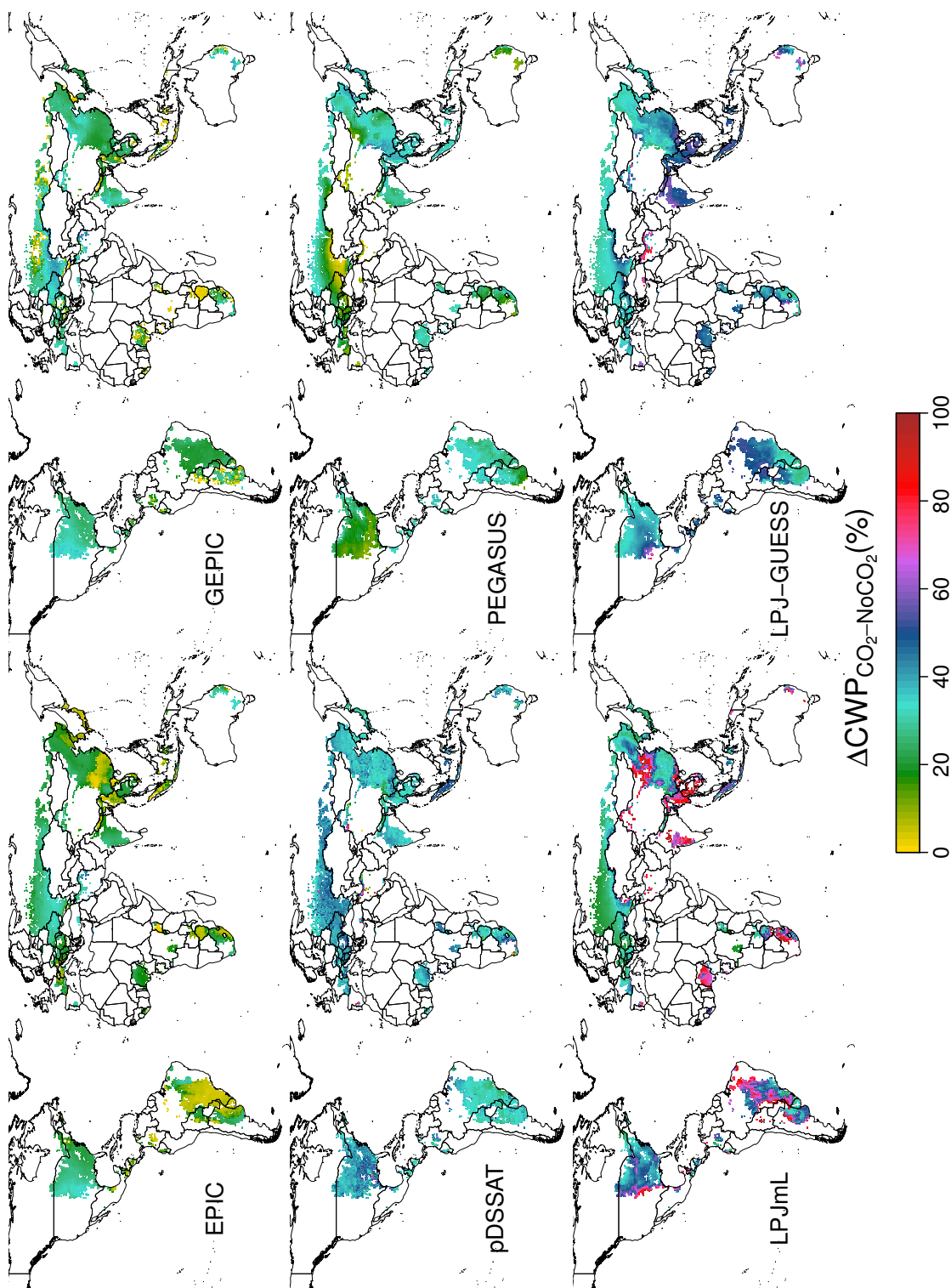
FIGURE 5.7: Map of actual soybean $\Delta\text{CWP}_{\Delta\text{CO}_2}$ (%) simulated by the six GGCMs in the 2050s under the RCP 8.5 HadGEM2-ES climate change scenario. Simulated area is masked by current soybean harvested area including both rainfed and irrigated soybean cultivations. Rainfed and fully irrigated simulations are combined using the MIRCA dataset on current irrigated soybean areas.

attenuated by higher transpiration demand driven by growing leaf area resulting from the strong photosynthesis enhancement effect. GGCMs tend to agree fairly well for wheat CO_2 response.Table 5.4 shows median and corresponding median absolute deviation (MAD) from median values of relative change as a metric to evaluate the spread in the results ensemble. By 2020s, the average MAD across the four crops amounts to 1.8% (and rises to 3.7% by the 2050s and 7.8% by the 2080s) when a single GGCM response is considered, whereas it amounts to 4.2% (and rises to 13.4% by 2050s and 24.8% by the 2080s) when all GGCMs responses are taken into account. The inclusion of the six GGCMs in this impact assessment of the role of elevated CO_2 on global CWP triples the range of uncertainties for medium and long time horizons. Finally, the MAD is higher in the case of soybean, which shows greater disagreement among GGCMs response to both climate and CO_2 fertilisation effects.

TABLE 5.4: Relative change in global CWP (%): Median and MAD values across all GCMs–GGCMs combinations for CC simulations and $CC_{w/o\ CO_2}$ simulations as shown in figures 1 & 2.

			2020: 418 ppm		2050: 545 ppm		2085: 794 ppm	
			CC	$CC_{w/o\ CO_2}$	CC	$CC_{w/o\ CO_2}$	CC	$CC_{w/o\ CO_2}$
	All GCMs	All GGCMs	2.8 ± 3.5	-1.9 ± 3.1	5.5 ± 14.2	-6.3 ± 9.1	12.4 ± 22.5	-14.0 ± 16.5
Maize	All GCMs	1 GGCM	2.6 ± 1.2	-1.1 ± 0.9	4.5 ± 2.4	-6.8 ± 2.0	9.2 ± 5.2	-15.1 ± 3.4
	1 GCM	All GGCMs	2.4 ± 3.5	-1.8 ± 2.5	4.5 ± 11.3	-7.3 ± 7.1	8.7 ± 19.1	-17.2 ± 11.7
	All GCMs	All GGCMs	2.7 ± 3.9	-1.2 ± 3.0	7.5 ± 15.6	-5.2 ± 4.0	5.6 ± 26.6	-19.5 ± 6.7
Rice	All GCMs	1 GGCM	5.1 ± 0.9	-1.7 ± 0.6	13.2 ± 0.9	-8.8 ± 0.9	19.9 ± 2.2	-22.7 ± 2.1
	1 GCM	All GGCMs	2.5 ± 2.8	-1.6 ± 3.6	7.8 ± 12.5	-4.9 ± 2.4	6.3 ± 20.7	-17.1 ± 4.6
	All GCMs	All GGCMs	3.3 ± 5.9	-3.9 ± 4.5	4.2 ± 13.9	-14.9 ± 10.0	7.1 ± 29.8	-28.4 ± 13.9
Soybean	All GCMs	1 GGCM	4.4 ± 1.8	-3.7 ± 1.8	10.8 ± 4.0	-14.0 ± 3.8	20.2 ± 8.2	-29.8 ± 5.7
	1 GCM	All GGCM	3.0 ± 4.8	-4.7 ± 2.7	3.8 ± 8.6	-16.1 ± 4.8	8.3 ± 20.5	-31.6 ± 8.3
	All GCMs	All GGCMs	2.7 ± 3.6	-3.1 ± 3.6	8.0 ± 9.7	-8.3 ± 7.6	17.3 ± 20.3	-19.5 ± 14.5
Wheat	All GCMs	1 GGCM	3.9 ± 0.6	-1.8 ± 0.4	11.5 ± 1.9	-6.8 ± 1.7	21.8 ± 2.7	-15.3 ± 2.5
	1 GCM	All GGCMs	2.9 ± 2.7	-2.9 ± 2.6	8.6 ± 6.6	-8.4 ± 6.3	16.5 ± 9.3	-17.5 ± 11.8
	All GCMs	All GGCMs	2.9 ± 4.2	-2.5 ± 3.5	6.3 ± 13.4	-8.7 ± 7.7	10.6 ± 24.8	-20.4 ± 12.9
All Crops	All GCMs	1 GGCM	3.7 ± 1.8	-2.2 ± 1.5	9.4 ± 3.7	-9.4 ± 3.4	17.1 ± 7.8	-21.2 ± 5.7
	1 GCM	All GGCMs	2.7 ± 3.4	-2.7 ± 2.9	6.2 ± 9.8	-9.2 ± 5.1	9.9 ± 17.4	-20.9 ± 9.1

5.4.2 Differences in global gridded crop models' approach to physiological processes

Even though the projected range of future CWP under climate change is wide across GGCMs, there is typically little overlap of the ranges for simulations with and without accounting for CO_2 (Figure 5.5(c)). Again, larger disparities among GGCMs are found for soybean and rice, with LPJmL and LPJ-GUESS displaying substantially higher ΔCWP; e.g. up to 50% in the case of rice for CC whereas ΔCWP show small reductions for all the other GGCMs. Although estimates of ΔCWP are very similar between

LPJmL and LPJ-GUESS in this case, it is interesting to note notable differences in their simulated ΔY and ΔAET. In fact, although both models use the same simplified Farquhar model (Collatz et al., 1991, 1992; Haxeltine and Prentice, 1996; Sitch et al., 2003), the main differences in their GGCM responses to elevated $[CO_2]$ are driven by the way those models were initially set up for this intercomparison exercise. LPJmL was calibrated to present-day yield by tuning a set of parameters that include the maximum leaf area index (LAI), which limits upper rates of photosynthesis. On the contrary, LPJ-GUESS was not calibrated to observed yield, and therefore allows for a much stronger positive feedback (via stronger expansion of leaves under high productivity) while this effect is much less pronounced in LPJmL and basically constrained to water-stressed regions (where the alleviated water stress also leads to larger leaf areas). As a result, LPJ-GUESS predicts much stronger positive response to CO_2 on yield than LPJmL. The large expansion in leaf area in LPJ-GUESS also counterbalances the reduction in stomatal conductance due to the physiological effect of elevated $[CO_2]$ (see section 5.2 for a description of the different modelling approaches and Chapter 4 section 4.4.1 for further details).

In general, magnitudes of Δyield and ΔCWP response tend to be weaker for the other GGCMs, especially for C_3 crops (Figure 5.5(c) & 5.5(a)). EPIC, GEPIC, PEGASUS and crop models from the CERES family (used in pDSSAT for maize, wheat and rice) all use a RUE approach to simulate photosynthesis. These models take CO_2 effects into account within the energy to biomass conversion equation, as well as in AET estimation through a reduction in plant transpiration demand (section 5.2 and Chapter 4). pDSSAT uses the SOYGRO model to simulate soybean, which contains a leaf-level photosynthesis simulation approach like LPJmL and LPJ-GUESS. Unlike those models, however, SOYGRO accounts for CO_2 effects on transpiration efficiency at the canopy scale (Hoogenboom et al., 1992). Nonetheless, RUE-like GGCMs do not necessarily agree with each other. EPIC and GEPIC, for instance, which come from the same crop model version (EPIC v0810) but differ in their initialisation and configuration, display larger differences in ΔCWP and ΔAET than when individually compared to pDSSAT and PEGASUS results.

5.4.3   The role of nitrogen

Some of these differences are driven by differences in calibration methodology, input data, and management assumptions (such as N fertiliser application and planting dates decisions). In the case of EPIC and GEPIC for instance, EPIC uses dynamic N fertiliser application constrained by an upper 200 kg-N Ha^{-1} application rate whereas GEPIC constrains N fertiliser application to observed national rates of fertiliser application. This difference in N management results in large differences in CO_2 response in low N-input regions. In the case of LPJmL and LPJ-GUESS, the latter assumes no N limitation whereas LPJmL has an implicit N reduction of yields through scaling of the RUE parameter α_a and the maximum LAI (see table 4.2 in Chapter 4). In general, differences in GGCM soil carbon (C) and N dynamics can have a major effect on crop sensitivity to CO_2 fertilisation effects. For instance, EPIC v0810 and the DSSAT models used in pDSSAT balance both C and N. Therefore, when there is not sufficient N uptake (from soil mineralised N and applied N fertiliser), the crop model limits the rate of photosynthesis that occurs as a function of the declining N concentration of the vegetative tissues while trying to hold relatively constant the concentration of N in the reproductive tissues. Consequently, yield decreases if N is relatively deficient, i.e. additional C gain causes even lower N concentration in vegetative tissue and that scales back photosynthesis reactivity to that increment of increased C. As a consequence, overall model responsiveness to CO_2 can be reduced under N limitation, especially for wheat, rice and maize. In the case of soybean, increased demand for N under higher [CO_2] stimulates increased carbohydrate allocation to increase N-fixation.

5.4.4   Difference in global gridded crop models' parameterisation and input data

A key aspect underlying GGCM's CWP sensitivity is the representation of management. Decisions over whether planting dates and crop cultivars are static or adaptive lead to notable differences in simulated length of growing seasons and ultimately Δyield and ΔAET. Unlike EPIC, LPJmL or pDSSAT, PEGASUS allows adaptation of both choice of crop cultivars and planting date decisions, which, in temperate regions for instance, take advantage of longer growing seasons to increase yield and inevitably total water use over that period; LPJ-GUESS uses fixed planting dates but allows adaptation of cultivars

to minimise yield reduction normally associated with temperature-induced shortening of life cycle; Finally GEPIC uses static cultivars but allows adaptation of planting date decisions. Further differences between EPIC and GEPIC estimates of ΔAET and ΔCWP can therefore be explained by different planting dates despite identical cultivars. In temperate regions for instance, longer growing periods counteract with crop water demand reduction, resulting in smaller decreases in AET for models allowing adaptation of choice of crop cultivars or/and planting date decisions (such as PEGASUS, GEPIC and LPJ-GUESS). Nevertheless, this effect is small in comparison to the other drivers of change in AET (i.e. CO_2 fertilisation effects on stomatal conductance and plant transpiration and increase in leaf area).

5.5   Discussion

This study presents results of multi-model and multi-scenario assessment of CWP under climate change and effects of CO_2 fertilisation that is unprecedented in its scope. Most studies on climate change impacts assessments have either focused on crop production, but missed evaluating impacts on underlying water use, or considered a single GGCM only (Gerten et al., 2011; Liu and Yang, 2010). Large discrepancies found in global estimates of CWP confirm previous findings that climate, irrigation water management and soil (nutrient) management, among other factors, greatly influence CWP (Zwart and Bastiaanssen, 2004), but also underscore that those factors and interactions need to be better understood and tested when implemented in GGCMs.

It is also important to highlight that evaluation and testing of GGCMs for CWP against observational data has been very minimal; rather, the evaluation has been for yield levels with less attention paid to the accompanying AET. To assess GGCMs' performance against current observations, we compiled existing results from FACE experiments reporting on CWP identified in four locations across the world and compared GGCM simulations against these FACE observations (i.e. at the grid-cell level) for rainfed and irrigated conditions. In general, ΔCWP of the GGCMs is found within the range of the observed ΔCWP values in FACE under comparable CO_2 enrichment (Figure 5.6 and Table 5.1). Measuring crop ET over the entire growing season is extremely challenging, hence the current limitation in available FACE data for validating simulated CO_2 effects on CWP in models (Leackey, personal communication).

The GGCMs have different approaches for predicting AET, which may lead to large disparities. However, the diversity in model results for CWP is not only due to model differences but also due to different assumptions in management decisions such as cultivar selection, sowing date and fertiliser application. Finally, some general mechanisms that are not addressed in any of our models may affect cropping systems in reality. For instance, lower transpiration rates cause higher leaf temperatures and may increase the likelihood to cross a heat-stress threshold or accelerate phenology. As well, the chemical composition of crops evolves under elevated CO_2 levels, which can increase crop susceptibility to insect pests and promote the formation of invasive species (Dermody et al., 2008; Zavala et al., 2008).

On a global average, CO_2 effects are projected here to exhibit a positive effect on yield and CWP. However, large spatial disparities are likely to remain (and potentially be exacerbated) between already water-scarce and water-rich regions. Along with better understanding and assessment of impacts of CO_2 effects on crops and water use, crop impact studies need to integrate knowledge on water availability and climate change impacts on global water resources to better evaluate hotspot areas where one can expect strong climate change impacts in the agriculture sector (Elliott et al., 2014a; Piontek et al., 2014). Adaptation of cropping periods by farmers may reduce detrimental impacts on yields but possibly at the expense of higher water requirements in some regions. Finally, the simulated responses of different crops vary widely (particularly soybean versus maize), so changes in crop distributions and rotations may also be a more secure way forward. Management adjustments, such as fertiliser inputs, may be needed to realise the full potential of CO_2 fertilisation.

5.6 Conclusion

This model intercomparison study is the first to report the large influence of CO_2 effects on crop yield and water use efficiency at the global scale, based on a suite of GGCMs of different design driven by an ensemble of climate data downscaled from five distinct GCMs. Results show CWP tend to increase by the end of this century under RCP 8.5 between $5.6 \pm 26.6\%$ and $17.3 \pm 20.3\%$ depending on crop type when both climate change and CO_2 fertilisation effects are taken into account in GGCMs. Without the effects of rising $[CO_2]$, the GGCM–GCM ensemble present a global decrease in CWP,

with changes ranging between $-14 \pm 16.5\%$ to $-28.4 \pm 13.9\%$ depending on crop type. Simulated CWP vary greatly not only among crop types but also among GGCMs. In addition, the range of CWP estimates doubles when taking into account carbon fertilisation effects. This study highlights strong GGCMs sensitivity on the choice of modelling methodology in respect to physiological and structural effects of elevated $[CO_2]$. GGCMs following a detailed mechanistic representation of photosynthesis and CO_2 effects at the leaf level are more sensitive to increases in $[CO_2]$ than GGCMs following a simpler RUE approach. Yet, differences between GGCM simulations are not systematically larger among GGCMs of different structure than among GGCMs of a same family but differently parameterised and calibrated. Agreement in the spatial distribution of the intensity of crop response to elevated CO_2 is low due to a combination of factors, including differences in agricultural management input data and calibration methods. Other factors important in crop–CO_2 response, such as response variation in nutrient stress environment and/or at temperature above 25℃ are not consistently taken into account by the GGCMs compared in this study, and may act to modify CO_2 responsiveness (Kimball, 2011).

Effects of elevated $[CO_2]$ are found in experiments to increase yields of C_3 crops substantially and also yields of C_4 crops to a lesser extent (Kimball, 2011). If the results found in these experimental settings are realised in farmers' fields, there could be a large beneficial impact at the global scale that might partly ease adverse impacts of the climatic changes associated with $[CO_2]$ rise. Global modelling analyses need to represent adequately the potential response to increasing atmospheric $[CO_2]$, scaled up from plot-scale experiments, and its interactions with changing climate conditions. Current gap in observational data across biomes impedes crop models to adequately simulate actual CO_2 fertilisation effects on crops and interactions with temperature, soil water and N availability. GGCM estimates of crop ET are largely uncertain due to their primary focus on yield simulations and challenges in finding useful global scale ET dataset to validate this type of model. To improve GGCM estimates of actual CO_2 fertilisation effects, modellers must address model limitations in simulating crop ET effectively across agro-ecosystems and under extreme climatic conditions that are expected to increase in frequency and intensity with climate change (Field et al., 2012).

These results, rather than providing robust and definite numbers on actual effects of CO_2 on CWP, show a large potential importance of CO_2, but qualify this result by

highlighting current modelling uncertainties and limitations at the global scale. They point to the urgent need for systematic global crop model validation and comparison exercises in order to improve assessment of CO_2 and climate change impacts on crop production and water use analyses. Finally, this study indicates the potential role of agricultural management practices, as illustrated by differences in model assumptions and settings in respect to fertiliser application, choice of crop cultivars and planting date decisions, and resulting disparities in outcomes among GGCMs simulating key processes with a similar approach. Assumptions about management practices appear to be more effective than the climate signal in some cases, which brings an optimistic message that adequate farming adaptation and planning could alleviate some of the risks posed by climate change and take advantage of the CO_2 fertilisation effects in producing "more crop per drop". The next chapter explores in more depth the role of farming management practices for adapting to and mitigating climate change.

Chapter 6

Development of global representative agricultural pathways to explore adaptive capacity and uncertainties in coordinated simulations

Preface

This chapter describes recent and ongoing AgMIP activities, as part of phase 1 of the global gridded crop model intercomparison and improvement initiative (GGCMI) described in Chapter 4, in which I have played and continue to play a leading role in the coordination of representative agricultural pathway (RAP) development for global gridded crop models (GGCMs). The RAPs aim to advance assessment of adaptive capacity in the agricultural sector in response to future climate change impacts and consist of qualitative storylines and scenarios to be used in a coherent fashion across scales and disciplines of food security. This scenario-based framework is designed to explore complex interaction among biophysical and socio-economic drivers of food security and uncertainties related to future climate change impacts, socio-economic development trends and farmers' adaptive capacity. I developed the initial ideas behind

96

RAP applications to GGCMs during the third annual AgMIP global workshop held in Rome in October 2012 along with Antle and colleagues from the AgMIP economic modelling teams. My role has since consisted of leading and coordinating RAP activities for the GGCMI in liaison with the AgMIP global and regional economic modelling teams. Thus, this chapter describes this major international initiative, my contribution and ideas for its development.

Abstract

Recent agricultural impact assessments and modelling intercomparisons demonstrate the need for coordinated scenario frameworks, designed to integrate biophysical and socio-economic dimensions of food security across scales. These can be used to explore near-, medium- and long-term agricultural development and adaptation pathways in response to future climate change and to better understand and constrain uncertainties. Here I present the background and motivation behind the development of representative agricultural pathways (RAPs), defined as "qualitative descriptions of synergies and tradeoffs between biophysical and socio-economic dimensions of agriculture development and food production" (Antle et al., 2013). Initiated by AgMIP, the RAPs complement a new generation of climate change and socio-economic pathways and scenarios developed for climate change research: chiefly the representative concentration pathways (RCP), the shared socio-economic pathways (SSPs) and the shared climate policy assumptions (SPAs). The RAPs encompass detailed storylines on land use change, biofuel policy, farming management practices, agricultural trade and food demand. The RAPs address conceptual challenges attributed to the multiplicity of dimensions and scales relevant to the agricultural sector: including soil and climatic factors; management practices; farmers' adaptation responses; and trade. In association to qualitative storylines, a set of quantitative parameters can then be developed to drive global gridded crop models (GGCMs) and global economic models, defined here as representative agricultural scenarios (RAS). An overview of RAP application to the AGMIP gridded crop modelling initiative (Ag-GRID) is presented along with a new harmonised global gridded dataset of farming management practices offering promising advancement for global assessments of agricultural impacts and farmers adaptation responses to climate change.

6.1   Introduction

Climate change is expected to impact crop productivity unevenly across regions, with large negative impacts occuring in more vulnerable countries (Deryng et al., 2014; Easterling et al., 2007; Porter et al., 2014; Rosenzweig et al., 2014). However, there are large uncertainties associated with climate change impacts on global agriculture due to: uncertainties in future climate change projections as shown in Chapter 3 and in Deryng et al. (2014); actual crop response to more variable temperature and precipitation conditions (Rosenzweig et al., 2014); increasing atmospheric carbon dioxide (CO_2) concentration further complicated by interactions with soil and atmospheric conditions as shown in Chapter 5; freshwater resources (Elliott et al., 2014a); and changes in pest and disease distribution (Easterling et al., 2007; Porter et al., 2014). Farmers can potentially employ an ensemble of farming management practices to alleviate some of the negative impacts of climate change, but assessment of farming adaptive capacity remains highly uncertain due to complex interactions between numerous biophysical and economic factors (Rötter, 2014; Warren, 2010).

The most comprehensive review on modelling adaptation to date (Challinor et al., 2014b; Porter et al., 2014) has compared 91 publications using simulations of crop-level adaptation to climate change. They (ibid) found various management practices, including changes in crop varieties, planting dates, irrigation, fertiliser application and residue management, could increase simulated yields by an average of 7-15%, with adaptations more effective for wheat and rice than maize. However, as Rötter (2014) pointed out, Challinor et al. (2014b), although providing a comprehensive review, was based on uncoordinated simulations (that used different climate scenarios, crop models, future periods, etc.) making it almost impossible to assess sources and significance of uncertainty. Their review combined results from various modelling methodologies, including statistical and process-based models. Some studies included CO_2 effects whereas others did not. In addition, the statistical relationship developed from the results of the paper in the review, gave more importance implicitly to a small number of global gridded modelling approaches, that contributed a much greater number of data points: only six global studies out of the 91 (i.e. ∼7%), including a previous study using PEGASUS version 1.0, comprised more than 30% of the entire dataset. Furthermore, the review identified incomplete and unequal representation of adaptation in crop modelling

studies, with most studies only considering one adaptation measure (predominantly changes in crop varieties) and just one study looking at the effect of increasing fertiliser application (contributing to 10 data point out of 1722) in sub-Saharan Africa. Finally, another limitation of the review was the focus on biophysical dimensions of crop response, excluding socio-economic dimensions of adaptation.

On the economics, Nelson and colleagues conducted an extensive global economic model intercomparison as part of the AgMIP/ISI-MIP fast-track process to assess the effects of climate change, bioenergy policy, and socio-economics on agriculture (Nelson and Shively, 2013; Nelson et al., 2014). For the first time, economic models were to some extent harmonised, using identical outputs of climate change impacts on cropland productivity generated from up to four GGCMs, driven by two distinct global climate models (GCMs) (Müller and Robertson, 2013; Nelson et al., 2014). Nonetheless, this economic study only presented a partial assessment of uncertainties as it excluded the role of carbon fertilisation on crops and did not account for adaptation in crop simulations. Even with harmonisation of key assumptions and the use of shared socio-economic pathways (SSPs) (see section 6.2), the spread in simulated commodity price between model results remained very large due to important differences in model structure and in their finer detail, highlighting the need for an exhaustive description of the agricultural sector beyond the SSPs for further model harmonisation (Nelson et al., 2013; Von Lampe et al., 2013).

Since agricultural development and adaptive capacity in farming depend equally on environmental and economic resources, the next phase of the model intercomparison programme calls for more systematic integration of crop and economic models, using a standardised set of agricultural storylines as a starting point. In this context, AgMIP is introducing new concepts and methods for the development of global and regional representative agricultural pathways (RAPs) and scenarios (RASs) for coordinated agricultural model intercomparison to explore future agricultural development, adaptive capacity, and improve assessment of uncertainties in biophysical and economic domains of agriculture (Antle et al., 2013; Rosenzweig et al., 2013) (see also www.agmip.org/representative-agricultural-pathways). Central to the RAPs is the idea that only a small number of distinct pathways suffice to represent a wide range of futures and help robust decision planning under current levels of uncertainty in regional climate change impacts and farmers' adaptive capacity. Another important aspect of

the RAPs is their versatility across scales and disciplines of agriculture impact models. This scenario and pathway framework is intended to improve robustness of exploratory analyses and facilitate decision makers to develop robust agricultural and land use policy.

This chapter addresses some of the key limitations highlighted in Challinor et al. (2014b) and Nelson and Shively (2013). After reviewing background and motivation behind the representative concentration pathways (RCPs) and the SSPs in section 6.2, I define the RAPs and discuss dimensionality and disaggregation challenges for developing trans-disciplinary RAPs applied at multiple scales in section 6.3. I then introduce in section 6.4 application of the RAPs to the global gridded crop model intercomparison and improvement initiative (GGCMI), which I coordinate, and my contribution to the AGMIP gridded crop modelling initiative (Ag-GRID) (see also Appendix B). I present recent Ag-GRID products developed by Müller and myself in section 6.5 and conclude with suggestions for further development of RAPs and scenarios for use in GGCMs in section 6.6.

6.2   A new scenario framework for climate change research

Scenarios provide a useful method for dealing with uncertainties in climate research by increasing awareness of unforeseeable events and expanding the scope of action for decision-making (Bell, 2003; Hallegatte et al., 2011; Kwakkel and Pruyt, 2013). Scenarios developed by the climate change community broadly aim to explore future climate change and its impacts and create a framework for the development and assessment of robust climate policies (Bell, 2003; Börjeson et al., 2006; Nakicenovic et al., 2014).

Previous scenarios developed for the IPCC Special Report on Emission Scenarios (SRES) followed a linear unidirectional process: initiated with the production of four narratives describing a range of driving forces behind GHG emissions and radiative forcing, including specific characterisation of demographic, social, economic, technological, and environmental development pathways (Nakicenovic et al., 2000). These qualitative storylines were then used by integrated assessment models (IAMs) to develop quantitative scenarios resulting in estimations of GHG emissions, which in turn were used as input to global climate models (GCMs) to simulate changes in climatic conditions, with the latter eventually used by impacts, adaptation and vulnerability

(IAV) models. Although widely used by the climate research community for more than ten years, this linear sequential approach caused the IAV simulations to lag behind the other modelling communities, and it became evident that a sequential scenario development process could not address adequately the complexity of climate interactions and feedbacks between biophysical and socio-economic factors nor mitigation and adaptation challenges (Ebi et al., 2014; Nakicenovic et al., 2014).

6.2.1 The representative concentration pathways and shared socio-economic pathways

In an effort to improve consistency across the climate change research community, to explore adaptation and mitigation options and better understand uncertainty, a parallel scenario development framework was established for the IPCC AR5 to design a new generation of storylines and scenarios to be used simultaneously by the climate, IAM and IAV modelling communities, and hence accelerate the research process (Moss et al., 2010; Nakicenovic et al., 2014).

These new pathways and scenarios are known as *Representative Concentration Pathways* (RCPs) and *Shared Socio-economic Pathways* (SSPs) (see Table 6.1 for a summary). They consist of qualitative narratives of climate change futures that include some quantitative information such as: the level of climate change and trends in human development (e.g. population), in relation to drivers of climate change; the ability to mitigate GHG emissions; and the ability to adapt to climate change (Kriegler et al., 2014; O'Neil et al., 2014; van Vuuren and Carter, 2014; van Vuuren et al., 2011). More specifically, the RCPs (see also section 2.3.2 in Chapter 2) were developed to describe the Earth's radiative forcing resulting from different levels of future GHG emissions (Moss et al., 2010; van Vuuren et al., 2012). Four main RCPs were selected to cover a range of climate change scenarios (Figure 6.1(a)). Similarly, SSPs were developed to represent different levels of future socio-economic challenges for mitigation and adaptation (Kriegler et al., 2014, 2012; O'Neil et al., 2014). Five main SSPs were identified to embrace a wide range of alternative futures in respect to different dimensions of mitigation and adaptation challenges (Figure 6.1(b)). While SSPs do not include elements of climate policy explicitly, they can be used in combination with RCPs to explore costs, risks and benefits associated with *Shared climate Policy Assumptions*

(a) Four RCPs (van Vuuren et al., 2011)   (b) Five SSPs (O'Neil et al., 2014)

(c) Scenario matrix of RCPs+SSPs+SPAs (van Vuuren et al., 2014)
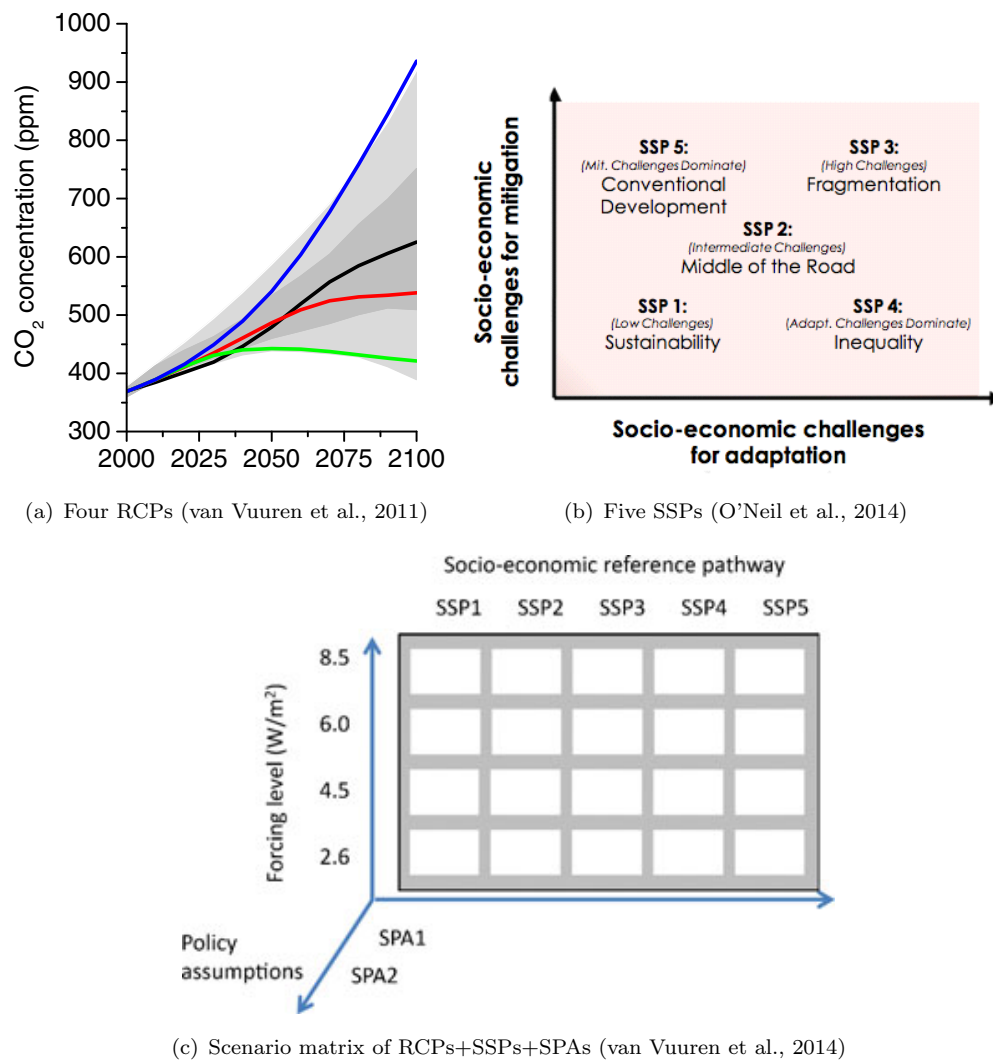
FIGURE 6.1: Figures representing the conceptual framework of RCPs (a) – here in terms of CO_2 concentration – and SSPs (b) and the scenario matrix of multiple RCP-SSP-SPA combinations (c).

(SPAs) on mitigation and adaptation (Kriegler et al., 2014), thus creating integrated scenarios to identify synergies and tradeoffs between different strategies and uncertainties (van Vuuren et al., 2014) (Figure 6.1(c) and Table 6.1).

6.2.2 Land use and agriculture in shared socio-economic pathways

The SSPs also contain very broad and high level assumptions on land use change regulation, trends in land productivity growth, environmental impact of food consumption, and international trade (Table 6.2) that are useful for guiding experimental designs of the agricultural impacts models. However, recent impact model intercomparison studies (ISI-MIP/AgMIP) have demonstrated the need for more

TABLE 6.1: Summary of acronyms and definitions of the new narratives and scenarios (*GDP=Gross Domestic Product).

Narrative/Scenario	Acronym	Key attributes	Group involved
Representative Concentration Pathway	RCP	GHG concentrations, radiative forcing	
Shared Socio-economic Pathway	SSP	Population, GDP*, global trade	IPCC
Shared climate Policy Assumption	SPA	Climate policy	
Representative Agricultural Pathway	RAP	Land demand, land productivity, agricultural trade	AgMIP

specific and standardised agricultural pathways across scales and disciplines – including the biophysical and economic dimensions of agriculture – to enhance intercomparison analyses and assessment of uncertainty (Nelson et al., 2014; Von Lampe et al., 2013).

TABLE 6.2: Agricultural storylines in SSPs. Adapted from O'Neil et al. (2011).

SSP1 **Sustainability**	Land use is strongly regulated, e.g. tropical deforestation rates are strongly reduced. Crop yields are rapidly increasing in low- and medium-income regions, leading to a faster catching-up with high income countries. Healthy diets with low animal-calorie shares and low waste prevail. In an open, globalised economy, food is traded internationally.
SSP2 **Continuation**	Land use change is incompletely regulated, i.e. tropical deforestation continues, although at slowly declining rates over time. Rates of crop yield increase decline slowly over time, but low-income regions catch up to a certain extent. Caloric consumption and animal calorie shares converge towards medium levels. International trade remains to large extent regionalised.
SSP3 **Fragmentation**	Land use change is hardly regulated, i.e. tropical deforestation continues at current rates. Rates of crop yield increase decline strongly over time, due to little investment. Unhealthy diets with high animal shares and high waste prevail. A regionalised world leads to reduced trade flows.
SSP4 **Inequality**	Land use change is strongly regulated in high income countries, but tropical deforestation still occurs in poor countries. High income countries achieve high crop yield increases, while low income countries remain relatively unproductive in agriculture. Caloric consumption and animal calorie shares converge towards medium levels. Food trade is globalised, but access to markets is limited in poor countries, increasing vulnerability for non-connected population groups.
SSP5 **Conventional** **Development First**	Land use change is incompletely regulated, i.e. tropical deforestation continues, although at slowly declining rates over time. Crop yields are rapidly increasing. Unhealthy diets with high animal shares and high waste prevail. Barriers to international trade are strongly reduced, and strong globalisation leads to high levels of international trade.

6.3 The representative agricultural pathways

6.3.1 Definition

Consequently, following the development of SSPs, *Representative Agricultural Pathways* (RAPs) are now under development to specifically explore the role of agricultural management practices and future adaptive capacity in a consistent manner across climate, economic and field-level management practices (Antle et al., 2013; Claessens
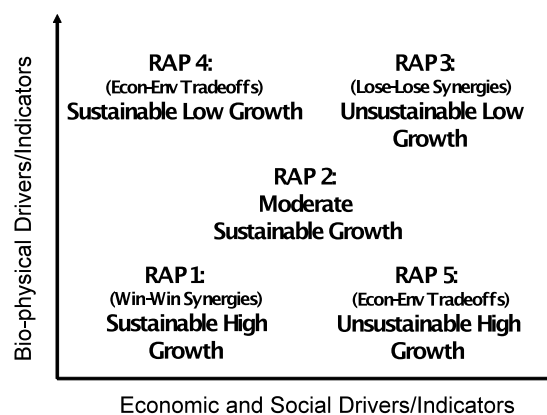
FIGURE 6.2: Five RAPs: synergy and tradeoff matrix with pathway descriptions (Antle et al., 2013, Figure 6)

et al., 2012). RAPs allow development of the agricultural sector to be represented in model simulations of future agricultural production and provide consistent, citable, storylines and associated scenarios for model execution to enable intercomparison (Table 6.1).

RAPs are intended to describe synergies and tradeoffs between biophysical and socio-economic dimensions of global and regional food production (Figure 6.2) and to fit logically into the broader framework of socio-economic mitigation and adaptation challenges described by the SSPs (Figure 6.3).

FIGURE 6.3: Diagram illustrating SSP-RAP correspondence. Colour of boxes illustrates synergy and tradeoff between socio-economic and biophysical factors. Red indicates important tradeoff whereas green indicates strong synergy. Orange and yellow boxes indicate medium tradeoff, with orange representing greater challenges than yellow, and blue boxes indicate neutrality.

Similar to the SSPs, RAPs should consist of a small number of pathways that together comprehensively represent the range of future agricultural development that is plausible in terms of environmental and socio-economic assumptions, and thus also incorporate

uncertainties (Antle et al., 2013; Ebi et al., 2014; van Vuuren and Carter, 2014). Hertel (2010) identified key factors driving global supply and demand for agricultural land and the role of environmental constraints, which are planned to be used in the development of RAP storylines (Table 6.3). On the demand side, RAPs should characterise not only food demand but also biofuel demand driven by global energy demand and oil prices. On the supply side, RAPs should inform trends in global cropland and pasture expansion (and contraction), crop yield increases driven by intensification and increases in yield frontiers (ongoing technological advancements in breeding varieties and genetics are expected to increase maximum achievable yield thresholds) and labour availability, which can play a major role especially at smaller scales (Chaudhury et al., 2012; Claessens et al., 2012; Keys and McConnell, 2005). RAPs should also account for environmental constraints to agricultural intensification, such as GHG emissions from agriculture, land degradation and water pollution, to enable full representation of tradeoffs and synergies between food security, energy security and ecosystem services (Figure 6.2). Finally, RAPs should describe those "shock factors" such as urban population expansion, which can cause urban areas to expand into peri-urban agricultural land, biodiversity loss, extreme climate variability and last but not least, specific land use policy (Table 6.3 & Hertel, 2010).

TABLE 6.3: Drivers of global land demand & agricultural development and drivers of environmental tradeoffs and production shocks (Hertel, 2010).

Land demand	Food supply	Environmental constraints	Production shocks
Population growth	Livestock		
Income growth	Fertiliser	Climate change	Urbanisation
Price elasticity	Yield frontiers	GHG emissions	Ecosystem services
of demand	Irrigation &	(N_2O, CH_4)	Biodiversity loss
Bioenergy &	water availability	Eutrophication	Climate variability
global land use	Harvested area	of lakes	Subsidies, price
Oil prices &	Waste management	& rivers	wedges & taxes
energy outlook	Labor cost		

These assumptions and storylines should be consistent across spatial and temporal scale and trans-disciplinary, i.e. describing biophysical drivers of crop productivity and land use change as well as socio-economic drivers of food demand, agricultural trade and land use change. Finally, RAP narratives should also offer flexibility for dealing with multiple spatio-temporal scales, i.e. embracing global and regional scales but also near-term and

long-term future conditions, and multiple dimensions of agriculture (Antle et al., 2013; Ebi et al., 2014; van Vuuren and Carter, 2014).

In correspondence to each RAP, quantitative *Representative Agricultural Scenarios* (RASs) will then be developed, consisting of a specific set of parameters to input to biophysical crop models and economic models. The term "scenario" is used here to describe a quantitative manifestation of a qualitative storyline or "pathway". The set of parameters forming a RAS should adhere to a particular RAP, and be guided by certain policy objectives, to represent, for example, measures of farming intensification levels, global food and biofuel demands, and global cultivated areas at various points in time.

6.3.2   Challenges across scales and disciplines

The development of RAPs across multiple scales and disciplines faces numerous challenges to ensure consistency between scenarios used in both global and regional agricultural models and harmonisation between socio-economic and biophysical drivers. At the global scale, RAPs should be broad enough to describe general trends according to SSPs but allowing room for disaggregation into regional RAPs, developed based on detailed information specific to the region of study (Figure 6.4). Antle et al. warn that some variables that are manifest at the global scale become drivers at regional scale, such as prices in economic models. A regional RAP should thus refer to some extent to a global RAP to ensure cohesion between pathways and scenarios (Antle et al., 2013; Claessens et al., 2012).

Characterisation of biophysical and socio-economic factors relevant to agricultural development should insure coherent storylines as some biophysical factors are directly dependent on socio-economic drivers, which eventually feedback on the economy. For instance, national rates of fertiliser use are related to fertiliser price and national incomes; land productivity increases with fertiliser application rates, increasing food production, which directly influences supply and demand equilibrium, and hence trade and food prices. In Nelson et al. (2014), fertiliser application rates were kept constant to the present-day; a one-way sequential approach was used in which GCM outputs (precipitation, temperatures...etc.) were used to drive GGCMs and generate crop yield outputs to drive global economic models (Figure 6.5(a)). Following this sequential approach, the RAPs enable two-way connections between biophysical and
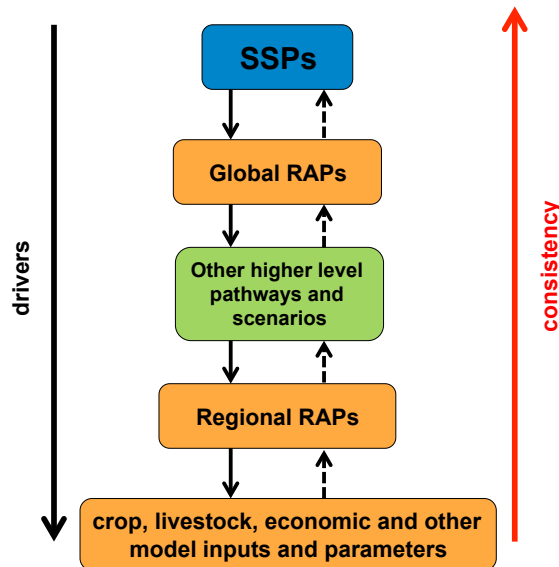
FIGURE 6.4: Linkages from global and regional pathways for disaggregation and development of model-specific scenarios (Antle et al., 2013, Figure 7)

economic models, to take into account feedback between both dimensions of agricultural development. In practice, global economic models prescribe monetary dependence of the level of farming intensification that correspond to a particular RAP in association with a particular SSP; then GGCMs provide corresponding crop yield outputs that finally feedback into the global economic models (Figure 6.5(b)). An important aspect of RAP's development and application should thus consist in facilitating and coordinating interaction between both modelling groups to ensure the coherence of each RAP storyline.

6.4 Application of representative agricultural pathways and scenarios to global gridded crop models

At the global scale, agricultural description within each SSP is directly extended into a more detailed RAP narrative on global land use change including: trends in deforestation and biofuel policy; global food production including land productivity and livestock; global food demand including diet and food waste; and global trade dynamics. Figure 6.3 illustrates the fit between SSPs and RAPs for global scale analyses and the degree of synergy and tradeoff for sustainable intensification. These RAP narratives allow for a more detailed and comprehensive description of future pathways of global agricultural development, which are required to develop RAS for models.

(a) Adapted from Nelson et al. (2014)

(b) with the new scenario framework
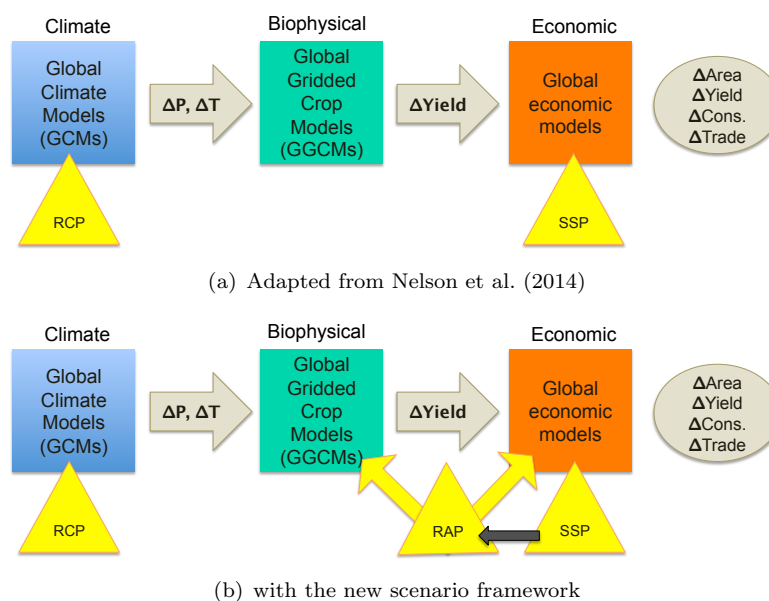
FIGURE 6.5: Flowchart illustrating relationship between GCMs, GGCMs, and global economic models as in recent model intercomparison (a) and using the new RAP framework (b). Adapted from Nelson et al. (2014)

Economic models can parameterise most and in certain instances all of the factors described in the RAPs, but biophysical crop models typically inform land productivity, i.e. crop yield, and land use change in terms of cropland suitability loss/gain due to climate change and soil fertility loss. "Yield shifters" are derived from crop models to quantify climate change impact on land productivity growth for use in economic models according to specified RAPs (Figure 6.5(a)) (Müller and Robertson, 2013).

RAS for GGCMs should consist of scenarios of farming management practices that affect crop yield, and describe farmers' adaptive capacity in response to climate change. Drivers of crop yield typically include fertiliser application, irrigation and timing and duration of crop growing period as determined by planting date decision and cultivar choice in terms of growing degree days (GDD). In addition, a general category of cultivar improvement standardised across scenarios should include factors such as improved tolerance to droughts and extreme temperatures, maximum yield potential thresholds and protein content (carbon–nitrogen ratio could play an important role especially in response to carbon fertilisation effects; see Chapter 5 and Taub et al., 2008).

Similarly to the creation of scenarios of GHG concentrations consistent with the RCPs, different scenarios of farming management practices will be produced in coherence with the RAPs, to represent different levels of land productivity growth on a yearly time-step:

none, slow, moderate, and rapid, and achieve different degrees of farming intensification over near, medium and long-time horizons (Figure 6.6) (personal communication with Ruane, Elliott, and Müller). These distinct levels of productivity will be defined to match the broader land use and agricultural trends description offered in the SSPs (see Table 6.3) and conditioned by recent observations of land productivity growth. In addition, these RAS could be developed through a consultation process involving experts and practitioners, such as the Delphi technique (Rikkonen et al., 2006). Overall, each RAS will consist of a set of gridded data of annual NPK fertiliser input, irrigation amount, change in planting date window and maturity rates evolving through time. In the next chapter (Chapter 7), I explore benefits associated with a scenario of high land productivity growth for maize in terms of achieving potential yield and tradeoffs for climate mitigation.
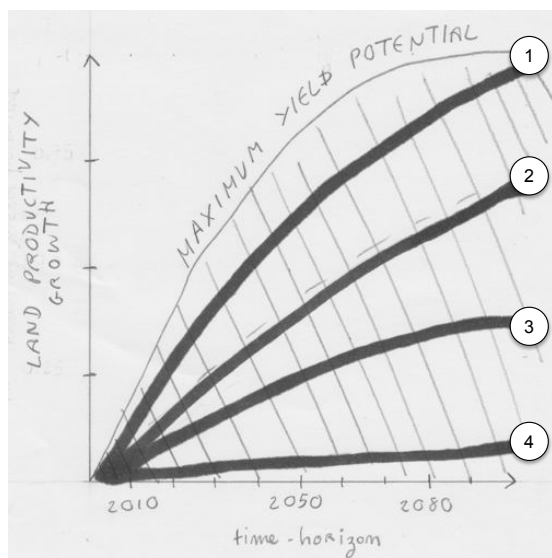
FIGURE 6.6: Four land productivity growth pathways for GGCMs. 1: "crop yields are rapidly increasing"; 2: "rates of crop yield increase decline over time"; 3: "rates of crop yield increase decline strongly over time"; 4: "relatively unproductive agriculture". These scenarios are still work in progress.

6.5 Harmonised gridded management input for global gridded crop models: the Ag-GRID framework

Since spring 2013, the GGCMI coordination team (including the co-leaders: Joshua Elliott and Christoph Müller; senior advisers: Cynthia Rosenzweig and Cesar Izaurralde; and leading activity coordinators: Alexander Ruane and myself; see Appendix B)

developed a new set of protocols for the next phase of analyses following the AgMIP/ISI-MIP fast-track process, centred on model evaluation, intercomparison and improvement. In response to the wide range of simulated crop productivity resulting from different GGCM management inputs and assumptions as discussed in Chapter 4 and also reported in Chapter 5, the AgMIP gridded crop modelling initiative (Ag-GRID) was launched to improve quality, accessibility and harmonisation of gridded datasets and scenario development to support the GGCMI. In particular, the use of such harmonised input datasets in GGCMs aims to reduce some of the uncertainties to better evaluate GGCM structural differences (www.agmip.org/ag-grid & Elliott et al., 2014b).

Harmonised gridded data on global crop calendar and fertiliser application rates for the present-day have already been created to be used in the historical evaluation phase of the GGCMI (Elliott et al., 2014b and Appendix B). These inputs are core to GGCMI and provide baseline for exploring effects of different RAPs on yields and other GGCM outputs. Present-day Ag-GRID data have been developed for 15 crops including wheat, maize, soybean and rice, considered priority-1 in GGCMs simulations, and cassava, groundnut, millet, potato, rapeseed, sorghum, sugarbeet, sugarcane, sunflower, cotton and coffee, considered priority-2 (see Appendix B). Although these crops are grown on defined harvested areas, each dataset has been produced to cover the entire land-surface using a specific gap filling approach.

6.5.1   Harmonised crop calendar data

Maps of present-day planting date, harvest dates and growing season length (Figure 6.7) have been compiled by Müller from two existing global crop calendars, MIRCA2000 (Portmann et al., 2009) and SAGE (Sacks et al., 2010), supplemented by a rule-based approach as implemented in LPJmL (Waha et al., 2011) to provide as much coverage of the global land surface as possible. Because MIRCA2000 has monthly resolution only, assuming the 1st of the month for planting dates and the last of the month for harvest dates, SAGE data with daily resolution is used where available. MIRCA2000 data is used only in regions where no SAGE data are available. MIRCA2000 data is ignored if growing seasons are longer than 330 days (e.g. wheat in large parts of Russia). LPJmL data is used to fill remaining areas globally with climate-driven rule-based estimates covering a large subset of cropping areas relevant for food security (Elliott et al., 2014b).

Both PEGASUS and LPJmL use a similar climate-rule based approach for planting date decisions (Deryng et al., 2011) but LPJmL was selected because of its larger range of simulated crops. LPJmL planting and harvesting date decision algorithm is described in detail in Waha et al. (2011).
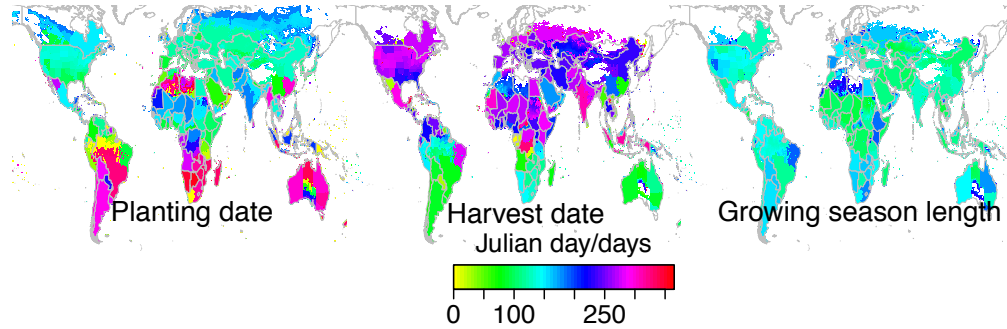
FIGURE 6.7: Harmonised crop calendar for present-day: Maize. Planting and harvest dates are shown in Julian day [1-365]. Growing season length is shown in number of days [1-365]. Same colour scale is applied in both cases. (Elliott et al., 2014b)

6.5.2 Harmonised fertiliser inputs data

I compiled global maps of present-day fertiliser nitrogen-phosphorus-potassium (NPK) application (Figure 6.8) based on published data on mineral NPK fertilisers and NP manure applications (Foley et al., 2011; Mueller et al., 2012; Potter et al., 2010). The mineral fertiliser dataset covers present-day harvested areas at sub-national levels, whereas the manure dataset covers present-day harvested areas at the grid-cell level. Thus mineral fertiliser and manure were aggregated using a state-level administrative boundary map of 372 units covering the entire land surface (Ramankutty and Foley, 1999). In addition, original manure data are reported in terms of atomic N and P and assumed to contain no K (Potter et al., 2010), whereas inorganic fertiliser data are reported as N, phosphate (P_2O_5) and potassium oxide (K_2O). The conversion from P manure to P_2O_5 is based on atomic masses: $P_2O_5eq = P/31(31 \times 2 + 5 \times 16)$, where 31 = atomic mass P, 16 = atomic mass of oxygen (O). Nutrients from manure are generally less available to plants than mineral fertilisers. 60% of applied N-manure is assumed to be available to the crop and 75% of applied P-manure similarly (Rosen and Bierman, 2005). Finally, since, the original data cover only crop-specific harvested areas, they are extrapolated in space to cover the entire land surface based on country income-level groups. First, the national average nutrient-specific fertiliser rate (area-weighted) is

assigned to all administrative units that do not apply any mineral fertiliser nor manure in the original data but are within a country actually reporting fertiliser application. Second, for all other countries that do not currently apply fertiliser to grow the specific crop, estimated nutrient-specific application rates are attributed by averaging fertiliser application rates over the corresponding income level group. Income level groups are based on the World Bank's definition to classify countries by income level (World Bank, 2013 and see Appendix D). Fertiliser application rates are averaged for all countries with fertiliser application larger than zero within the income level group and applied to all countries without fertiliser data within that group.
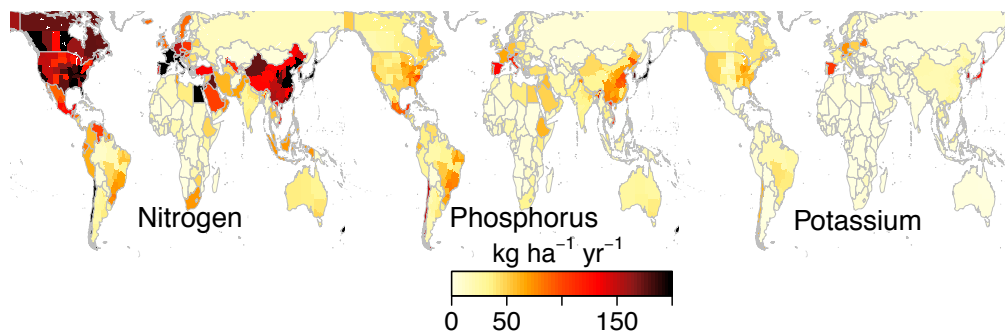
FIGURE 6.8: Harmonised fertiliser application rates for present-day: Maize (compiled by myself, Elliott et al., 2014b)

6.5.3 Harmonised input data for future simulations

Additional maps of harmonised management factors and inputs will be created for the 2030s, 2050s and 2080s according to each RAP and environmental limitations of agricultural development. The difference between the present-day map of crop yield and the 2050s map, for example, would be greater in a RAP associated with the "rapid" land productivity growth in SSP1 than would be the difference in a RAP associated with the "slow" land productivity growth in SSP3. The differences would also be greater in areas with larger yield gaps, as there is generally more room for adjustment in each factor before plausible limitations are met. A RAS for each RAP would then be published as a time series of maps linearly interpolated between the present-day, 2030s, 2050s and 2080s time periods and thus describe different degrees of global yield gap closure. In the current stage of Ag-GRID development, additional factors (e.g. planting dates) are not expected to be explicitly defined, but should be determined using approaches that allow for autonomous local adaptation (e.g. simulations with planting windows). This setup

will thus allow economic modellers to either draw entirely from a single GGCM RAS or to construct new maps in which different regions follow different productivity curves.

6.6 Summary and conclusion

I have described a framework for developing RAPs and RASs for enhancing global IAV assessment of the interactions between climate change and agriculture. The RAPs provide a novel scenario-based approach for exploring plausible agricultural development trends along with adaptive capacity and uncertainty using a coordinated set of model simulations. The RAPs are part of a broader scenario framework designed for integrated climate change research. A RAP is defined as a model-independent narrative using synergies and tradeoffs between biophysical and economic factors to characterise the evolution of agricultural sector development. A RAS is defined as a model-specific manifestation of a RAP, consisting of a set of quantified parameters that adhere to a particular RAP. RAPs should be broad enough to address a wide range of research and policy questions relevant to both biophysical and socio-economic dimensions of agriculture. A global RAP should be consistent with the land use and agricultural storylines of a particular SSP; similarly, a regional RAP should exhibit some degree of coherence with a particular global RAP, to ensure consistent disaggregation of global trends to regions for IAV analysis. At the global level, RASs designed to drive GGCMs could cover a range of four distinct levels of land productivity growth rates described in the RAPs to cover a representative but minimal range of plausible futures, similar to the four RCPs. GGCMs will therefore be able to produce four distinct maps of future simulated crop yields driven by each of these RASs. The four RASs will consist in global gridded data of fertiliser inputs, irrigation amounts, planting dates and growing period lengths. Gridded crop yield outputs will then be aggregated in relevant economic regions for use in global economic models. Finally, different RAS-specific aggregated yield trends will be combined depending on regional agricultural development trends as described in a given RAP. Currently present-day harmonised gridded management data have been developed for Ag-GRID and GGCMI and gridded RAS time-series dataset are planned to be developed comparably. To conclude, the RAP framework presented here is intended to provide better integration of biophysical and socio-economic factors

in agricultural impact simulations to better characterise adaptive capacity and identify sources of uncertainty.

To illustrate the theoretical framework proposed here, I present in the next chapter (Chapter 7) an exploratory analysis using PEGASUS driven by a prototype RAS of intensive fertiliser application rates to evaluate effects of increasing global N fertiliser use on global crop yield and associated nitrous oxide emissions from soils for maize. Regional disparities in the benefits and tradeoffs for climate mitigation are discussed.

Chapter 7

Conceiving agricultural intensification in representative agricultural pathways: balancing yield increase and nitrous oxide emissions resulting from global maize cultivation

Preface

As a preliminary modelling analysis of how representative agricultural pathway (RAP), presented in the previous chapter, could be applied this chapter addresses opportunities and challenges related to intensification of fertiliser use to increase global crop yield. The analysis presented here employs the global crop model PEGASUS. An initial version of the work was presented at the Planet Under Pressure conference, held in London in March 2012 (see Appendix C), led by myself, and co-authored by Navin Ramankutty, with whom I had started the global yield gap analysis, and Nathan Mueller and Jon Foley, who provided the higher resolution version of global fertiliser inputs data. I designed and performed the overall research, and wrote the text, which is aimed to be

submitted for publication to *Global Environmental Change.* Declan Conway advised on the presentation and discussion of the results and revised the text.

Abstract

Since most of the land suitable for agriculture is already in use, additional food is likely to be produced by increasing yield rather than through cropland expansion, unless further tropical deforestation occurs. Great opportunities for increasing crop yields exist in many parts of the world where low rates of fertiliser are currently applied. However, complex interactions between socio-economic and biophysical drivers of food production must be carefully analysed to comprehend the nature and the extent of challenges to future agricultural development. This study explores tradeoffs between maize intensification through nitrogen (N) fertiliser and greenhouse gas (GHG) emissions through a representative agricultural pathway (RAP) that optimises application of N inputs globally. Using the global gridded crop model PEGASUS, we estimate an additional 332 Gt yr^{-1} of maize could be produced on current rainfed and irrigated maize areas using intensive levels of N fertilisers, representing a 62% increase in current global maize supplies. In terms of GHG emissions, we find with the current level of N application rates to maize harvested areas, 91.6 [24 ; 406] 10^9 kgCO2e emissions are produced with an emission rate of 695 [182 ; 3,080] kg CO_2eq ha^{-1} yr^{-1}. Under higher N inputs, total nitrous oxide (N_2O) emissions increase by $\sim$60%, reaching 147 [38 ; 654] 10^9 kg CO_2eq with an emission rate of 1,115 [288 ; 4,962] kg CO_2eq ha^{-1} yr^{-1}. The range here represent uncertainties related to N_2O emissions factors estimated by the IPCC. We find efficiency of N application depends on many factors including water stress and occurrence of leaching, suggesting that for some areas present tradeoffs exist; increasing N fertiliser application produces a large positive response in terms of yield relative to N_2O emissions, including South Africa, Kenya, Madagascar, and large maize producers: India, central and southern Brazil and Argentina. In contrast, our analysis suggests a lose-lose outcome for other key maize producing countries such as China and northeast Brazil as well as Nigeria and Tanzania, where increasing N fertiliser only – without addressing other limiting factors such as soil nutrients imbalance and water scarcity and, in the case of China for instance, overuse of N fertiliser and manure resulting in

nitrate leaching – causes negative results by raising N_2O emissions without enhancing crop production.

7.1 Introduction

Agriculture in the 21st century faces the major challenge of sustaining world food demand while reducing pressure on global land and water resources (Foley et al., 2011). Historical trends in global crop production illustrate the success of the *green revolution*, which largely resulted from escalating yields (25% increase during 1985-2005, Foley et al., 2011) thanks to intensive mineral fertiliser and pesticide application, irrigation expansion, and the advancement of cultivars (Cassman, 1999; Tilman et al., 2002). Yet, intensification of agricultural systems occurred with large environmental consequences (Foley et al., 2005; Rosegrant and Cline, 2003): agriculture today uses ∼34% of terrestrial land (12% for cropland and 22% for pasture) (Ramankutty et al., 2008), 70% of global freshwater withdrawal (Gleick et al., 2009; Postel et al., 1996), and contributes 15-25% of global GHG emissions (∼2,198–6,567 $MtCO_2e$ as carbon dioxide (CO_2) from land use change in 2008, ∼1,945–2,324 as N_2O $MtCO_2e$ emissions mainly from agricultural soils in 2005 and ∼1,638–1,952 $MtCO_2e$ CH_4 emissions from livestock, manure and rice cultivation in 2005, Vermeulen et al., 2012b). Moreover, inadequate timing of fertiliser application and overuse on agricultural soils are leading to critical degradation of freshwater resources with large amounts of nitrate leaching to groundwater and rivers (e.g. Mississippi, Danube, Nile, and Yangtze and Yellow river basins), and N_2O emissions, a GHG which is 300 times more potent than CO_2 in terms of global warming potential (Stocker et al., 2013). Negative effects of intensive chemical use such as water and soil quality degradation and climate change are pervasive. These issues are increasing environmental awareness and calling for a "greener revolution" that takes environmental concerns into account (Beddington, 2009; Beddington et al., 2012; Conway, 1997; Rosegrant and Cline, 2003).

Since most of the land suitable for agriculture is already in use (Foley et al., 2007), additional food is likely to be produced by intensifying agriculture, i.e. increasing yield rather than through cropland expansion, unless further tropical deforestation occurs, which would be potentially disastrous for biodiversity, tropical ecosystems and the Earth's climate (Foley et al., 2007, 2011). Many areas across the world lack sufficient

water and soil nutrients for achieving potential crop yield, thus presenting further opportunities for increasing global crop production by using additional fertiliser and irrigation water to currently harvested areas. In fact, most of the world experiences some level of yield gap, defined as: the difference between actual yield observed in the field and corresponding maximum yield achievable under optimum management practices given agroclimatic constraints (Lobell et al., 2009; van Ittersum et al., 2013). At local levels, methods to estimate crop yield gap are based on site-specific simulations using process-based crop models along with detailed agroclimatic data and maximum yield measurements in experimental field trials (van Ittersum et al., 2013). As well, van Ittersum et al. (2013) reviewed global scale assessments of crop yield gap developed upon empirical relationships between global actual yield data (e.g. national/gridded crop yield statistics, Monfreda et al., 2008) and global agroclimatic data (e.g. gridded soil characteristics, Batjes, 2005; and climatic data for present-day, New et al., 2002) and farm management practices (e.g. gridded irrigated and rainfed areas, Portmann et al., 2009; and national/subnational fertiliser application rates, IFA, 2002/Mueller et al. (2012)). Foley et al. (2011) estimated global crop production could increase by 58% when closing yield gaps of 16 important food and feed crops. In particular, global potential maize yield is estimated at 50–64% higher than current actual yield (Licker et al., 2010; Mueller et al., 2012; Neumann et al., 2010). Alternatively, global scale estimates of yield gap can be derived from a process-based model run at the global scale. Again van Ittersum et al. (2013) reported potential yield estimated by various modelling studies (including DayCent, Stehfest et al., 2007; PEGASUS 1.0, Deryng et al., 2011; LPJmL, Bondeau et al., 2007; DSSAT, Nelson et al., 2010; GEPIC, Liu et al., 2007). However, for the same reasons listed in Chapters 4 and 6 of this thesis, these results differed largely across models due to the use of different datasets for present-day climate, soil and actual yield observations, making it difficult to compare and assess the robustness of these estimates.

In Chapter 6, I presented a new scenario framework based on representative agricultural pathways (RAPs) to coordinate and harmonise trans-disciplinary modelling analyses of future food supply accounting for alternative trends in agricultural development, climate change impacts, and farmers' adaptive capacity. Based on global RAPs and representative agricultural scenarios (RASs), the next phase of gridded crop modelling intercomparison and improvement initiative (GGCMI) aims to explore the range of

plausible trends in global yield increases according to alternative assumptions on socio-economic and biophysical drivers of food production and their interaction. Drawing upon previous global scale yield gap analyses and the RAPs, this chapter presents a simple exploratory modelling analysis looking at tradeoffs between closing the yield gap through intensive N fertiliser use to increase global crop production and N_2O emissions. The main hypothesis here is that while some places could benefit greatly from increasing rates of fertiliser application to increase crop yields, some other regions of currently low yields are either primarily constrained by temperature conditions, or are water deficient due to limited rainfall and the lack of irrigation infrastructure and/or water resources for irrigation, suggesting that increasing fertiliser application alone in these regions could mostly contribute to large N_2O emissions, without any gain in yields. This chapter aims at validating this hypothesis and identifying regions of important tradeoffs.

The global crop yield model PEGASUS is applied to estimate present-day and potential – i.e. non-N limited – yield for maize in current rainfed and irrigated areas and to quantify the corresponding N_2O emissions. Note for simplicity in the text, the term *potential* is used throughout the following sections of this chapter to refer to non-N limited yields independent of water limitations. The next section describes the crop modelling methodology and approach to estimating N_2O emissions from fertiliser application to soils (section 7.2). Section 7.3 presents N_2O emissions estimates and potential maize production estimates. The significance and limitations of the analysis are discussed in section 7.4 before concluding in section 7.5.

7.2 Methods

7.2.1 Crop yield simulation

In this study, we use the global crop yield model PEGASUS capable of simulating global crop response to climate and farm management practices. PEGASUS has been used in several studies assessing climate change impacts on global crop yields (Chapter 3 and Deryng et al., 2014, 2011; Rosenzweig et al., 2014) and was used in the first GGCMI exercise jointly led by AgMIP and ISI-MIP (see Chapters 4 5 and Rosenzweig et al., 2014). The advantages of using PEGASUS here is that, contrasting with other GGCMs, PEGASUS includes a range of management practices and relies on a minimum set of

data inputs making it a suitable tool for global scale climate impact assessment on agriculture.

PEGASUS' structure and processes are described in detail in Deryng et al. (2014, 2011) and reviewed in Chapter 2. PEGASUS 1.1 is used (as in Chapters 3 and 5) with an updated nutrient stress function, described in the following section, along with the methodology used to estimate potential yield and N_2O emissions resulting from N fertiliser inputs.

7.2.2 Nutrient-stress factor in PEGASUS

The nutrient stress factor in PEGASUS (f_N) is estimated from annual rates of fertiliser application and remains constant throughout the growing season as described in Chapter 2 section 2.2.4 and in Deryng et al. (2011). The nutrient stress function was updated using sub-national fertiliser and manure application rates (Elliott et al., 2014b; Mueller et al., 2012) as opposed to national estimates reported by IFA (IFA, 2002) used in previous PEGASUS' studies. The finer spatial resolution of the data gives a more accurate distribution of fertiliser application and the corresponding yield gap. The nutrient-stress factor was determined by analysing the correlation between rates of chemical fertiliser application and spatial yield gap fraction data in irrigated cropland, assuming nutrient deficit is the main factor limiting crop yield in those areas (see Deryng et al., 2011, and Chapter 2, section 2.2.4, for a detailed rationale behind this assumption). We used the harmonised global mineral fertiliser (including nitrogen–phosphorus–potassium, i.e. NPK) and manure (including NP only) dataset developed for the GGCMI (see Chapter 6, section 6.5.2) and spatial yield-gap fraction data developed by Mueller et al. (2012).

The nutrient stress function in PEGASUS used a linear relationship between rate of fertiliser application and nutrient stress factor. The modified version follows a non-linear least-square algorithm approach proposed by Mueller et al. (2012). The rationale for this approach is that crop yield reaches a plateau at high inputs and NKP fertilisers are not substitutable. In other words, crops require sufficient amounts of all N, P and K, and deficiency in one chemical type is not compensated by adding more of the other chemical types. As in Mueller et al. (2012), the yield response to nutrient follows a standard functional form (Frank et al., 1990; Paris, 1992) and followed the von Liebig
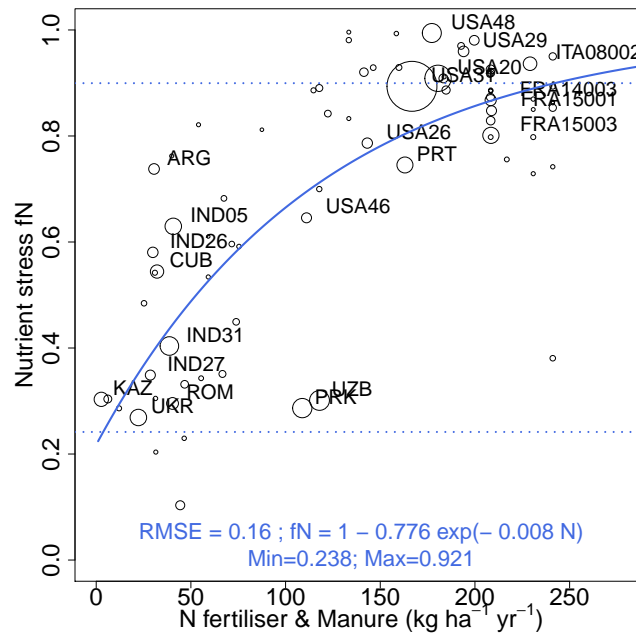
FIGURE 7.1: Scatterplots of sub-national average yield gap fractions in irrigated areas versus total N fertiliser application. We calculated weighted average yield gap fractions by selecting only pixels where more than 20% of the crop-harvested area is irrigated, using global maps of yield gap fraction (Mueller et al., 2012), irrigated areas (Portmann et al., 2009), and harvested area (Monfreda et al., 2008) for maize. The spatial weighting to derive the national averages was based on crop-irrigated areas. We used the harmonised N fertiliser application from Ag-GRID (Chapter 6, section 6.5.2). Areas of circles represent crop-irrigated area.

"law of the minimum" (Paris, 1992) to assess the combined effects of NPK inputs. State-level rates of NPK fertiliser application are then compared to corresponding yield gap data from Mueller et al., 2012 in irrigated grid-cells, assuming that yield gap could be attributed entirely to nutrient limitation as in Deryng et al. (2011).

The regression analysis (Figure 7.1) is weighted to maize irrigated areas – to be consistent with PEGASUS' overall development method (see Deryng et al., 2011) – excluding data points for China. Indeed, China is a major maize producing country known for overusing N fertiliser application and exercises a bias on the weighted regression, resulting in an unrealistic maximum N application threshold value to achieve non-N limited yield. As expected, the regression analysis confirmed maize to be more strongly influenced by N and f_N is expressed as $f_N = 1 - b_N e^{-c_N N} + \xi$, where $b_N = 0.776$, $c_N = 0.008$, and $\xi = b_N e^{-c_N N_{max}}$ so that $f_N = 1$ at N_{max}. Figure 7.1 shows the resulting non-linear regressions between yield gap fraction and the rate of chemical N fertiliser application.

Following Licker et al. (2010), f_N (a value from 0 to 1) indicates the level of potential
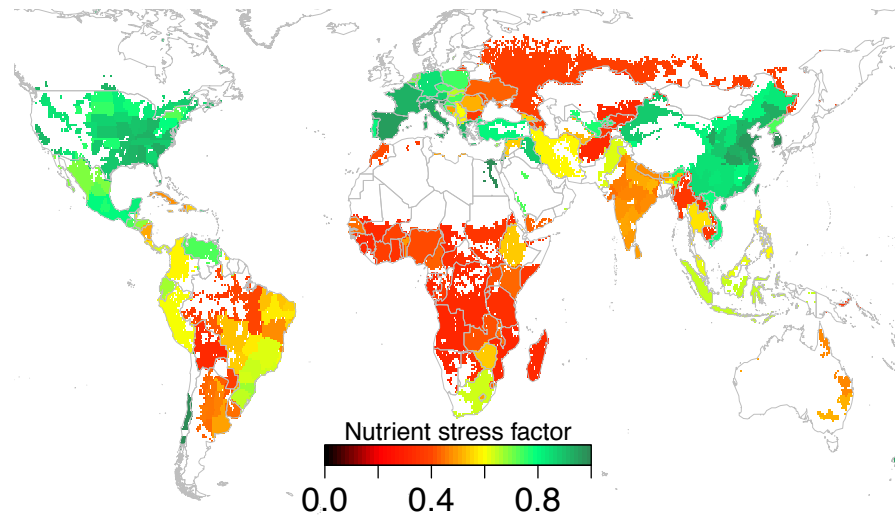
FIGURE 7.2: Spatial variation of nutrient stress factor (f_N) according to current N fertiliser application rates. Dark green areas achieve yield levels close to potential values. Red and orange areas face large yield gaps and thus present great opportunities for increasing yields with more N fertiliser inputs.

yield that is achieved given N fertiliser inputs and climatic conditions. Most developed countries apply high levels of fertiliser and thus exhibit a nutrient stress closer to 1, except Russia, which along with less developed countries – including most of Africa, India and parts of South America – apply low levels of fertiliser resulting in f_N values closer to 0 (Figure 7.2) .

7.2.3   Simulated actual and potential yield

PEGASUS is driven by a six-year subset (1996-2002) from the WATCH daily climate time-series (Weedon et al., 2011) as described in Chapter 2. Other input data consist of soil AWC (Batjes, 2005) and harmonised Ag-GRID crop calendar and fertiliser application data for maize in the present-day (Elliott et al., 2014b and Chapter 6). Earthstat harvested area (Monfreda et al., 2008) and MIRCA2000 irrigated and rainfed areas (Portmann et al., 2009) for maize are used to compute actual and potential yields on current maize harvested areas in a post processing step, after simulating rainfed and full irrigation runs independently.

Similarly to section 3.4 in Chapter 2, the radiation use efficiency (RUE) coefficient under ambient [CO$_2$] (ϵ_{amb}) is tuned to calibrate simulated yield to observed yield at the grid-cell level. Maize ϵ_{amb} value is tuned in this case to 0.035 molC m^{-2}s^{-1}APAR. Figure 7.2 shows PEGASUS performance in simulating present-day observed yield

(Monfreda et al., 2008). Unweighted r^2 (= 0.61) is much higher than in the previous version of PEGASUS ($r^2 = 0.41$, see section 3.4) owing to the use of the non-linear nutrient stress function and the use of prescribed planting and harvesting dates for the present day.

Potential yield is simulated by ensuring that the nutrient stress factor is kept above 0.9, resulting in a minimum N application rate threshold of 183 kg ha^{-1}yr^{-1}. The simulation does not account for improved nutrient assimilation due to enhanced soil management. Therefore, the potential yield simulations allow for application of more than 183 kg ha^{-1}yr^{-1} in areas currently over-applying N fertiliser. In the Mueller et al. dataset, the highest N application rate for maize is currently found in Egypt with up to 372 kgha^{-1}yr^{-1}. Other noticeable regions applying intensive rates of N fertilises (> 200 kg ha^{-1}yr^{-1}) include New Zealand, Western European countries such as Spain, Italy and France, Chile, South Korea, Japan, Manitoba and British Columbia in Canada and several American states, especially located along the Corn Belt. The question of NUE and optimum N fertiliser application rates is discussed further in section 7.5.

Potential yield estimated here includes both water-limited and irrigated potential yields – as defined by Lobell et al. (2009) – based on current maize rainfed and irrigated areas (Portmann et al., 2009). Exploring scenarios of plausible irrigated area expansion is beyond the scope of this study. Thus the term potential yield is used here for simplicity in the text but refers to non-N limited yield on present-day rainfed and irrigated areas.

7.2.4 Nitrous oxide emissions factors

Annual N$_2$O emissions from N inputs to maize harvested area are quantified following the IPCC Tier 1 set of equations for estimating direct and indirect N$_2$O-N emissions from managed soils (Eggleston et al., 2006, Chapter 11). Since N inputs data used here explicitly differentiate synthetic and organic fertilisers, N$_2$O-N emissions are calculated using the IPCC equations for each source of fertilisers. Indirect N$_2$O emissions include atmospheric deposition of volatilised N (N$_2$O-N$_{volatil}$) and N leaching and runoff (N$_2$O-N$_{leach}$) and together with direct N$_2$O-N emissions (N$_2$O-N$_{direct}$) are expressed in
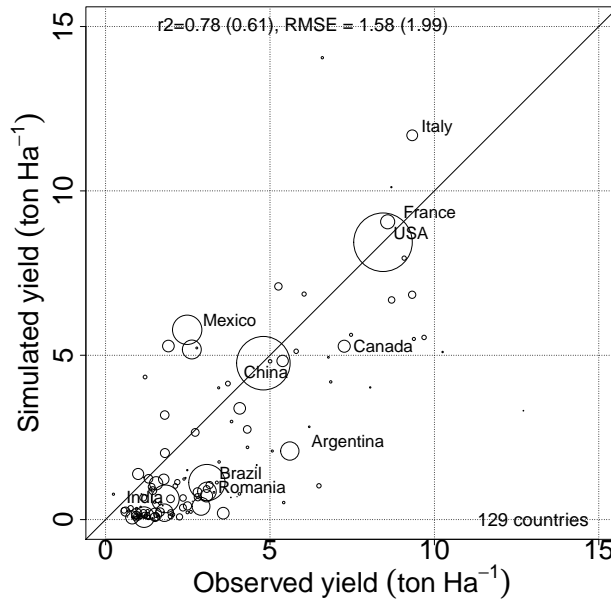
FIGURE 7.3: Scatterplots of national average maize yield from Earthstat present-day yield data versus PEGASUS simulation for the year 2000. Comparison of simulated crop yields and corresponding observations (Monfreda et al., 2008) aggregated by country for maize. Areas of circles represent crop-harvested area. We show both unweighted and weighted R^2 as well as the corresponding root-mean-square error (RMSE) (with the weighting based on crop-harvested area for each country).

units of kg N_2O-N yr^{-1} (see Eggleston et al., 2006, Equations 11.1, 11.9 & 11.10):

$$N_2O_{direct}-N = EF_1(N_f + N_m) \times \mathcal{A}_\mathcal{H} \tag{7.1}$$

$$N_2O_{volatil}-N = EF_4(f_{GASf}N_f + f_{GASm}N_m) \times \mathcal{A}_\mathcal{H} \tag{7.2}$$

$$N_2O_{leach}-N = EF_5 f_{leach}(N_f + N_m) \times \mathcal{A}_\mathcal{W} \tag{7.3}$$

where N_f and N_m (kg N $ha^{-1}yr^{-1}$) correspond to synthetic fertiliser and manure N application rates respectively. $EF_1[$kg $N_2O-N($kg $N)^{-1}]$ is the emission factor for direct N_2O emission from N inputs, EF_4 [kg $N_2O-N($kg $NH_3-N+NO_x-N)^{-1}]$ is the emission factor for atmospheric deposition of N on soils and water surfaces, and EF_5 [kg $N_2O-N($kg N leaching/runoff$)^{-1}]$ is the emission factor for N leaching and runoff. f_{GASf} and f_{GASm} [kg $NH_3-N+NO_x-N($kg N applied$)^{-1}]$ are the fractions of synthetic and organic fertiliser N that volatilises as NH_3 and NO_x. f_{leach} [kg N(kg of N additions$)^{-1}]$ is the fraction of all N added to/mineralised in managed soils in regions where leaching/runoff occurs that is lost through leaching and runoff. Following the approach described in Eggleston et al. (2006, Table 11.3), we assumed leaching to occur on irrigated land and
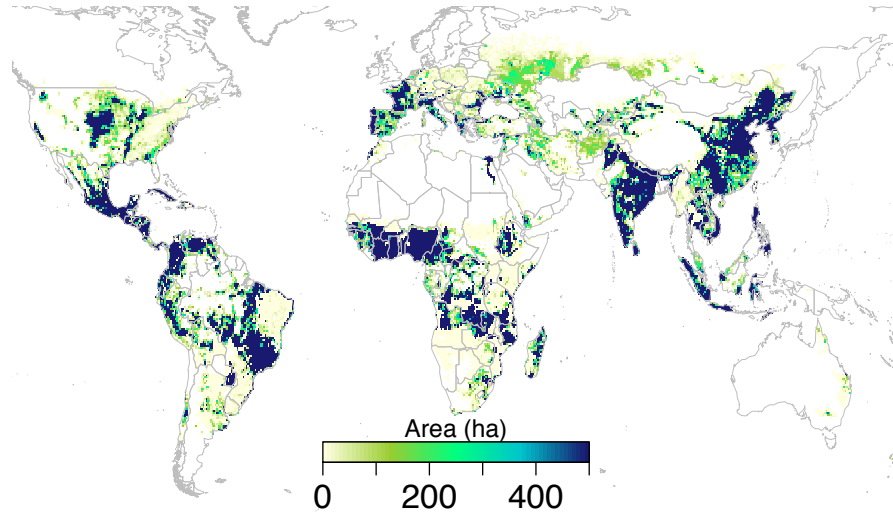
FIGURE 7.4: Area where leaching/runoff occurs: this includes irrigated land and areas where the difference between growing season rainfall minus growing season potential evapotranspiration exceed soil AWC of the top-third layer as estimated in PEGASUS.

in grid-cells where the difference between growing season rainfall minus growing season potential evapotranspiration exceed soil AWC of the top-third layer as estimated in PEGASUS (Deryng et al., 2011) (Figure 7.4).

Finally $\mathcal{A}_{\mathcal{H}}$ (ha) represents maize harvested area and $\mathcal{A}_{\mathcal{W}}$ (ha) in Equations 7.1 to 7.3 represents maize harvested areas including only regions where soil water-holding capacity (i.e. AWC used in PEGASUS) is exceeded, as a result of rainfall and/or irrigation. Note that the IPCC recommends excluding regions using drip irrigation but since the global irrigation dataset does not provide this information, we included all irrigated areas.

Values of each parameter and range of estimates are given in Table 7.1.

TABLE 7.1: Emission factors from IPCC Tier 1 equations to estimate direct and indirect N_2O emissions (Eggleston et al., 2006, Tables 11.1 & 11.3)

Emission factor	Default value	Uncertainty range
EF_1	0.01	0.003–0.03
EF_4	0.01	0.002–0.05
EF_5	0.0075	0.0005–0.025
f_{GASf}	0.1	0.03–0.3
f_{GASm}	0.2	0.05–0.5
f_{leach}	0.3	0.1–0.8

Total N_2O emissions ($kg\ N_2O\ yr^{-1}$) from N inputs to maize cultivated soils are the sum of $N_2O_{direct} - N$, $N_2O_{volatil} - N$ and $N_2O_{leach} - N$, multiplied by $\frac{44}{28}$, the N to N_2O conversion factor. Finally, CO_2 equivalent emissions ($kg\ CO_{2eq}\ yr^{-1}$) are estimated

by multiplying N_2O emissions by 298, the global warming potential (GWP) for N_2O (Stocker et al., 2013, Chapter 8).

7.3   Results

7.3.1   Baseline simulation: maize production circa the year 2000

In the baseline simulation, calibrated to simulate maize yield circa the year 2000 under corresponding farming management practices, PEGASUS estimates global maize production at 546.96 Gt (Table 7.2) using a total of 16.6 Gt of N fertiliser (including both mineral fertiliser and manure). Resulting global N_2O emissions total 307.37 [80.43; 1,362.12] Mt-N_2O yr^{-1}, representing 20% of total N_2O emissions from global cereals, and double N_2O emissions from rice crops (Stehfest and Bouwman, 2006). We find 85% of total annual N_2O emissions from N inputs to managed soils result from direct emissions; 11% comes from N volatilisation and the remaining 4% from N leaching or/and runoff. The range in N_2O emission estimates results from the range in Tier 1 IPCC emission factors (Table 7.1).

Most of the developed world – including North America and Western Europe – achieve optimum land productivity today (Figure 7.5-a) resulting in low rates of N_2O emissions per unit of crop produced (Figure 7.6-a). Western China exhibits higher land productivity while the Eastern regions achieve lower yields, resulting in a national average yield of 5 t ha^{-1} yr^{-1} as opposed to 8.6 t ha^{-1} yr^{-1} in the United States. Finally, the rest of the world – including South America, Africa, the Middle East, Eastern Europe, Russia, India and South East Asia – exhibit relatively low yields (Figure 7.5-a). N_2O emission per unit of crop production varies greatly across the developing world (Figure 7.6-a), suggesting the relatively low yields are only partially caused by nutrient stress and that other factors, such as water stress in rainfed cropland, may also play a major limiting role. Yet regions of particularly elevated N_2O emissions rates per unit of crop production include sub-Saharan Africa, India and South-East Asia and Central America and Brazil.
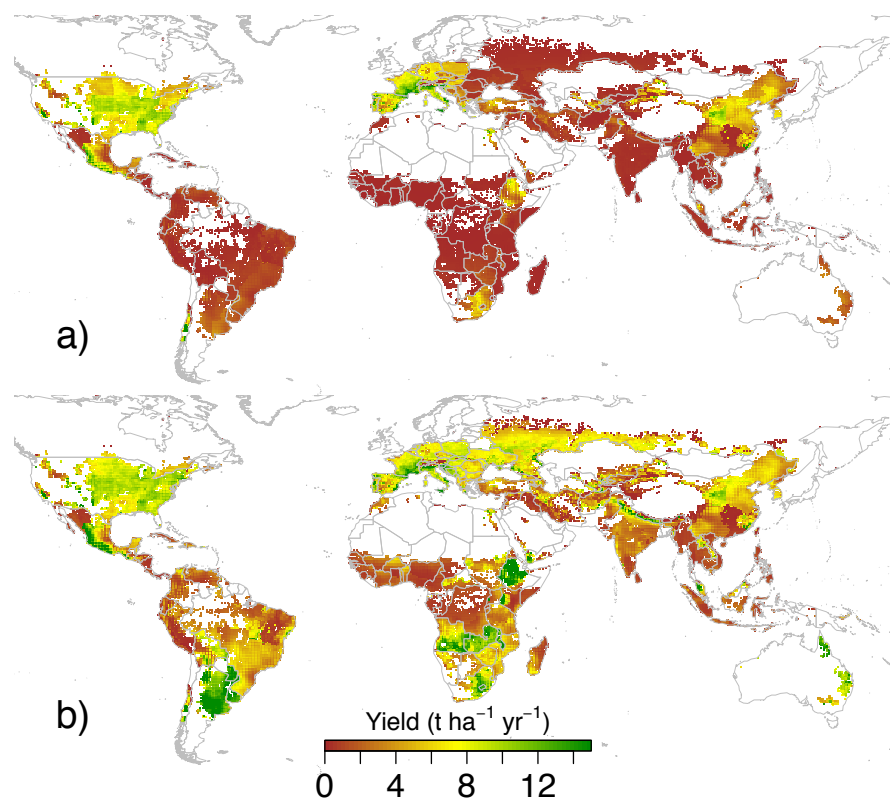
FIGURE 7.5: Simulated actual (a) and potential yields (b).

7.3.2 Nitrous oxide emissions and yield gap closure

We estimate potential maize yield and production on current harvested areas and increase in N_2O emissions resulting from the additional N fertiliser application required to achieve potential land productivity. We find an additional 332 Gt of maize could be produced when maize production systems are not N limited (N application rates > 183 kg ha^{-1} yr^{-1}), representing a 62% increase in global maize production (Table 7.2). Global N_2O emissions from maize due to additional N fertiliser application could reach 493.59 [128.50 ; 2,194.05] Mt-N_2O yr^{-1}. This additional production comes principally from medium and low income countries as richer countries are already close to achieving potential yields (Figure 7.8(a) and section 7.3.3).

We find maize production in Central and South America, Southern and Eastern Africa, Eastern Europe, northern India and China increases as a result of intensive N fertiliser application (up to 183 kg-N ha^{-1} yr^{-1}) confirming the importance of N in boosting yield in these regions (Figure 7.5-b). Yet, as expected, these increases are accompanied by large quantities of N_2O emissions from African, Asian and South American soils (Figure 7.7-b and 7.8(c)). We find the largest increase in N_2O emissions resulting from maize
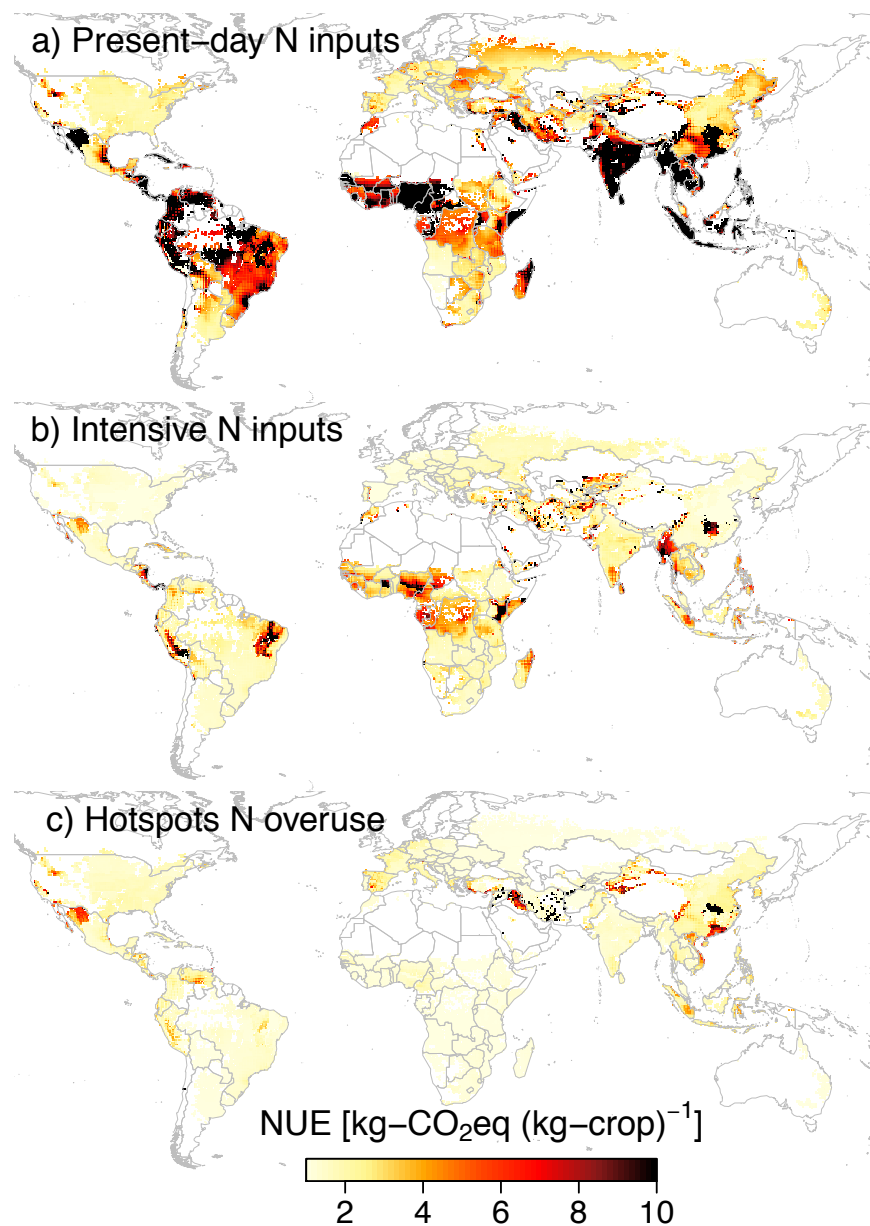
FIGURE 7.6: a) N_2O emissions per unit of crop production (kg CO_2eq/kgcrop) for present-day N inputs; b) Increase in N_2O emissions per kg of crop yield gains under intensive N fertiliser inputs relative to present-day yield (darker areas highlight regions of lower NUE); c) Difference between maps (a) and (b), pointing out regions currently over-applying N fertiliser.

TABLE 7.2: Results for world total, aggregated income economies, top-5 maize producers and top-5 countries presenting lowest f_N values among large producers (harvest area > 10^5 ha and potential yield > 3 t ha^{-1} yr^{-1}). The range in N_2O emissions results from the range in the emission factors. Yield, production and N_2O emissions are to be read as: values corresponding to present-day (top-row) and to potential N inputs (bottom row).

Country	Income group	Harvest area (10^6ha)	Obs.Y (t/ha)	Napp.rates (kg/ha/yr)	Yield gap fraction (f_N)	Yield (t/ha)	Production (1000Mt)	N_2O emissions (10^6kg N_2O)
Global		131.81	4.5	126	0.70	4.1	546.96	307.37 [80.43 ; 1362.12]
						6.7	878.51	493.59 [128.50 ; 2194.05]
Aggregated income economies								
HI		35.80	8.3	182	0.86	8.4	298.98	116.02 [31.44 ; 492.56]
						9.3	332.18	128.33 [34.81 ; 543.96]
MHI		59.36	3.8	135	0.74	3.6	214.34	149.96 [38.92 ; 671.00]
						6.3	375.66	221.59 [57.88 ; 982.14]
MLI		24.15	2.1	68	0.53	0.8	19.45	33.10 [8.03 ; 159.06]
						3.7	88.46	98.21 [24.11 ; 463.44]
LI		12.47	1.4	33	0.42	1.1	14.13	8.15 [2.01 ; 38.83]
						6.6	82.15	45.32 [11.66 ; 203.83]
Top-5 maize producers								
United States	HI	29.1	8.4	180	0.87	8.6	251.1	92.55 [25.2 ; 390.63]
						9.5	275.8	101.13 [27.57 ; 426.15]
China		24.3	4.8	209	0.90	5.0	120.5	93.36 [24.59 ; 410.19]
						5.4	130.6	93.36 [24.59 ; 410.19]
Brazil		11.2	3.1	76	0.60	1.2	12.9	16.39 [4.17 ; 75.33]
	MHI					4.7	53.1	41.68 [10.8 ; 186.22]
Mexico		7.2	2.5	137	0.79	5.9	42.1	19.63 [4.78 ; 94.08]
						8.6	61.5	28.1 [6.9 ; 133.09]
Argentina		2.8	5.6	42	0.48	2.1	14.4	2.11 [0.56 ; 9.27]
						5.9	40.1	9.49 [2.6 ; 39.68]
Top-5 countries with lowest f_N								
Paraguay	MLI	0.36	2.4	21	0.38	0.7	0.24	0.16 [0.04 ; 0.80]
						14.3	5.21	1.41 [0.34 ; 6.80]
Tanzania		1.34	1.5	11	0.34	0.2	0.22	0.30 [0.08 ; 1.45]
	LI					3.8	5.06	4.65 [1.22 ; 20.39]
Mozambique		0.89	0.9	4	0.33	0.2	0.17	0.06 [0.02 ; 0.31]
						5.6	4.98	3.12 [0.80 ; 14.06]
Bolivia	MLI	0.28	2.0	12	0.33	0.2	0.06	0.07 [0.02 ; 0.31]
						7.0	1.95	0.97 [0.26 ; 4.17]
Angola	MHI	0.70	0.6	2	0.31	0.2	0.17	0.03 [0.01 ; 0.16]
						9.5	6.70	2.46 [0.63 ; 11.14]

production in Africa, which currently uses very little amount of N fertiliser. In fact, if Africa and Latin America use intensive rates of N fertiliser on all maize cultivated land, we find N_2O emissions could equal those of the United States and China (Figure 7.8(d)).

N_2O emission rate per unit of crop production is reduced globally, indicating that maize is largely positively responsive to N application in PEGASUS (Figure 7.6-b). Particularly successful regions include most of Africa and India, Madagascar, Eastern Europe, central and southern parts of Brazil, northern Argentina and central Mexico. However, a few regions remain relatively inefficient in terms of yield even with intensive N use: Peru and the Andean regions, Guatemala and north-west of Mexico (Sonora states) and north-east Brazil in Latin America; Nigeria and Tanzania in Africa; Spain in
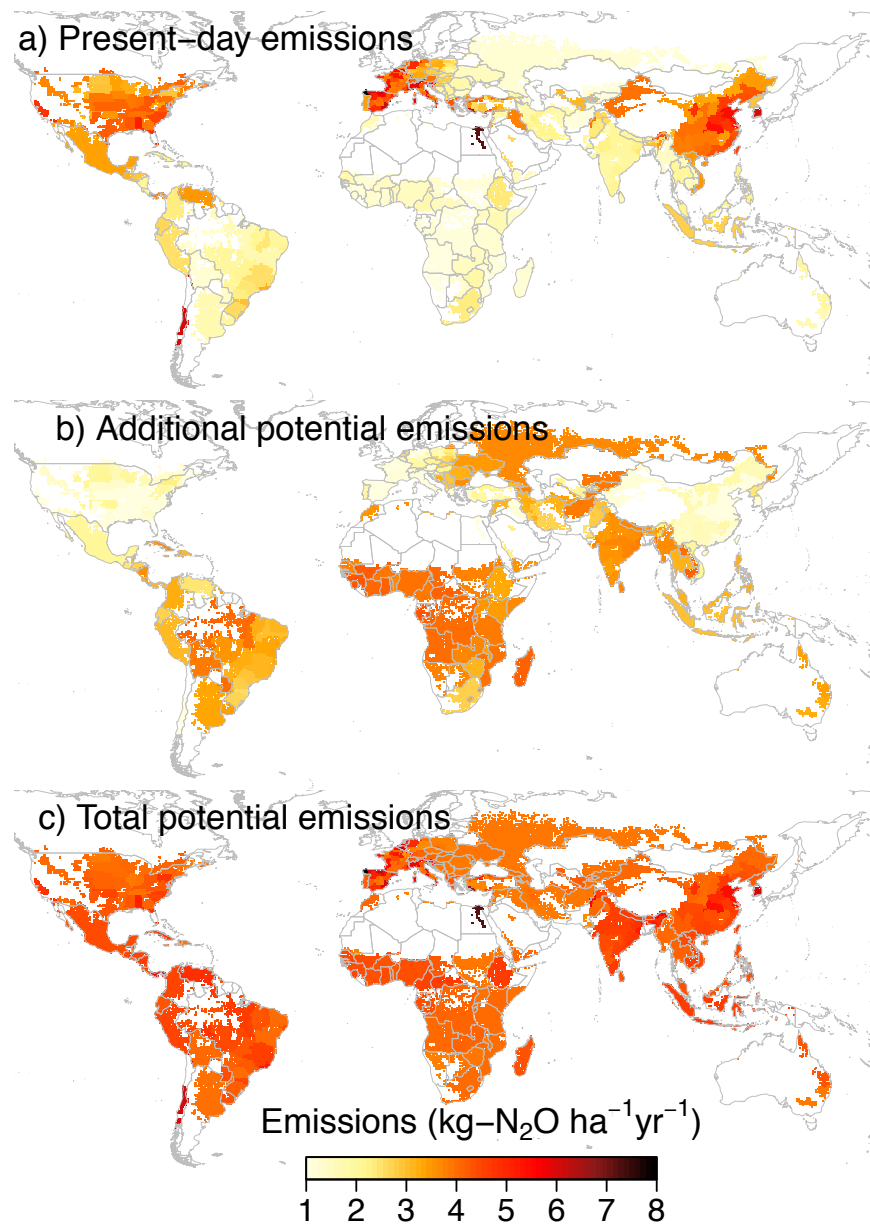
FIGURE 7.7: Estimated N_2O emission rates (kg N_2O ha^{-1} yr^{-1}) for current N inputs levels (a). Additional N_2O emission rates resulting from closing yield gaps (b), and total N_2O emission rates from closing yield gaps (c).

Western Europe and most of the Middle East and Turkey; the Philippines and southern parts of China as well as north-west China. The relative inefficiency of increasing N fertiliser can indicate that other limiting factors need to be addressed in these regions in addition to N deficits.

7.3.3   Country ranking and income levels

The top-5 maize producing countries (see Appendix D for definitions of income groups), chiefly the United States, China, Brazil, Mexico and Argentina, contribute to 80% of global maize production (Figure 7.8(e)) and 70% of global N_2O emissions resulting from N fertiliser use (Table 7.2). The largest shares are emitted by the United States and China (each accounting for 30% of total emissions). Latin American countries, in particular Brazil, Mexico and Argentina, account for another 12% of total emissions (Figure 7.8(f)). High income (HI) countries produce more than half of global maize production and contribute to 38% of total N_2O emissions (including the United States, France, Italy, Canada, and Spain among the largest producing countries) whereas medium high income (MHI) countries contribute to 47% of total N_2O emissions resulting from 38% of global maize production (including China, Brazil, Mexico, Argentina, and Romania) (Tables 7.2 and 7.3 and Figure 7.8(b)). Medium low income (MLI) countries contribute to 11% of total N_2O emissions from 8% of global maize production (including India, Indonesia, Egypt, Nigeria and Ukraine among the largest producing countries in this category) while low income (LI) countries contribute to only 3% of total N_2O emissions from 3% of global maize production (including Kenya, Ethiopia, Tanzania, Nepal, and North Korea among the largest producing countries in this category) (Table 7.3 and Figure 7.8(b)). Finally, parts of China, the Middle East, and the West coast of the United States show overuse of N fertiliser (Figure 7.6-c)

Among the most important maize growing countries (harvest areas $> 1 \times 10^5$ ha), the top-5 countries experiencing the largest nutrient stress whilst being able to produce a minimum maize yield of 3 t ha^{-1} yr^{-1} with sufficient N inputs are Paraguay, Tanzania, Mozambique, Bolivia and Angola.

We further classify countries by their N use efficiency (NUE), defined here as the amount of N_2O emissions relative to crop production (kg-N2O/kg-crop). With intensive N inputs among the 73 most important maize growing countries, the top-5 five most efficient countries include Malawi, Ethiopia, Lesotho, Argentina and Paraguay, which produce average yields above 14 t ha^{-1} yr^{-1}, higher than potential yields estimated for the United States and Western Europe (Figure 7.6 and Table 7.3). This suggests that environmental conditions are exceptionally favourable for maize cultivation in these places, but that N availability is currently severely limiting (Sanchez, 2010). Other

remarkably productive countries include the United States, Mexico, France, Italy, South Africa, Hungary and Serbia, where yields achieve > 8.5 t ha^{-1} yr^{-1}. In contrast, the top-5 least efficient countries include Myanmar, Nigeria, Cameroon, the Philippines and Nicaragua, where yields remain low, suggesting that other environmental limiting factors must be addressed in these regions to increase yields. The case of Nigeria raises particular attention as it ranks seventh in terms of maize harvest area: increasing N inputs could increase risk of nitrate leaching and further N$_2$O emissions from cultivated soils without gaining much for land productivity. Other notable countries signalling some degree of low NUE include China, Brazil, India, Indonesia, Egypt, Thailand and Tanzania (Figure 7.6 and Table 7.3).

TABLE 7.3: Most and least N efficient countries relative to potential N$_2$O emissions and potential maize production capacity

Country	Income group	% of total maize harvest area	NUE (kg N$_2$O (kg-crop)$^{-1}$)
		top-5 most efficient countries	
Malawi	LI	4.9	0.21 [0.06 ; 0.87]
Ethiopia		8.8	0.23 [0.06 ; 1.06]
Lesotho		0.9	0.23 [0.06 ; 0.96]
Argentina	MLI	21.1	0.24 [0.06 ; 0.99]
Paraguay		2.8	0.27 [0.07 ; 1.30]
		Top-5 least efficient countries	
Myanmar	LI	1.6	3.84 [1.06 ; 16.03]
Nigeria		27.6	4.11 [0.98 ; 19.99]
Cameroon		2.4	4.33 [1.03 ; 21.08]
Philippines	MHI	16.0	4.77 [1.12 ; 23.41]
Nicaragua		2.2	6.24 [1.46 ; 30.78]

Among the top-20 countries with the largest maize harvested areas (Table 7.4), we find twelve face significant nutrient stress ($f_N < 0.6$): the Democratic Republic of Congo, Tanzania, Kenya and Ethiopia among LI economies; India, Nigeria and the Philippines among MLI economies; and Brazil, Romania, Argentina, Serbia and Thailand among MHI economies. Increasing N application levels in these countries could bring an additional 120 Gt of maize (equivalent to half of current United States' maize production and 22% of global maize production) and an additional 112 Gt of N$_2$O to the atmosphere (equivalent to 36% of current estimated N$_2$O emissions).

The top-5 biggest N$_2$O emitters are China, the United States, Mexico, Brazil and India. Under current maize harvested areas, assuming elevated N inputs globally results in the same ranking of top-5 emitters.
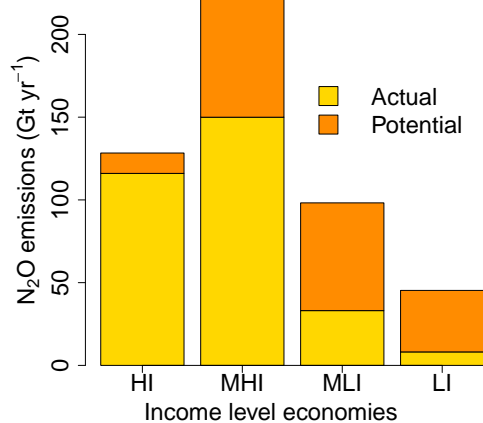
(a) N₂O emissions by income groups
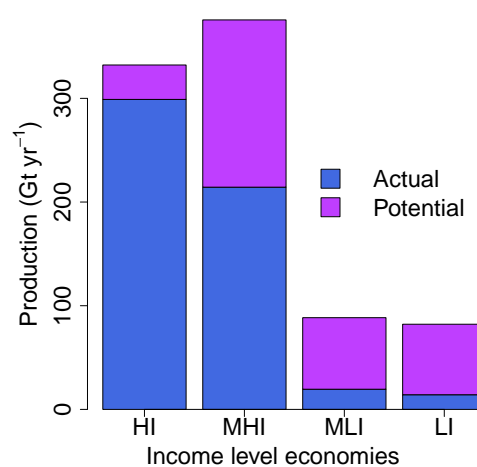
(b) Maize production by income groups
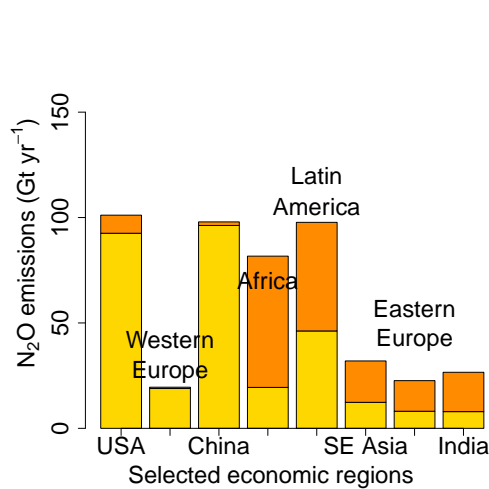
(c) N₂O emissions by economic regions
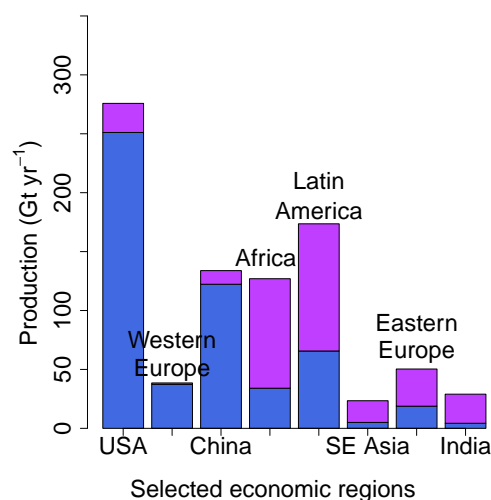
(d) Maize production by economic regions
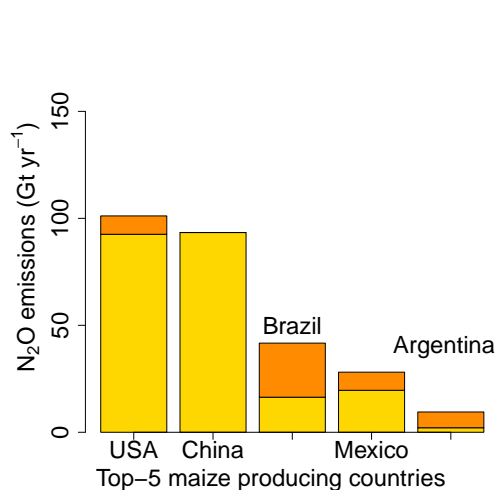
(e) N₂O emissions by top-5 countries
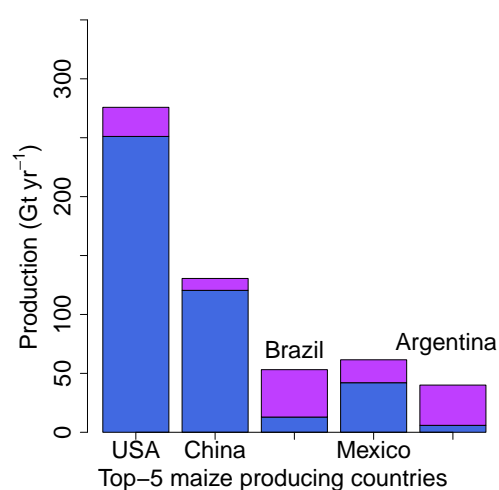
(f) Maize production by top-5 countries

FIGURE 7.8: Actual and potential total N_2O emissions ($Gt\ yr^{-1}$) by income groups (a), economic regions (c) and for the top-5 producers (d). Figures (b-d-e) show corresponding actual and potential maize production ($Gt\ yr^{-1}$)

TABLE 7.4: Results for top-20 countries of largest harvested areas. Yield, production and N_2O emissions are to be read as: values corresponding to present-day (top-row) and to potential N inputs (bottom row).

Country	Income group	Harvest area (10^6ha)	Obs.Y (t/ha)	Napp.rates (kg/ha/yr)	Yield gap fraction (f_N)	Yield (t/ha)	Production (1000Mt)	N_2O emissions (10^6kg N_2O)
United States	HI	29.1	8.4	180	0.87	8.6	251.1	92.55 [25.2 ; 390.63]
						9.5	275.8	101.13 [27.57 ; 426.15]
France		1.7	8.6	238	0.93	9.1	15.6	7.41 [1.97 ; 32.11]
						9.1	15.6	7.41 [1.97 ; 32.11]
China	MHI	24.3	4.8	209	0.90	5.0	120.5	93.36 [24.59 ; 410.19]
						5.4	130.6	93.36 [24.59 ; 410.19]
Brazil		11.2	3.1	76	0.60	1.2	12.9	16.39 [4.17 ; 75.33]
						4.7	53.1	41.68 [10.8 ; 186.22]
Mexico		7.2	2.5	137	0.79	5.9	42.1	19.63 [4.78 ; 94.08]
						8.6	61.5	28.1 [6.9 ; 133.09]
South Africa		3.0	2.6	83	0.64	5.2	15.8	4.54 [1.22 ; 19.56]
						10.7	32.3	10.55 [2.86 ; 44.66]
Romania		3.0	3.1	44	0.51	0.9	2.6	2.36 [0.64 ; 10.18]
						6.0	17.8	9.74 [2.68 ; 40.51]
Argentina		2.8	5.6	42	0.48	2.1	5.9	2.11 [0.56 ; 9.27]
						14.4	40.1	9.49 [2.6 ; 39.68]
Serbia		1.3	4.1	67	0.59	3.4	4.3	1.49 [0.41 ; 6.31]
						8.5	10.8	4.17 [1.15 ; 17.3]
Thailand		1.2	3.6	61	0.57	0.2	0.3	1.4 [0.35 ; 6.45]
						1.1	1.3	4.3 [1.1 ; 19.44]
Hungary		1.1	5.4	114	0.69	4.8	5.4	2.22 [0.61 ; 9.32]
						8.5	9.4	3.7 [1.02 ; 15.36]
India	MLI	6.5	1.8	59	0.49	0.7	4.3	7.93 [1.88 ; 39.15]
						4.5	29	26.59 [6.51 ; 126.05]
Nigeria		3.6	1.2	24	0.41	0.1	0.3	1.87 [0.43 ; 9.52]
						0.9	3.4	14.13 [3.36 ; 68.67]
Indonesia		2.5	2.9	96	0.64	0.4	1.0	4.89 [1.16 ; 24.03]
						1.4	3.4	10.43 [2.49 ; 50.58]
Philippines		2.1	1.8	66	0.60	0.2	0.5	2.94 [0.68 ; 14.63]
						0.8	1.7	8.32 [1.96 ; 40.83]
Ukraine		1.3	3.1	30	0.43	0.7	0.9	0.68 [0.18 ; 2.99]
						7.7	9.7	4.21 [1.15 ; 17.7]
Kenya	LI	1.5	1.5	39	0.43	1.1	1.7	1.14 [0.29 ; 5.21]
						7.2	11	5.42 [1.48 ; 22.85]
Congo Dem. Rep.		1.5	0.8	5	0.32	0.1	0.1	0.14 [0.03 ; 0.7]
						1.6	2.3	5.18 [1.31 ; 23.63]
Tanzania		1.3	1.5	11	0.34	0.2	0.2	0.3 [0.08 ; 1.45]
						3.8	5.1	4.65 [1.22 ; 20.39]
Ethiopia		1.2	1.9	76	0.54	5.3	6.2	1.79 [0.43 ; 8.81]
						18.3	21.2	4.81 [1.2 ; 22.45]

7.4 Discussion

There are some published studies on quantifying yield gaps and potential yields using results from field experiments and trial contests (Gustafson et al., 2014; Lobell et al., 2009), statistical analyses of global crop and climatic datasets (Licker et al., 2010; Mueller et al., 2012; Neumann et al., 2010) and more sophisticated approaches based on crop modelling and agroecological zones (van Wart et al., 2013a,b, the Global Yield Gap Atlas: www.yieldgap.org). Our analysis is unique in linking yield gap closure and the resulting N_2O emissions and consequences for GHG emissions. The

results presented here give a partial view on the tradeoffs between increasing fertiliser applications to increase crop yields and GHG emissions. A full analysis needs to include other important crops and contrast the N_2O emissions to the avoided CO_2 emissions from deforestation. For instance, Valin et al. (2013) considered the climate mitigation benefits of closing the yield gap but related this to CO_2 emission reduction resulting from avoided land use change. They found that intensive use of fertilisers to increase global crop production could reduce total agricultural GHG emissions by 8% when accounting for CO_2 emissions from land use change, N_2O emissions from cultivated soils and livestock manure and methane (CH_4) emissions from livestock manure, enteric fermentation and rice cultivation.

Although definition of potential yield used here differs from that used by Gustafson et al. (2014), it is interesting to note our estimate that the additional 332 Gt of maize produced by increasing N inputs using PEGASUS is remarkably close to the additional 335 Gt of maize estimated using an empirical-data driven approach. The two approaches also differ by several assumptions, such as the baseline year (2000 here, versus 2010) and the degree of yield gap closure (here 90% versus 83.5%) as well as their consideration of improving irrigation and other optimum management practices (which are not included here).

Regarding N_2O emissions, the results for the baseline simulation can be compared to those recently published by Perlman et al. (2014), who used a metamodelling approach based on the DeNitrification-DeComposition (DNDC) model. Their (ibid) approach aimed to capture better regional variation in N_2O estimates due to soil organic matter and climatic conditions. They estimated total N_2O emissions from soil growing maize at 157 10^9 kg CO_2eq and an average emissions rate of 1038 kg CO_2eq ha^{-1}. We find much lower total N_2O emissions from maize soils (91.6 [24 ; 406] 10^9 kg CO_2eq) and a lower average emissions rate of 695 [182 ; 3080] kg CO_2eq ha^{-1}, which is also much lower than that reported by Linquist et al. (2011) (1,399 kg CO_2eq ha^{-1}). One reason for these low estimates is that emissions from N inputs to soils only were included, whereas DNDC captures more complex soil biogeochemistry responsible for N_2O emissions. However, when comparing national emissions estimates, our study does not produce systematically lower estimates (Table 7.5). In fact, Perlman et al. (2014) acknowledged their study overestimated emissions in some places, and was very sensitive to irrigation, which could be reasons for some of the difference in the estimates. Finally, Perlman et al.

(2014) identify important emissions in the Andean region, southern and north-east China, Central America and Western Europe and low emissions in Eastern Europe and Argentina; similar to our findings (Figure 7.7-a).

TABLE 7.5: Comparison of N_2O emission estimates (10^6 kg CO_2eq) between this study, using PEGASUS and Perlman et al. (2014, Appendix S6), using a metamodel version of DNDC (metaDNDC).

Country	metaDNDC	PEGASUS
Argentina	2,677	629
Brazil	12,037	4,886
China	15,874	27,580
Ethiopia	765	534
France	3,605	2210
India	6,323	2,363
Indonesia	10,327	1,458
Mexico	23,131	5,850
Nepal	1,400	264
Nigeria	3,625	556
Romania	543	704
South Africa	975	1364
Ukraine	1,446	203
United States	23,134	27,580

It should be noted that the N_2O emissions estimates presented here involve large uncertainties, as highlighted by the huge range of global emission factors and estimates, and should therefore be used with caution. In fact, this study is mainly aimed at exploring tradeoffs between increasing use of N inputs and GHG emissions rather than providing precise estimates of N_2O emissions from maize cultivation. Indeed, the approach uses single emission factors provided by the IPCC, which has been widely criticised for underestimating N_2O emissions, and not capturing spatial and temporal variations in emissions due to timing of fertiliser application, climate conditions and other factors (Berdanier and Conant, 2011; Good and Beatty, 2011; Nishina et al., 2012; Olander et al., 2013; Reay et al., 2012). However, the currently available methods for quantifying emissions are often too expensive or complex, or not sufficiently user friendly for widespread use (Olander et al., 2013; Philibert et al., 2013), so that global assessments remain limited to using the IPCC Tier 1 emission factors as a default method (Berdanier and Conant, 2011; Hénault et al., 2012). In addition, although PEGASUS is used to identify areas where leaching and runoff occurs, it does not take into account tropical soil characteristics relevant for N_2O emissions, and the estimate of leaching

and runoff-related N_2O does not capture adequately variation across watersheds and agricultural systems (Nevison, 2000). Another source of uncertainty includes the fact that we only consider one (the main) cropping season, so that maize grown in the tropics matures quicker than that in temperate regions; thus simulated annual maize production in the tropics is often lower than actual production due to the inclusion of only one growing season. Finally, there are uncertainties associated with the global fertiliser dataset and the use of a single crop modelling approach to simulate yield and yield potential (as demonstrated in Chapter 5).

7.5 Conclusion

Acknowledging the wide range of uncertainties in global N_2O emissions estimates, this study provides useful insights to the tradeoffs between increasing N fertiliser to raise maize yields in developing countries and reducing global GHG emissions. We estimate global maize production could increase by 60% as a result of more intensive N application rates. However, some regions show greater yield increase than others, confirming that N application alone will not improve yield successfully if other limiting factors, such as PK unbalance and water scarcity, are not addressed simultaneously. South Africa, Kenya, Madagascar, and large maize producers such as India, central and southern Brazil and Argentina benefit extensively from increasing rates of N fertiliser application. However, other key maize producing areas do not gain in crop productivity from additional application of N fertiliser. These areas include northeast Brazil, Nigeria and Tanzania, where factors such as soil nutrients imbalance and water scarcity limits N fertilisation effects (Barros et al., 2005; Sanchez, 2010); and China, where current overuse of N fertiliser lead to large amount of nitrate pollution in rivers (Ju et al., 2006, 2009).

These findings confirm the importance of targeted farming management options to improve sustainability of cropping systems and further increase global crop supply (Cassman, 1999; Foley et al., 2011; Godfray and Garnett, 2014). The methodology employed here, using a global gridded crop model, will benefit from improvement in global N_2O estimates from soils and representation of spatial variations in emissivity and from further links to global climate change and agroeconomic modelling (Havlík et al., 2014) to explore in more detail the tradeoffs involved in increasing fertiliser inputs, not

only in terms of yield and emissions, but also in the broader context of future food and energy security to identify better options for a "real green revolution".

Chapter 8

Conclusion

8.1 Overview of results and hypotheses

The overall ambition of this thesis was to improve global scale assessments of climate change impacts on global crop production and agricultural adaptive capacity by addressing key knowledge gaps in simulating key influences on crop yield and quantifying multiple sources of uncertainty. This chapter first summarises the main results and how they support the hypotheses raised throughout this thesis, and then provides a discussion of the main findings. Finally, I conclude with implications of this research followed by an outlook for future research and a broader perspective about the role of scientific knowledge in informing policy and decision making.

Chapters 3 and 5 covered some understudied biophysical processes at the global scale and thus presented new knowledge related to two fundamental drivers of climate change impacts on crop yield: the effect of extreme temperatures occurring around crop flowering and the role of elevated atmospheric CO_2 concentration ($[CO_2]$). Chapter 6 presented a new framework to address the role of adaptation and link socio-economic drivers of food production to climate change impacts assessments on global crop yields. Illustrating the theoretical framework introduced in Chapter 6, Chapter 7 then presented an exploratory analysis of tradeoffs associated with nitrogen (N) fertiliser application to increase global maize yield and subsequent increases in greenhouse gas (GHG) emissions as a result of nitrous oxides (N_2O) emissions from agricultural soils and discussed implications for global food security and climate adaptation and mitigation policy.

The frequency and severity of extreme climatic events are expected to increase with global warming (Stocker et al., 2013), raising the chance of seasonal heatwaves, which can be highly detrimental to crops especially when occurring around their flowering period. However, none of the previous global scale agricultural impact assessments of the effects of climate change published before Deryng et al. (2014) (presented in Chapter 3) had accounted explicitly for this process. Moreover, only a few smaller scale studies have been conducted; two on long-term impacts of extreme temperature stress over the Mediterranean basin (Moriondo et al., 2011) and one over India (Challinor et al., 2007a), and a few large scale studies have focused on regional historical impacts (Africa, Lobell et al., 2011a; France, Hawkins et al., 2013; and the United States, Schlenker and Roberts, 2009. Yet, along with increasing risks of water scarcity and floods, extreme heat stress poses a major threat to future crop yields and necessitates much greater consideration. I therefore quantified for the first time at the global scale the impacts of extreme heat stress at anthesis on yields of maize, spring wheat and soybean using the global crop model PEGASUS. First, I showed extreme heat stress at anthesis (HSA) reduces substantially relative gains, expected as a result of carbon fertilisation of C_3 crops, in global crop yields of spring wheat and soybean. Second, I established that HSA doubles global maize losses; maize is a C_4 crop and thus does not benefit much from elevated CO_2 enhancement on photosynthesis. Third, I showed HSA impacts vary widely by regions and that large producers of the crops as well as vulnerable countries could experience negative effects of HSA, which could seriously affect global crop supply and food security. In particular, I found the United States and Brazil could experience up to 15–50% reductions in average soybean yield, respectively, and 3–15% reductions in average maize yield. Fourth, I found the range of uncertainties in simulated impacts resulting directly from uncertainties in simulated climate change produced by eighteen global climate models (GCMS) doubles between the 2050s and the 2080s as radiative forcing increases under RCP 8.5. Soybean presented the highest level of uncertainty with results exhibiting both positive and negative impacts, while maize was generally negative and spring wheat generally positive. Finally, when assuming CO_2 fertilisation effects to be negligible, I demonstrated drastic climate mitigation policy as in RCP 2.6 could avoid more than 80% of the global average yield losses otherwise expected by the 2080s under RCP 8.5.

Overall, this chapter confirms the hypothesis that HSA induced by climate change could

severally harm crop yields globally and threaten global food security. Changes in spring wheat yields remain positive even after HSA halves global average gains, but Maize yield losses worsen almost uniformly when including HSA effects. Unexpectedly, climate change impacts on soybean yields are the most contrasting around the world due to strong HSA effects in some key producing regions. As well, the conclusion from this chapter leans towards strong climate mitigation efforts to reduce the risk of negative impacts on crop yields as the range of uncertainty increases with radiative forcing, mostly due to rising differences in climate change signals and debatable CO_2 fertilisation effects.

In Chapter 3, I presented results both with and without including CO_2 fertilisation as it is not clear yet whether and by how much this specific driver of climate change impacts on crop yield will be realised in the field (Kirkham, 2012). In fact, there is still a strong debate among the scientific community (Ainsworth et al., 2008; Long et al., 2006; Tubiello et al., 2007) about this effect and further investigations are urgently needed to better understand the role of CO_2 on crop physiology and its interaction with multiple drivers of crop yield – such as temperature, water, N and ozone (O_3), the effects of which can vary substantially among crop types and also among agroecosystems (Leakey et al., 2012). Understanding the role of CO_2 fertilisation is therefore a key priority for agricultural impacts assessment of climate change because, with relatively strong CO_2 fertilisation effects based on FACE observations, global average yields of C_3 crops are projected to increase in some regions despite negative impacts from adverse climatic conditions. Research published prior to the study presented in Chapter 5 generally followed the same approach as in Chapter 3, consisting of two sets of results with and without CO_2 fertilisation effects (e.g. Müller et al., 2010; Parry et al., 2004). Some other studies have not accounted for CO_2 fertilisation effects at all, primarily focusing on the direct drivers of climate change impacts (e.g. Deryng et al., 2011). However none of these approaches satisfy either the information demands of policy makers or those of climate impacts modellers and agronomists. First, policy makers need better transparency related to current uncertainties on the role of elevated CO_2 on crops. Second, climate impacts modellers and agronomists need to work more closely to resolve the key sources of uncertainties. Climate impacts modellers need to perform robust evaluation of model performance, its strengths and limitations such as the research design I presented in Chapter 5, while agronomists must extend FACE experiments to sub-tropical and tropical cropping systems.

I therefore addressed this central source of uncertainty in crop models in Chapter 5. Results presented in Chapter 5 were made possible thanks to the coordination of the first GGCMs intercomparison analysis, in which I took an active part as one of the leading project coordinators, which I described in detail in Chapter 4. I compared estimates of simulated crop yield and actual evapotranspiration (AET) over the growing season for maize, wheat, rice and soybean among six GGCMs driven by five GCMs and both including and excluding CO_2 fertilisation effects in the models. I presented results in terms of simulated impacts on crop water productivity (CWP), which is defined as the ratio of crop yield to AET to encompass both CO_2 effects in one metric.

First I showed the six GGCMs tend to agree in the sign of change in global average simulated yield, AET and CWP when accounting for direct effects of climate change but excluding CO_2 fertilisation, with net decreases simulated for each variable. However, when including CO_2 fertilisation effects by the end of the 21st century under RCP 8.5, the sign of change in global average yield differ considerably among GGCMs, especially for rice and soybean, which is reflected in estimated global average CWP. Relative change in global average CWP between the 2080s and the 1980s show smaller increases in the median for rice and soybean but was associated with a larger range of uncertainties (5.6 ± 26.6 and $7.1 \pm 29.8\%$ respectively) than for maize and wheat (12.4 ± 22.5 and $17.3 \pm 20.3\%$ respectively). Second, I identified large differences in GGCM response as a result of the different approaches used to simulate photosynthesis. GGCMs using an empirically derived equation of radiation use efficiency (RUE) tend to simulate lower CO_2 fertilisation effects than those using a complex leaf-level biogeochemistry description (also known as the Farquhar approach). Third I showed that results vary widely across crops, not only due to the C_3 versus C_4 photosynthesis pathway distinction but also due to other factors simulated differently by the GGCMs. For instance, I found effects of HSA that were simulated by only one of the GGCMs (i.e. PEGASUS) systematically led to lower decreases in global average yield and CWP. In addition, I found results to be more negative when nutrient stress was fully represented in the GGCMs. Then, I also showed the importance of the choice of evapotranspiration equations in driving some of the regional differences in results, confirming similar findings for global hydrological models (Federer et al., 2010; Harding et al., 2011) and highlighting the need for further GGCM intercomparison and sensitivity analyses of water and temperature stress. Finally I also found significant differences in results due to contrasting parameterisation and

calibration methods, which contributed to large differences in results generated by multiple versions of the same model run by different research groups. Fourth, I presented the first GGCM evaluation against FACE measurements and showed CWP simulations broadly cover the range of CWP observations, with differences between wet and dry conditions well represented. However, the extent of FACE data on CWP remain very limited due to the scarcity of AET data, which are very difficult to measure from an experimental perspective (Bernacchi, personal communication) and hence limits the comparison. Overall, I demonstrated substantial differences among GGCMs simulations reflecting fundamental gaps in our understanding of crop response to elevated CO_2. Furthermore the main findings of Chapter 5 call for much needed large scale observations to be conducted under a wider range of agroecological conditions as well as more thorough GGCM intercomparison and sensitivity analyses to be performed on both yield and water use.

The large potential positive effects of elevated $[CO_2]$ on crop yields and crop water use are receiving greater attention in the literature. In fact, if realised in the fields, carbon fertilisation effects could alleviate largely the negative impacts of temperature and water stresses on global crop yields. In addition, effect of elevated $[CO_2]$ on transpiration crop demand could provide an opportunity for increasing CWP and thus reducing pressure on water use in some regions. However, results presented in this chapter confirm the hypothesis that modelling skills of global crop responses to CO_2 are limited due to scarce availability of FACE experimental results on both crop yields and ET in diverse agroclimatic conditions. Furthermore, the traditional focus of GGCMs on yield have left behind analyses on CO_2 effects on crop quality, which is even more crucial for global food security (Myers et al., 2014; Taub et al., 2008). Both complex leaf-level representation and RUE modelling approaches need to be rigorously tested against observations and compared to constrain the range of uncertainty and improve predictions. Yet it is expected that these improvements will take some times due to FACE experimental constraints. As decision-makers must plan for adaptation and mitigation regardless of predictive skills of impact models, it is therefore advisable to pursue modelling intercomparison exercises such as this one to improve transparency and clarity of existing carbon fertilisation uncertainties and thus increase usefulness of results from agricultural impact assessments.

In response to biophysical impacts of climate change on crop yields, farmers are

expected to adapt their agricultural management practices to reduce some of the negative impacts and/or take advantage of eventual opportunities. The adaptive capacity of the agricultural sector across the world will, however, depend on local infrastructures and economic resources, such as farmers' access to new cultivars and costs associated with increasing irrigation and fertiliser application (Claessens et al., 2012; Vermeulen et al., 2012a), and general trends in socio-economic and technological development pathways (Adger et al., 2005; Barnett, 2010; Berry et al., 2006).

Therefore, in Chapter 6, I addressed the role of agricultural adaptation options in response to climate change with a trans-disciplinary approach designed to account for socio-ecological drivers of food production and underlying complex interactions between the environment, the economy and society. Drawing upon findings and methodologies presented in Chapters 4 and 5, I presented in Chapter 6 the coordinated representative agricultural pathway (RAP) framework initiated by AgMIP and in which I took a central role by directing the design of RAPs for use in GGCMs. First, I showed how the RAPs contribute to the broader mechanism of scenarios development in climate research (Moss et al., 2010) by specifically targeting the agricultural sector. Second, I demonstrated how the RAPs enable integration of both biophysical and socio-economic dimensions of food productions systems at multiple scales to produce consistent evaluation of the role of farming management practices and adaptive capacity under different levels of climate change impacts and socio-economic development trends. In addition, I reviewed emerging challenges for designing RAPs that require them to be coherent and flexible across multiple scales and disciplines. Third, I introduced methods for applying RAPs to GGCM and for designing specific representative agricultural scenarios (RASs) to drive GGCMs that are consistent with the agricultural and land use storylines described in the shared socio-economic pathways (SSPs) (O'Neil et al., 2014). I showed how RASs for GGCM could rely on a minimum number of variables and parameters given the level of detail currently represented in GGCMs, such as level of fertiliser application, irrigation area and capacity to switch cultivars. Finally, I presented a new harmonised agricultural gridded datasets, developed by Ag-GRID (Elliott et al., 2014b), for the global gridded crop modelling intercomparison and improvement initiative (GGCMI). Ongoing and future GGMCI activities include historical model validation analyses, sensitivity analyses to change in biophysical factors, as mentioned earlier in Chapter 5, and assessments of future climate impacts on crop yields and agricultural adaptation

responses (see www.agmip.org/ag-grid/ggcmi and Appendix B).

This chapter aimed to resolve the hypothesis that biophysical and socio-economic factors of future crop production and demand must be integrated within a flexible and systematic framework carefully designed to explore a wide range of possible and unknown futures in respect of agricultural impacts, vulnerability and adaptation. While RAPs and RASs are currently under development for use within global and regional agro-economic models, this chapter focused on their potential relevance to and use within GGCMs, and proposed a list of actions to move forward with pathway and scenario development. Central to the success of the development and use of the RAPs is a clear and systematic documentation of proposed pathways, and most importantly a constant interaction across the disciplines of agricultural impact modelling. The main recommendation for the next phase of AgMIP and GGCMI activities consists in developing a small number of RAPs applicable to both global agro-economic models and GGCMs that span a wide range of farmers' adaptive capacity futures and broad enough to allow models from various disciplines, origins and philosophies to develop suitable quantitative RASs, thus enabling co-ordinated and transdisciplinary multi-model intercomparison studies, useful for decision-makers.

Then in Chapter 7, in parallel with undergoing RAP development activities within AgMIP, I used the crop model PEGASUS to explore tradeoffs associated with one of the main agricultural development strategies for increasing crop yields: increasing N fertiliser application. This development will be necessary to raise crop yields in regions currently suffering from N deficit, chiefly most of sub-Saharan Africa, India, Latin America and Eastern Europe. This study aimed to take climate change impacts assessments on crop yield to a greater level of complexity; one in which farming adaptive capacity and technological development pathways are taken into account, along with biophysical drivers of climate change impacts on crop yields, as explored in Chapters 3 and 5. I presented in Chapter 7 an exploratory analysis focusing on present-day yield change for maize due to potential increases in fertiliser application to close the global yield gap. This allowed an evaluation of tradeoffs associated with subsequent increases in N_2O emissions. The main motivation behind this analysis was to identify and illustrate tradeoffs associated with a RAS of high land productivity growth driven by intensive fertiliser application for use in a GGCM, here PEGASUS. The eventual objective is to fully explore synergies and tradeoffs linked to diverse agricultural intensification options

within a coordinated GGCMI exercise that will involve participation of multiple GGCMs and global economic models (see www.agmip.org/ag-grid/ggcmi and Appendix B).

First I showed global maize production could increase by 62% when applying optimum N fertiliser to the current maize harvested areas, resulting in an additional 332 Gt of maize production. However, I estimated that current level of N application rates to maize harvested areas produce 91.6 [24 ; 406] 10^9 kg CO_2eq emissions, representing 20% of estimated total N_2O emissions from current cereal production. Second, I estimated total N_2O emissions could reach 147 [38 ; 654] 10^9 kgCO_2eq under high N inputs, with an emission rate of 1,115 [288 ; 4,962] kg CO_2eq ha^{-1} yr^{-1} in contrast to 695 [182 ; 3,080] kg CO_2eq ha^{-1} yr^{-1} for the present-day. Third, I found large regional disparities in nutrient use efficiency (NUE) in terms of yield increase relative to N_2O emissions. I identified large potential for increasing N fertiliser application in South Africa, Kenya, Madagascar, and some of the main maize producing countries: India, central and southern Brazil and Argentina. However, I found important tradeoffs in some other key maize producing countries such as China and north-east Brazil as well as Nigeria and Tanzania, suggesting increasing N fertiliser use without addressing other limiting factors such as water scarcity and, in the case of China for instance, overuse of N fertiliser and manure application, could result in large increases in global N_2O emissions without any benefit on local crop yields. Overall, I demonstrated an original integrated analysis looking at tradeoffs associated with N fertiliser applications in maize cropping systems, which could contribute to the development of improved international policy to achieve sustainable intensification and a "greener" revolution.

Results from this chapter confirm the hypothesis that important tradeoffs need to be negotiated in order to increase crop yields sustainably in many parts of the world. Yet the large uncertainties accompanying N_2O emissions estimates and the use of a single GGCM call for further research and modelling analyses to better integrate regional N_2O emission estimates and provide robust information on the opportunities and tradeoffs associated with intensive N fertiliser applications globally.

8.2 Discussion

Results presented in this thesis contribute advances to the quantitative analysis of future climate impacts on crop yields. However some important sources of uncertainty were left out and thus, will require detailed examination to further constrain the range of uncertainties in climate impacts assessments on crop yield.

First of all, the analysis of the effects of HSA on crop yield presented in Chapter 3 included some assumptions and uncertainties such as the specific choice of global temperature threshold parameters for HSA and the use of monthly average climate data produced by the Community Integrated Assessment System (CIAS) (coupled to PEGASUS weather generator), which did not account for changes in the frequency of extreme temperatures. In fact, relative impacts on yields presented in Chapter 5 were found to be more negative than results reported in Chapter 3. Reasons for these differences can be explained, in part, by the use of daily climate data from the CMIP5 climate data ensemble instead of monthly mean climate data; Climate data from CMIP5 represent more adequately changes in extreme precipitation patterns, droughts and extreme temperature, to which GGCMs are highly sensitive.

Moreover, only spring variety of wheat was simulated in Chapter 3. In Chapter 5, PEGASUS spring wheat simulations were extrapolated to winter wheat harvested areas to enable comparison with the other GGCM wheat simulations.

Secondly, none of the crop simulations performed in this thesis accounted for potential limitation in irrigation water resources due to climate change impacts on freshwater flows, which is likely to be a key driver of future irrigated crop yields. Furthermore other important drivers of climate change impacts on crop yields such as negative effects of pests, diseases, air pollutants, floods and storms were excluded from the analyses. Some complex interactions and feedbacks between the variety of drivers of climate change impacts, such as CO_2-O_3-N_2O interactions, are unaccounted for in current state of the art crop modelling analysis.

Additionally, the use of a single GGCM in Chapters 3 and 7 led to a partial estimate of the range of uncertainties that did not account for crop model sensitivity. In fact, the use of multiple GGCMs in Chapter 5 proved the importance of better understanding and evaluating multi-crop model performance, as results showed a large range of impacts and

discrepancy among GGCMs. Yet the GGCM intercomparison analyses included some limitations, such as the partial harmonisation of GGCMs inputs data, calibration and parameterisation making it difficult to identify accurately sources of uncertainty.

Finally, results presented in Chapter 7 were based on global average N_2O emissions factors, which resulted in large underestimation of emissions from tropical croplands. Moreover, the fertiliser and yield gap dataset used to run PEGASUS contained some additional uncertainties. Last but not least, this study accounted only for quantity of fertiliser application and omitted the role of timing on crop growth and yield, which interact with climatic conditions to affect nitrate leaching and N_2O emissions. Detrimental effects of N fertiliser application on surrounding water quality, eutrophication and biodiversity must be included in future analyses to fully address environmental challenges for agricultural intensification.

8.3 Implications

Despite the limitations listed above, this doctoral research has addressed some important gaps in climate change impact assessments on global crop yields. I showed extreme temperatures could result in large negative impacts on crop yield of key producing regions and vulnerable countries. I identified areas showing larger disagreement in estimated crop yields, resulting from uncertainty in climate model projections; I confirmed the likelihood of strong negative impacts over most of Africa and south-east Asia, South America and Australia; and potential positive impacts on yield in the higher latitudes. I also demonstrated the role of elevated CO_2 on crops to be the most sensitive factor in global crop model simulations and thus needs careful examination to improve future climate impact assessments. I identified key research questions to be explored in the next phase of climate impact assessments on crops: chiefly, future crop modelling studies must prioritise evaluation of the role of elevated CO_2 on crops across biomes and the role of different model assumptions and choice of parameterisation. Finally, I presented a detailed conceptual framework integrating the multiple dimensions of agricultural production to assess their complex interactions and the role of adaptation to climate change; and a concrete example of a RAP looking at tradeoffs between optimising fertiliser application on crop yield and GHG emissions. Establishing adaptive capacity at the global scale presents a major challenge, which needs to be examined urgently.

In the first part of this thesis, I focused on analysing the impacts of key processes for crops, altered by climate change: the role of extreme heat stress and the role of carbon fertilisation effects. Modelling results comprise of two sets of simulation ensembles: (1) made of eighteen different simulations generated by one GGCM (PEGASUS) driven by eighteen GCMs (Chapter 3) and (2) thirty different simulations generated by six GGCMs driven by five GCMs (Chapter 5). The key implications of the findings are:

- the use of daily climate data as opposed to monthly mean climate data interpolated to daily more adequately represents crop response to climate variability. It is therefore strongly recommended to use daily climate data to drive crop models when possible;

- there are poorly understood processes currently limiting knowledge of impact assessments, including: CO_2 effects on photosynthesis and ET in tropical and sub-tropical climate; N-CO_2 interaction; FACE experiments located in tropical and sub-tropical sites, especially looking at carbon-temperature-water-nitrogen interactions and effects on crop growth and yields are urgently needed;

- there are nonetheless well established drivers of crop yields, including: temperature, light and precipitation; the broad patterns of impacts on yield remains consistent with results from early agricultural impact studies such as Parry et al. (2004); Rosenzweig and Parry (1994);

- divergence among results ensembles calls for better and consistent documentation and standardisation of farming management options in models;

- additional geospatial data are urgently needed, especially to cover sub-tropic and tropical cropland including: 1) historical yield and harvested areas for model validation, 2) historical N fertiliser applications; 3) irrigation areas; 4) crop calendar data and multiple cropping systems; Novel techniques combining remote-sensing images and census data could be extremely valuable;

- there has been little effort to run GGCMs at regional scales; modelling intercomparison projects such as AgMIP can offer better interactions among experts across the world to encourage such regional analyses; there is no doubt that use and application of GGCMs to carefully targeted regions of study would improve both predictive and exploratory analyses. First, regional data can be

accessed more easily for model calibration, validation and sensitivity analyses; Additionally, interaction with local stakeholders and regional experts can provide a better sense of regional vulnerability to a particular adaptation policy and increase the chance of implementing successful adaptation planning supported by an ensemble of impact model simulations.

- most GGCMs are designed to simulate large monoculture cropping systems and do not represent adequately the complexity of multiple cropping often found in tropical and subtropical regions, which may consist in either growing more than one crop on a field at the same time, after each other in a sequence or with overlapping growing periods (Waha et al., 2013).

In the second part of this thesis, I focused on developing and testing a new coordinated framework for studying opportunities and tradeoffs of different farming adaptation measures. Findings support the statement that climate change can also offer opportunities for the agriculture sector and global food security if the right adaptation measures are implemented and economic resources provided. These adaptations include switching to more suitable crop varieties, delaying or advancing crop planting dates, carefully targeted increased N fertiliser applications, especially as it would not just raise crop yield but also interact with elevated $[CO_2]$, to further amplify the fertilisation effects.

8.4   Outlook

This doctoral research has been driven by the motivation to produce valuable quantitative knowledge to inform policy and decision-making, intended to enhance global food security while fundamentally reducing the ecological footprint of the world's population and create a sustainable society for future generations. When performing this research I faced a knowledge/action dilemma, that is to say questioning the utility of producing "global kinds of knowledge" as Hulme neatly put it (Hulme, 2010), while in parallel, climate and land use policy – needed more than ever to solve the global environmental crisis – depend nonetheless on the extent and quality of scientific knowledge of global climate impacts on agriculture. Of course absolute accuracy is a

utopia in modelling and risk assessments of climate change impacts and real plans must be made in light of incomplete knowledge and deep uncertainty (Haasnoot et al., 2013).

Already, enough diversion has fuelled the political discourse of climate change to delay concrete actions to reduce GHG emissions and achieve a 2°C limit to global warming (Edwards, 2011; Sarewitz, 2011). In fact, a shift towards localised systemic problem solving (Fiscus, 2013) and polycentric governance (Ostrom, 2008, 2010) have been proposed to empower grassroots initiatives, encourage collective action to deal with global environmental issues and resolve global governance inertia (Manuel-Navarrete, 2010).

Furthermore, there are strong geographical biases related to climate knowledge production that originate mostly from western scientific institutions and climate impacts and vulnerability that are likely to be much stronger in the developing world (Deryng et al., 2014; Field et al., 2014; Hulme, 2010; Rosenzweig et al., 2014). To conclude, future impact assessment research must not only explore the frontiers of scientific knowledge but, importantly, must also address complex interactions across scales and disciplines to connect researchers and encourage active involvement of regional stakeholders, local practitioners and scientists in the design and application of climate impact research and policy (Dessai et al., 2004; Khagram et al., 2010; Krueger et al., 2012).

Appendix A

AgMIP & ISI-MIP publications

"How do various maize crop models vary in their responses to climate change factors?" in *Global Change Biology*. Bassu et al. (2014)

Abstract: Potential consequences of climate change on crop production can be studied using mechanistic crop simulation models. While a broad variety of maize simulation models exist, it is not known whether different models diverge on grain yield responses to changes in climatic factors, or whether they agree in their general trends related to phenology, growth, and yield. With the goal of analysing the sensitivity of simulated yields to changes in temperature and atmospheric carbon dioxide concentrations [CO_2], we present the largest maize crop model intercomparison to date, including 23 different models. These models were evaluated for four locations representing a wide range of maize production conditions in the world: Lusignan (France), Ames (USA), Rio Verde (Brazil) and Morogoro (Tanzania). While individual models differed considerably in absolute yield simulation at the four sites, an ensemble of a minimum number of models was able to simulate absolute yields accurately at the four sites even with low data for calibration, thus suggesting that using an ensemble of models has merit. Temperature increase had strong negative influence on modelled yield response of roughly –0.5 Mg ha^{-1} per °C. Doubling [CO_2] from 360 to 720 μmol mol^{-1} increased grain yield by 7.5% on average across models and the sites. That would therefore make temperature the main factor altering maize yields at the end of this century. Furthermore, there was a large uncertainty in the yield response to [CO_2] among models. Model responses to temperature and [CO_2] did not differ whether models were simulated with low calibration information or, simulated with high level of calibration information.

Author contributions: The first eight authors are members of leading group of AgMIP-Maize Team. All other authors made equivalent contributions and are listed in

alphabetical order by surnames.

"Constraints and potentials of future irrigation water availability on agricultural production under climate change" in the *Proceedings of the National Academy of Sciences*. Elliott et al. (2014a)

Abstract: We compare ensembles of water supply and demand projections from 10 global hydrological models and six global gridded crop models. These are produced as part of the Inter-Sectoral Impacts Model Intercomparison Project, with coordination from the Agricultural Model Intercomparison and Improvement Project, and driven by outputs of general circulation models run under representative concentration pathway 8.5 as part of the Fifth Coupled Model Intercomparison Project. Models project that direct climate impacts to maize, soybean, wheat, and rice involve losses of 400–1,400 Pcal (8–24% of present-day total) when CO_2 fertilisation effects are accounted for or 1,400–2,600 Pcal (24–43%) otherwise. Freshwater limitations in some irrigated regions (western United States; China; and west, south, and central Asia) could necessitate the reversion of 20–60 Mha of cropland from irrigated to rainfed management by end-of-century, and a further loss of 600–2,900 Pcal of food production. In other regions (northern/eastern United States, parts of South America, much of Europe, and south-east Asia) surplus water supply could in principle support a net increase in irrigation, although substantial investments in irrigation infrastructure would be required.

Author contributions: Elliott, Frieler, Gerten, Rosnezweig, and Ruane designed research; Elliott, **Deryng**, Müller, Konzmann, Gerten, Glotter, Flörke, Wada, Best, Eisner, Fekete, Folberth, Gosling, Haddeland, Khabarov, Ludwig, Masaki, Olin, Satoh, Schmid, Stacke, Tang, and Wisser performed research; Elliott, **Deryng**, Müller, Gerten, Flörke, Wada, Eisner, Folberth, Gosling, Haddeland, Khabarov, Ludwig, Masaki, Olin, Satoh, Schmid, Stacke, and Tang contributed new analytic tools; Elliott, Frieler, and Konzmann analysed data; and Elliott, **Deryng**, Müller, and Foster wrote the paper.

"Climate change effects on agriculture: Economic responses to biophysical shocks" in the *Proceedings of the National Academy of Sciences*. Nelson et al. (2014)

Abstract: Agricultural production is sensitive to weather and thus directly affected by climate change. Plausible estimates of these climate change impacts require combined use of climate, crop, and economic models. Results from previous studies vary substantially due to differences in models, scenarios, and data. This paper is part of a collective effort to systematically integrate these three types of models. We focus

on the economic component of the assessment, investigating how nine global economic models of agriculture represent endogenous responses to seven standardised climate change scenarios produced by two climate and five crop models. These responses include adjustments in yields, area, consumption, and international trade. We apply biophysical shocks derived from the Intergovernmental Panel on Climate Change's representative concentration pathway with end-of-century radiative forcing of 8.5 W/m^2. The mean biophysical yield effect with no incremental CO_2 fertilisation is a 17% reduction globally by 2050 relative to a scenario with unchanging climate. Endogenous economic responses reduce yield loss to 11%, increase area of major crops by 11%, and reduce consumption by 3%. Agricultural production, cropland area, trade, and prices show the greatest degree of variability in response to climate change, and consumption the lowest. The sources of these differences include model structure and specification; in particular, model assumptions about ease of land use conversion, intensification, and trade. This study identifies where models disagree on the relative responses to climate shocks and highlights research activities needed to improve the representation of agricultural adaptation responses to climate change.

Author contributions: Nelson, Valin, Sands, Von Lampe, Lotze-Campen, van Meijl, van der Mensbrugghe, and Müller designed research; Nelson, Valin, Sands, Havlík, Ahammad, **Deryng**, Elliott, Fujimori, Hasegawa, Heyhoe, Kyle, Von Lampe, Lotze-Campen, Mason d'Croz, van Meijl, van der Mensbrugghe, Müller, Popp, Robertson, Robinson, Schmid, Schmitz, Tabeau, and Willenbockel performed research; Nelson, Valin, Sands, Havlík, Ahammad, **Deryng**, Elliott, Fujimori, Hasegawa, Heyhoe, Kyle, Von Lampe, Lotze-Campen, Mason d'Croz, van der Mensbrugghe, Müller, Popp, Robertson, Robinson, Schmid, Schmitz, Tabeau, and Willenbockel analysed data; and Nelson and Valin wrote the paper.

"Multisectoral climate impact hotspots in a warming world" in the *Proceedings of the National Academy of Sciences.* Piontek et al. (2014)

Abstract: The impacts of global climate change on different aspects of humanity's diverse life-support systems are complex and often difficult to predict. To facilitate policy decisions on mitigation and adaptation strategies, it is necessary to understand, quantify, and synthesise these climate-change impacts, taking into account their uncertainties. Crucial to these decisions is an understanding of how impacts in different sectors overlap, as overlapping impacts increase exposure, lead to interactions of impacts, and are likely to raise adaptation pressure. As a first step we develop herein a framework to study coinciding impacts and identify regional exposure hotspots. This framework can then be used as a starting point for regional case studies on vulnerability and multifaceted

adaptation strategies. We consider impacts related to water, agriculture, ecosystems, and malaria at different levels of global warming. Multisectoral overlap starts to be seen robustly at a mean global warming of 3℃ above the 1980–2010 mean, with 11% of the world population subject to severe impacts in at least two of the four impact sectors at 4℃. Despite these general conclusions, we find that uncertainty arising from the impact models is considerable, and larger than that from the climate models. In a low probability-high impact worst-case assessment, almost the whole inhabited world is at risk for multisectoral pressures. Hence, there is a pressing need for an increased research effort to develop a more comprehensive understanding of impacts, as well as for the development of policy measures under existing uncertainty.

Author contributions: Piontek, Frieler, Schellnhuber, Warszawski, and Schewe designed research; Piontek performed research; Piontek, Müller, Pugh, Clark, **Deryng**, Elliott, de Jesus, Colón González, Flörke, Folberth, Franssen, Friend, Gosling, Hemming, Khabarov, Kim, Lomas, Masaki, Mengel, Morse, Neumann, Nishina, Ostberg, Pavlick, Ruane, Schewe, Schmid, Stacke, Tang, Tessler, Tompkins, and Wisser analysed data; and Piontek, Müller, Pugh wrote the paper.

"Assessing agricultural risks of climate change in the 21st century in a global gridded crop model intercomparison" in the *Proceedings of the National Academy of Sciences.* Rosenzweig et al. (2014)

Abstract: Here we present the results from an intercomparison of multiple global gridded crop models (GGCMs) within the framework of the Agricultural Model Intercomparison and Improvement Project and the Inter-Sectoral Impacts Model Intercomparison Project. Results indicate strong negative effects of climate change, especially at higher levels of warming and at low latitudes; models that include explicit nitrogen stress project more severe impacts. Across seven GGCMs, five global climate models, and four representative concentration pathways, model agreement on direction of yield changes is found in many major agricultural regions at both low and high latitudes; however, reducing uncertainty in sign of response in mid-latitude regions remains a challenge. Uncertainties related to the representation of carbon dioxide, nitrogen, and high temperature effects demonstrated here show that further research is urgently needed to better understand effects of climate change on agricultural production and to devise targeted adaptation strategies.

Author contributions: Rosenzweig, Elliott, **Deryng**, Ruane, Müller, Boote, Glotter, Piontek, and Jones designed research; Elliott, **Deryng**, Müller, Arneth, Folberth, Glotter, Khabarov, Neumann, Pugh, Schmid, Stehfest, and Yang performed research; Elliott, **Deryng**, Ruane, and Müller contributed analytic tools; Rosenzweig, Elliott,

Deryng, Ruane, Müller, and Boote analysed data; and Rosenzweig, Elliott, **Deryng**, Ruane, and Müller wrote the paper.

Appendix B

Global Gridded Crop Model Intercomparison and Improvement Initiative. Guidance document

Co-Leaders:

Joshua Elliott, University of Chicago and Argonne National Laboratory

Christoph Müller, Potsdam Institute for Climate Impact Research

Senior Advisors:

Cynthia Rosenzweig, NASA Goddard Institute of Space Studies

Cesar Izaurralde, University of Maryland and Pacific Northwest National Laboratory

Scenario/RAP coordinator:

Delphine Deryng, University of East Anglia

Climate data coordinator:

Alexander Ruane, NASA Goddard Institute of Space Studies

For more information, please visit www.agmip.org/ggcmi

Reproduction from draft-version dated: 3 april 2013

B.1 Overview and motivation

The Agricultural Model Intercomparison and Improvement Project (AgMIP; Rosenzweig et al., 2013; www.agmip.org) is leading a coordinated, international, trans-disciplinary process to improve regional and global assessments of climate change impacts on agricultural production and food security. Although there have been many agricultural impact studies in the past, the lack of consistency in the data, models, and assumptions used has generally caused problems in interpreting and using results. Additionally, recent research has shown that the use of multiple crop models in assessments greatly helps in our understanding of uncertainties.

In 2012 AgMIP led a Global Gridded Crop Model (GGCM) Intercomparison fast-track project in coordination with the PIK-led Inter-Sectoral Impacts Model Intercomparison Project (ISI-MIP). This fast-track included seven GGCMs and focused primarily on updating the state of knowledge on the expected impacts of climate change on crop systems using the most modern data and models. This fast-track culminated with the January 31st submission of six papers to a PNAS special issue that is expected in print by fall 2013.

B.2 A new generation of model intercomparison and improvement for the international GGCM community

Starting in spring 2013, we are developing a new set of protocols for the first phase of the GGCMI, which will focus on model evaluation, skill, and improvement. Phase 1 will run for three years and include three overlapping stages of increasing duration:

1. Historical simulation and model evaluation

2. Analysis of model sensitivity to NCTW (nitrogen, carbon, temperature, and water)

3. Coordinated global climate assessment

Each stage will include planning, simulation, analysis, and publication components that will build on the previous stage while proceeding in parallel to the extent possible (Table B.1).

Planning stages will include the preparation and dissemination of the requisite harmonised weather/climate, environmental, and management datasets used as model inputs. The development of these products will be coordinated by the Ag-GRID

		Year 1				Year 2				Year 3			
	Quarter	1	2	3	4	1	2	3	4	1	2	3	4
Stage 1: Historical simulation and model evaluation	Planning												
	Simulation												
	Analysis												
	Publication												
Stage 2: Analysis of NCTW sensitivity	Planning												
	Simulation												
	Analysis												
	Publication												
Stage 3: Coordinated Inter-Sectoral global assessment	Planning												
	Simulation												
	Analysis												
	Publication												
Other key activities	IT and data services												
	Scenarios and RAPs												

Table B.1. Three year time-line for GGCMI phase 1

leadership team in partnership with the AgMIP and ISI-MIP climate teams, the AgMIP soils initiative, and the AgMIP economics team and RAP group. This design takes maximum advantage of available data, resources, and expertise available within AgMIP and ISI-MIP and frees up the active modelling teams as much as possible to focus on core model development and simulations.

Publication will include article submissions to top quality journals timed to coincide with public releases of input data and simulation outputs, published through an Earth Systems Grid (ESG) node and metadata catalog maintained at the University of Chicago and Argonne National Lab.

As of now, we have engaged modelling groups from fourteen institutions in eight countries to participate in this next phase of the project (Table B.2). Key to the success of this activities will be the team's ability to leverage existing AgMIP strengths by bringing together AgMIP members from the climate, crop modelling, information technology (IT), Representative Concentration Pathways (RAPs), scaling, uncertainty, and economic teams to develop new initiatives for improving quality and access to gridded data, models, computing, and scenario development and coalesce the international community of large-scale gridded crop modellers around the most important topics at the interface of food and climate.

In order to ensure success of the core activities of the Ag-GRID GGCMI team, we will pursue several additional activities that integrate with other AgMIP groups and strengths to maximally leverage our participation in the project.

Stage 1: Historical simulation and model evaluation. In the first stage, models will be run using various observation and reanalysis-based historical weather products so that the models can be evaluated over the historical period globally and in various key

Model	Institution	Contact	Notes
pDSSAT	U Chicago, USA	jelliott@ci.uchicag.edu	Based on DSSAT4.5; mai, whe, soy, ric
LPJmL	PIK, Germany	cmueller@pik-potsdam.de	Ecosystem-type model; ~16 crops
PEGASUS	Tyndall, UEA, UK	d.deryng@uea.ac.uk	Ecosystem-type model; mai, whe, soy
EPIC-Boku	Boku, Austria	erwin.schmid@boku.ac.at	Based on EPIC; ~16 crops modeled
GEPIC	EAWAG, Switzerland	christian.folberth@eawag.ch	Based on EPIC; mai, whe, soy, ric
LPJ-GUESS	Lund, Germany	stefan.olin@nateko.lu.se	Ecosystem-type model
CropSyst-WU	Washington U, USA	stockle@wsu.edu	Based on field-scale CropSyst
GLAM	Walker Inst., UK	t.m.osborne@reading.ac.uk	
ORCHIDEE-mil	IPSL, France	nathalie.de-noblet@lsce.ipsl.fr	DGVM type with STICS crop model
CGMS	Wageningen, NL	allard.dewit@wur.nl	Based on WOFOST
EPIC-IIASA	IIASA, Austria	velde@iiasa.ac.at	Based on EPIC
DAYCENT	Colorado State, USA	dennis.ojima@colostate.edu	**[Confirmation pending]**
MCWLA	IGSNRR, China	taofl@igsnrr.ac.cn	**[Confirmation pending]**
EPIC-JGCRI	JGCRI, USA	cesar.lzaurralde@pnnl.gov	Based on EPIC

Table B.2. Models and groups engaged thus far for the AgMIP GGCMI team

interest regions and so that inter-model differences can be compared to the variation induced by the choice of historical data product.

Stage 2: Analysis of NCTW sensitivity. In the second stage, model sensitivity to individual climatic drivers will be analysed followed by an analysis of the influence of implicit and explicit assumptions on modelling results.

Stage 3: Coordinated Inter-Sectoral global assessment. Throughout the project we will coordinate activities and data with the ongoing ISI-MIP project. This collaboration will culminate in a new global inter-sectoral assessment of climate vulnerabilities, impacts, and adaptations for which we will begin simulations near the end of year 2.

B.3 Other key activities and coordination with other AgMIP teams

B.3.1 Gridded data assimilation, validation, and distribution improves all models

Simulations with field scale crop and climate impact models, require daily time series of detailed weather data over one or more years. Primary variables in the weather series are

daily max/min temperatures, precipitation, and incoming solar radiation. Models can typically also take one or more secondary weather variables if available, such as surface wind speeds and relative humidity. Key environmental data for models is typically encoded in soil and surface profiles and includes the slope and aspect, albedo, surface permeability and soil water retention properties, organic carbon, nitrogen, pH, rooting depth, and many more. Key management inputs include nitrogen fertiliser application rates, irrigation capacity, and cultivar choice, and secondary management inputs can include phosphorous fertiliser application rates, pest control, and tillage methods.

One immediate way to improve gridded modelling capacity within AgMIP and more broadly is to improve the quality, availability, and usability of the gridded data products that are the backbone of any gridded modelling effort or assessment. AgMIP is in a unique position to leverage climate, soil, management, and IT expertise to create integrated and scalable solutions to the data challenges posed by large-scale gridded crop modelling. Members of the GGCMI team are already making substantial strides towards cataloguing, gathering, preparing, and synthesising high resolution (in space and time) observational weather data, multi-terabyte ensembles of (raw and bias-corrected) climate model output, environmental data (such as soil properties) at regional or global scales, and information on local planting, management, and cultivar decisions. With the formalisation of these activities under the GGCMI initiative, we will accelerate these activities and facilitate better utilisation of these data products in the scientific community.

B.3.2   Information technology and scalable data solutions are key

In order to make use of the results of this massive data organisation and standardisation activity we require IT solutions for data ingest, processing, storage, and delivery that can scale from the point-based AgMIP data standards to high-resolution multi-terabyte archives of integrated crop modelling data. These efforts require a modern and sustained effort to leverage High-Performance Computing (HPC) and modern workflow technologies to improve gridded data and the "data experience" within AgMIP. The University of Chicago and Argonne National Laboratory Computation Institute, in close partnership with the AgMIP IT team and other participants like iPlant and the Texas Advanced Computing Centre (TACC), are developing tools to facilitate this agenda. In fact, a key to the success of the 2012 fast-track intercomparison exercise was the development and maintenance of a synced 10 TB mirror for the ISI-MIP data server in Hamburg, installed on the Earth Systems Grid (ESG) node at Argonne National Laboratory. This server used Global Online and GridFTP to serve data to project participants at rates 10-100 times faster than traditional methods. This archive will be

made public in fall 2013 and will act as a prototype for future high-performance data management.

Another key initiative required for the success of the GGCMI team core activities will be a strong engagement with the AgMIP IT team (and partners at the University of Chicago, Argonne National Lab, and iPlant) to scale existing computing, data storage, processing (translation), and distribution technologies to the level needed for large-scale gridded modelling. Here we will leverage existing resources and expertise in high-performance computing, rapid and robust data transfer using Globus Online, and existing big-data archives developed during the fast-track exercise and mirrored on the Argonne National Lab Earth Systems Grid (ESG) server (currently serving more than 10 TB of climate data and model outputs to the gridded modelling team).

B.3.3   Global and regional RAPs for GGCMI

Long-term projections of agricultural productivity as typical in assessments of climate impacts heavily depend on assumptions on changes in technology, management and land-use patterns as well as climate scenarios. Projections of climate change and future agricultural markets and food security, on the other hand, depend on assumptions on agricultural productivity and environmental externalities, such as greenhouse gas emissions. Harmonising assumptions and analysing feedbacks between these sectors is of central importance for the interpretation of results and for the understanding and reduction of uncertainties.

GGCMI members will work closely with the Representative Agricultural Pathways (RAPs) group to develop RAPs specifically designed for use in GGCM. This effort will be led by Delphine Deryng (University of East Anglia, UK) who will liaison with the AgMIP RAP group and work with researchers on both teams to develop regional and global scale baseline and adaptation scenarios with the appropriate representational complexity for use in gridded model simulations and intercomparisons.

A set of global RAPs will be developed along regional ones to enable a simulation framework with consistent climate, economics and field-levels farming adaptation assumptions for use by both the CGMI and economic teams. The global RAPs will provide the GGCM with a number of necessary variables related to the various management inputs listed in section B.3.1.

The RAPs will be a direct extension of the Shared Socio-economic Pathways (SSPs) compatible with the Radiative Concentration Pathways (RCPs) (Moss et al., 2010; O'Neil et al., 2011; van Vuuren et al., 2011). The RAPs will also be linked to the

development of Shared climate Policy Assumptions (SPAs; Kriegler et al., 2012 to specifically address the issue of farmers vulnerability and adaptation capabilities across regions.

Finally, in parallel to the aggregation and scaling group, this activity will focus on dimensionality and disaggregation challenges, to ensure consistencies between many different combinations of regional RAPs and global trends.

B.4 Funding requirements and opportunities

In order to be successful in the two core activities of the Ag-GRID GGCMI group, we will seek funding from a number of sources to cover meetings and travel, technical support and IT costs, and leadership and organisational assistance. Even though these activities are fundamentally separate, connecting them under a single organisational platform within AgMIP will allow us to exploit overlaps to take maximum advantage of available funds.

B.4.1 Data and information technology needs for the GGCMI

Key to the success of both activities will be a scalable and accessible long-term solution to data storage, management, and distribution.

B.4.2 Meetings and travel

Virtual meetings will be held as much as possible to reduce travels and encourage low-carbon research practices.

B.5 GGCMI Coordination and Contact Details

GGCMI is coordinated from the NASA Goddard Institute for Space Studies in New York City, the site of the AgMIP Coordination Office, the University of Chicago and Argonne National Laboratory Computation Institute, and the Potsdam Institute for Climate Impact Research. The Coordination Team is led by Joshua Elliott and Christoph Müller. The GGCMI Coordinators welcome questions, comments and ideas and can be contacted at ggcmi@agmip.org. For more information, materials, and updates, please visit www.agmip.org/ggcmi.

Appendix C

More Fertiliser for More Food? An analysis of future fertiliser use and resulting greenhouse gases emissions using the global crop yield model PEGASUS

This appendix section presents the poster I exhibited at the Planet Under Pressure conference (www.planetunderpressure2012.net), held in London in March 2012, on the preparatory analysis, further developed and presented in chapter 7.

More Fertiliser for More Food?

An analysis of future fertiliser use and resulting greenhouse gases emissions using the global crop yield model PEGASUS

Tyndall°Centre®
for Climate Change Research

UEA
University of East Anglia

Delphine Deryng[*,1], Rachel Warren[1], Navin Ramankutty[2], Nathan Mueller[3] and Jon Foley[3]

[*]d.deryng@uea.ac.uk

[1]Tyndall Centre, University of East Anglia, Norwich UK; [2]McGill University, Montreal Canada; [3]Institute on the Environment (IonE) University of Minnesota, USA

Closing the Yield Gap within Planetary Boundaries

In this study, we explore scenarios of future food production and fertiliser use to meet global demand and account for the effects of climate change. Since most of the land suitable for agriculture is already in use, additional food is likely to be produced by increasing yield rather than through cropland expansion, unless further tropical deforestation occurs. Cropland across the world lack sufficient soil nutrients to achieve potential yield. Hence, there are opportunities to increase global crop production by using additional fertiliser and reducing the yield gap. However, agriculture intensification is also a major environmental threat (Foley et al., 2011).

Climate Change

Climate change is projected to reduce crop yields in many parts of the world. Although the addition of nitrogen fertilisers enhances CO_2 uptake and hence crop yield, it also emits N_2O to the atmosphere. Therefore, this potential adaptation process has a positive feedback on climate change.

The Nitrogen Cycle

N_2O Emission from Cropland

Nitrogen addition to cultivated soils represents the largest source of N_2O emissions, which amount an average of 5.2 Tg N_2O/year (Stehfest & Bouwman, 2006). Large uncertainties are associated with this estimate, often based on a single emission factor for the globe and neglecting regional disparities due to climate conditions and other factors (Berdanier & Conant, 2012).

This is How

we quantified additional fertiliser needed to increase crop yields and how these estimates relate to N_2O emissions from the agricultural sector. We used:

1. the global crop yield model PEGASUS (Deryng et al., 2011),
2. a new global fertiliser and manure dataset (Mueller et al., submitted),
3. estimates of direct and indirect N_2O emissions from fertiliser use (Tier 1 equations from the IPCC (2006), including average, lower and upper values of emission factors of N_2O from fertiliser and from manure application),
4. crop specific harvested areas (Monfreda et al., 2008) to quantify total emissions for the current global cultivated area.

Actual N2O Emissions from Fertiliser Use

Preliminary Results

Total actual N_2O emissions from fertiliser use for maize production amount to an average of 0.28 Tg-N_2O/yr

Uncertainties in estimates are large with a lower estimate of 0.065 Tg-N_2O/yr and a upper estimate of 1.7 Tg-N_2O/yr due to the range in emission factors

Projected Additional Emission (Preliminary Results)

An additional 0.97 (min=0.23,max=5.9) Tg-N_2O/yr could be emitted to close the yield gap for Maize

Nutrient-stress factor in PEGASUS

The nutrient-stress factor was determined after analysing the correlation between rates of chemical fertiliser application and spatial yield gap fraction data in irrigated cropland, assuming nutrient deficit is the main factor limiting crop yield in those regions. We used the new global fertiliser (NPK) and manure (NP) dataset by Mueller et al. (submitted) and spatial yield-gap fraction data developed by Licker et al. (2010). The yield gap fraction data were developed by comparing potential yield given optimum supply of nutrients and water, and actual yield.

Uncertainties

- The use of average emission factors across the globe involves large uncertainties in global estimates of N_2O, and depends on the use of average, lower or upper emission factors.
- These preliminary results show N_2O emissions for one single crop, which are a fraction of estimates for global cropland.
- The global fertiliser dataset includes some uncertainties (see Mueller et al., submitted).
- Finally, there are uncertainties related to PEGASUS' ability to simulate actual and potential crop yields (Deryng et al., 2011).

Fertiliser and Manure dataset (Mueller et al., submitted)

Next Steps

1. Fully calibrate PEGASUS with the new global fertiliser dataset for maize, spring wheat and soybean and recent updates, in particular, the inclusion of a daily stochastic weather generator and a heat-stress function to account for the effect on crop yield of extreme hot temperature events (Deryng et al., in preparation).
2. Explore spatial variations of emission factors due to variations in climate condition and other factors.

References

Berdanier & Conant (2012) Regionally differentiated estimates of cropland N2O emissions reduce uncertainty in global calculations. Global Change Biology, 18, 928–935, doi: 10.1111/j.1365-2486.2011.02554.x

Deryng et al. (2011), Simulating the effects of climate and agricultural management practices on global crop yield, Global Biogeochem. Cycles, 25, GB2006, doi:10.1029/2009GB003765.

Foley et al. 2011. Solutions for a Cultivated Planet. Nature. doi:10.1038/nature10452.

IPCC, 2006. IPCC Guidelines for National Greenhouse Gas Inventories, IGES, Japan.

Licker et al. (2010), Mind the gap: How do climate and agricultural management explain the 'yield gap' of croplands around the world?, Global Ecol. Biogeogr., 19(6), 769–782.

Monfreda et al. (2008), Farming the planet: 2. Geographic distribution of crop areas, yields, physiological types, and net primary production in the year 2000, Global Biogeochem. Cycles, 22, GB1022, doi:10.1029/2007GB002947.

Mueller et al. (submitted), Closing the 'yield gap': Boosting global crop production by changing nutrient and water management.

Stehfest & Bouwman (2006), N2O and NO emission from agricultural fields and soils under natural vegetation: summarizing available measurement data and modeling of global annual emissions. Nutrient Cycling in Agroecosystems, 74, 207–228.

Appendix D

World Bank database: country classifications

Country and lending groups according to 2012 gross national income per capita (World Bank, 2013)

High Income ($12,616 or more)	Medium High Income ($4,086 − $12,615)	Medium Low Income ($1,036 − $4,085)	Low Income ($1,035 or less)
Aruba	Angola	Armenia	Afghanistan
Andorra	Albania	Bolivia	Burundi
United Arab Emirates	Argentina	Bhutan	Benin
Antigua and Barbuda	American Samoa	Cote d'Ivoire	Burkina Faso
Australia	Azerbaijan	Cameroon	Bangladesh
Austria	Bulgaria	Congo	Central African Republic
Belgium	Bosnia	Cape Verde	Congo Democratic Republic
Bahrain	Belarus	Djibouti	Comoros
Bahamas	Belize	Egypt	Eritrea
Bermuda	Brazil	Micronesia	Ethiopia
Barbados	Botswana	Georgia	Guinea
Brunei Darussalam	China	Ghana	Gambia
Canada	Colombia	Guatemala	Guinea Bissau
Switzerland	Costa Rica	Guyana	Haiti
Chile	Cuba	Honduras	Kenya
Cayman Islands	Dominica	Indonesia	Kyrgyzstan
Cyprus	Dominican Republic	India	Cambodia
Czech Republic	Algeria	Kiribati	Liberia
Germany	Ecuador	Laos	Madagascar
Denmark	Fiji	Sri Lanka	Mali
Spain	Gabon	Lesotho	Myanmar
Estonia	Grenada	Morocco	Mozambique
Finland	Hungary	Moldova	Malawi
France	Iran	Mongolia	Niger
Faroe Islands	Iraq	Mauritania	Nepal
United Kingdom	Jamaica	Nigeria	Korea Democratic Republic
Equatorial Guinea	Jordan	Nicaragua	Rwanda
Greece	Kazakhstan	Pakistan	Sierra Leone
Greenland	Lebanon	Philippines	Somalia
Guam	Libya	Papua New Guinea	Chad
Hong Kong	Saint Lucia	Paraguay	Togo
Croatia	Maldives	Sudan	Tajikistan
Ireland	Mexico	Senegal	Tanzania
Iceland	Marshall Islands	Solomon Islands	Uganda
Israel	Macedonia	ElSalvador	Zimbabwe
Italy	Montserrat	Sao Tome and Principe	
Japan	Mauritius	Swaziland	
Saint Kitts and Nevis	Malaysia	Syria	
Korea Rep	Namibia	Timor–Leste	
Kuwait	Panama	Ukraine	

Table D.1 – *Continued from previous page*

High Income ($12,616 or more)	Medium High Income ($4,086 − $12,615)	Medium Low Income ($1,036 − $4,085)	Low Income ($1,035 or less)
Liechtenstein	Peru	Uzbekistan	
Lithuania	Palau	Viet–Nam	
Luxembourg	Romania	Vanuatu	
Latvia	Serbia	Samoa	
Macao	Suriname	Yemen	
Monaco	Seychelles	Zambia	
Malta	Thailand		
Northern Mariana Islands	Turkmenistan		
New Caledonia	Tonga		
Netherlands	Tunisia		
Norway	Turkey		
New Zealand	Tuvalu		
Oman	Saint Vincent		
Poland	Venezuela		
Puerto Rico	South Africa		
Portugal			
French Polynesia			
Qatar			
Russia			
SaudiArabia			
Singapore			
San Marino			
Slovakia			
Slovenia			
Sweden			
Turks and Caicos			
Trinidad and Tobago			
Uruguay			
United States			
Virgin Islands UK			
Virgin Islands US			

Bibliography

Abbott, P. C., Hurt, C., and Tyner, W. E. (2008). What's driving food prices? Farm foundation. Issue report.

Adam, M., van Bussel, L. G. J., Leffelaar, P. A., Van Keulen, H., and Ewert, F. (2011). Effects of modelling detail on simulated potential crop yields under a wide range of climatic conditions. *Ecological Modelling*, 222(1):131–143.

Adger, W. N., Arnell, N. W., and Tompkins, E. (2005). Successful adaptation to climate change across scales. *Global Environmental Change*, 15.

Ainsworth, E. A. (2008). Rice production in a changing climate: A meta-analysis of responses to elevated carbon dioxide and elevated ozone concentration. *Global Change Biology*, 14(7):1642–1650.

Ainsworth, E. A., Leakey, A. D. B., Ort, D. R., and Long, S. P. (2008). FACE-ing the facts: Inconsistencies and interdependence among field, chamber and modeling studies of elevated $[CO_2]$ impacts on crop yield and food supply. *New Phytologist*, 179(1):5–9.

Ainsworth, E. A. and Rogers, A. (2007). The response of photosynthesis and stomatal conductance to rising $[CO_2]$: mechanisms and environmental interactions. *Plant, Cell and Environment*, 30(3):258–270.

Aksoy, H. (2000). Use of Gamma distribution in hydrological analysis. *Turkish Journal of Enginneering and Environmental Sciences*, pages 1–10.

Antle, J., Valdivia, R., Claessens, L., Nelson, G. C., Rosenzweig, C., Ruane, A. C., and Vervoort, J. (2013). Representative Agricultural Pathways and Scenarios: A trans-disciplinary approach to agricultural model inter-comparison, improvement and climate impact assessment. AgMIP.

Asseng, S., Ewert, F., Rosenzweig, C., Jones, J. W., Hatfield, J. L., Ruane, A. C., Boote, K. J., Thorburn, P. J., Rötter, R. P., Cammarano, D., Brisson, N., Basso, B., Martre, P., Aggarwal, P. K., Angulo, C., Bertuzzi, P., Biernath, C., Challinor, A. J., Doltra,

J., Gayler, S., Goldberg, R., Grant, R., Heng, L., Hooker, J., Hunt, L. A., Ingwersen, J., Izaurralde, R. C., Kersebaum, K. C., Müller, C., Naresh Kumar, S., Nendel, C., O'Leary, G., Olesen, J. E., Osborne, T. M., Palosuo, T., Priesack, E., Ripoche, D., Semenov, M. A., Shcherbak, I., Steduto, P., Stöckle, C., Stratonovitch, P., Streck, T., Supit, I., Tao, F., Travasso, M., Waha, K., Wallach, D., White, J. W., Williams, J. R., and Wolf, J. (2013). Uncertainty in simulating wheat yields under climate change. *Nature Climate Change*, 3(9):827–832.

Baker, J. T., Hartwell Allen, L., Boote, K. J., and Pickering, N. B. (1997). Rice responses to drought under carbon dioxide enrichment. 2. Photosynthesis and evapotranspiration. *Global Change Biology*.

Barnett, J. (2010). Adapting to climate change: three key challenges for research and policy-an editorial essay. *Wiley Interdisciplinary Reviews: Climate Change*.

Barros, I. d., Williams, J. R., and Gaiser, T. (2005). Modeling soil nutrient limitations to crop production in semiarid NE of Brazil with a modified EPIC version. *Ecological Modelling*, 181(4):567–580.

Bassu, S., Brisson, N., Durand, J.-L., Boote, K., Lizaso, J., Jones, J. W., Rosenzweig, C., Ruane, A. C., Adam, M., Baron, C., Basso, B., Biernath, C., Boogaard, H., Conijn, S., Corbeels, M., Deryng, D., De Sanctis, G., Gayler, S., Grassini, P., Hatfield, J., Hoek, S., Izaurralde, C., Jongschaap, R., Kemanian, A. R., Kersebaum, C. K., Kumar, N. S., Makowski, D., Müller, C., Nendel, C., Priesack, E., Pravia, M. V., Kim, S.-H., Sau, F., Shcherbak, I., Tao, F., Teixeira, E., Timlin, D., and Waha, K. (2014). How do various maize crop models vary in their responses to climate change factors? *Global Change Biology*.

Batjes, N. H. (2005). ISRIC-WISE global data set of derived soil properties on a 0.5 by 0.5 degree grid (Version 3.0). Report 2005/08, ISRIC – World Soil Information, Wageningen (with data set).

Beddington, J. R. (2009). Food, energy, water and the climate: a perfect storm of global events? World Development. London , UK : Government Office for Science.

Beddington, J. R., Asaduzzaman, M., Clark, M. E., Fernandez Bremauntz, A., Guillou, M. D., Howlett, D. J. B., Jahn, M. M., Lin, E., Mamo, T., Negra, C., Nobre, C. A., Scholes, R. J., Van Bo, N., and Wakhungu, J. (2012). What next for Agriculture after Durban? *Science*, 335(6066):289–290.

Bell, W. (2003). *Foundations of futures studies: human science for a new era*, volume vol. 1: History, Purposes, and Knowledge. Transaction Publishers.

Berdanier, A. B. and Conant, R. T. (2011). Regionally differentiated estimates of cropland N_2O emissions reduce uncertainty in global calculations. *Global Change Biology.*

Berkhout, F. (2010). Reconstructing boundaries and reason in the climate debate. *Global Environmental Change*, 20(4):565–569.

Bernacchi, C. J., Kimball, B. A., Quarles, D. R., Long, S. P., and Ort, D. R. (2006). Decreases in stomatal conductance of soybean under open-air elevation of $[CO_2]$ are closely coupled with decreases in ecosystem evapotranspiration. *Plant Physiology*, 143(1):134–144.

Berry, J. and Bjorkman, O. (1980). Photosynthetic response and adaptation to temperature in higher plants. *Annual Review of Plant Physiology.*

Berry, P. M., Rounsevell, M. D. A., Harrison, P. A., and Audsley, E. (2006). Assessing the vulnerability of agricultural land use and species to climate change and the role of policy in facilitating adaptation. *Environmental Science and Policy*, 9(2):189–204.

Bondeau, A., Smith, P., Zaehle, S., Schaphoff, S., Lucht, W., Cramer, W., Gerten, D., Lotze-Campen, H., Müller, C., and Reichstein, M. (2007). Modelling the role of agriculture in the 20th century global terrestrial carbon balance. *Global Change Biology*, 13:679–706.

Booker, F. L. (2000). Influence of carbon dioxide enrichment, ozone and nitrogen fertilization on cotton (Gossypium hirsutum L.) leaf and root composition. *Plant, Cell and Environment.*

Booker, F. L., Miller, J. E., Fiscus, E. L., Pursley, W. A., and Stefanski, L. A. (2005). Comparative responses of container – versus ground-grown soybean to elevated carbon dioxide and ozone. *Crop Science.*

Börjeson, L., Höjer, M., Dreborg, K.-H., Ekvall, T., and Finnveden, G. (2006). Scenario types and techniques: towards a user's guide. *Futures*, 38(7):723–739.

Boucher, O., Myhre, G., and Myhre, A. (2004). Direct human influence of irrigation on atmospheric water vapour and climate. *Climate Dynamics.*

Bouwman, A. F., Kram, T., Klein, T., and Goldewijk, K., editors (2006). *Integrated modelling of global environmental change. An overview of IMAGE 2.4.* PBL Netherlands Environmental Assessment Agency, The Hague.

Brooks, T. J., Wall, G. W., Pinter, Jr, P. J., Kimball, B. A., Lamorte, R. L., Leavitt, S. W., Matthias, A. D., Adamsen, F. J., Hunsaker, D. J., and Webber,

A. N. (2000). Acclimation response of spring wheat in a free-air CO_2 enrichment (FACE) atmosphere with variable soil nitrogen regimes. 3. Canopy architecture and gas exchange - Springer. *Photosynthesis Research*.

Burkart, S., Manderscheid, R., Wittich, K. P., Löpmeier, F. J., and Weigel, H. J. (2011). Elevated CO_2 effects on canopy and soil water flux parameters measured using a large chamber in crops grown with free-air CO_2 enrichment. *Plant Biology*, 13(2):258–269.

Burke, M. B., Lobell, D. B., and Guarino, L. (2009). Shifts in African crop climates by 2050, and the implications for crop improvement and genetic resources conservation. *Global Environmental Change-Human and Policy Dimensions*, 19(3):317–325.

Campbell, G. S. and Norman, J. M. (2000). *An introduction to environmental biophysics*. Springer.

Carter, T. R. (2010). Assessing impacts of climate change: an editorial essay. *Wiley Interdisciplinary Reviews: Climate Change*, 1(4):479–482.

Cassman, K. G. (1999). Ecological intensification of cereal production systems: Yield potential, soil quality, and precision agriculture. *Proceedings of the National Academy of Sciences*.

Challinor, A. J., Martre, P., Asseng, S., Thornton, P., and Ewert, F. (2014a). Making the most of climate impacts ensembles. *Nature Climate Change*, 4(2):77–80.

Challinor, A. J., Osborne, T., Morse, A., and Shaffrey, L. (2009). Methods and resources for climate impacts research. *Bulletin of the American Meteorological Society*.

Challinor, A. J., Smith, M. S., and Thornton, P. (2013). Use of agro-climate ensembles for quantifying uncertainty and informing adaptation. *Agricultural and Forest Meteorology*, 170:2–7.

Challinor, A. J., Watson, J., Lobell, D. B., Howden, S. M., Smith, D. R., and Chhetri, N. (2014b). A meta-analysis of crop yield under climate change and adaptation. *Nature Climate Change*.

Challinor, A. J., Wheeler, T. R., Craufurd, P., Ferro, C. A. T., and Stephenson, D. B. (2007a). Adaptation of crops to climate change through genotypic responses to mean and extreme temperatures. *Agriculture, Ecosystems & Environment*, 119(1-2):190–204.

Challinor, A. J., Wheeler, T. R., Craufurd, P., and Slingo, J. M. (2005). Simulation of the impact of high temperature stress on annual crop yields. *Agricultural and Forest Meteorology*, 135(1-4):180–189.

Challinor, A. J., Wheeler, T. R., Garforth, C., Craufurd, P., and Kassam, A. (2007b). Assessing the vulnerability of food crop systems in Africa to climate change. *Climatic Change*, 83(3):381–399.

Chaudhury, M., Vervoort, J., Kristjanson, P., Ericksen, P., and Ainslie, A. (2012). Participatory scenarios as a tool to link science and policy on food security under climate change in East Africa. *Regional Environmental Change*, 13(2):389–398.

Chen, Y. and Cournède, P.-H. (2014). Data assimilation to reduce uncertainty of crop model prediction with Convolution Particle Filtering. *Ecological Modelling*.

Chun, J. A., Wang, Q., Timlin, D., Fleisher, D., and Reddy, V. R. (2011). Effect of elevated carbon dioxide and water stress on gas exchange and water use efficiency in corn. *Agricultural and Forest Meteorology*.

Claessens, L., Antle, J. M., Stoorvogel, J. J., Valdivia, R. O., Thornton, P. K., and Herrero, M. (2012). A method for evaluating climate change adaptation strategies for small-scale farmers using survey, experimental and modeled data. *Agricultural Systems*, 111(C):85–95.

Clausen, S. K., Frenck, G., Linden, L. G., Mikkelsen, T. N., Lunde, C., and Jørgensen, R. B. (2011). Effects of single and multifactor treatments with elevated temperature, CO_2 and ozone on oilseed rape and barley. *Journal of Agronomy and Crop Science*, 197(6):442–453.

Cline, W. R. (2007). *Global warming and agriculture: Impact estimates by country*. The Peterson Institute for International Economics.

Collatz, G. J., Ball, J., Grivet, C., and Berry, J. A. (1991). Physiological and environmental regulation of stomatal conductance, photosynthesis and transpiration: a model that includes a laminar boundary layer. *Agricultural and Forest Meteorology*.

Collatz, G. J., Ribas-Carbo, M., and Berry, J. A. (1992). Coupled photosynthesis-stomatal conductance model for leaves of C_4 plants. *Aust J Plant Physiol.*, 19:519–538.

Conley, M. M., Kimball, B. A., Brooks, T. J., Pinter, Jr., P. J., Hunsaker, D. J., Wall, G. W., Adam, N. R., LaMorte, R. L., Matthias, A. D., Thompson, T. L., Leavitt, S. W., Ottman, M. J., Cousins, A. B., and Triggs, J. M. (2001). CO_2 enrichment increases water-use efficiency in sorghum. *New Phytologist*, 151(2):407–412.

Conway, D., Persechino, A., Ardoin-Bardin, S., Hamandawana, H., Dieulin, C., and Mahe, G. (2009). Rainfall and water resources variability in sub-Saharan Africa during the twentieth century. *Journal of Hydrometeorology*, 10(1).

Conway, G. (1997). *The Double Green Revolution*. Penguin Books, London, UK.

Cosby, B., Hornberger, G., Clapp, R., and Ginn, T. (1984). A statistical exploration of the relationships of soil moisture characteristics to the physical properties of soils. *Water Resources Research*, 20(6):682–690.

Dasgupta, S., Laplante, B., Murray, S., and Wheeler, D. (2011). Exposure of developing countries to sea-level rise and storm surges. *Climatic Change*, 106(4):567–579.

Dermody, O., O'Neill, B. F., Zangerl, A. R., Berenbaum, M. R., and DeLucia, E. H. (2008). Effects of elevated CO_2 and O_3 on leaf damage and insect abundance in a soybean agroecosystem. *Arthropod-Plant Interactions*, 2(3):125–135.

Deryng, D. (2009). Simulating the effects of climate and land management practices on global crop yield. Master's thesis, McGill University, Montreal, Canada.

Deryng, D., Conway, D., Ramankutty, N., Price, J., and Warren, R. (2014). Global crop yield response to extreme heat stress under multiple climate change futures. *Environmental Research Letters*, 9(3):034011.

Deryng, D., Elliott, J., Ruane, A. C., Folberth, C., Müller, C., Pugh, T. A. M., Schmid, E., Boote, K. J., Gerten, D., Jones, J. W., Khabarov, N., Olin, S., Schaphoff, S., Yang, H., and Rosenzweig, C. (in review). Disentangling uncertainties in future crop water productivity under climate change.

Deryng, D., Sacks, W. J., Barford, C. C., and Ramankutty, N. (2011). Simulating the effects of climate and agricultural management practices on global crop yield. *Global Biogeochemical Cycles*, 25(GB2006):1–18.

Dessai, S., Adger, W. N., Hulme, M., Turnpenny, J., Löhler, J., and Warren, R. (2004). Defining and experiencing dangerous climate change. *Climatic Change*, 64.

Dessai, S. and Hulme, M. (2004). Does climate adaptation policy need probabilities? *Climate Policy*, 4(2):107–128.

Dessai, S. and Hulme, M. (2007). Assessing the robustness of adaptation decisions to climate change uncertainties: A case study on water resources management in the East of England. *Global Environmental Change*, 17(1):59–72.

Dessai, S., Hulme, M., Lempert, R., and Pielke, Jr., R. (2011). Do We Need Better Predictions to Adapt to a Changing Climate? *EOS, Transactions American Geophysical Union*, 90(13):111–112.

Dessai, S., Lu, X., and Risbey, J. S. (2005). On the role of climate scenarios for adaptation planning. *Global Environmental Change*, 15(2):87–97.

Dieleman, W. I. J., Vicca, S., Dijkstra, F. A., Hagedorn, F., Hovenden, M. J., Larsen, K. S., Morgan, J. A., Volder, A., Beier, C., Dukes, J. S., King, J., Leuzinger, S., Linder, S., Luo, Y., Oren, R., De Angelis, P., Tingey, D., Hoosbeek, M. R., and Janssens, I. A. (2012). Simple additive effects are rare: a quantitative review of plant biomass and soil process responses to combined manipulations of CO_2 and temperature. *Global Change Biology*, 18(9):2681–2693.

Dobos, E. (2006). Albedo. In Encyclopedia of Soil Science, Second Edition (pp. 64-66).

Doorenbos, J. and Pruitt, W. O. (1984). *Guidelines for predicting crop water requirements.* FAO Irrigation and Drainage Paper 24., FAO, Rome.

Easterling, W., Aggarwal, P., Batima, P., Brander, K., Erda, L., Howden, S., Kirilenko, A., Morton, J., Soussana, J.-F., Schmidhuber, J., and Tubiello, F. (2007). *Climate change 2007: impacts, adaptation and vulnerability. Contribution of Working Group II to the fourth assessment report of the Intergovernmental Panel on Climate Change,* chapter 5. Food, fibre and forest products. Cambridge University Press, Cambridge, UK.

Easterling, W., Rosenburg, N., McKenney, M., Jones, C., Dyke, P., and Williams., J. (1992). *Preparing the erosion productivity impact calculator (EPIC) model to simulate crop response to climate change and the direct effects of CO_2.* Agricultural and Forest Meteorology, 59:17-34.

Ebi, K. L., Hallegatte, S., Kram, T., Arnell, N. W., Carter, T. R., Edmonds, J. A., Kriegler, E., Mathur, R., O'neill, B. C., and Riahi, K. (2014). A new scenario framework for climate change research: background, process, and future directions. *Climatic Change*, 122(3):1–10.

Edwards, N. R. (2011). Mitigation: Plausible mitigation targets. *Nature Climate Change*, 1(8):395–396.

Eggleston, H., Buendia, L., Miwa, K., Ngara, T., and Tanabe, K., editors (2006). *IPCC 2006. IPCC guidelines for national greenhouse gas inventories, prepared by the national greenhouse gas inventories programme.* Institute for Global Environmental Strategies (IGES), Japan.

Ehrlich, P. R. and Ehrlich, A. H. (2013). Can a collapse of global civilization be avoided? *Proceedings of the Royal Society B: Biological Sciences*, 280(1754).

Ejeta, G. (2010). African green revolution needn't be a mirage. *Science*, 327(5967):831–832.

Elliott, J., Deryng, D., Müller, C., Frieler, K., Konzmann, M., Gerten, D., Glotter, M., Flörke, M., Wada, Y., Best, N., Eisner, S., Fekete, B. M., Folberth, C., Foster, I., Gosling, S. N., Haddeland, I., Khabarov, N., Ludwig, F., Masaki, Y., Olin, S., Rosenzweig, C., Ruane, A. C., Satoh, Y., Schmid, E., Stacke, T., Tang, Q., and Wisser, D. (2014a). Constraints and potentials of future irrigation water availability on agricultural production under climate change. *Proceedings of the National Academy of Sciences*, 111(9):3239–3244.

Elliott, J., Glotter, M., Best, N., Kelly, D., Wilde, M., and Foster, I. (2013). The parallel system for integrating impact models and sectors (pSIMS). *Proceedings of the Conference on Extreme Science and Engineering Discovery Environment: Gateway to Discovery (XSEDE '13). Association for Computing Machinery*, 21:1–8.

Elliott, J., Müller, C., Deryng, D., Büchner, M., Chryssanthacopoulos, J., Foster, I., Glotter, M., Heinke, J., Iizumi, T., Izaurralde, C., LeBauer, D., Mueller, N., Ray, D., Ruane, A., and Rosenzweig, C. (2014b). The Global Gridded Crop Model Intercomparison (GGCMI): Data and modeling protocol for phase 1 (v1.0). *Geoscientific Model Development*, 7:4383–4427.

Fader, M., Rost, S., Müller, C., Bondeau, A., and Gerten, D. (2010). Virtual water content of temperate cereals and maize: Present and potential future patterns. *Journal of Hydrology*, 384.

Falloon, P., Challinor, A. J., Dessai, S., Hoang, L., Johnson, J., and Koehler, A.-K. (2014). Ensembles and uncertainty in climate change impacts. *Frontiers in Environmental Science*, 2.

FAO (1991). The digitized soil map of the world (release 1.0). Food and Agriculture Organization of the United Nations.

FAO/IIASA (2012). Harmonized World Soil Database (version 1.2). FAO, Rome Italy and IIASA, Laxenburg, Austria.

FAOSTAT (Accessed in July 2013). Food and Agriculture Organization (FAO). FAOSTAT, Statistical Databases, http://faostat.fao.org/default.aspx, United Nations, Rome, Italy.

Farage, P. K., McKee, I. F., and Long, S. P. (2013). Does a low nitrogen supply necessarily lead to acclimation of photosynthesis to elevated CO_2? *Plant Physiology*.

Farquhar, G. D., Caemmerer, S., and Berry, J. A. (1980). A biochemical model of photosynthetic CO_2 assimilation in leaves of C_3 species. *Planta*, 149.

Federer, C. A., Vörösmarty, C., and Fekete, B. (2010). Intercomparison of Methods for Calculating Potential Evaporation in Regional and Global Water Balance Models. *Water Resources Research*, 32(7):2315–2321.

Feng, Z. and Kobayashi, K. (2009). Assessing the impacts of current and future concentrations of surface ozone on crop yield with meta-analysis. *Atmospheric Environment*, 43(8):1510–1519.

Ferris, R., Ellis, R., Wheeler, T. R., and Hadley, P. (1998a). Effect of high temperature stress at anthesis on grain yield and biomass of field-grown crops of wheat. *Annals of Botany*.

Ferris, R., Wheeler, T. R., Hadley, P., and Ellis, R. H. (1998b). Recovery of Photosynthesis after Environmental Stress in Soybean Grown under Elevated CO_2. *Crop Science*.

Field, C., Barros, V., Mach, K., Mastrandrea, M., and co-authors (2014). *Climate change 2014: impacts, adaptation and vulnerability. Contribution of Working Group II to the fourth assessment report of the Intergovernmental Panel on Climate Change. Technical summary.* Cambridge University Press, Cambridge, UK.

Field, C. B., Barros, V., Stocker, T., Qin, D., Dokken, D., Ebi, K., Mastrandrea, M., Mach, K., Plattner, G.-K., Allen, S., Tignor, M., , and Midgley, P., editors (2012). *IPCC 2012. Managing the risks of extreme events and disasters to advance climate change adaptation. a special report of Working Groups I and II of the Intergovernmental Panel on Climate Change.* Cambridge University Press, Cambridge, UK.

Fischer, G., Shah, M., Tubiello, F. N., and Velhuizen, H. v. (2005). Socio-economic and climate change impacts on agriculture: an integrated assessment, 1990–2080. *Philosophical Transactions of the Royal Society B*.

Fischer, G., Shah, M., Velthuizen, H., and Nachtergaele, F. (2002). Global Agro-ecological Assessment for Agriculture in the 21st Century. IIASA and FAO.

Fiscus, D. (2013). Life, Money, and the Deep Tangled Roots of Systemic Change for Sustainability. *World Futures*, 69:555–571.

Fleisher, D., Timlin, D., Reddy, K. R., and R., R. V. (2011). Effects of CO_2 and temperature on crops: Lessons from SPAR growth chambers. In Hillel, D. and Rosenzweig, C., editors, *Handbook of Climate Change and Agroecosystems – Impacts, Adaptation, and Mitigation*, volume 1 of *ICP Series on Climate Change Impacts, Adaptation, and Mitigation*. Imperial College Press.

Folberth, C., Gaiser, R., Abbaspour, K., Schulin, R., and Yang, H. (2012). Regionalization of a large-scale crop growth model for sub-saharan africa: Model setup, evaluation, and estimation of maize yields. *Agriculture Ecosystems & Environment Environment*, 151:21–33.

Foley, J. A. (1994). Net primary productivity in the terrestrial biosphere: the application of a global model. *Journal of Geophysical Research.*

Foley, J. A., Asner, G. P., Costa, M. H., Coe, M. T., DeFries, R., Gibbs, H. K., Howard, E. A., Olson, S., Patz, J., Ramankutty, N., and Snyder, P. (2007). Amazonia revealed: forest degradation and loss of ecosystem goods and services in the Amazon Basin. *Frontiers in Ecology and the Environment*, 5(1):25–32.

Foley, J. A., Defries, R. S., Asner, G. P., Barford, C. L., and Bonan, G. B. (2005). Global consequences of land use. *Science.*

Foley, J. A., Ramankutty, N., Brauman, K. A., Cassidy, E. S., Gerber, J. S., Johnston, M., Mueller, N. D., O'Connell, C., Ray, D. K., West, P. C., Balzer, C., Bennett, E. M., Carpenter, S. R., Hill, J., Monfreda, C., Polasky, S., Rockström, J., Sheehan, J., Siebert, S., Tilman, D., and Zaks, D. P. M. (2011). Solutions for a cultivated planet. *Nature.*

Frank, M. D., Beattie, B. R., and Embleton, M. E. (1990). A comparison of alternative crop response models. *American Journal of Agricultural Economics*, 72(3):597–603.

Fujino, J., Nair, R., Kainuma, M., Masui, T., and Matsuoka, Y. (2006). Multi-gas mitigation analysis on stabilization scenarios using AIM global model. *The Energy Journal.*

Galloway, J. N., Townsend, A. R., Erisman, J. W., Bekunda, M., Cai, Z., Freney, J. R., Martinelli, L. A., Seitzinger, S. P., and Sutton, M. A. (2008). Transformation of the nitrogen cycle: recent trends, questions, and potential solutions. *Science.*

Garnett, T., Appleby, M. C., Balmford, A., Bateman, I. J., Benton, T. G., Bloomer, P., Burlingame, B., Dawkins, M., Dolan, L., Fraser, D., Herrero, M., Hoffmann, I., Smith, P., Thornton, P. K., Toulmin, C., Vermeulen, S. J., and Godfray, H. C. J. (2013). Sustainable intensification in agriculture: premises and policies. *Science*, 341(6141):33–34.

Gassman, P. W., Williams, J. R., Benson, V. W., Izaurralde, R. C., Hauck, L. M., Jones, C. A., Atwood, J. D., Kiniry, J., and Flowers, J. D. (2004). Historical development and applications of the EPIC and APEX models. SAE/CSAE meeting paper no. 042097. Available at www.card.iastate.edu.

Geng, S. (1986). A simple method for generating daily rainfall data. *Agricultural and Forest Meteorology*, 36(4):363–376.

Gerten, D., Heinke, J., Hoff, H., Biemans, H., Fader, M., and Waha, K. (2011). Global water availability and requirements for future food production. *Journal of Hydrometeorology*, 12:885–899.

Gerten, D., Schaphoff, S., Haberlandt, U., Lucht, W., and Sitch, S. (2004). Terrestrial vegetation and water balance – Hydrological evaluation of a dynamic global vegetation model. *Journal of Hydrology*, 286(1-4):249–270.

Giddens, A. (2009). *Politics of Climate Change*. Polity Press.

Gleick, P., Cooley, H., and Morikawa, M., editors (2009). *The World's Water 2008–2009: The biennial report on freshwater resources*. Island Press.

Godfray, H. C. J. and Garnett, T. (2014). Food security and sustainable intensification. *Philosophical Transactions of the Royal Society B*, 369(1639).

Good, A. G. and Beatty, P. H. (2011). Fertilizing nature: a tragedy of excess in the commons. *PLoS biology*, 9(8):e1001124.

Gornall, J., Betts, R. A., Burke, E., Clark, R., Camp, J., Willett, K., and Wiltshire, A. (2010). Implications of climate change for agricultural productivity in the early twenty-first century. *Philosophical Transactions of the Royal Society B*, 365(1554):2973–2989.

Gourdji, S. M., Sibley, A. M., and Lobell, D. B. (2013). Global crop exposure to critical high temperatures in the reproductive period: historical trends and future projections. *Environmental Research Letters*.

Gustafson, D. I., Jones, J. W., Porter, C. H., Hyman, G., Edgerton, M. D., Gocken, T., Shryock, J., Doane, M., Budreski, K., Stone, C., Healy, D., and Ramsey, N. (2014). Climate adaptation imperatives: untapped global maize yield opportunities. *International Journal of Agricultural Sustainability*, pages 1–16.

Haasnoot, M., Kwakkel, J. H., Walker, W. E., and ter Maat, J. (2013). Dynamic adaptive policy pathways: A method for crafting robust decisions for a deeply uncertain world. *Global Environmental Change*, 23(2):485–498.

Haddeland, I., Clark, D. B., Franssen, W., Ludwig, F., Voß, F., Arnell, N. W., Bertrand, N., Best, M., Folwell, S., Gerten, D., Gomes, S., Gosling, S. N., Hagemann, S., Hanasaki, N., Harding, R., Heinke, J., Kabat, P., Koirala, S., Oki, T., Polcher, J., Stacke, T., Viterbo, P., Weedon, G. P., and Yeh, P. (2011). Multimodel estimate of the

global terrestrial water balance: Setup and first results. *Journal of Hydrometeorology*, 12(5):869–884.

Haddeland, I., Lettenmaier, D. P., and Skaugen, T. (2006). Effects of irrigation on the water and energy balances of the Colorado and Mekong river basins. *Journal of Hydrology*, 324(1-4):210–223.

Hallegatte, S., Przyluski, V., and Vogt-Schilb, A. (2011). Building world narratives for climate change impact, adaptation and vulnerability analyses. *Nature Climate Change*, 1(3):151–155.

Harding, R., Best, M. J., Blyth, E., Hagemann, S., Kabat, P., Tallaksen, L. M., Warnaars, T., Wiberg, D., Weedon, G. P., van Lanen, H., Ludwig, F., and Haddeland, I. (2011). WATCH: current knowledge of the terrestrial global water cycle. *Journal of Hydrometeorology*, 12(6).

Havlík, P., Valin, H., and Herrero, M. (2014). Climate change mitigation through livestock system transitions. In *Proceedings of the National Academy of Sciences*, pages 3709–3714.

Hawkins, E., Fricker, T. E., Challinor, A. J., Ferro, C. A. T., Ho, C. K., and Osborne, T. (2013). Increasing influence of heat stress on French maize yields from the 1960s to the 2030s. *Global Change Biology*, 19(3):937–947.

Haxeltine, A. and Prentice, I. C. (1996). BIOME3: An equilibrium terrestrial biosphere model on ecophysiological constraints, resource availability, and competition among plant functional types. *Global Biogeochemical Cycles*, 10(4):17.

Heagle, A. S., Miller, J. E., and Pursley, W. A. (2000). Growth and yield responses of winter wheat to mixtures of ozone and carbon dioxide. *Crop Science*.

Hempel, S., Frieler, K., Warszawski, L., Schewe, J., and Piontek, F. (2013). A trend-preserving bias correction – the ISI-MIP approach. *Earth System Dynamics Discussions*, 4(1):49–92.

Hénault, C., Grossel, A., Mary, B., Roussel, M., and Léonard, J. (2012). Nitrous oxide emission by agricultural soils: a review of spatial and temporal variability for mitigation. *Pedosphere*.

Hertel, T. (2010). The global supply and demand for agricultural land in 2050: a perfect storm in the making? GTAP Working Paper No. 63.

Hertel, T. W., Burke, M. B., and Lobell, D. B. (2010). The poverty implications of climate-induced crop yield changes by 2030. *Global Environmental Change*, 20(4):577–585.

Hillel, D. and Rosenzweig, C. (2011). Climate change and agroecosystems: main findings and future research directions. In Hillel, D. and Rosenzweig, C., editors, *Handbook of climate change and agroecosystems – Impacts, adaptation, and mitigation*, volume 1 of *ICP series on climate change impacts, adaptation, and mitigation*. Imperial College Press.

Hoogenboom, G., Jones, J. W., and Boote, K. J. (1992). Modeling growth, development, and yield of grain legumes using CROPGRO: SOYGRO, PNUTGRO and BEANGRO: a review. *Trans. ASAE*, 35:2043–2056.

Horlings, L. G. and Marsden, T. K. (2011). Towards the real green revolution? Exploring the conceptual dimensions of a new ecological modernisation of agriculture that could 'feed the world'. *Global Environmental Change*, 21(2):441–452.

Hulme, M. (2010). Problems with making and governing global kinds of knowledge. *Global Environmental Change*, 20(4):558–564.

Hunsaker, D. J., Kimball, B. A., Pinter, P. J., LaMorte, R. L., and Wall, G. W. (1996). Carbon dioxide enrichment and irrigation effects on wheat evapotranspiration and water use efficiency. *Transactions of the ASAE*, 39(4):1345–1355.

Hunsaker, D. J., Kimball, B. A., Pinter, Jr., P. J., Wall, G. W., LaMorte, R. L., Adamsen, F. J., Leavitt, S. W., Thompson, T. L., Matthias, A. D., and Brooks, T. J. (2000). CO2 enrichment and soil nitrogen effects on wheat evapotranspiration and water use efficiency. *Agricultural and Forest Meteorology*, 104(2):85–105.

IFA (2002). Fertilizer Use by Crop, Fifth edition, http://www.fertilizer.org/ifa/statistics.asp. International Fertilizer Industry Association, International Fertilizer Development Center, International Potash Institute, Phosphate and Potash Institute, Food and Agriculture Organization of the United Nations, Rome, Italy.

Izaurralde, R. C., Williams, J. R., McGill, W. B., Rosenberg, N. J., and Jakas, M. C. Q. (2006). Simulating soil C dynamics with EPIC: Model description and testing against long-term data. *Ecological Modelling*, 192(3-4):362–384.

Jones, J. W., Hoogenboom, G., Porter, C., Boote, K. J., Batchelor, W. D., Hunt, L., Wilkens, P., Singh, U., Gijsman, A., and Ritchie, J. C. (2003). The DSSAT cropping system model. *European Journal of Agronomy*, 18.

Joos, F. and Spahni, R. (2008). Rates of change in natural and anthropogenic radiative forcing over the past 20,000 years. *Proceedings of the National Academy of Sciences*, 105(5):6.

Ju, X. T., Kou, C. L., Zhang, F. S., and Christie, P. (2006). Nitrogen balance and groundwater nitrate contamination: Comparison among three intensive cropping systems on the North China Plain. *Environmental Pollution*, 143(1):117–125.

Ju, X. T., Xing, G. X., Chen, X. P., Zhang, S. L., Zhang, L. J., Liu, X. J., Cui, Z. L., Yin, B., Christie, P., Zhu, Z. L., and Zhang, F. S. (2009). Reducing environmental risk by improving N management in intensive Chinese agricultural systems. *Proceedings of the National Academy of Sciences*, 106(9):3041–3046.

Kassam, A. and Smith, M. (2001). FAO methodologies on crop water use and crop water productivity. Presented at the expert meeting on crop water productivity, Rome , 3 to 5 December.

Keys, E. and McConnell, W. J. (2005). Global change and the intensification of agriculture in the tropics. *Global Environmental Change*, 15(4):320–337.

Khagram, S., Nicholas, K. A., Bever, D. M., Warren, J., Richards, E. H., Oleson, K. L. L., Kitzes, J., Katz, R., Hwang, R., Goldman, R., Funk, J., and Brauman, K. A. (2010). Thinking about knowing: conceptual foundations for interdisciplinary environmental research. *Environmental Conservation*, 37(04):388–397.

Kim, H.-Y., Lieffering, M., Kobayashi, K., Okada, M., Mitchell, M. W., and Gumpertz, M. (2003). Effects of free-air CO_2 enrichment and nitrogen supply on the yield of temperate paddy rice crops. *Field Crops Research*.

Kimball, B. (2011). Lessons from FACE: CO_2 effects and interactions with water, nitrogen and temperature. In Hillel, D. and Rosenzweig, C., editors, *Handbook of Climate Change and Agroecosystems – Impacts, Adaptation, and Mitigation*, volume 1 of *ICP Series on Climate Change Impacts, Adaptation, and Mitigation*. Imperial College Press.

Kimball, B. A., LaMorte, R. L., Pinter, Jr., P. J., Wall, G. W., Hunsaker, D. J., Adamsen, F. J., Leavitt, S. W., Thompson, T. L., Matthias, A. D., and Brooks, T. J. (1999). Free-air CO_2 enrichment and soil nitrogen effects on energy balance and evapotranspiration of wheat. *Water Resources Research*, 35(4):1179–1190.

Kirkham, M. B. (2012). Research needs for agriculture under elevated carbon dioxide. In Hillel, D. and Rosenzweig, C., editors, *Handbook of Climate Change and Agroecosystems – Global and Regional Aspects and Implications*, volume 2 of *ICP Series on Climate Change Impacts, Adaptation, and Mitigation*. Imperial College Press.

Knox, J., Hess, T., Daccache, A., and Wheeler, T. R. (2012). Climate change impacts on crop productivity in Africa and South Asia. *Environmental Research Letters*, 7(3):034032.

Kriegler, E., Edmonds, J. A., Hallegatte, S., Ebi, K. L., Kram, T., Riahi, K., Winkler, H., and Van Vuuren, D. P. (2014). A new scenario framework for climate change research: the concept of shared climate policy assumptions. *Climatic Change*, 122(3):401–414.

Kriegler, E., O'neill, B. C., Hallegatte, S., Kram, T., Lempert, R. J., Moss, R. H., and Wilbanks, T. (2012). The need for and use of socio-economic scenarios for climate change analysis: A new approach based on shared socio-economic pathways. *Global Environmental Change*, 22(4):807–822.

Krueger, T., Page, T., Hubacek, K., Smith, L., and Hiscock, K. (2012). The role of expert opinion in environmental modelling. *Environmental Modelling & Software*, pages 1–15.

Kucharik, C. J. (2003). Evaluation of a process-based agro-ecosystem model (Agro-IBIS) across the U.S. cornbelt: simulations of the inter-annual variability in maize yield. *Earth Interactions*, 7:1–33.

Kucharik, C. J. (2008). Contribution of planting date trends to increased maize yields in the Central United States. *Agronomy Journal*, 100(2):1–9.

Kundzewicz, Z. W., Mata, L., Arnell, N. W., Döll, P., Jimenez, B., Miller, K., Oki, T., Sen, Z., and Shiklomanov, I. (2008). The implications of projected climate change for freshwater resources and their management. *Hydrological Sciences Journal*, 53(1):8.

Kwakkel, J. H. and Pruyt, E. (2013). Exploratory Modeling and Analysis, an approach for model-based foresight under deep uncertainty. *Technological Forecasting and Social Change*, 80(3):419–431.

Lambin, E. F. and Geist, H. J. (2006). *Land-use and land-cover change, local processes and global impacts*. IGBP.

Lambin, E. F. and Meyfroidt, P. (2011). Global land use change, economic globalization, and the looming land scarcity. *Proceedings of the National Academy of Sciences*, 108(9).

Lawrence, D. M. and Slater, A. (2008). Incorporating organic soil into a global climate model. *Climate Dynamics*, 30(2-3):145–160.

Leakey, A. D. B., Ainsworth, E. A., Bernacchi, C. J., Rogers, A., Long, S. P., and Ort, D. R. (2009). Elevated CO_2 effects on plant carbon, nitrogen, and water relations: six important lessons from FACE. *Journal of Experimental Botany*, 60(10):2859–2876.

Leakey, A. D. B., Bishop, K. A., and Ainsworth, E. A. (2012). A multi-biome gap in understanding of crop and ecosystem responses to elevated CO_2. *Current Opinion in Plant Biology*, 15(3):228–236.

Lee, L. A., Carslaw, K. S., Pringle, K. J., Mann, G. W., and Spracklen, D. V. (2011). Emulation of a complex global aerosol model to quantify sensitivity to uncertain parameters. *Atmospheric Chemistry and Physics*, 11(23):12253–12273.

Leemans, R. and Solomon, A. (1993). Modeling the potential change in yield and distribution of the earth's crops under a warmed climate . *Climate Research*.

Levis, S. (2010). Modeling vegetation and land use in models of the Earth System. *Wiley Interdisciplinary Reviews: Climate Change*.

Li, Y., Ye, W., Wang, M., and Yan, X. (2009). Climate change and drought: a risk assessment of crop-yield impacts. *Climate Research*, 39:31–46.

Licker, R., Johnston, M., Foley, J. A., Barford, C. C., Ramankutty, N., and Monfreda, C. (2010). Mind the Gap: How do climate and agricultural management explain the "yield gap" of croplands around the world? *Global Ecology and Biogeography*.

Lindeskog, M., Arneth, A., Bondeau, A., Waha, K., Seaquist, J., Olin, S., and Smith, B. (2013). Implications of accounting for land use in simulations of ecosystem services and carbon cycling in Africa. *Earth Syst. Dynam. Discuss.*, 4:235–278.

Linquist, B., Groenigen, K. J., Adviento-Borbe, M. A., Pittelkow, C., and Kessel, C. (2011). An agronomic assessment of greenhouse gas emissions from major cereal crops. *Global Change Biology*, 18(1):194–209.

Liu, J., Williams, J. R., Zehnder, A., and Yang, H. (2007). GEPIC – modelling wheat yield and crop water productivity with high resolution on a global scale. *Agricultural Systems*, 94(2):478–493.

Liu, J. and Yang, H. (2010). Spatially explicit assessment of global consumptive water uses in cropland: Green and blue water. *Journal of Hydrology*, 384(3-4):187–197.

Lobell, D. B. (2013). Errors in climate datasets and their effects on statistical crop models. *Agricultural and Forest Meteorology*, 170:58–66.

Lobell, D. B., Bänziger, M., Magorokosho, C., and Vivek, B. (2011a). Nonlinear heat effects on African maize as evidenced by historical yield trials. *Nature Climate Change*, 1(1):42–45.

Lobell, D. B. and Burke, M. B. (2010). On the use of statistical models to predict crop yield responses to climate change. *Agricultural and Forest Meteorology*, 150(11):1443–1452.

Lobell, D. B., Cassman, K. G., and Field, C. B. (2009). Crop yield gaps: their importance, magnitudes, and causes. *Annual Review of Environment and Resources.*

Lobell, D. B. and Gourdji, S. (2012). The influence of climate change on global crop productivity. *Plant Physiology.*

Lobell, D. B., Hammer, G. L., McLean, G., Messina, C., Roberts, M. J., and Schlenker, W. (2013). The critical role of extreme heat for maize production in the United States. *Nature Climate Change*, 3(4):1–5.

Lobell, D. B., Schlenker, W., and Costa-Roberts, J. (2011b). Climate trends and global crop production since 1980. *Science.*

Long, S. P. (1991). Modification of the response of photosynthetic productivity to rising temperature by atmospheric CO_2 concentrations: Has its importance been underestimated? *Plant, Cell and Environment*, 14(8):729–739.

Long, S. P., Ainsworth, E. A., Leakey, A. D. B., Nösbsrger, J., and Ort, D. R. (2006). Food for thought: lower-than-expected crop yield stimulation with rising CO_2 concentrations. *Science*, 312(5782):1918–1921.

Manderscheid, R., Erbs, M., and Weigel, H.-J. (2012). Interactive effects of free-air CO_2 enrichment and drought stress on maize growth. *European Journal of Agronomy.*

Manderscheid, R. and Weigel, H.-J. (2007). Drought stress effects on wheat are mitigated by atmospheric CO_2 enrichment. *Agronomy for Sustainable Development.*

Manuel-Navarrete, D. (2010). Power, realism, and the ideal of human emancipation in a climate of change. *Wiley Interdisciplinary Reviews: Climate Change*, 1(6):781–785.

Markelz, R. J. C., Strellner, R. S., and Leakey, A. D. B. (2011). Impairment of C_4 photosynthesis by drought is exacerbated by limiting nitrogen and ameliorated by elevated [CO_2] in maize. *Journal of Experimental Botany*, 62(9):3235–3246.

McMurtrie, R. E., Comins, H. N., Kirschbaum, M., and Wang, Y.-P. (1992). Modifying existing forest growth models to take account of effects of elevated CO_2. *Australian Journal of Botany.*

McMurtrie, R. E. and Wang, Y.-P. (1993). Mathematical models of the photosynthetic response of tree stands to rising CO_2 concentrations and temperatures. *Plant, Cell and Environment.*

Meehl, G. A., Boer, G. J., Covey, C., Latif, M., and Stouffer, R. J. (1997). Intercomparison makes for a better climate model. *EOS, Transactions American Geophysical Union*, 78(41):445.

Meehl, G. A., Covey, C., Taylor, K. E., Delworth, T., Stouffer, R. J., Latif, M., McAvaney, B., and Mitchell, J. F. B. (2007). The WCRP CMIP3 multimodel dataset: a new era in climate change research. *Bulletin of the American Meteorological Society.*

Meinshausen, M., Raper, S. C. B., and Wigley, T. M. L. (2011). Emulating coupled atmosphere-ocean and carbon cycle models with a simpler model, MAGICC6 – Part 1: Model description and calibration. *Atmospheric Chemistry and Physics.*

Mendelsohn, R., Nordhaus, W. D., and Shaw, D. (1994). The impact of global warming on agriculture: a Ricardian analysis. *The American Economic Review*, pages 753–771.

Mitchell, T. D. and Jones, P. D. (2005). An improved method of constructing a database of monthly climate observations and associated high-resolution grids. *International Journal of Climatology.*

Modhej, A., Naderi, A., Emam, Y., Aynehband, A., and Normohamadi, G. (2008). Effects of post-anthesis heat stress and nitrogen levels on grain yield in wheat (T. durum and T. aestivum) genotypes. *International Journal of Plant Production.*

Monfreda, C., Ramankutty, N., and Foley, J. A. (2008). Farming the planet: 2. Geographic distribution of crop areas, yields, physiological types, and net primary production in the year 2000. *Global Biogeochemical Cycles*, 22(1):19.

Monteith, J. (1965). Evaporation and environment. *Symposia of the Society for Experimental Biology*, 19:205–224.

Moriondo, M., Bindi, M., and Kundzewicz, Z. W. (2010). Impact and adaptation opportunities for European agriculture in response to climatic change and variability. *Mitigation and Adaptation Strategies for Global Change.*

Moriondo, M., Giannakopoulos, C., and Bindi, M. (2011). Climate change impact assessment: the role of climate extremes in crop yield simulation. *Climatic Change*, 104(3-4):679–701.

Moss, R. H., Edmonds, J. A., Hibbard, K. A., Manning, M. R., Rose, S. K., Van Vuuren, D. P., Carter, T. R., Emori, S., Kainuma, M., Kram, T., Meehl, G. A., Mitchell, J. F. B., Nakicenovic, N., Riahi, K., Smith, S. J., Stouffer, R. J., Thomson, A. M., Weyant, J. P., and Wilbanks, T. J. (2010). The next generation of scenarios for climate change research and assessment. *Nature*, 463(7282):747.

Mueller, N. D., Gerber, J. S., Johnston, M., Ray, D. K., Ramankutty, N., and Foley, J. A. (2012). Closing yield gaps through nutrient and water management. *Nature*, pages 1–4.

Müller, C., Bondeau, A., Popp, A., Waha, K., and Fader, M. (2010). WDR 2010: Development and climate change. World development report.

Müller, C., Cramer, W., Hare, W. L., and Lotze-Campen, H. (2011). Climate change risks for African agriculture. *Proceedings of the National Academy of Sciences*, 108(11):4313–4315.

Müller, C. and Lucht, W. (2007). Robustness of terrestrial carbon and water cycle simulations against variations in spatial resolution. *Journal of Geophysical Research.*

Müller, C. and Robertson, R. D. (2013). Projecting future crop productivity for global economic modeling. *Agricultural Economics*, 45(1):37–50.

Myers, S. S., Zanobetti, A., Kloog, I., Huybers, P., Leakey, A. D. B., Bloom, A. J., Carlisle, E., Dietterich, L. H., Fitzgerald, G., Hasegawa, T., Holbrook, N. M., Nelson, R. L., Ottman, M. J., Raboy, V., Sakai, H., Sartor, K. A., Schwartz, J., Seneweera, S., Tausz, M., and Usui, Y. (2014). Increasing CO_2 threatens human nutrition. *Nature.*

Nakicenovic, N., Davidson, O., Davis, G., Grübler, A., Kram, T., Rovere, E. L. L., Metz, B., Morita, T., Pepper, W., Pitcher, H., Sankovski, A., Shukla, P., Swart, R., Watson, R., and Dadi, Z. (2000). *IPCC 2000. Special report on emissions scenarios. Working Group III of the Intergovernmental Panel on Climate Change.* Cambridge University Press, Cambridge, UK.

Nakicenovic, N., Lempert, R. J., and Janetos, A. C. (2014). A framework for the development of new socio-economic scenarios for climate change research: introductory essay. *Climatic Change*, 122(3):351–361.

Neitsch, S. L., Arnold, J. G., Kiniry, J. R., and Williams, J. R. (2005). *Soil and water assessment tool. Theoretical documentation, version 2005.* Grassland, soil and water research laboratory, Agricultural research service 808 East Blackland road, Temple, Texas 76502.

Nelson, G. C., Rosegrant, M. W., Koo, J., Robertson, R., Sulser, T., Zhu, T., Ringler, C., Msangi, S., Palazzo, A., Batka, M., Magalhaes, M., Valmonte-Santos, R., Ewing, M., and Lee, D. (2009). *Climate change: Impact on agriculture and costs of adaptation.* International Food Policy Research Institute (IFPRI).

Nelson, G. C., Rosegrant, M. W., Palazzo, A., Gray, I., Ingersoll, C., Robertson, R., Tokgoz, S., Zhu, T., Sulser, T. B., Ringler, C., Msangi, S., and You, L. (2010). *Food security, farming, and climate change to 2050.* International Food Policy Research Institute (IFPRI).

Nelson, G. C. and Shively, G. E. (2013). Modeling climate change and agriculture: an introduction to the special issue. *Agricultural Economics*, 45(1):1–2.

Nelson, G. C., Valin, H., Sands, R. D., Havlík, P., Ahammad, H., Deryng, D., Elliott, J., Fujimori, S., Hasegawa, T., Heyhoe, E., Kyle, P., Von Lampe, M., Lotze-Campen, H., Mason d'Croz, D., van Meijl, H., van der Mensbrugghe, D., Müller, C., Popp, A., Robertson, R., Robinson, S., Schmid, E., Schmitz, C., Tabeau, A., and Willenbockel, D. (2014). Climate change effects on agriculture: Economic responses to biophysical shocks. *Proceedings of the National Academy of Sciences*, 111(9):3274–3279.

Nelson, G. C., van der Mensbrugghe, D., Ahammad, H., Blanc, E., Calvin, K., Hasegawa, T., Havlík, P., Heyhoe, E., Kyle, P., Lotze-Campen, H., Von Lampe, M., Mason d'Croz, D., van Meijl, H., Müller, C., Reilly, J. M., Robertson, R., Sands, R. D., Schmitz, C., Tabeau, A., Takahashi, K., Valin, H., and Willenbockel, D. (2013). Agriculture and climate change in global scenarios: why don't the models agree. *Agricultural Economics*, 45(1):85–101.

Neumann, K., Verburg, P. H., Stehfest, E., and Müller, C. (2010). The yield gap of global grain production: A spatial analysis. *Agricultural Systems*.

Nevison, C. (2000). Review of the IPCC methodology for estimating nitrous oxide emissions associated with agricultural leaching and runoff. *Chemosphere - Global Change Science*, 2(3-4):493–500.

New, M., Lister, D., Hulme, M., and Makin, I. (2002). A high-resolution data set of surface climate over global land areas. *Climate Research*.

Nishina, K., Akiyama, H., Nishimura, S., Sudo, S., and Yagi, K. (2012). Evaluation of uncertainties in N_2O and NO fluxes from agricultural soil using a hierarchical Bayesian model. *Journal of Geophysical Research*, 117(G4).

Olander, L., Wollenberg, E., Tubiello, F., and Herold, M. (2013). Advancing agricultural greenhouse gas quantification. *Environmental Research Letters*.

O'Neil, B., Carter, T., Ebi, K., Edmonds, J., Hallegatte, S., Kemp-Benedict, E., Kriegler, E., Mearns, L., Moss, R., Riahi, K., van Ruijven, B., and van Vuuren, D. (2011). Meeting report of the workshop on the nature and use of new socioeconomic pathways for climate change research, Boulder, CO, November 2-4, 2011. Available at: http://www.isp.ucar.edu/socio- economic-pathways.

O'Neil, B. C., Kriegler, E., Riahi, K., Ebi, K. L., Hallegatte, S., Carter, T. R., Mathur, R., and Van Vuuren, D. P. (2014). A new scenario framework for climate change research: the concept of shared socioeconomic pathways. *Climatic Change*, 122(3):387–400.

Osborn, T. J. (2009). *User guide for ClimGen: a flexible tool for generating monthly climate data sets and scenarios. 19.* Climatic Research Unit, University of East Anglia.

Osborne, T., Rose, G., and Wheeler, T. R. (2013). Variation in the global-scale impacts of climate change on crop productivity due to climate model uncertainty and adaptation. *Agricultural and Forest Meteorology*, 170:183–194.

Osborne, T. M., Lawrence, D. M., Challinor, A. J., Slingo, J. M., and Wheeler, T. R. (2007). Development and assessment of a coupled crop-climate model. *Global Change Biology*.

Ostrom, E. (2008). Frameworks and theories of environmental change. *Global Environmental Change*, pages 1–4.

Ostrom, E. (2010). Polycentric systems for coping with collective action and global environmental change. *Global Environmental Change*, 20(4):550–557.

Paris, Q. (1992). The von Liebig hypothesis. *American Journal of Agricultural Economics*, 74(4):1019–1028.

Parlange, M. B. and Katz, R. W. (2000). An extended version of the Richardson model for simulating daily weather variables. *Journal Of Applied Meteorology*.

Parry, M., Rosenzweig, C., Iglesias, A., Livermore, M., and Fischer, G. (2004). Effects of climate change on global food production under SRES emissions and socio-economic scenarios . *Global Environmental Change*, 14:53–67.

Patt, A. (2007). Assessing model-based and conflict-based uncertainty. *Global Environmental Change*, 17(1):37–46.

Penman, H. L. (1948). Natural evaporation from open water, bare soil, and grass. *Proceedings of the Royal Society*, A(193):120–146.

Penning de Vries, F. W. T., Jansen, D. M., ten Berge, H. F. M., and Bakema, A. (1989). *Simulation of ecophysiological processes of growth in several annual crops.* Pudoc.

Perlman, J., Hijmans, R. J., and Horwath, W. R. (2014). A metamodelling approach to estimate global N_2O emissions from agricultural soils. *Global Ecology and Biogeography*.

Phalan, B., Green, R., and Balmford, A. (2014). Closing yield gaps: perils and possibilities for biodiversity conservation. *Philosophical Transactions of the Royal Society B*, 369(1639):20120285–20120285.

Philibert, A., Loyce, C., and Makowski, D. (2013). Prediction of N_2O emission from local information with Random Forest. *Environmental Pollution*.

Piesse, J. and Thirtle, C. (2009). Three bubbles and a panic: An explanatory review of recent food commodity price events. *Food Policy.*

Piontek, F., Müller, C., Pugh, T. A. M., Clark, D. B., Deryng, D., Elliott, J., de Jesus Colón González, F., Flörke, M., Folberth, C., Franssen, W., Frieler, K., Friend, A. D., Gosling, S. N., Hemming, D., Khabarov, N., Kim, H., Lomas, M. R., Masaki, Y., Mengel, M., Morse, A., Neumann, K., Nishina, K., Ostberg, S., Pavlick, R., Ruane, A. C., Schewe, J., Schmid, E., Stacke, T., Tang, Q., Tessler, Z. D., Tompkins, A. M., Warszawski, L., Wisser, D., and Schellnhuber, H. J. (2014). Multisectoral climate impact hotspots in a warming world. *Proceedings of the National Academy of Sciences*, 111(9):3233–3238.

Pleijel, H. and Uddling, J. (2011). Yield vs. quality trade-offs for wheat in response to carbon dioxide and ozone. *Global Change Biology.*

Poppy, G. M., Jepson, P. C., Pickett, J. A., and Birkett, M. A. (2014). Achieving food and environmental security: new approaches to close the gap. *Philosophical Transactions of the Royal Society B*, 369.

Porter, J. R. and Gawith, M. (1999). Temperatures and the growth and development of wheat: a review. *European Journal of Agronomy.*

Porter, J. R., Xie, L., Challinor, A., Cochrane, K., Howden, M., Iqbal, M. M., Lobell, D., Travasso, M. I., Chhetri, N., Garrett, K., Ingram, J., Lipper, L., McCarthy, N., McGrath, J., Smith, D., Thornton, P., Watson, J., and Ziska, L. (2014). *Climate change 2014: impacts, adaptation, and vulnerability. Contribution of working group II to the fifth assessment report of the intergovernmental panel on climate change*, chapter 7. Food security and food production systems. Cambridge University Press, Cambridge, UK.

Portmann, F. T., Siebert, S., and Döll, P. (2009). MIRCA2000 – Global Monthly Irrigated and Rainfed Crop Areas around the year 2000: a new high-resolution data set for agricultural and hydrological modeling. *Global Biogeochemical Cycles.*

Postel, S. L., Daily, G. C., and Ehrlich, P. R. (1996). Human Appropriation of Renewable Fresh Water. *Science.*

Potter, P. A., Ramankutty, N., Bennett, E. M., and Donner, S. (2010). Characterizing the Spatial Patterns of Global Fertilizer Application and Manure Production. *Earth Interactions*, 14(2):1–22.

Priestley, C. H. B. and Taylor, R. J. (1972). On the Assessment of Surface Heat Flux and Evaporation Using Large-Scale Parameters . *Monthly Weather Review.*

Ramankutty, N., Evan, A., Monfreda, C., and Foley, J. A. (2008). Farming the planet: 1. Geographic distribution of global agricultural lands in the year 2000. *Global Biogeochemical Cycles.*

Ramankutty, N. and Foley, J. A. (1999). Estimating historical changes in global land cover: Croplands from 1700 to 1992. *Global Biogeochemical Cycles.*

Ramankutty, N., Foley, J. A., Norman, J., and McSweeney, K. (2002). The global distribution of cultivable lands: current patterns and sensitivity to possible climate change. *Global Ecology and Biogeography.*

Reay, D. S., Davidson, E. A., Smith, K. A., Smith, P., Melillo, J. M., Dentener, F., and Crutzen, P. (2012). Global agriculture and nitrous oxide emissions. *Nature Climate Change.*

Reid, C. D. and Fiscus, E. L. (1998). Effects of elevated $[CO_2]$ and/or ozone on limitations to CO_2 assimilation in soybean (Glycine max). *Journal of Experimental Botany.*

Riahi, K., Grubler, A., and Nakicenovic, N. (2007). Scenarios of long-term socio-economic and environmental development under climate stabilization. *Technological Forecasting and Social Change.*

Richardson, C. W. (1981). Stochastic simulation of daily precipitation, temperature, and solar radiation. *Water Resources Research*, 17(1):182–190.

Richardson, C. W. and Wright, D. A. (1984). *WGEN: a model for generating daily weather variables.* U.S. Department of Agriculture, Agricultural Research Service, ARS–8.

Rikkonen, P., Kaivo-oja, J., and Aakkula, J. (2006). Delphi expert panels in the scenario-based strategic planning of agriculture. *foresight*, 8(1):66–81.

Rockström, J., Steffen, W., Noone, K., Persson, A., Chapin, III, F. S., Lambin, E. F., Lenton, T. M., Scheffer, M., Folke, C., Schellnhuber, H. J., Nykvist, B., de Wit, C. A., Hughes, T., van der Leeuw, S., Rodhe, H., Sorlin, S., Snyder, P., Costanza, R., Svedin, U., Falkenmark, M., Karlberg, L., Corell, R. W., Fabry, V. J., Hansen, J., Walker, B. H., Liverman, D., Richardson, K., Crutzen, P., and Foley, J. A. (2009). A safe operating space for humanity. *Nature*, 461(7263):472–475.

Romanova, A., Mudrik, V., Novichkova, N., Demidova, R., and Polyakova, V. (2002). Physiological and biochemical characteristics of sugar beet plants grown at an increased carbon dioxide concentration and at various nitrate doses. *Russian Journal of Plant Physiology*, 49:204–210.

Rosegrant, M. W. and Cline, S. (2003). Global Food Security: Challenges and Policies. *Science*, 302(5652):1917.

Rosen, C. J. and Bierman, P. M. (2005). Nutrient management for fruit & vegetable crop production in using manure and compost as nutrient sources for vegetable crops. Ed. University of Minnesota.

Rosenthal, D. M., Slattery, R. A., Miller, R. E., Grennan, A. K., Cavagnaro, T. R., Fauquet, C. M., Gleadow, R. M., and Ort, D. R. (2012). Cassava about-FACE: Greater than expected yield stimulation of cassava (Manihot esculenta) by future CO2 levels. *Global Change Biology*, 18(8):2661–2675.

Rosenzweig, C., Elliott, J., Deryng, D., Ruane, A. C., Müller, C., Arneth, A., Boote, K. J., Folberth, C., Glotter, M., Khabarov, N., Neumann, K., Piontek, F., Pugh, T. A. M., Schmid, E., Stehfest, E., Yang, H., and Jones, J. W. (2014). Assessing agricultural risks of climate change in the 21st century in a global gridded crop model intercomparison. *Proceedings of the National Academy of Sciences*, 111(9):3268–3273.

Rosenzweig, C., Jones, J. W., Hatfield, J. L., Ruane, A. C., Boote, K. J., Thorburn, P., Antle, J. M., Nelson, G. C., Porter, C., Janssen, S., Asseng, S., Basso, B., Ewert, F., Wallach, D., Baigorria, G., and Winter, J. M. (2013). The Agricultural Model Intercomparison and Improvement Project (AgMIP): Protocols and pilot studies. *Agricultural and Forest Meteorology*, 170:166–182.

Rosenzweig, C. and Neofotis, P. (2013). Detection and attribution of anthropogenic climate change impacts. *Wiley Interdisciplinary Reviews: Climate Change*, 4(2):121–150.

Rosenzweig, C. and Parry, M. (1994). Potential impact of climate change on world food supply. *Nature*, 367.

Rosenzweig, C., Tubiello, F. N., Goldberg, R., Mills, E., and Bloomfield, J. (2002). Increased crop damage in the US from excess precipitation under climate change. *Global Environmental Change*, 12(3):197–202.

Rosenzweig, C., Yang, X. B., Epstein, P. R., and Chivian, E. (2001). Climate change and extreme weather events – Implications for food production, plant diseases, and pests. *Global Change & Human Health*, 2(2):15.

Rotmans, J., Hulme, M., and Downing, T. E. (1994). Climate change implications for europe: An application of the escape model. *Global Environmental Change*, 4:97–124.

Rötter, R. P. (2014). Agricultural Impacts: Robust uncertainty. *Nature Climate Change*, 4(4):251–252.

Rötter, R. P., Carter, T. R., Olesen, J. E., and Porter, J. R. (2011). Crop–climate models need an overhaul. *Nature Climate Change*, 1(4):175–177.

Ruane, A. C., Cecil, L. D., Horton, R. M., Gordón, R., McCollum, R., Brown, D., Killough, B., Goldberg, R., Greeley, A. P., and Rosenzweig, C. (2013a). Climate change impact uncertainties for maize in Panama: Farm information, climate projections, and yield sensitivities. *Agricultural and Forest Meteorology*, 170:132–145.

Ruane, A. C., Major, D. C., Yu, W. H., Alam, M., Hussain, S. G., Khan, A. S., Hassan, A., Al Hossain, B. M. T., Goldberg, R., Horton, R. M., and Rosenzweig, C. (2013b). Multi-factor impact analysis of agricultural production in Bangladesh with climate change. *Global Environmental Change*, 23(1):338–350.

Sacks, W., Cook, B., Buenning, N., and Levis, S. (2008). Effects of global irrigation on the near-surface climate. *Climate Dynamics*.

Sacks, W., Deryng, D., Foley, J. A., and Ramankutty, N. (2010). Crop planting dates: an analysis of global patterns. *Global Ecology and Biogeography*.

Sanchez, P. A. (2010). Tripling crop yields in tropical Africa. *Nature Geoscience*, 3(5):299–300.

Sarewitz, D. (2011). Does climate change knowledge really matter? *Wiley Interdisciplinary Reviews: Climate Change*, 2(4):475–481.

Savage, N. (2013). Modelling: Predictive yield. *Nature*.

Sayer, J. and Cassman, K. G. (2013). Agricultural innovation to protect the environment. *Proceedings of the National Academy of Sciences*, 110(21):8345–8348.

Schaap, M. G. and Bouten, W. (1996). Modeling water retention curves of sandy soils using neural networks. *Water Resources Research*, 32(10):3033–3040.

Schellnhuber, H. J., Frieler, K., and Kabat, P. (2014). The elephant, the blind, and the intersectoral intercomparison of climate impacts. *Proceedings of the National Academy of Sciences*, 111(9):3225–3227.

Schiermeier, Q. (2011). Extreme measures. Can violent hurricanes, floods and droughts be pinned on climate change? Scientists are beginning to say yes. *Nature*, 477:1–2.

Schlenker, W. and Roberts, M. (2009). Nonlinear temperature effects indicate severe damages to US crop yields under climate change. *Proceedings of the National Academy of Sciences*, 106(37).

Schlesinger, W. (2008). On the fate of anthropogenic nitrogen. *Proceedings of the National Academy of Sciences*.

Schmitz, C., Biewald, A., Lotze-Campen, H., Popp, A., Dietrich, J. P., Bodirsky, B., and Krause, M. (2012). Trading more food: Implications for land use, greenhouse gas emissions, and the food system. *Global Environmental Change*, 22:189–209.

Semenov, M. A. and Shewry, P. (2011). Modelling predicts that heat stress and not drought will limit wheat yield in Europe. *Scientific Reports*, 1(66).

Shimono, H., Nakamura, H., Hasegawa, T., and Okada, M. (2013). Lower responsiveness of canopy evapotranspiration rate than of leaf stomatal conductance to open-air CO_2 elevation in rice. *Global Change Biology*, 19(8):2444–2453.

Siebert, S., Burke, J., Faures, J.-M., Frenken, K., Hoogeveen, J., Döll, P., and Portmann, F. T. (2010). Groundwater use for irrigation – a global inventory. *Hydrology and Earth System Science*, pages 1863–1880.

Singels, A., Jones, M., Marin, F., Ruane, A., and Thorburn, P. (2013). Predicting climate change impacts on sugarcane production at sites in Australia, Brazil and South Africa using the Canegro model. *Sugar Tech*.

Sitch, S., Smith, P., Prentice, I. C., Arneth, A., Bondeau, A., Cramer, W., Kaplan, J., Levis, S., Lucht, W., Sykes, M. T., Thonicke, K., and Venevsky, S. (2003). Evaluation of ecosystem dynamics, plant geography and terrestrial carbon cycling inthe LPJ dynamic global vegetation model . *Global Change Biology*, 9:25.

Smith, B., Prentice, I. C., and Sykes, M. T. (2001). Representation of vegetation dynamics in the modelling of terrestrial ecosystems: comparing two contrasting approaches within European climate space. *Global Ecology and Biogeography*, 10(6):621–637.

Solomon, S., Qin, D., Manning, M., Chen, Z., Marquis, M., Averyt, K. B., Tignor, M., and Miller, H. L., editors (2007). *Climate change 2007: the physical science basis. Contribution of Working Group I to the fourth assessment report of the Intergovernmental Panel on Climate Change.* Cambridge University Press, Cambridge, UK.

Spiertz, J. H. J., Hamer, R. J., Xu, H., Primo-Martin, C., Don, C., and van der Putten, P. E. L. (2006). Heat stress in wheat (Triticum aestivum L.): Effects on grain growth and quality traits. *European Journal of Agronomy*.

Stehfest, E. and Bouwman, L. (2006). N_2O and NO emission from agricultural fields and soils under natural vegetation: summarizing available measurement data and modeling of global annual emissions. *Nutrient Cycling in Agroecosystems*.

Stehfest, E., Heistermann, M., Priess, J. A., Ojima, D., and Alcamo, J. M. (2007). Simulation of global crop production with the ecosystem model DayCent. *Ecological Modelling.*

Stocker, T. F., Qin, D., Plattner, G. K., Tignor, M., Allen, S. K., Boschung, J., Nauels, A., Xia, Y., Bex, V., and Midgley, P. M., editors (2013). *Climate change 2013: the physical science basis. Contribution of Working Group I to the fifth assessment report of the Intergovernmental Panel on Climate Change.* Cambridge University Press, Cambridge, UK.

Stuhlfauth, T. and Fock, H. P. (1990). Effect of whole season CO_2 enrichment on the cultivation of a medicinal plant, Digitalis lanata. *Journal of Agronomy and Crop Science*, 164(3):168–173.

Sumner, D. M. and Jacobs, J. M. (2005). Utility of Penman-Monteith, Priestley-Taylor, reference evapotranspiration, and pan evaporation methods to estimate pasture evapotranspiration. *Journal of Hydrology*, 308(1-4):81–104.

Taub, D. R., Miller, B., and Allen, H. (2008). Effects of elevated CO_2 on the protein concentration of food crops: a meta-analysis. *Global Change Biology.*

Teixeira, E. I., Fischer, G., van Velthuizen, H., Walter, C., and Ewert, F. (2011). Global hot-spots of heat stress on agricultural crops due to climate change. *Agricultural and Forest Meteorology*, pages 1–10.

The Millennium Development Goals Report (2013). *Scaling Up Nutrition; UNDP; UNDP-IKEA, FAO (The State of Food and Agriculture 2013); UNICEF; ILO; WFP, Zero Hunger Challenge.* United Nations.

Thuzar, M., Puteh, A. B., Abdullah, N. A. P., Lassim, M. B. M., and Jusoff, K. (2010). The effects of temperature stress on the quality and yield of soya bean. *Journal of Agricultural Science.*

Tilman, D., Balzer, C., Hill, J., and Befort, B. L. (2011). Global food demand and the sustainable intensification of agriculture. *Proceedings of the National Academy of Sciences*, 108(50):20260–20264.

Tilman, D., Cassman, K. G., Matson, P., Naylor, R., and Polasky, S. (2002). Agricultural sustainability and intensive production practices. *Nature.*

Tubiello, F. N., Amthor, J. S., Boote, K. J., Donatelli, M., Easterling, W., Fischer, G., Gifford, R. M., Howden, M., Reilly, J. M., and Rosenzweig, C. (2007). Crop response to elevated CO_2 and world food supply - A comment on "Food for Thought.

. .” by Long et al., Science 312:1918–1921, 2006. *European Journal of Agronomy*, 26(3):215–223.

USDA/NRCS (2012). Soil Survey Staff, Natural Resources Conservation Service, Soil Survey Geographic (SSURGO) Database for [Survey Area, State]. Available online at http://soildatamart.nrcs.usda.gov. Accessed Feb 2012.

Utset, A., Farre, I., Martinez-Cob, A., and Cavero, J. (2004). Comparing Penman–Monteith and Priestley–Taylor approaches as reference-evapotranspiration inputs for modeling maize water-use under Mediterranean conditions. *Agricultural Water Management*, 66(3):205–219.

Valin, H., Havlík, P., Mosnier, A., Herrero, M., Schmid, E., and Obersteiner, M. (2013). Agricultural productivity and greenhouse gas emissions: trade-offs or synergies between mitigation and food security? *Environmental Research Letters*.

Van Dingenen, R., Dentener, F. J., Raes, F., Krol, M. C., Emberson, L., and Cofala, J. (2009). The global impact of ozone on agricultural crop yields under current and future air quality legislation. *Atmospheric Environment*, 43(3):604–618.

van Genuchten, M., Kaveh, F., and Russell, W. (1988). Direct and indirect methods for estimating the hydraulic properties of unsaturated soils. Land qualities in space and time : proceedings of a symposium, Wageningen, the Netherlands,.

van Ittersum, M. K., Cassman, K. G., Grassini, P., Wolf, J., Tittonell, P., and Hochman, Z. (2013). Yield gap analysis with local to global relevance – A review. *Field Crops Research*, 143:4–17.

van Vuuren, D. P. and Carter, T. R. (2014). Climate and socio-economic scenarios for climate change research and assessment: reconciling the new with the old. *Climatic Change*, 122(3):415–429.

van Vuuren, D. P., den Elzen, M. G. J., Lucas, P. L., Eickhout, B., Strengers, B. J., van Ruijven, B., Wonink, S., and van Houdt, R. (2007). Stabilizing greenhouse gas concentrations at low levels: an assessment of reduction strategies and costs. *Climatic Change*.

van Vuuren, D. P., Edmonds, J. A., Kainuma, M., Riahi, K., Hibbard, K., Hurtt, G. C., Kram, T., Krey, V., Lamarque, J.-F., Masui, T., Meinshausen, M., Nakicenovic, N., Smith, S. J., and Rose, S. K. (2011). The representative concentration pathways: an overview. *Climatic Change*.

van Vuuren, D. P., Kriegler, E., O’neill, B. C., Ebi, K. L., Riahi, K., Carter, T. R., Edmonds, J. A., Hallegatte, S., Kram, T., Mathur, R., and Winkler, H. (2014). A

new scenario framework for Climate Change Research: scenario matrix architecture. *Climatic Change*, 122(3):373–386.

van Vuuren, D. P., Meinshausen, M., Plattner, G.-K., Joos, F., Strassmann, K. M., Smith, S. J., Wigley, T. M. L., Raper, S. C. B., Riahi, K., de la Chesnayel, F., Den Elzen, M. G., Fujino, J., Jiang, K., Nakicenovic, N., Paltsev, S., and Reilly, J. M. (2008). Temperature increase of 21st century mitigation scenarios. *Proceedings of the National Academy of Sciences*.

van Vuuren, D. P., Riahi, K., Moss, R., Edmonds, J. A., Thomson, A., Nakicenovic, N., Kram, T., Berkhout, F., Swart, R., Janetos, A., Rose, S. K., and Arnell, N. (2012). A proposal for a new scenario framework to support research and assessment in different climate research communities. *Global Environmental Change*, 22(1):21–35.

van Wart, J., Kersebaum, K. C., Peng, S., Milner, M., and Cassman, K. G. (2013a). Estimating crop yield potential at regional to national scales. *Field Crops Research*.

van Wart, J., van Bussel, L. G. J., Wolf, J., Licker, R., Grassini, P., Nelson, A., Boogaard, H., Gerber, J., Mueller, N. D., Claessens, L., van Ittersum, M. K., and Cassman, K. G. (2013b). Use of agro-climatic zones to upscale simulated crop yield potential. *Field Crops Research*.

Vanuytrecht, E., Raes, D., Willems, P., and Geerts, S. (2012). Quantifying field-scale effects of elevated carbon dioxide concentration on crops. *Climate Research*, 54(1):35–47.

Vermeulen, S. J., Aggarwal, P. K., Ainslie, A., Angelone, C., Campbell, B. M., Challinor, A. J., Hansen, J. W., Ingram, J. S. I., Jarvis, A., Kristjanson, P., Lau, C., Nelson, G. C., Thornton, P. K., and Wollenberg, E. (2012a). Options for support to agriculture and food security under climate change. *Environmental Science and Policy*, 15(1):136–144.

Vermeulen, S. J., Campbell, B. M., and Ingram, J. S. I. (2012b). Climate change and food systems. *Annual Review of Environment and Resources*, 37(1):195–222.

Vermeulen, S. J., Challinor, A. J., Thornton, P. K., Campbell, B. M., Eriyagama, N., Vervoort, J. M., Kinyangi, J., Jarvis, A., Läderach, P., Ramirez-Villegas, J., Nicklin, K. J., Hawkins, E., and Smith, D. R. (2013). Addressing uncertainty in adaptation planning for agriculture. *Proceedings of the National Academy of Sciences*, 110(21):8357–8362.

Vilhena-Cardoso, J. and Barnes, J. (2001). Does nitrogen supply affect the response of wheat (Triticum aestivum cv. Hanno) to the combination of elevated CO_2 and O_3? *Journal of Experimental Botany*, 52:1901–1911.

Vincent, K. (2007). Uncertainty in adaptive capacity and the importance of scale. *Global Environmental Change*, 17(1):12–24.

Vinukollu, R. K., Wood, E. F., Ferguson, C. R., and Fisher, J. B. (2011). Global estimates of evapotranspiration for climate studies using multi-sensor remote sensing data: Evaluation of three process-based approaches. *Remote sensing of environment*, 115(3):801–823.

Von Lampe, M., Willenbockel, D., Ahammad, H., Blanc, E., Cai, Y., Calvin, K., Fujimori, S., Hasegawa, T., Havlík, P., Heyhoe, E., Kyle, P., Lotze-Campen, H., Mason d'Croz, D., Nelson, G. C., Sands, R. D., Schmitz, C., Tabeau, A., Valin, H., van der Mensbrugghe, D., and van Meijl, H. (2013). Why do global long-term scenarios for agriculture differ? An overview of the AgMIP Global Economic Model Intercomparison. *Agricultural Economics*, 45(1):3–20.

Vörösmarty, C. J., McIntyre, P. B., Gessner, M. O., Dudgeon, D., Prusevich, A., Green, P., Glidden, S., Bunn, S. E., Sullivan, C. A., Liermann, C. R., and Davies, P. M. (2010). Global threats to human water security and river biodiversity. *Nature*, 467(7315):555–561.

Waha, K., Müller, C., Bondeau, A., Dietrich, J. P., Kurukulasuriya, P., Heinke, J., and Lotze-Campen, H. (2013). Adaptation to climate change through the choice of cropping system and sowing date in sub-Saharan Africa. *Global Environmental Change*, 23(1):130–143.

Waha, K., van Bussel, L. G. J., Müller, C., and Bondeau, A. (2011). Climate-driven simulation of global crop sowing dates. *Global Ecology and Biogeography*, 21(2):247–259.

Wahid, A., Gelani, S., Ashraf, M., and Foolad, M. R. (2007). Heat tolerance in plants: an overview. *Environmental and Experimental Botany*, 61(3):199–223.

Wang, D., Heckathorn, S. A., Barua, D., Joshi, P., Hamilton, E. W., and LaCroix, J. J. (2008). Effects of elevated CO_2 on the tolerance of photosynthesis to acute heat stress in C_3, C_4, and CAM species. *American journal of botany*, 95(2):165–176.

Warren, R. (2010). The role of interactions in a world implementing adaptation and mitigation solutions to climate change. *Philosophical Transactions of the Royal Society A: Mathematical, Physical and Engineering Sciences*.

Warren, R., de la Nava Santos, S., Arnell, N. W., Bane, M., Barker, T., Barton, C., Ford, R., Füssel, H.-M., Hankin, R., Klein, R., Linstead, C., Kohler, J., Mitchell, T., Osborn, T., Pan, H., Raper, S. C. B., Riley, G., Schellnhuber, H. J., Winne, S., and Anderson,

D. (2008). Development and illustrative outputs of the Community Integrated Assessment System (CIAS), a multi-institutional modular integrated assessment approach for modelling climate change. *Environmental Modelling & Software.*

Warren, R., Yu, R., Osborn, T. J., and de la Nava Santos, S. (2012). European drought regimes under mitigated and unmitigated climate change: application of the Community Integrated Assessment System (CIAS). *Climate Research.*

Warszawski, L., Frieler, K., Huber, V., Huber, V., Piontek, F., Serdeczny, O., and Schewe, J. (2014). The Inter-Sectoral Impact Model Intercomparison Project (ISI-MIP): Project framework. *Proceedings of the National Academy of Sciences*, 111(9):3228–3232.

Wassmann, R., Hien, N. X., Hoanh, C. T., and Tuong, T. P. (2004). Sea level rise affecting the Vietnamese Mekong Delta: water elevation in the flood season and implications for rice production. *Climatic Change*, 66(1-2):89–107.

Weart, S. R. (2010). The idea of anthropogenic global climate change in the 20th century. *Wiley Interdisciplinary Reviews: Climate Change*, 1(1):67–81.

Weedon, G. P., Gomes, S., Viterbo, P., Shuttleworth, W. J., Blyth, E., Österle, H., Adam, J. C., Bellouin, N., Boucher, O., and Best, M. (2011). Creation of the WATCH forcing data and its use to assess global and regional reference crop evaporation over land during the twentieth century. *Journal of Hydrometeorology.*

Weerakoon, W., Ingram, K., and Moss, D. (2000). Atmospheric carbon dioxide and fertilizer nitrogen effects on radiation interception by rice. *Plant and Soil*, 220:99–106.

Wheeler, T. R., Craufurd, P. Q., Ellis, R. H., Porter, J. R., and VaraPrasad, P. V. (2000). Temperature variability and the yield of annual crops. *Agriculture, Ecosystems & Environment.*

Wheeler, T. R. and von Braun, J. (2013). Climate change impacts on global food security. *Science.*

White, J. W., Hoogenboom, G., Kimball, B. A., and Wall, G. W. (2011). Methodologies for simulating impacts of climate change on crop production. *Field Crops Research*, 124(3):357–368.

Widodo, W., Vu, J. C., Boote, K. J., Baker, J. T., and Allen, Jr, L. H. (2003). Elevated growth CO_2 delays drought stress and accelerates recovery of rice leaf photosynthesis. *Environmental and Experimental Botany.*

Wigley, T. M. L. (2001). Interpretation of High Projections for Global-Mean Warming. *Science.*

Wilby, R. and Dessai, S. (2010). Robust adaptation to climate change. *Weather*, 65(7):180–185.

Williams, J. R. (1990). *EPIC-Erosion/Productivity Impact Calculator*. USDA. Agricultural Research Service, Technical Bulletin Number 1768. Springfield, VA,.

Williams, J. R. (1995). *Computer Models of Watershed Hydrology*, chapter 25: The EPIC Model., pages 909–1000. Water Resources Publications. Highlands Ranch, CO.

Willmott, C. J., Ackleson, S. G., Davis, R. E., Feddema, J. J., Klink, K. M., Legates, D. R., O'Donell, J., and Row, C. M. (1985). Statistics for the Evaluation and Comparison of Models . *Journal of Geophysical Research*.

Wise, M., Calvin, K., Thomson, A. M., Clarke, L., Bond-Lamberty, B., Sands, R., Smith, S. J., Janetos, A., and Edmonds, J. A. (2009). Implications of Limiting CO_2 Concentrations for Land Use and Energy. *Science*.

Wood, S. and Dent, F. (1983). LECS : a land evaluation computer system methodology. Part of: Manual / Food and Agriculture Organization Nr. no. 5, version 1.

World Bank (2013). World Bank country and lending groups. http://data.worldbank.org/about/country-classifications/country-and-lending-groups. Accessed in July 2013.

Wullschleger, S. D., Tschaplinski, T. J., and Norby, R. J. (2002). Plant water relations at elevated CO_2 – implications for water-limited environments. *Plant, Cell and Environment*, 25(2):319–331.

Zavala, J. A., Casteel, C. L., DeLucia, E. H., and Berenbaum, M. R. (2008). Anthropogenic increase in carbon dioxide compromises plant defense against invasive insects. *Proceedings of the National Academy of Sciences*, 105(13):5129–5133.

Ziervogel, G. and Ericksen, P. J. (2010). Adapting to climate change to sustain food security. *Wiley Interdisciplinary Reviews: Climate Change*, 1(4):525–540.

Zwart, S. J. and Bastiaanssen, W. G. M. (2004). Review of measured crop water productivity values for irrigated wheat, rice, cotton and maize. *Agricultural Water Management*, 69(2):115–133.